

THE DEVELOPMENT OF CHIRAL TITANOCENES AS PHOTOREDOX CATALYSTS

DISSERTATION

ZUR

ERLANGUNG DES DOKTORGRADES (DR. RER. NAT.)

DER MATHEMATISCH-NATURWISSENSCHAFTLICHEN FAKULTÄT
DER RHEINISCHEN FRIEDRICH-WILHELMS-UNIVERSITÄT BONN

VORGELEGT VON

DANIEL SLAK

AUS

CLOPPENBURG

BONN

2022

Angefertigt mit Genehmigung der Mathematisch-Naturwissenschaftlichen Fakultät
der Rheinischen Friedrich-Wilhelms-Universität Bonn.

Betreuer/Gutachter:	Prof. Dr. Andreas Gansäuer
Gutachter:	Prof. Dr. Arne Lützen
Tag der Promotion:	13.01.2023
Erscheinungsjahr:	2023

The work and research towards this dissertation were carried out between November 2019 and October 2022 at the Kekulé Institute of Organic Chemistry and Biochemistry of the *Rheinische Friedrich-Wilhelms-Universität Bonn* under supervision of *Prof. Dr. A. Gansäuer*.

Parts of this work have already been published:

TITANOCENES AS PHOTOREDOX CATALYSTS USING GREEN LIGHT IRRADIATION

Z. Zhang, T. Hilche, **D. Slak**, N. R. Rietdijk, U. N. Oloyede, R. A. Flowers II, A. Gansäuer, *Angew. Chem. Int. Ed.* **2020**, 59, 9355–9359; *Angew. Chem.* **2020**, 132, 9441–9445.

DOI: 10.1002/anie.202001508 and 10.1002/ange.202001508.

THERE ARE ONLY TWO DAYS IN THE YEAR THAT NOTHING CAN BE DONE.
ONE IS CALLED YESTERDAY AND THE OTHER IS CALLED TOMORROW.

DALAI LAMA XIV

Table of Content

1 Introduction	1
1.1 Sustainability and Environmental Protection	1
1.2 Green Chemistry	2
2 General Part	6
2.1 Nature as Model for Synthetic Chemistry	6
2.2 Stereoselective Catalysis	13
2.3 Titanocenes in Epoxide Opening Reactions	23
2.4 Photoredox Catalysis	27
3 Special Part	34
3.1 Task and Objective of this Work	34
3.2 Applications of the Photoactive Properties of Titanocenes	35
3.3 Expansion to Other Systems	41
3.4 Arylations	51
3.5 REO and DEO Substrates	64
3.6 Photochemical REO and DEO Reactions	77
4 Summary and Outlook	97
5 Experimental Part	100
5.1 General Information	100
5.2 General Procedures	104
5.3 Photoexcited Titanocene Catalyzed Epoxide Openings	109
5.4 Pinacol Couplings	115
5.5 Radical Arylations and REO-Arylations of Epoxides	117
5.6 REO Substrate Syntheses	126
5.7 DEO Substrate Syntheses	149
5.8 Diastereodivergent Epoxide Openings	150
5.9 Regiodivergent Epoxide Openings with Organic Photocatalysts	160
5.10 Regiodivergent Epoxide Openings with Sulfonamides	165
5.11 Regiodivergent Epoxide Openings under other Conditions	174
5.12 Other Syntheses	176

6 References.....	198
7 Abbreviations.....	213
8 Appendix	217
8.1 List of Figures	217
8.2 List of Tables	219
8.3 List of Schemes	220
8.4 List of Publications	224
9 Acknowledgement – Danksagung	225
10 Zusammenfassung	226
11 Abstract	227

For clarity, chemical structures in this thesis are abbreviated according to their respective topic. These employed abbreviations followed by a consecutive number are:

- A** Arylation substrates and products
- C** Intermediates in catalytic cycles
- D** DEO substrates and products
- E** General epoxides and opening products
- H** *Hantzsch* esters
- I** Structures of introductory examples
- N** Nucleophiles for REO substrate synthesis
- P** Pinacol coupling substrates and products
- R** REO substrates and products
- S** Other chemicals
- T** Titanocene carboxylates
- X** Commonly used reagents and substrates
- Z** Chloride-acceptors

1 Introduction

The world-wide effects of climate change, global-warming and environmental degradation have become increasingly perceptible and measurable in recent years.^[1] Finding solutions to environmental and economic problems regarding renewable energy sources is one of the most crucial long-term investments into a sustainable, livable future. The rapid decrease of conventional fossil energy and resource stocks threatens the society and life standards we know.^[2] The dependency on energy in everyday life as well as in public infrastructure, agriculture and industry becomes especially visible these days due to global political conflicts, and resulting sanctions and energy embargos or shortages.

For this reason, innovative, independent and sustainable technologies and production methods are indispensable to keep today's lifestyle and standards without destruction of the environment and a total and irretrievable depletion of fossil feedstocks.^[1,2]

1.1 Sustainability and Environmental Protection

There is an unquestionable relation between renewable energies and sustainability.^[1] The global demand for energy by the 25% of the world's wealthiest industrial economies amounts to 75% of the total energy supply.^[2] A major advantage of fossil energy sources is the independency from weather and climate as well as their on demand availability. In contrast, a reliable power provision from sustainable resources requires continuous research and investment into new technologies and methods.^[3]

“Anthropogenic greenhouse gas emissions [...] are *extremely likely* to have been the dominant cause of the observed warming since the mid-20th century.”^[4] This statement by the *Intergovernmental Panel on Climate Change* (IPCC) confirms and emphasizes the man-made influence on climate change and environmental destruction. Hence, a reduction of these emissions is crucial to diminish and eventually stop further global warming. In 2017, fossil fuels contributed 73.5% to the global electricity production.^[5] Although there is a tendency to replace conventional energy sources by renewable feedstocks, the majority of this change is yet to be fulfilled.^[6] From a chemical point of view, the most apparent approach to this crisis is the development of more sustainable, energy saving and resource efficient syntheses – the *German Federal Statistic Office* (Statistisches Bundesamt) states that the chemical industry contributed the major part (33%) of the industrial primary energy consumption in Germany in 2019.^[7] This fact shows that sustainability in this industrial sector has a lot of influence and potential.

1.2 Green Chemistry

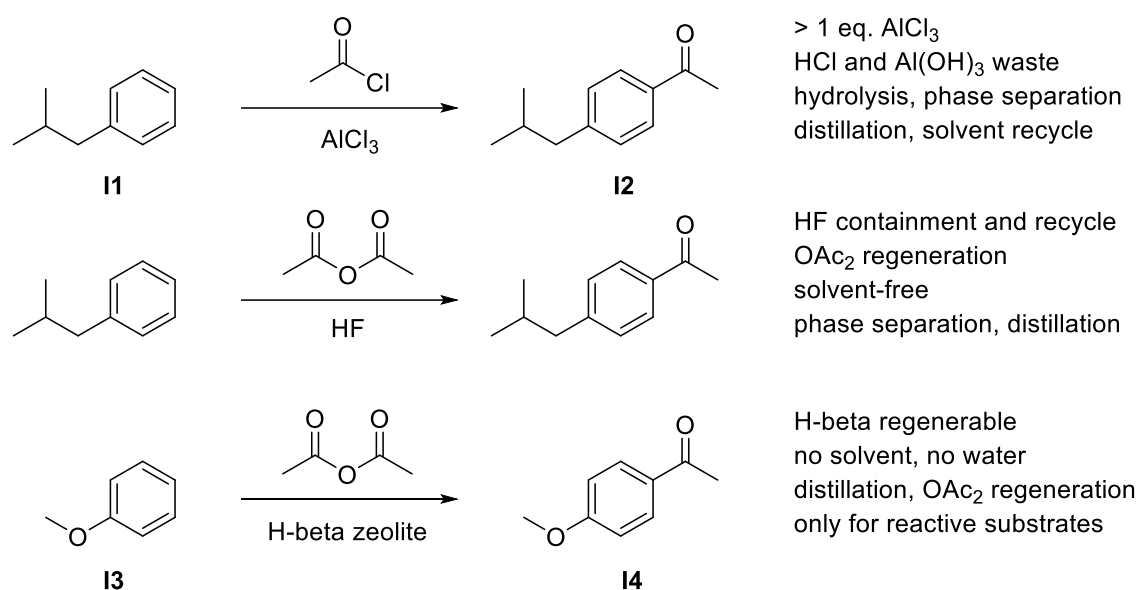
Around the turn of the millennium a new approach to improve the compatibility of the chemical industry and the natural environment and thereby also change the unfavorable image of the chemical industry arose.^[8,9] As more and more people and governments accepted the necessity of sustainable processes and development in their economies to maintain their high standards of living in a growing global population, the term 'Green Chemistry' was implemented to specify a number of principles by which this goal should be achieved. The key point of this approach was the reduction of waste or, in the best case, the total elimination of the generation of any hazardous substance in a chemical synthesis.^[10] An ideal synthesis would additionally be atom efficient, environmentally acceptable, safe and simple, give 100% yield and only use readily available materials.^[8] In this context, the term hazardous includes physical, toxicological, and also global harm.^[10] In 2000, *P. Anastas* published the twelve principles of Green Chemistry for the design of environmentally friendly and sustainable syntheses and products.^[11,12] A selection of these is shown in **Figure 1**, which focusses on applicability in the development for chemical syntheses in a research laboratory rather than on industrial scale application.

- I. Prevention of waste.
- II. Reduction of the use of auxiliary substances.
- III. Minimization of energy requirement.
- IV. Use of renewable, earth-abundant feedstocks.
- V. Application of catalysts rather than stoichiometric reagents.

Figure 1: Selection of principles of Green Chemistry by *Anastas*.^[10,11]

Not only is the disposal of waste a major reason for environmental pollution, but also a huge cost factor for any kind of industrial process. New synthetic methodologies in industrial processes and academia enable the minimization of waste generation by the application of reactions with a higher atom-economy, which is determined by the amount of atoms of the substrates found in the reaction products.^[10,13,14] For example, the synthesis of the well-known nonsteroidal anti-inflammatory drug *Ibuprofen* has been improved to a three-step route with about 80% atom-economy, compared to the originally developed six-step method, which already requires "greater than stoichiometric quantities of AlCl_3 "^[8] in a *Friedel-Crafts* acylation as the first synthesis step and below 40% atom utilization in the overall process.^[8,10] Additionally, the classical, widely-used homogeneous *Friedel-Crafts* acylation generates HCl as byproduct in the acylation itself and in the preparation of the required acetyl chloride.^[15] **Scheme 1** summarizes a comparison of the originally used and the modern, atom-efficient

modification of the acylation employed in the *Ibuprofen* synthesis as well a heterogeneous, solvent-free acylation method.



Scheme 1: Comparison of sustainability in different acylations for *Ibuprofen* precursor **I2**.^[8,10,15]

While the 2nd and 3rd method generate acetic acid as byproduct, which can be regenerated to the respective anhydride, the HCl and aluminum hydroxide that are formed in the 1st reaction must be disposed and cannot be easily recycled for the generation of acetyl chloride or AlCl₃. Additionally, AlCl₃ is used in over-stoichiometric amounts and in contrast, HF and H-beta zeolite are used catalytically. The 3rd reaction minimizes the required chemicals even further as it can be performed solvent-free. However, only reactive substrates such as **I3** can be used and the synthesis requires one additional reaction-step, the application is therefore limited.^[8,10,15] Particularly in industrial scale synthesis, the reduction of waste by application of recyclable chemicals and catalysts are key parts to stop the depletion of raw materials and feedstocks. The reduction of auxiliary substances is another important aspect of Green Chemistry. Auxiliary substances are for example solvents or separation agents,^[10,11] which are necessary to perform a reaction and may also be recycled. However, they thereby increase the production cost and potentially require elaborate purification to be reused. In addition, they might be hazardous themselves and therefore add risks in the reaction process and purification.

As already stated above, the chemical industry requires an enormous amount of energy. Especially with exploitation of fossil resources and rising costs for electricity, saving energy is not only an economic, but also an environmentally beneficial task.^[9,16] Probably the most apparent measure to reduce energy requirements in industry as well as in a research laboratory is the development of reactions that can be performed at ambient conditions,

meaning room temperature and atmospheric pressure. The aspect of saving energy also relates to waste minimization and renunciation of auxiliaries, as avoidable purification, transport and disposal demand substantial amounts of energy.

Although energy from fossil sources is a limited good, in principle, renewable energy sources such as wind, water and solar energy are inexhaustible and, thus, syntheses demanding higher amounts of energy are preferable, if chemicals can be saved.^[10] Of course, this demands large investments in suitable reactions and processes and the expansion of sustainable, renewable energy production in the future.

1.2.1 Renewable Energies and Feedstocks

There are several renewable and sustainable energy sources used for power generation these days. Wind, water, biomass, geothermal and solar energy can be utilized depending on the regional availability and climatic factors. Overall, the worldwide need for renewables is growing rapidly due to an increasing demand for energy, reduced cost compared to fossil sources and environmental concerns.^[17] The most general and globally almost omnipresent source of renewable energy is the sunlight.^[3] The annual power of incoming solar radiation is about 178,000 TW (= 178,000,000,000,000 kW).^[18] Nevertheless, a seasonal variation in solar radiation might cause problems, as storage of large amounts of electrical energy needs high-capacity batteries and thus is not as convenient as fossil feedstock storage. For this reason, a reliable power supply system based on various sustainable energy sources is the key to lose dependency on fossil fuels.

Another possibility of exploiting (artificial) light energy is the immediate use in chemical reactions by irradiation of suitable molecules. This photochemical approach will be discussed in following parts of this thesis and a new synthetic route enabling the reduction of hazardous chemicals in epoxide opening reactions will be introduced.

Not only the generation of 'practical' energy from renewable sources is important, but also the utilization of earth-abundant resources to ensure a sustainable supply for all kinds of manufacturing and syntheses. As organic material mainly consists of hydrogen, carbon, oxygen and nitrogen and three of these elements can also be produced from water and air, their feedstock is large enough to guarantee an inexhaustible supply. This is however not true for many other elements and especially transition metals, which are indispensable in modern societies. Prominent examples in large scale chemical processes are the use of iron in the *Haber-Bosch* process^[19], vanadium for the production of sulfuric acid^[20], platinum in fuel cells or for the production of nitric acid^[21,22] or nickel and rhodium in hydrogenation processes.^[23,24] While iron can be found in relatively large amounts in the earth's crust (46.5 g/kg)^[25] and iron ore is often found in discrete regions as banded iron formations and therefore easy to mine,

the other above mentioned transition metals are much rarer: vanadium (0.09 g/kg)^[25], nickel (0.03 g/kg)^[25], platinum (5 µg/kg)^[26] and rhodium (1 µg/kg).^[26] Iridium, which will play a key role in later parts of this work as it is used as central part of photocatalysts is also very rare (1 µg/kg)^[26] and therefore, a substitution is beneficial.

High demand or depletion of rare transition metals inevitably leads to high prices. Consequently, processes using readily available, earth-abundant elements are preferred. In this thesis, titanocene catalyzed epoxide opening reactions will be discussed. In fact, titanium is the 9th most abundant element in the earth's crust (5.7 g/kg)^[26] and thus inexpensive and quite sustainable.

1.2.2 Catalysis

The fifth selected principle of Green Chemistry is catalysis. In contrast to stoichiometric reagents, catalysts facilitate or accelerate a reaction without being consumed and thereby, they may be used in sub-stoichiometric amounts due to their high turnover numbers. Catalysts are no human invention, as natural enzymes can also be considered as catalysts. Because of the regeneration after performing a reaction cycle, catalysts can be reused many times, which makes them superior in contrast to stoichiometric reagents under the aspect of Green Chemistry.^[10,27,28]

Catalysts can be classified into two main sub-groups: homogeneous catalysts, which are present in the same phase as the other reaction components (mostly liquid/dissolved) and heterogeneous catalysts, where the reaction occurs at the interface between two phases (often solid catalyst and liquid reactants).^[29]

The overall standard *Gibbs* energy of the reaction or the chemical equilibrium are not influenced by the catalyst, only the reaction rate is accelerated.^[29,30] Today, over 90% of all chemically manufactured products have at least one catalyzed step in their synthesis.^[28] In fact, the above mentioned uses of transition metals in chemical industry for the *Haber-Bosch* process, the synthesis of sulfuric or nitric acid, running fuel cells or performing hydrogenations are mostly heterogeneous catalytic reactions. Synthesis on a laboratory scale relies on the power of catalytic reactions as well. Cross-coupling reactions enable the formation of carbon-carbon or carbon-heteroatom bonds. There are catalyzed oxidations, reductions, rearrangements, condensations or substitutions to name only a few.^[31–35] The importance of catalysis in general can be highlighted by the fact that since the year 2000, four *Nobel-Prizes* in chemistry have been awarded for the development of catalytic reactions.^[36–39]

This work will focus on the fields of (chiral) titanocene catalyzed epoxide opening reactions and photocatalysis in detail and explain them in the following chapters.

2 General Part

In this part of the thesis, the theoretical background and concepts to understand the research topic of (chiral) titanocenes as photoredox catalysts and titanocene catalyzed epoxide opening reactions will be described and explained.

2.1 Nature as Model for Synthetic Chemistry

Every living species on earth exists because of innumerable chemical reactions taking place inside of them. These organisms have evolved from times with hostile conditions being hot, with very low amounts of oxygen and high UV-radiation and evolved over 3.8 trillion years into the nature we know today.^[18,40] Probably the most commonly known chemical process developed over this period of time, and that human and vegetal life relies on, is the photosynthesis taking place in the chloroplasts of plants, converting carbon dioxide into sugars by transforming sunlight into chemically usable energy. However, photosynthesis does not only generate organic carbon compounds, but also plays an important role in the generation of oxidants, which are often oxidized forms of sulfur, iron, or water. Without these oxidants, the evolution of life would have been impossible.^[18] As mentioned before, enzymes can be understood as biochemical catalysts with a discrete space for one very specific reaction each, and thus, catalysis is also a natural tool for synthesis – and life.

Since the chemical properties of a substance determine the reactions it can undergo, synthetic chemistry cannot simply combine atoms to obtain a desired structure and function. Successful synthesis requires elaborate concepts and feasible reaction pathways. Often complex sequences are therefore necessary to obtain the desired product. Nature had trillions of years to develop and improve those, and therefore, in synthetic chemistry it can often be used as a model to gain new ideas for reactions.

2.1.1 Stereochemistry and Chirality

To understand the importance of the shape of chemical substances, explaining the concepts of stereochemistry and chirality is crucial. Already in 1886, the Italian chemist *A. Piutti* discovered that the two enantiomers of asparagine had a difference in taste, although there is only a tiny difference in their chemical structure (**Figure 2**). The two molecules appear as image and mirror image. He found that L-asparagine was without taste, whereas D-asparagine tasted intensively sweet.^[41] L-asparagine naturally occurs in proteins as one of the proteinogenic amino acids, its enantiomer is much more rare: it was isolated by *Piutti* from vetches in very small amounts. He extracted 100 g of the compound from 6500 kg of plants.^[41]

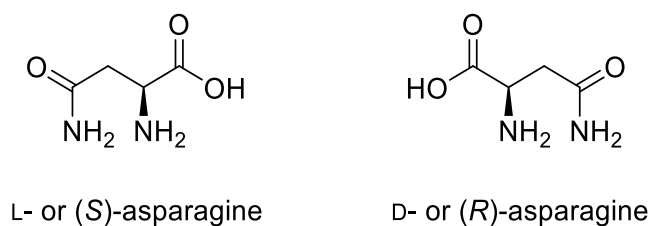


Figure 2: Structures of the two enantiomers of asparagine.

This example shows that the structure of a chemical compound can have a huge influence on its perception by the human taste sense. A second example of stereoisomers having a different influence on a human body is the effect of *Escitalopram*, an antidepressant, belonging to the selective serotonin reuptake inhibitors (SSRI), and *Citalopram*, the mixture of both enantiomers of the compound (**Figure 3**).^[42] As before, the molecules behave like image and mirror image, but the desired effect on the receptors in the human body almost exclusively resides from the (S)-enantiomer, *Escitalopram*.^[42,43]

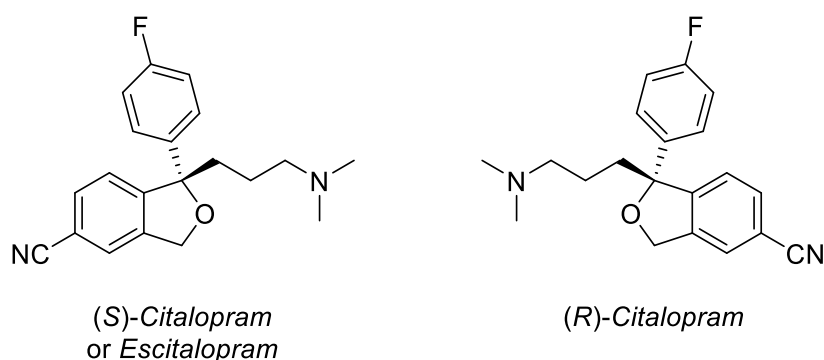


Figure 3: Structures of the two enantiomers of *Citalopram*.

These cases clearly indicate that the absolute geometrical structure of a compound can be distinguished by interaction with the human body, which can differentiate between image and mirror-image of a molecule. A third example is the different smell of the enantiomers of cavone, one smells like mint and the other like caraway.^[44] These findings can be explained by the fact that the human body is chiral itself, which is a prerequisite for distinguishing between enantiomers. This is easily noticeable by the comparison of the two hands, they also appear like image and mirror image and cannot be held in a way that they are identical.

In general, isomerism describes molecules which have the same sum formula, but may differ in their bonding sequence (constitutional isomers) or three-dimensional orientation of the atoms in space (stereoisomers). **Figure 4** displays different forms of isomerism and their respective terms.^[45] Enantiomers are a form of stereoisomers, which behave like image and mirror image. They are not superimposable. In the shown example, the central carbon atom is called the chiral center of the molecule, which bears four different substituents. This phenomenon is called central chirality. There are other forms of chirality which will not be

discussed at this point. A 1:1-mixture consisting of both enantiomers is called a racemic mixture. Enantiomers have the same physical and chemical properties in achiral environments. However, they differ under chiral conditions.^[45]

Stereoisomers that are not defined as enantiomers and are non-identical are called diastereoisomers. This can be the case, if more than one chiral center is present, or, as shown above, a double bond is restricting the molecule's rotation and two different substituents are thereby fixed relative to each other. Conformers, however, can interconvert into each other by rotation around one or more formal single bonds. One conformer of a molecule is often energetically favored, but the energy difference is very small and can be compensated by surrounding conditions (room temperature) so that the isolation of different conformers is not possible.^[45]

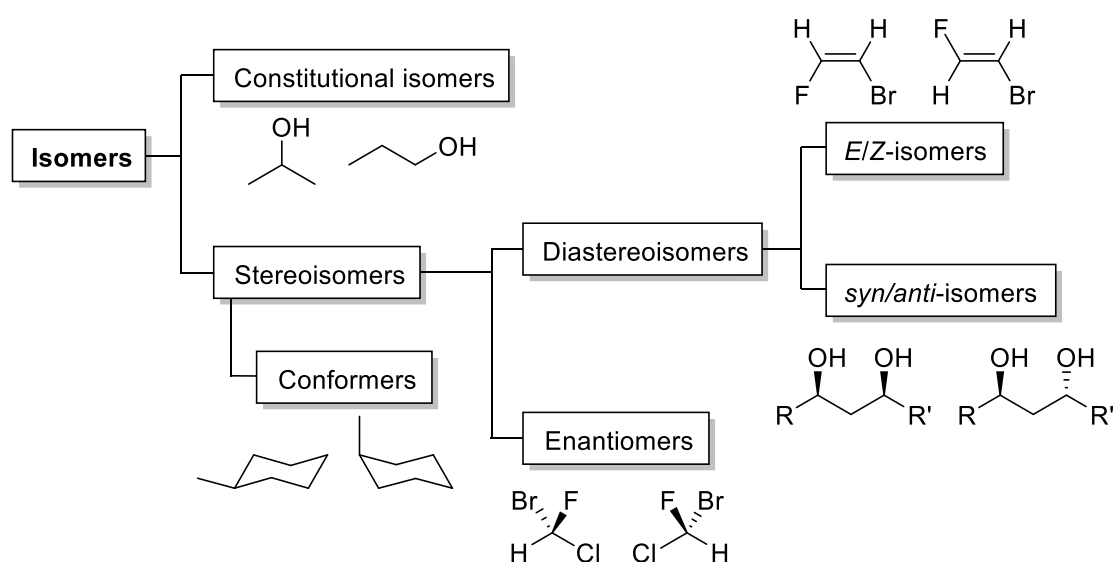
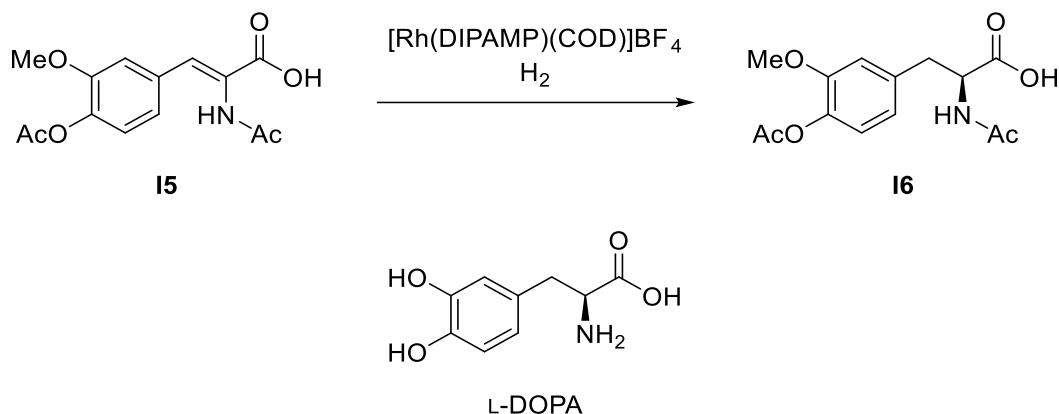


Figure 4: Basic overview of isomerism.

While nature has its enzymes to ensure a chemo-, regio- and stereoselective synthesis^[46,47] by providing a specifically shaped, discrete 'reactor' only made for one single reaction,^[48] in a chemical lab, stereoselective synthesis has to be performed in much more simple reactions with only a few, yet effective reagents and catalysts. However, the possibility to use 'every' element of the periodic table extends the chemical toolbox immensely compared to nature.

2.1.2 Stereoselective Synthesis

Obtaining enantiomerically and diastereoisomerically pure products in chemical synthesis is often realized by employing enantiomerically pure ligands, auxiliaries or catalysts.^[49,50] The pioneers in design and development of efficient ligand-catalyst-systems^[51,52] are *Knowles*,^[53] *Noyori*^[54] and *Sharpless*,^[55] who were awarded with the *Nobel-Prize* for their work and contributions on this field in 2001.^[36] The first industrially applied enantioselective synthesis was used for the generation of pharmaceutical drug L-DOPA (**Scheme 2**).^[23,56] The obtained enantioselectivity in the product of this hydrogenation reaction is based on a chiral ligand: (*R,R*)-DIPAMP (**Figure 5**).^[57] In its synthesis, menthol serves as chirality resolving agent,^[23] which is isolated as chiral-pool substance from natural origin, which means that the chirality has originally been induced by an enzyme, which is chiral itself consisting of single enantiomer amino acids.



Scheme 2: Simplified depiction of the enantioselective hydrogenation in the synthesis of L-DOPA.^[52,56,58]

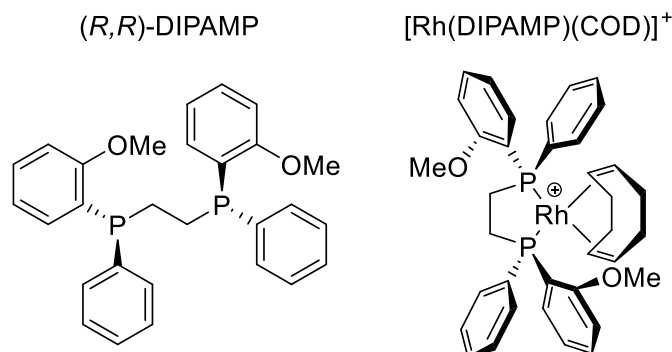
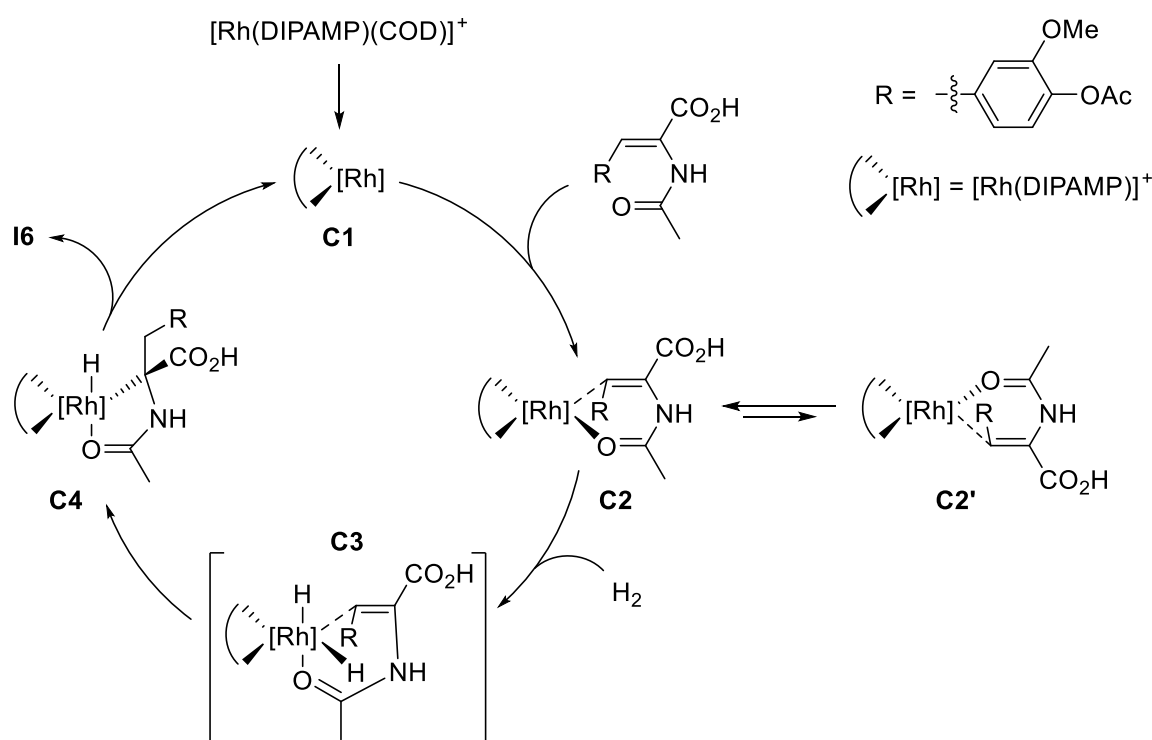


Figure 5: Structure of (*R,R*)-DIPAMP and the (*R,R*)-DIPAMP rhodium(I) COD complex.^[57]

The mechanism (**Scheme 3**) of the asymmetric enantioselective hydrogenation proceeds via the formation of the active catalyst species $[\text{Rh}(\text{DIPAMP})]^+$ **C1** by losing the COD-ligand (compare **Figure 5**). Upon bonding of substrate **I5**, square planar Rh(I)-complex **C2** is formed, in which the diastereoisomers (**C2** and **C2'**) equilibrate rapidly. The rhodium center oxidatively adds to H_2 to yield octahedral complex **C3**. Subsequently one hydride is transferred to the former prochiral carbon atom in a migratory insertion. The alkyl hydride complex **C4** reductively eliminates and the active catalyst as well as **I6**, containing the enantiomerically pure desired chiral center, are released.^[52,56]



Scheme 3: Catalytic cycle of the asymmetric enantioselective hydrogenation DIPAMP employed enantiomerically pure.^[56]

Knowles suggested that the stereochemical control of this reaction originated in the hydrogen addition to form **C3** or the alkyl species **C4**.^[56] This selectivity is possible, as the enantiomerically pure DIPAMP ligand on the rhodium center blocks specific orientations of the binding **I5**, which results in one energetically favored diastereoisomer of the complex. A similar but much more substrate specific behavior can be seen in the binding of molecules in the active site of enzymes.^[59–61] In addition to the perfect enantio- or diastereoselectivity, enzymes are also regio- and chemoselective which goes hand in hand with functional group tolerance. The fact that for example of all the different molecules in a cell, only the ‘correct’ ones are reacted in the enzyme unveils a high level of complexity and substrate selection, which is unmatched in any artificial synthesis. However, this greatly limits the ‘applicability’ of enzymes, as they are often only designed for one reaction of one specific substrate.

2.1.3 Photosynthesis and Photochemistry

The process of photosynthesis in the chloroplasts of plants is probably the most important photochemical reaction for life on Earth. It involves numerous enzymes and highly specialized cell structures. The commonly known reaction products of this process are glucose and oxygen made from water and carbon dioxide (**Scheme 4**).^[62]



Scheme 4: Net equation of the photosynthesis.^[62]

For this reaction to occur, capturing sunlight as radiation energy and transforming it into an electrical potential is necessary. This happens at the photosystem II, where an enzyme called P680, the chlorophyll *a* (**Figure 6**) dimer in the photosystem's center, absorbs red visible light with a maximum of 680 nm at its Mg^{2+} -ion centers.^[62,63] The excited P680^* then transfers an electron to pheophytin and therefore gets oxidized to a radical cation $\text{P680}^{+\bullet}$, which is reduced by tyrosine. The resulting tyrosine radical is reduced by water.^[62,64] In summary, the P680 enzyme is able to convert photons of a specific wavelength and therefore energy into chemical energy. Without the absorption of light, the reaction does not occur. This is the key concept of photochemistry, a field that has grown immensely in the past years.^[65–69]

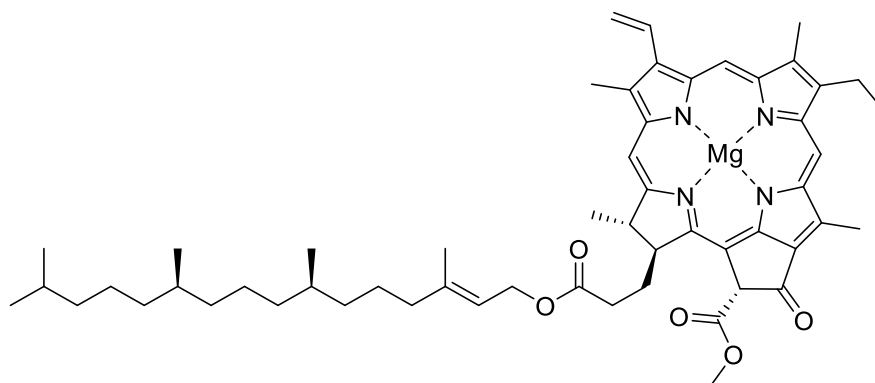


Figure 6: Structure of chlorophyll *a*.^[70]

As depicted in **Figure 6**, chlorophyll *a* contains a porphyrin ring which chelates a magnesium cation. In synthetic chemistry, photochemical reactions often use special photoredox catalysts (PRCats). Various photoredox catalysts have been developed that resemble this motif of a metal-centered complex.^[71] Especially transition metals are widely used and by derivatization of the respective ligands, their photoredox properties can be modified.^[72] A selection of metal-centered photoredox catalysts is depicted in **Figure 7**. They contain rare and expensive transition metals and therefore do not match the desired criteria for Green Chemistry. A detailed discourse of photoredox catalysts can be found in chapter 2.4.

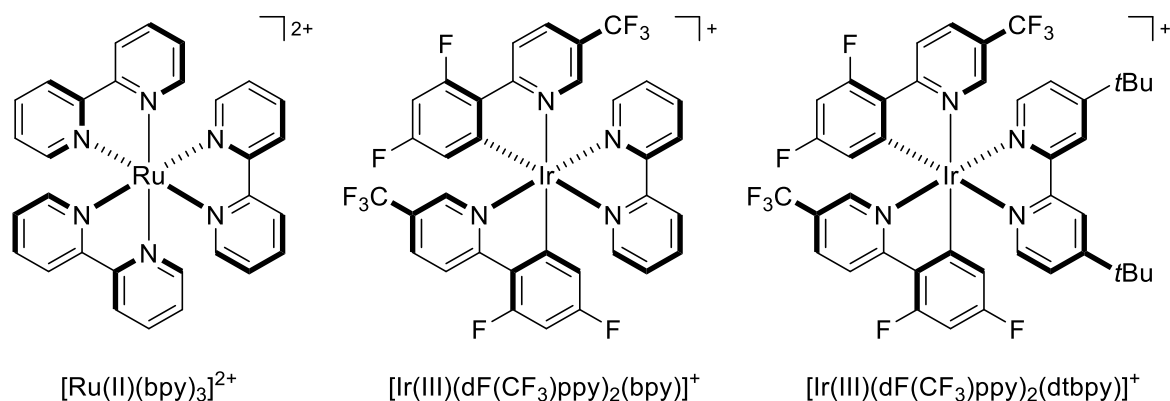
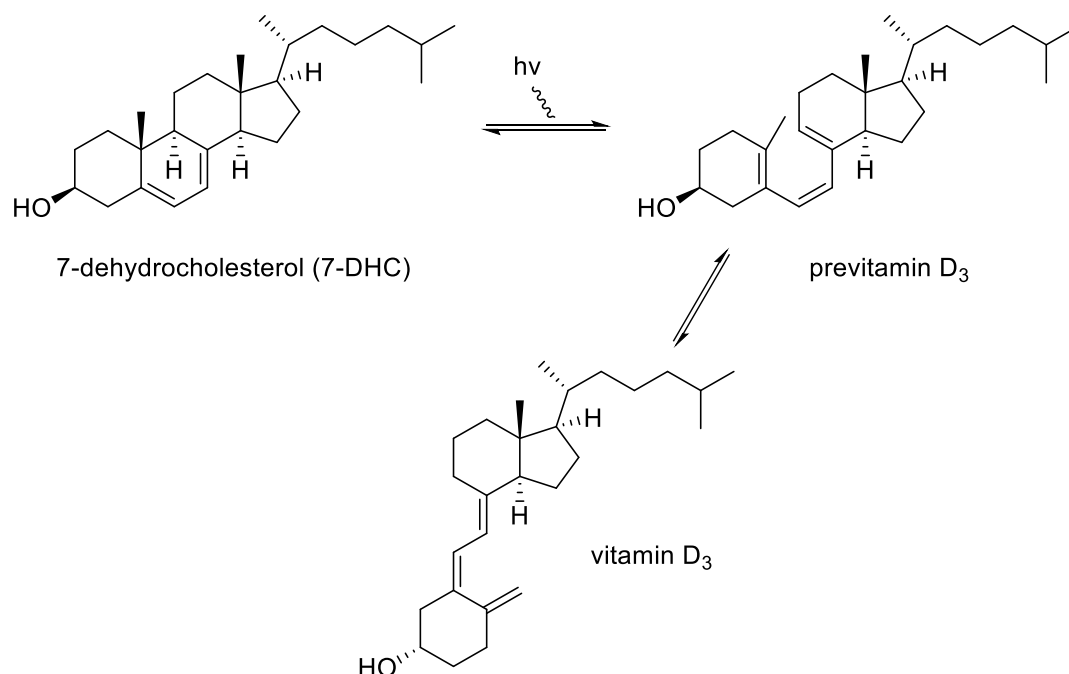


Figure 7: Ru(II) and Ir(III) photoredox catalysts.^[66,69,73]

Photochemistry is however not limited to the use of photoredox catalysts. Two other examples are isomerization reactions and radical (de)cyclizations.^[74–79] For instance, the synthesis of vitamin D₃ in human skin by irradiation of precursors with UV-B light (280–315 nm)^[80] combines a thermally forbidden six-electron electrocyclic conrotatory decyclization with a subsequent isomerization reaction (**Scheme 5**). The isomerization in this case is not photochemically induced but occurs due to the thermodynamically unfavored structure of previtamin D₃. For simplicity, only the conversion of 7-DHC (7-dehydrocholesterol) is shown, other precursors are lumisterol₃ and tachysterol₃.^[78]



Scheme 5: Synthesis of vitamin D₃.^[78,79]

2.2 Stereoselective Catalysis

Making chiral centers in a stereoselective manner is a tremendous challenge in organic synthesis. One possibility is the deracemization reaction or kinetic resolution, meaning that a racemic mixture of a chiral compound is converted in a way that one enantiomer reacts faster than the other.^[81] This reaction type can be further specified as *kinetic* or *dynamic kinetic* resolution.^[58,82,83] In a kinetic resolution, a maximum of 50% yield can be obtained, as only one enantiomer reacts either to give the product or to be converted to enable separation (compare to chapter 5.6.1). In a dynamic kinetic resolution one enantiomer reacts faster as well, but the slowly reacting enantiomer racemizes and can therefore reenter the kinetic resolution reaction. By this method, the yield is potentially 100%.^[83]

Without going into detail, other obvious possibilities for stereoselective synthesis are the formation of the chiral center during the reaction via the addition to a prochiral site of the substrate or the conversion of or close to an already existing chiral center. The synthesis of L-DOPA presented in **Scheme 2** is one example of a prochiral olefin reacting with an enantiomerically pure catalyst to form a stereodefined chiral center in a high enantiomeric ratio (*e.r.*).

As the majority of this thesis will focus on epoxide opening reactions, the important concepts for understanding stereoselective catalysis will be explained using this reaction type. The detailed mechanisms will be explained later. For epoxide openings, enantio- and diastereoselectivity are the two possible stereoselectivity distinctions. The enantiomerically pure catalyst used in the reactions is a titanocene dichloride derivative with either D- or L-menthol derived substituents, known as *Kagan's complex*.^[84,85] It will be referred to as D- or L-Kagan (-Cl₂ omitted for clarity) and its structure is depicted in **Figure 8**.

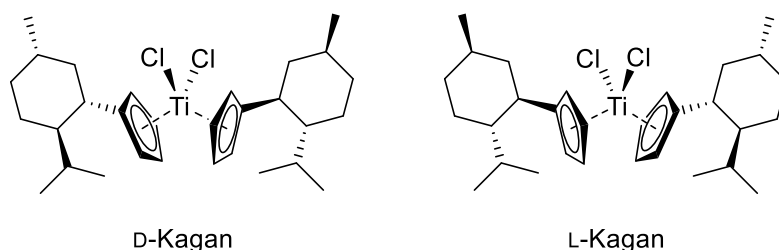
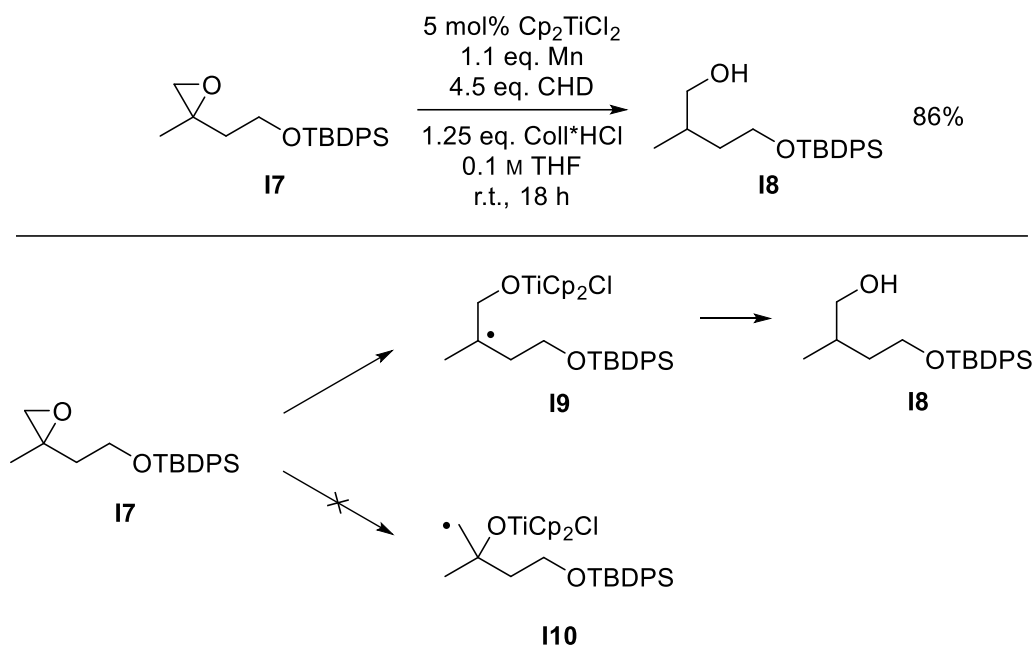


Figure 8: Structures of D- and L-Kagan complex.^[84]

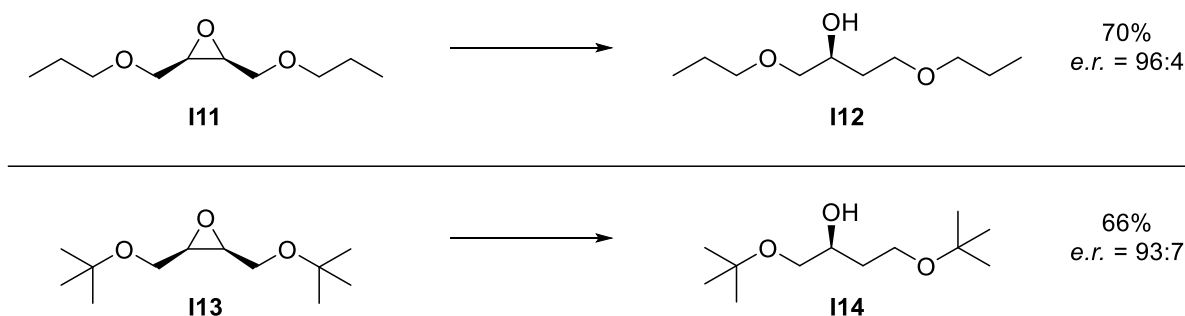
Due to their structure, a large number of epoxides possess two chiral centers. Exceptions are, if the two substituents at each of the epoxide's carbon atoms or all four are identical. Because of that, these epoxides are either chiral or *meso*-compounds (containing a mirror plane). In epoxide opening reactions the regioselectivity of the reaction also has to be considered. It can either be substrate- or catalyst-controlled, as well as a combination of both (matched/mismatched substrate- and catalyst-regioselectivity).

An early example of substrate-controlled regioselectivity with achiral titanocene dichloride as catalyst is shown in **Scheme 6** (the mechanistic details of titanocene catalyzed epoxide opening reactions are explained in chapter 2.3). In this case, a 1,1-disubstituted epoxide **17** is opened in a single-electron transfer reaction (SET). In this way, two possible regioisomers **19** and **110** can be formed and due to the higher stability of the tertiary radical in **19**, this pathway is observed exclusively. A primary radical is not formed. Product **18** is obtained as racemic mixture.



Scheme 6: Regioselective epoxide opening using titanocene dichloride as achiral catalyst.^[86]

If the epoxide is however 1,2-disubstituted the radical formed in an opening reaction is in both cases a secondary radical. Consequently, substrate control of the regioselectivity cannot longer be expected. For *meso*-epoxides, a reaction with an enantiomerically pure titanocene catalyst, a desymmetrization is observed, yielding an enantiomerically enriched product.^[87,88]



Scheme 7: Titanocene catalyzed enantioselective opening of *meso*-epoxides. Conditions: 10 mol% L-Kagan, 2.5 eq. Coll*HCl, 1.0 eq. epoxide, 1.0 eq. CHD, 2.0 eq. Zn, 0.1 M in THF, rt, 22 h.^[88]

Two examples are given in **Scheme 7**, in which *meso*-epoxides are opened by chiral L-Kagan as catalyst. In contrast to the kinetic resolution of a racemic mixture described earlier, in this case the catalyst distinguishes between two enantiotopic C–O bonds (at the epoxide), rather than two enantiomers. Enantiotopic groups or bonds in a molecule are mirror images of each other across an internal symmetry plane. When one of them is substituted they form enantiomers and the symmetry plane is lost.^[89]

2.2.1 Regiodivergence

If an enantiomerically pure catalyst is employed with a non-symmetric substrate in which two different positions of similar reactivity can be differentiated,^[90] the reaction can be called regiodivergent. In the past years, *Gansäuer et al.* developed several methods for regiodivergent epoxide opening reactions, as well as regiodivergent carbopalladations.^[91–97] To understand the reason how the enantiomerically pure catalyst can distinguish the two ‘sides’ of an epoxide in regiodivergent reactions (and in desymmetrisations of *meso*-epoxides), the interaction of catalyst and substrate **I11** prior to the opening is depicted in **Figure 9**.^[94,98–100]

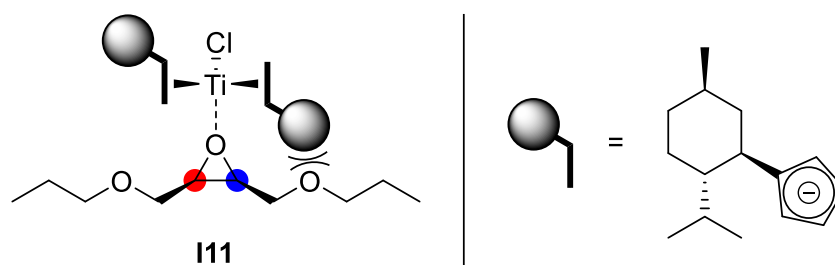
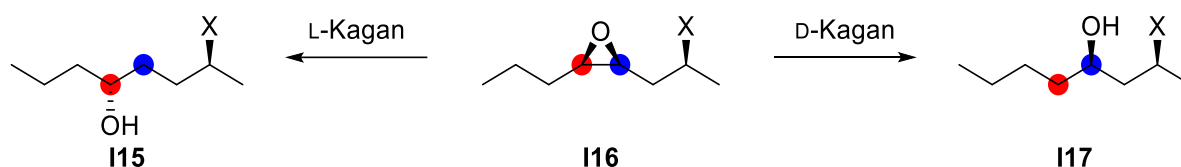


Figure 9: Interaction of reduced L-Kagan catalyst and substrate **I11** prior to the epoxide opening.^[94]

The selectivity of the catalyst is controlled by its absolute configuration. Upon binding to the epoxide as *Lewis* acid, the adduct with **I11** becomes chiral. As a consequence of steric repulsion with one chain of the substrate, one of the enantiotopic carbon-oxygen bonds (blue side) is weakened. This is why this bond is favorably cleaved in the following opening reaction.^[94] The structure of the catalyst-substrate-adduct has been supported for an ethoxy-substituted *meso*-epoxide by DFT calculations.^[100]

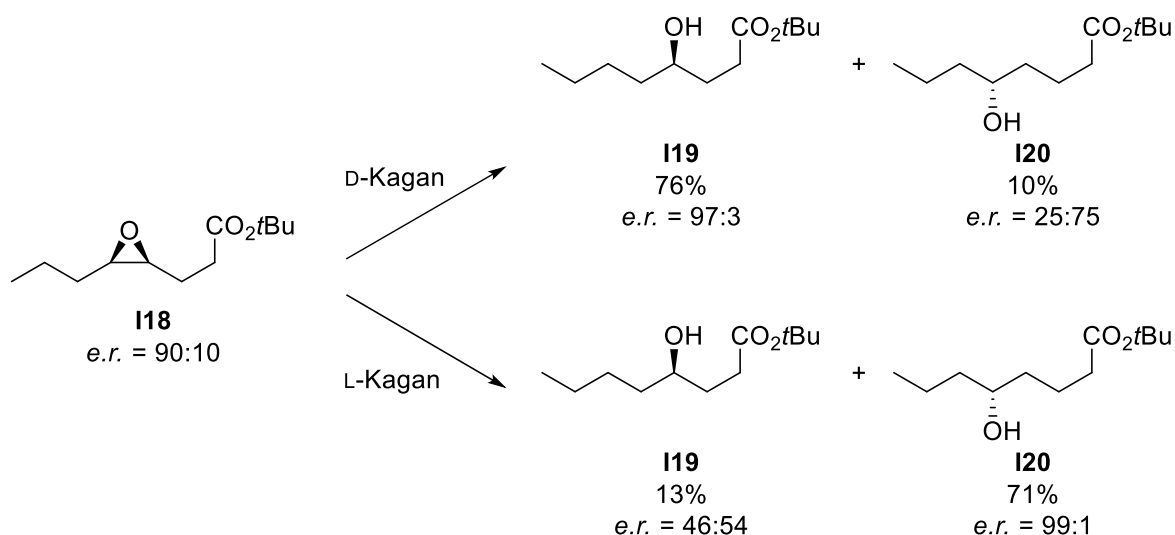
If the same concept is applied to a chiral, enantiomerically pure substrate, the reaction is regiodivergent, as constitutional isomers result as products depending on the enantiomer of the catalyst used. **Scheme 8** shows the ideal case, in which an enantiomerically pure substrate **I16** is converted into two different products. In this example, the L-Kagan opens the blue carbon-oxygen-bond to form product **I15**, whereas the D-Kagan yields **I17**, a constitutional isomer of **I15**.^[93]



Scheme 8: Regiodivergent epoxide opening (REO) by application of different catalyst enantiomers.

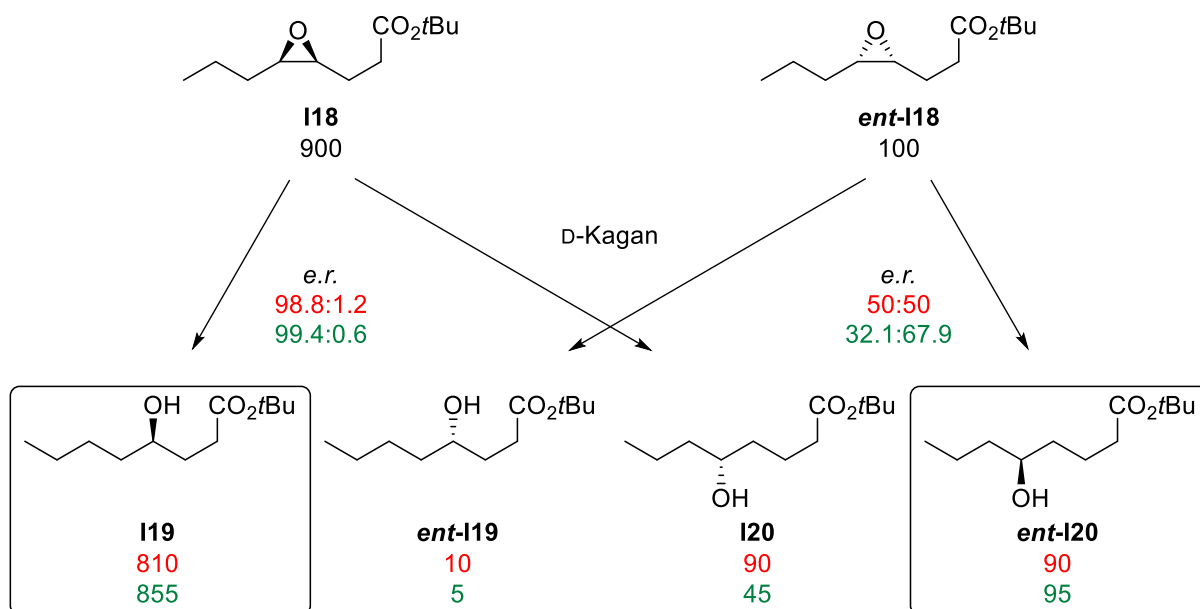
This theoretical description of regiodivergency could be verified by *Gansäuer* in practice for regiodivergent epoxide openings (REO).^[95,96,101] The investigated reaction of an enantiomerically enriched substrate (**I18**) in a REO is given in **Scheme 9**. In contrast to the ideal case above, the substrate is not enantiomerically pure, but possesses an *e.r.* of 90:10. Because of this, the regioisomeric byproduct is also obtained in a small amount. The reaction is however mainly catalyst-controlled.^[101]

What is really interesting is the development of the *e.r.* in the products. In the upper case, the *e.r.* = 90:10 of **I18** improves greatly to *e.r.* = 97:3 for the main product **I19**, whereas it decreases to *e.r.* = 25:75 for byproduct **I20**. In the lower case, the opposite product is mainly formed as to be expected, though the enantiomeric ratios of **I19** and **I20** differ even more. This deviation of the *e.r.* values can be explained by minor influence of the substrate on the catalyst's selectivity.^[95] The regioselectivity of the REO matches the established model of diastereomeric *Lewis* acid-base complexes formed with the different enantiomers of **I18** (compare to **Figure 9**).^[94,99,100]

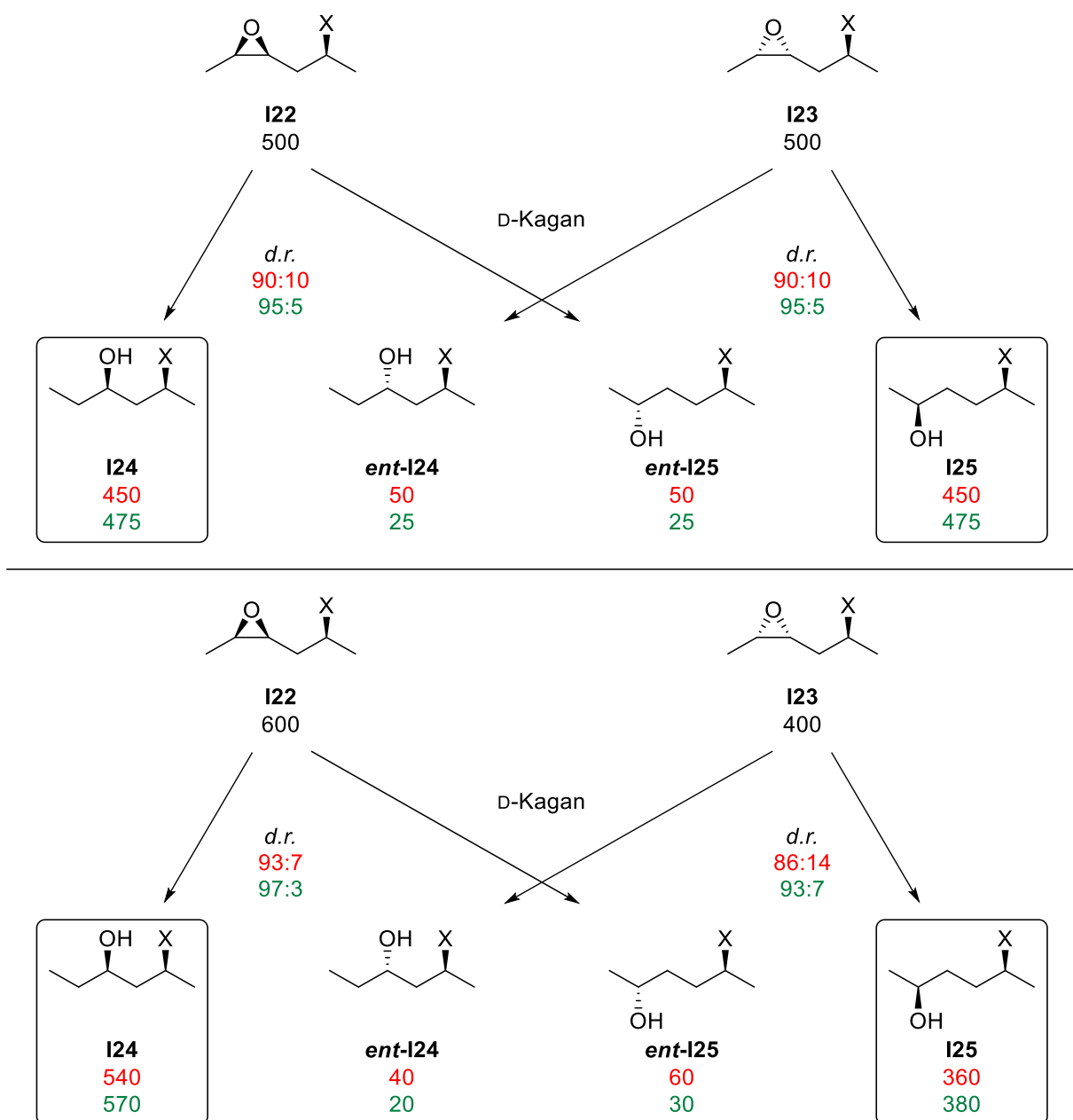


Scheme 9: Regiodivergent epoxide opening of an enantiomerically enriched substrate. Conditions: 10 mol% D- or L-Kagan, 1.0 eq. epoxide, 1.5 eq. Coll*HCl, 1.5 eq. Mn, 4.4 eq. CHD, 0.3 M in THF, rt, 16 h.^[95,96]

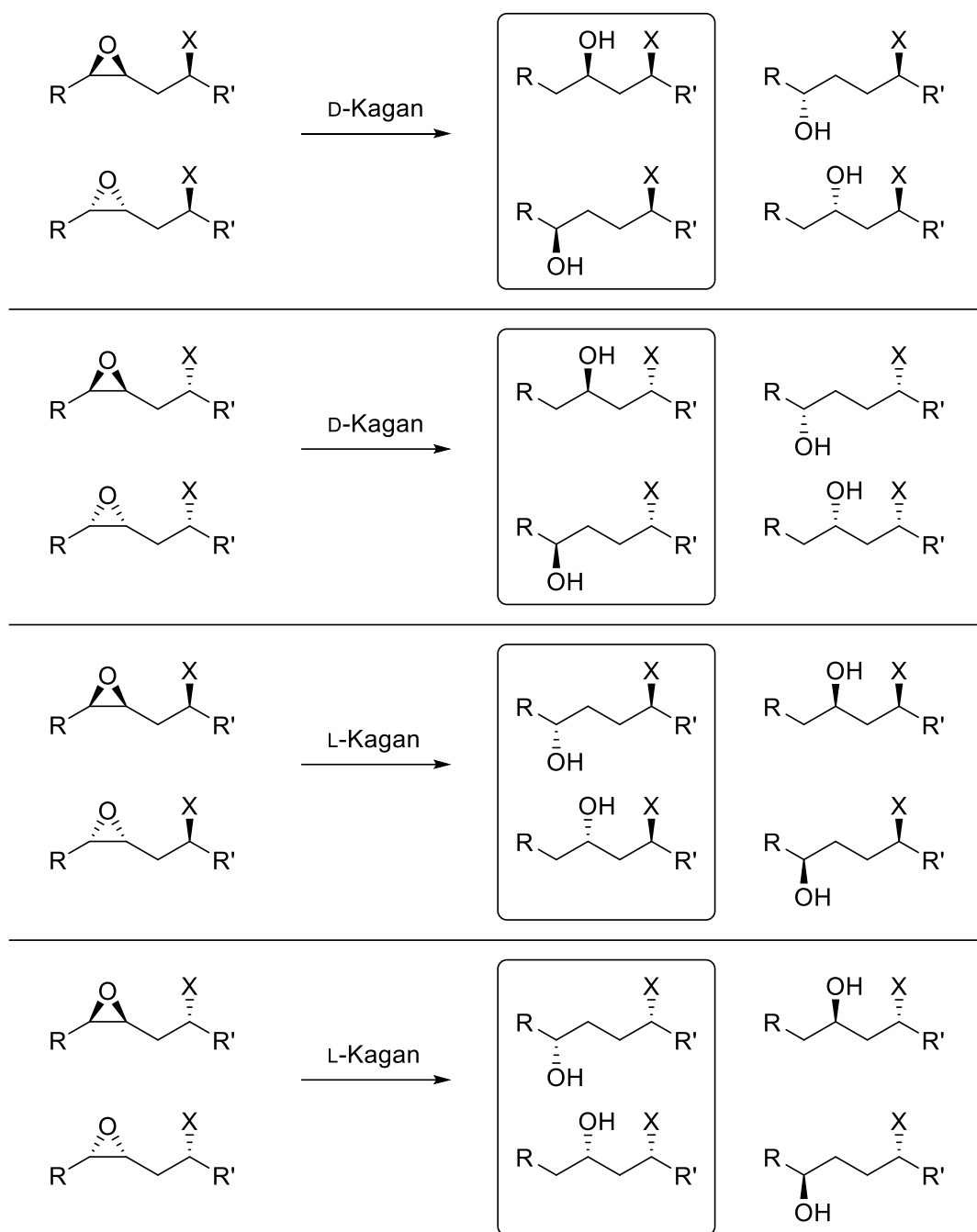
To elucidate the enantiomeric enrichment of the main products, a thought experiment assuming 1000 molecules and a catalyst selectivity of 90% (red) and 95% (green) and the substrate *e.r.* = 900:100 of **I18** is shown in **Scheme 10**. The resulting *e.r.* is calculated from the corresponding product ratio. Substrate influences are neglected.



Scheme 10: Calculation of enantiomeric ratios in a REO with D-Kagan and a catalyst selectivity of 90% (red) and 95% (green) exclusively under catalyst-control.



Scheme 11: Calculation of diastereoisomeric ratios in a DEO with D-Kagan and a catalyst selectivity of 90% (red) and 95% (green) exclusively under catalyst-control.



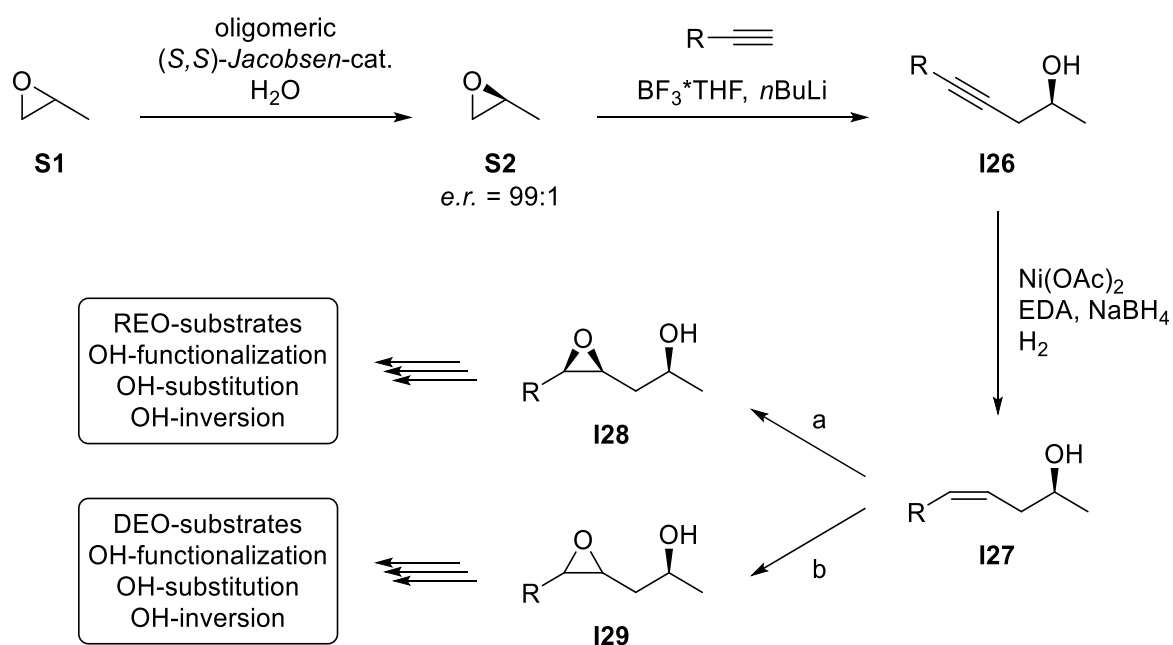
Scheme 12: Overview of possible DEO reaction products. Main products encircled.

In contrast to the REO reactions, in a DEO two regioisomers of the products can be obtained in a single reaction, as technically a DEO can be classified as parallel resolution of a *pseudo*-racemic mixture of two diastereomers. Due to the product's difference in polarity, they can be separated by column chromatography. Although the *d.r.* of the minor reaction product is slightly decreased compared to the major product, it is still diastereomerically enriched. **Scheme 12** shows all possible DEO reaction products and unequivocally the potential power of DEO reactions in preparing molecular libraries containing all possible diastereomers and enantiomers of these 1,3- and 1,4-diol-derived structures.

2.2.3 Diversity-Oriented Synthesis

Both REO and DEO approaches for the synthesis of substituted, stereodefined alcohols are especially appealing for natural product synthesis and drug development. The majority of pharmaceutical agents consist of so called *small molecules*,^[104] which are often derived from natural compounds or extracts.^[105] In drug development, one approach is to search for molecules that have a specific influence on a target inside the body. This is mainly done by copying privileged structures from natural sources in a so called target-oriented synthesis (TOS).^[105–108]

In contrast, REO and DEO reactions fit the second big strategy for finding biologically active substances: diversity-oriented synthesis (DOS). By accessing molecular libraries through synthesis of many chemically and physically diverse molecules from common precursors without a specific target structure, the probability of finding lead structures for biologically active compounds is vastly increased.^[109] By splitting reaction pathways of mutual precursors, diversity is generated without prior long synthetic sequences for each molecule.^[108] As already shown in **Scheme 12**, all possible diastereoisomers and enantiomers of the four starting substances can be made in four reactions. Additionally, **Scheme 13** depicts the synthesis of these starting substrates, which is also derived from common molecules and only requires three steps up to the branching point for REO and DEO substrates. Because of this simple synthetic approach, REO and DEO provide an appealing approach to synthesize molecular libraries in a DOS manner.



Scheme 13: General synthesis of REO and DEO substrates from simple common precursors.

a) $\text{VO}(\text{acac})_2$, TBHP; b) *m*CPBA.^[103,110]

2.2.4 Diols in Biologically Active Natural Compounds

1,3- and 1,4-diols are prominent motifs in natural products and pharmaceutical drugs.^[111–115] **Figure 11** contains a selection of molecules containing 1,3-diols highlighted in blue and 1,4-diols in red (not all highlighted). Especially interesting and ‘alcohol rich’ is the fused ring structure of paclitaxel, not only as it is sold as chemotherapy medication in cancer treatment (*Taxol*®),^[116] but also due to its multiple stereodefined diol-structures in close proximity. Chivosazol A is an antibiotic substance,^[117] picrotoxinin is a highly potent neurotoxin^[118] and esters of phorbol act as tumor promoters.^[119]

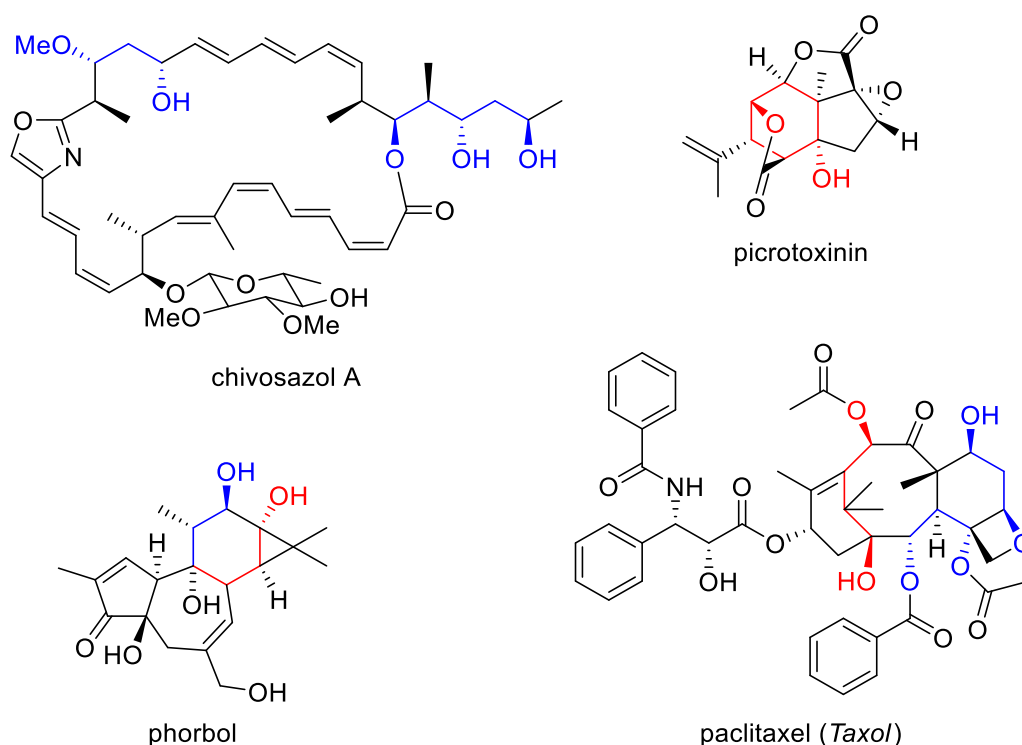
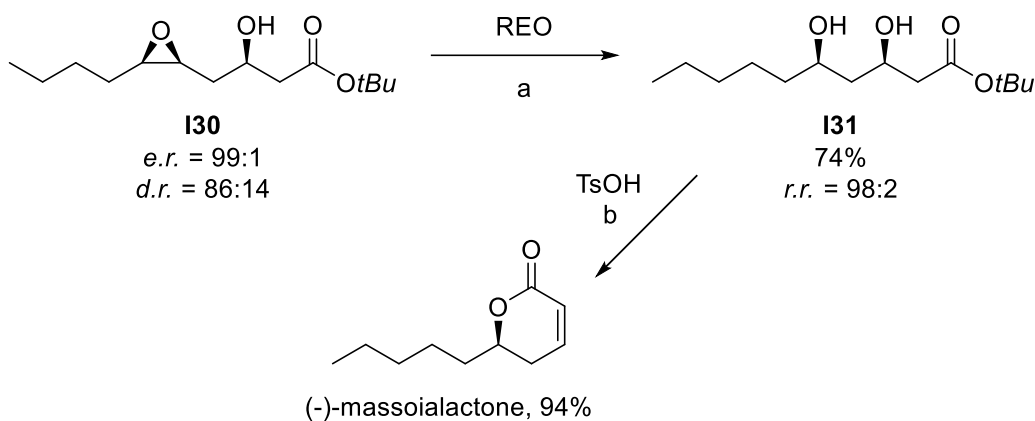


Figure 11: 1,3- and 1,4-diol-motif in natural products and pharmaceutical drugs.^[112,113]

Discrete 1,3-diol-structures in open chains as found in chivosazol A could readily be synthesized by REO or DEO methods, which provide an easy and reliable synthetic approach to diols and are therefore a powerful tool for any synthetic organic chemist. Particularly the regiodivergent epoxide opening reactions enable synthesizing these valuable structural motifs in good yields and facilitate excellent control over enantio- and diastereoselectivity. An example of a successful application of a REO for the synthesis of a small biologically active compound is shown in **Scheme 14**. The antifungal^[120] (-)-massoialactone was synthesized by *Gansäuer* in a REO and subsequent lactonization in excellent yields and regioisomeric ratio, emphasizing the potential of this type of reaction.^[93,110]



Scheme 14: Synthesis of (-)-massoialactone via REO. Conditions: a) 1.0 eq. epoxide **I30**, 1.5 eq., Lut⁺HCl, 1.5 eq. Mn, 7 mol% D-Kagan, 2.2 eq. Bu₃SnH, 0.17 M in THF, rt, 72 h; b) 1.0 eq. 1,3-diol **I31**, 0.5 eq. TsOH, 0.05 M in benzene, reflux, 7 h.^[93,110]

2.3 Titanocenes in Epoxide Opening Reactions

Titanocenes consist of two cyclopentadienyl ligands in a sandwich-complex with a titanium center. In contrast, titanocene dihalides such as Cp₂TiCl₂ have a tetrahedral structure with the Cp-ligands and the halide ligands around the titanium atom. In this work, exclusively titanocene dihalides are discussed and used. The term titanocene always refers to these.

Titanium is an earth-abundant 1st row transition metal, present in almost every rock on the planet.^[121] It is also one of the most common elements found in the earth's crust, ranking number 9 in total and number 2 in the list of transition metals with 5.7 g/kg, only iron is found more often.^[121] Therefore, the use of titanium-based reagents in organic synthesis matches the criteria of Green Chemistry (chapter 1.2) very well, as they can be considered to be readily available not toxic. Titanium is cheap and safe enough that its main use (as TiO₂) is as white pigment in paint.^[26,121–124]

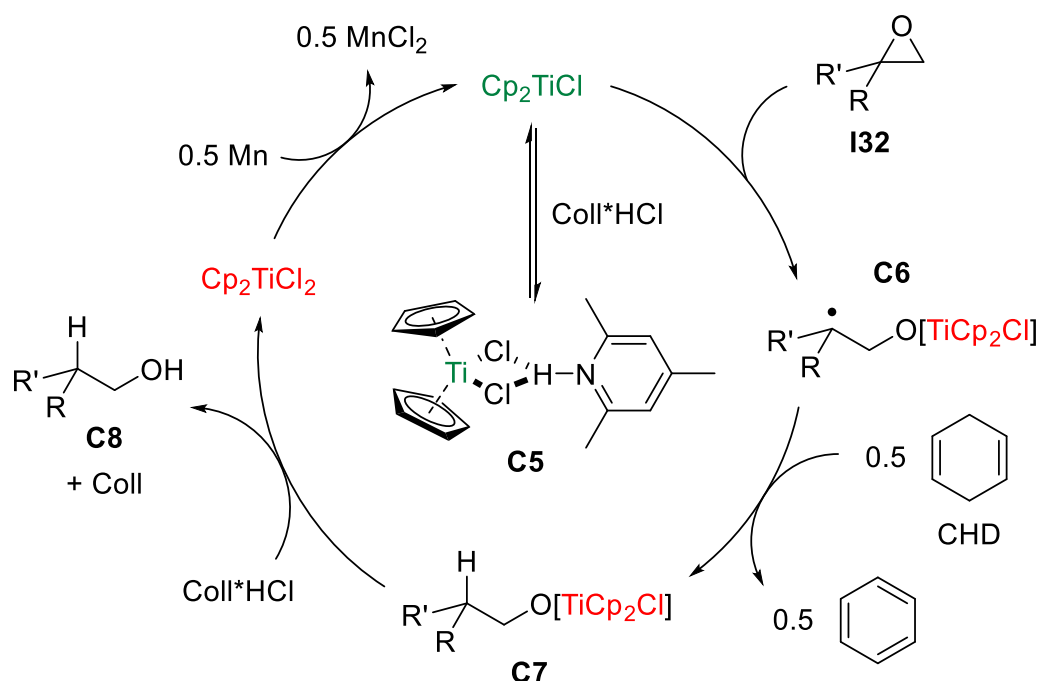
Titanocenes can easily undergo single-electron oxidations and reductions (Ti(III)/Ti(IV)) and are hence very well suited compounds for single-electron transfer catalysis or metalloradical chemistry.^[125]

In previous chapters many examples of titanocene catalyzed epoxide opening reactions have been shown. However, the mechanistic details of these have not been elucidated so far. In 1988 *W. Nugent* and *T. RajanBabu* discovered that epoxides can be opened in a single-electron-transfer (SET) reaction by stoichiometric amounts of Cp₂Ti(III)Cl leading to the formation of β-titanoxy radicals.^[126,127] One carbon-oxygen bond is thereby homolytically cleaved, releasing the epoxide's high ring strain of 27 kcal·mol⁻¹.^[128] In the following years, *Gansäuer et al.* improved this reaction by developing a *catalytic* method with either reduction of the β-titanoxy radical formed or alternatively further functionalization.^[86] Until today, the

system has been improved even further and various methods for catalyst activation compared to the original *in situ* reduction by manganese or zinc powder^[86,129] have been found.

Upon *in situ* reduction by a photocatalyst,^[130] electrochemically,^[131] with chromium-hydride complexes,^[132–134] or as recently discovered by irradiation with visible light and subsequent quenching with a tertiary amine,^[135,136] the bench-stable precatalyst titanocene dichloride (Cp_2TiCl_2) is transformed into its catalytically active species. The corresponding catalytic cycle is depicted in **Scheme 15**, with titanocene(IV) dichloride activation by reduction with manganese.^[137,138]

The catalytically active $\text{Cp}_2\text{Ti(III)Cl}$ species (Ti(III) depicted in green, Ti(IV) in red) is formed upon single-electron reduction with manganese powder from the air-stable precatalyst $\text{Cp}_2\text{Ti(IV)Cl}_2$. It undergoes an equilibrium with Coll^*HCl , forming a catalyst resting state (**C5**). Therefore, only a small amount of free active catalyst species is present in the reaction mixture. This sounds paradoxical at first, but the stabilization of active catalyst in a resting state prevents catalyst decomposition or undesired side reactions.^[139,140]



Scheme 15: General catalytic cycle of the titanocene catalyzed epoxide opening with *in situ* catalyst activation by reduction with manganese powder. Depiction of the resting state **C5** by complex formation with Coll^*HCl .^[92,137,138]

For some reactions, manganese has been unveiled to be superior to zinc, as ZnCl_2 can itself slowly open epoxides via a *Meinwald* rearrangement due to its more *Lewis* acidic character compared to MnCl_2 .^[141–143] Epoxide **132** is then opened via a one-electron oxidative addition to $\text{Cp}_2\text{Ti(III)Cl}$ via homolytic cleavage of the carbon-oxygen-bond of the higher substituted carbon

atom, exclusively forming the tertiary β -titanoxy radical **C6**. The driving force of this reaction step is the release of the epoxide's ring strain as well as the formation of the stable titanium-oxygen-bond.^[144] The radical is reduced by a hydrogen atom transfer (HAT) from CHD or a similar hydrogen atom donor (HAD) to form **C7**. Instead of the direct reduction, a radical translocation to unsaturated compounds such as olefins^[145] or aromatic systems^[139] with a carbon-carbon-bond formation is also possible and will be discussed in later parts of this work. The catalytic cycle is closed with the regeneration of precatalyst Cp_2TiCl_2 and alcohol **C8**. The cleavage of the titanium-oxygen-bond is mediated by the protonation of the oxygen by Coll^*HCl and chloride-donation to the titanium center.

The properties of the employed titanocene catalyst in epoxide opening reactions can be modified by various approaches. To ensure a successful reaction, the ideal catalyst has to be evaluated first in thorough screening and test reactions. Upon exchanging the anion of the catalyst, properties like redox-potential, geometrical structure or influence on regioselectivity in regiodivergent radical arylations can be modified.^[144,146–149]

The catalyst's reactivity can additionally be tuned by application of halide-ion-acceptors that activate the titanium-halide-bond for dissociation.^[131,150,151] Prominent structures for these acceptors are sulfonamides (**Z1**), ureas (**Z2**), or squaramides (**Z3**). A selection of these is depicted in **Figure 12**. They form hydrogen-bonds to the catalyst's anions and thereby activate the bonds for cleavage.^[150] Their binding abilities can be increased by substitution with electron withdrawing groups, such as trifluoromethyl, as shown below. In addition, using the sulfur-analogues of urea and squaric acid enhances the binding ability even further. Moreover, sulfonamides like **Z1** are able to stabilize the active titanocene species (chapter 3.6.3).^[150]

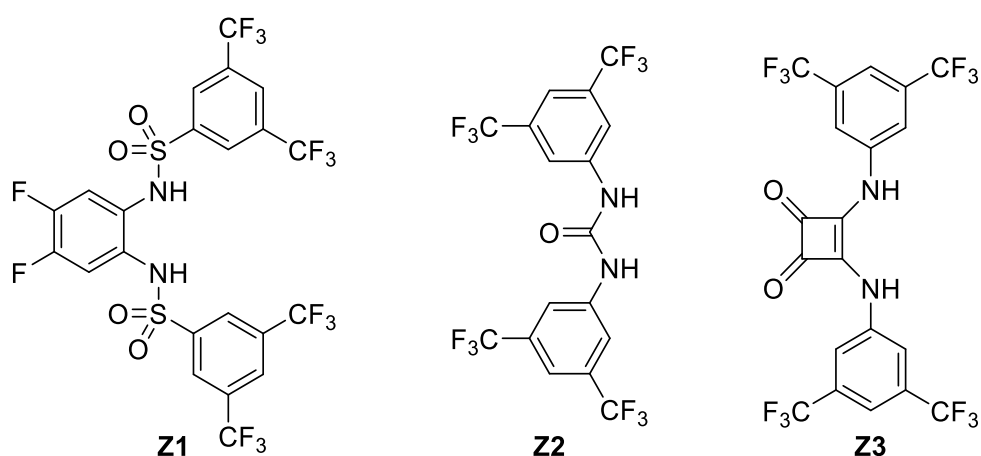
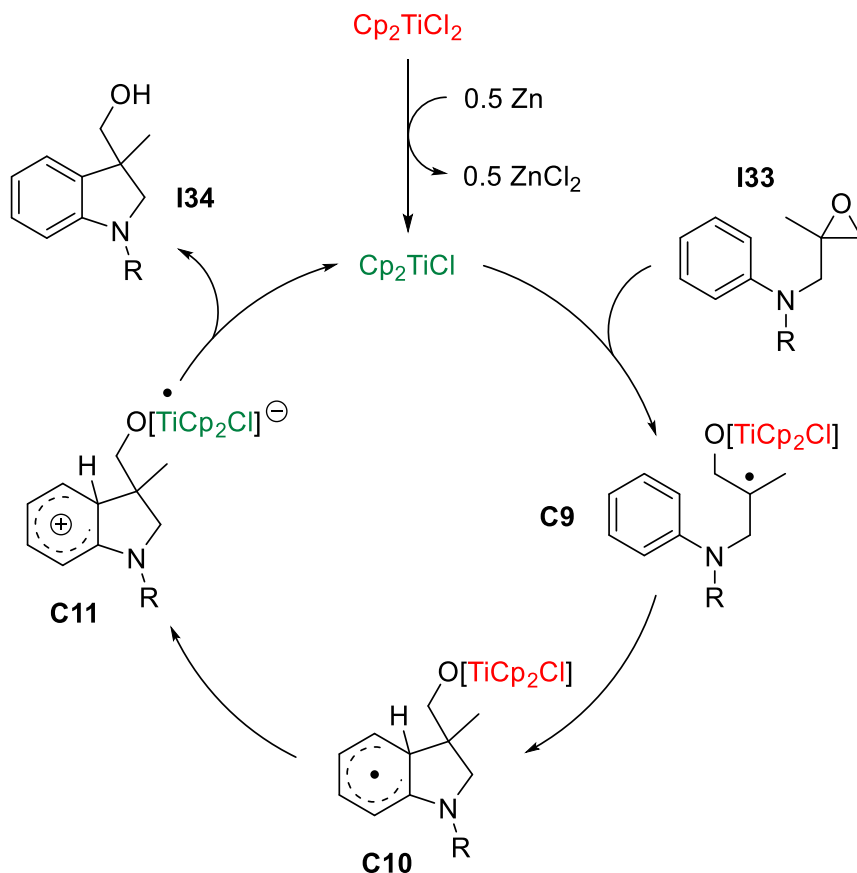


Figure 12: Prominent structures of halide-ion-acceptors.^[131,136,150,151]

The third modification for tuning the titanocene catalyst's reactivity and redox-potential is a substitution on the Cp-ligands of the titanium. More electron-rich titanocenes facilitate the oxidative addition to the epoxides but are harder to reductively eliminate and vice versa for electron deficient complexes.^[144,152,153]

In addition to the epoxide opening displayed in **Scheme 15**, in which CHD was used as hydrogen atom donor, atom-economic radical arylations developed by *Gansäuer et al.* in 2012 proceed via a different mechanism.^[139] The catalytic cycle is shown in **Scheme 16**.

In this case, only catalytic amounts of metal reductant (here zinc) are necessary to reduce titanocene dichloride to yield the catalytically active species. An aryl-substituted epoxide **I33** is opened in a single-electron oxidative addition to form tertiary β -titanoxy radical **C9**. The radical is subsequently added to the arene forming a radical σ -complex **C10**, which transfers an electron to the titanium(IV) center, giving cationic σ -complex **C11**. This electron transfer is coupled with a proton transfer (PCET) in a formal single-electron reductive elimination, cleaving the titanium-oxygen-bond upon release of product **I34** and catalytically active $\text{Cp}_2\text{Ti(III)Cl}$.^[139] Regarding substrate **I33** and product **I34**, the reaction proceeds with perfect atom-economy. A regiodivergent variant of this reaction employing *Kagan's* complex as catalyst will be discussed in chapter 3.4.



Scheme 16: General catalytic cycle of the titanocene catalyzed radical arylation.^[139]

In addition to the given examples of epoxide opening reactions, *Gansäuer et al.* developed titanocene catalyzed pinacol-couplings,^[129,154] hydrosilylations,^[155–157] deuteriosilylations,^[158] and acetalizations.^[159] This shows that titanocenes are in fact a broadly applicable class of catalysts for many types of single-electron transfer reactions.^[160] Especially the photochemical properties of titanocenes are of high interest, as they enable the renunciation of toxic reagents that were necessary under previous reaction conditions. Aspects of this 'greener' approach to titanocene catalyzed epoxide opening reactions are given in the *Special Part* (chapter 3) of this thesis.

2.4 Photoredox Catalysis

As discussed in chapter 1.2.1, using renewable energy sources is an important part of fulfilling the requirements of Green Chemistry. This is not only true for electricity generation, but light energy can also be employed directly as 'reagent' in chemical reactions. For this, numerous photoredox catalysts (PRCats) have been developed, matching the requirements of various reaction conditions in organic synthesis.^[72,161] Visible light photoredox catalysts exploit the energy of visible light, which is in a region of 380–750 nm.^[162] Mainly used and well investigated 2nd and 3rd row transition metal complexes are established as PRCats (compare **Figure 7**). However, there are many purely organic PRCats known today.^[163–167] In addition, 1st row transition metals recently became more popular as PRCats, especially appealing due to their lower price and higher abundance.^[72,135,168–170]

Photoredox catalysis (PRC) finds broad application in organic synthesis nowadays, especially in reductions,^[171,172] oxidations,^[173–176] or dehalogenations,^[68,177–179] as these reactions are based on redox processes and hence (single-) electron transfer. Additionally, the substrate of a reaction can participate in both oxidative and reductive process with the overall reaction being redox neutral. Here photoredox catalysis can enable reaction pathways not possible under other conditions. Well known examples are *Diels-Alder* reactions,^[180] (thermally forbidden) [2+2]-cycloadditions,^[181–183] or decarboxylations.^[184–188]

The basic mechanism of a transition metal PRCat can be understood by illustrating the molecular orbitals of the complex. For this, a simplified molecular orbital scheme of [Ir(III)(ppy)₃] (tris(2-phenylpyridine)iridium(III)) is depicted in **Figure 13**.^[71]

Upon irradiation with 375 nm light (the absorption maximum of the complex), one electron is excited from the ground-state S₀ into the π*-orbital of the ligands via a single-electron transfer (SET) and subsequent intersystem crossing into triplet-state T₁ (drawn in violet), which is 56 kcal·mol⁻¹ higher in energy than the ground-state S₀.^[71,72,189,190]

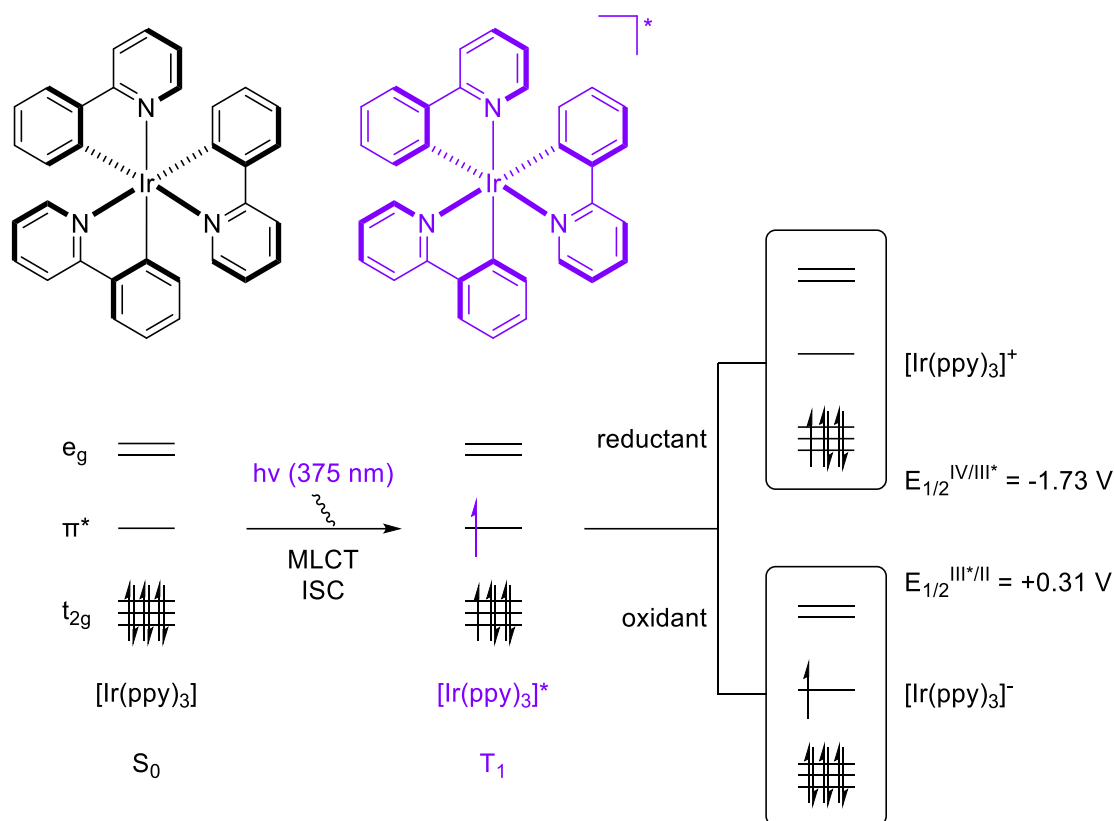


Figure 13: Simplified photochemical molecular orbital scheme of $[\text{Ir}(\text{ppy})_3]$ under irradiation with 375 nm light.^[71,189]

The process of electron donation upon excitation from S_0 at the metal core of the PRCat to the lowest unoccupied molecular orbital (LUMO) at the ligand sphere (here π^* -orbital) is called metal-to-ligand charge transfer (MLCT).

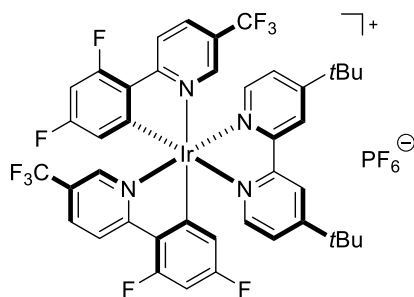
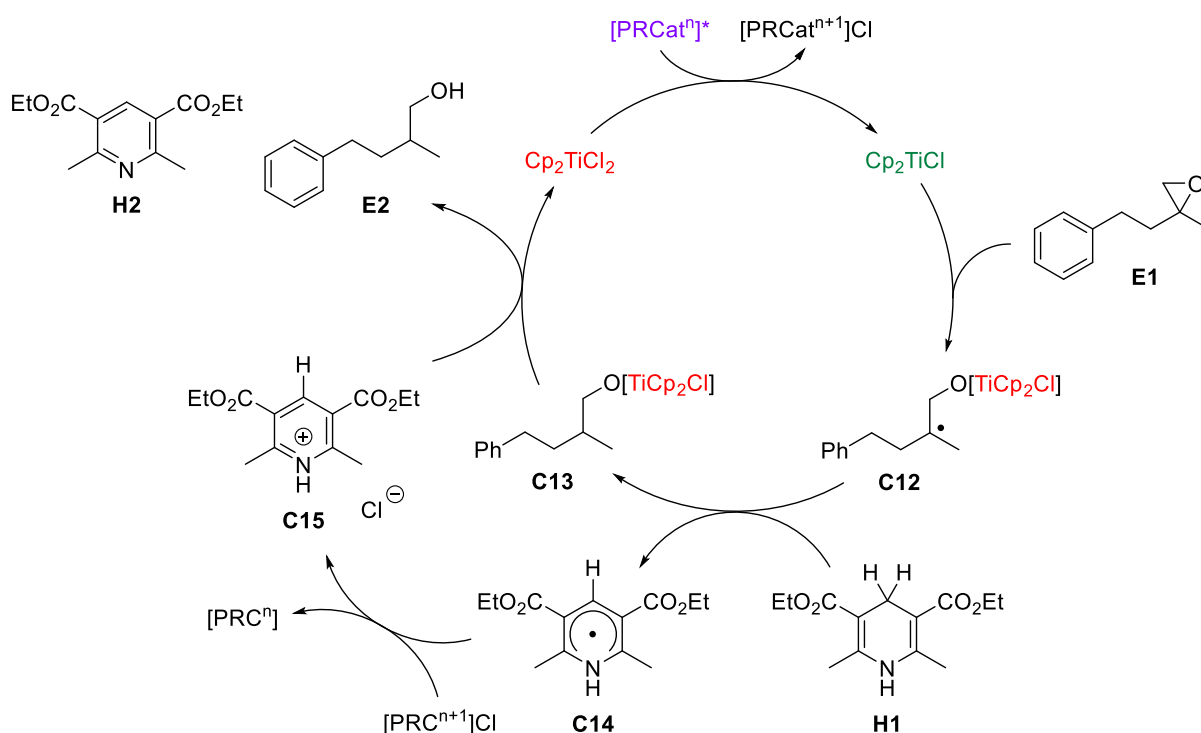
As T_1 is an open-electron-shell species, it can react both as oxidant upon uptake of an electron into the t_{2g} -orbitals (yielding $[\text{Ir}(\text{II})(\text{ppy})_3]^-$) and as reductant, donating the π^* -orbital electron (yielding $[\text{Ir}(\text{IV})(\text{ppy})_3]^+$). An important feature of most PRCats is that the excited state is long-living (here $\tau = 1.9 \mu\text{s}$).^[71] Otherwise, no intermolecular electron transfer can occur.

The application of visible light PRCats in organic synthesis offers a number of advantages: compared to high-energy UV-radiation which can cause side-reactions or destroy sensitive functional groups, visible light possesses longer wavelengths and is therefore lower in energy. By irradiation solely at the PRCat's absorption maximum the possibility of undesired reactions is minimized further. As described before, PRCats react via single-electron transfer and hence are suited for radical processes, which in general can be classified as mild reaction conditions with high functional group tolerance.^[191–193]

Combining the benefits of photochemistry and established radical reactions, *Gansäuer et al.* developed a titanocene catalyzed epoxide opening reaction merged with a photoredox process for catalyst activation.^[73,130] By this approach, radical arylations were realized without the need

of a metal reductant. **Scheme 17** shows the catalytic cycle of combining both photoredox catalysis and the titanocene catalyzed epoxide opening.

In this example, *Hantzsch* ester **H1** is used as a stoichiometric HAT reagent. The activation of the precatalyst Cp_2TiCl_2 is achieved by reduction with the photochemically excited Ir-PRCat. The active catalyst oxidatively opens epoxide **E1** to form a β -titanoxy radical **C12** which is reduced upon HAT from **H1**. The resulting radical **C14** is oxidized to yield a stabilized cation (**C15**) and thereby the oxidized PRCat is reduced. Thus, the photocatalytic cycle (depicted in two half-cycles for clarity) is completed and the PRCat can be irradiated again. **C15** is protonating the titanium-oxygen bond of **C13**, liberating Cp_2TiCl_2 and products **E2** and **H2**.

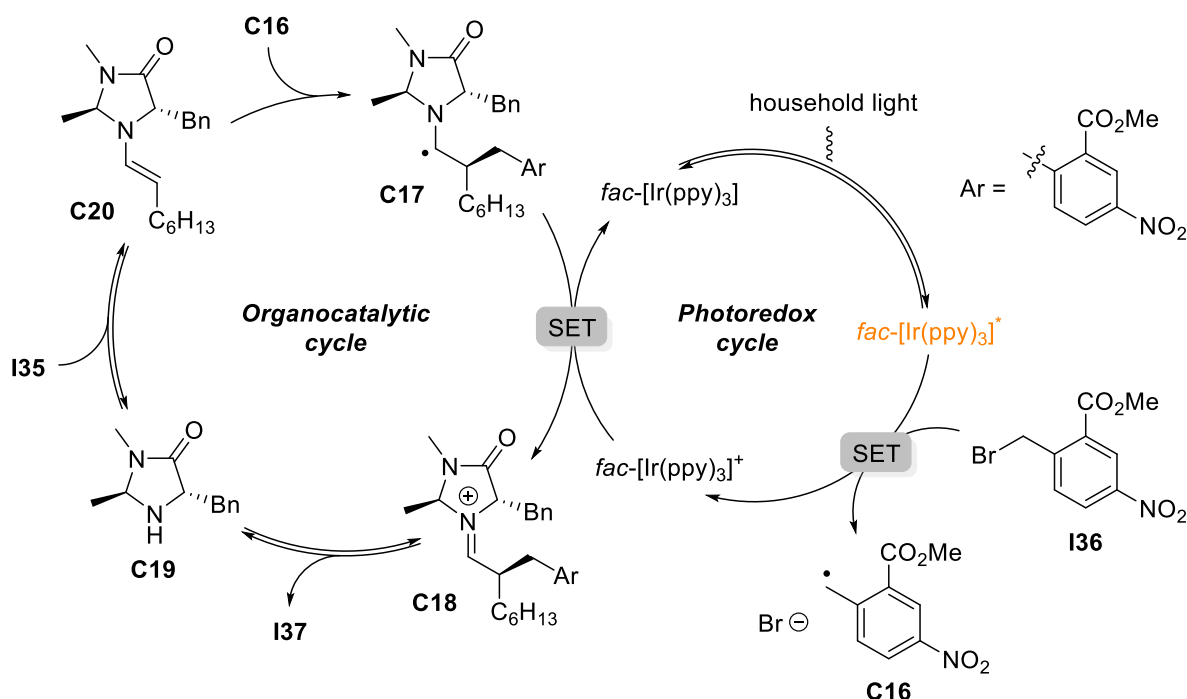
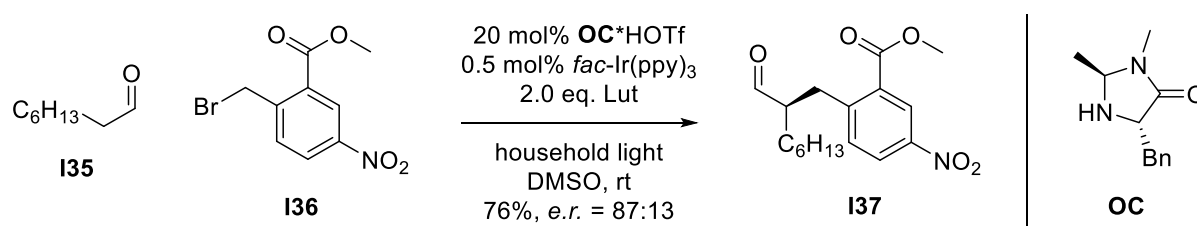


Scheme 17: Catalytic cycle of photoredox catalysis coupled with the titanocene catalyzed epoxide opening.^[130]

Condition optimization by *Zhang* resulted in an exchange of chloride for trifluoroacetate in the titanocene catalyst. However, that does not affect the concept of the catalytic cycle.^[130] Regarding sustainability and atom economy, the use of 2.0 equivalents of *Hantzsch* ester as HAT reagent leaves room for improvement, as only 0.8 wt% of the molecule is made up by the desired hydrogen ($MW_{H1} = 253.3$ g/mol; $MW_{H2} = 251.3$ g/mol). Furthermore, the PRCat is an Ir-based complex and thus cheaper and more earth-abundant alternatives could replace it.

2.4.1 Stereoselectivity in PRC

As stated above, **Scheme 17** does not accurately display the two catalytic cycles, which are merged together. Generally, in most cases in photoredox chemistry the PRCat transfers or receives an electron to/from a second redox cycle which is responsible for the actual organic transformation. This dual-catalysis approach enables various reactions that are not possible with either one of the cycles separately.



Scheme 18: Dual-catalysis by *MacMillan* coupling photoredox catalyst with imidazolidinone-based organocatalyst in enantioselective α -benzylation of aldehydes.^[194]

A noticeable example of such a dual system by Nobel Prize laureate *D. W. C. MacMillan* is given in **Scheme 18**. He used an enantiomerically pure imidazolidinone organocatalyst in an enantioselective α -benzylation of aldehydes.^[194] In the photocatalytic cycle, visible-light excited PRCat $fac-[Ir(ppy)_3]^*$ serves as reductant for benzyl bromide **I36**, forming benzyl radical **C16** and oxidized $fac-[Ir(ppy)_3]^+$, an Ir(IV)-complex.

In the organocatalytic cycle, radical **C16** accepts one electron from the double bond of enamine **C20** forming radical **C17**. In another SET, $fac-[Ir(ppy)_3]^+$ gets reduced to its Ir(III)-species, ready for another turn in the photoredox cycle.

Simultaneously, iminium ion **C18** is formed, which can dissociate to yield enantioenriched α -benzyl aldehyde **I37** and **C19** as free organocatalyst. **C19** can subsequently activate another aldehyde for the reaction. Besides this system, *MacMillan et al.* have developed several similar photochemical organocatalytic reactions enabling various functionalizations of aldehydes.^[66,194–196]

Most examples of photocatalyzed stereoselective reactions in the literature follow an approach alike the one displayed above. The chirality in an asymmetric reaction is induced in the organocatalytic cycle of a dual-catalysis with the PRCat solely serving as one-electron reductant and oxidant.^[72,197,198]

There are only a few exceptions of bifunctional photocatalysts known,^[199] one of them using a bimetallic Ru(II)-Pd(II)-complex $[Ru(bpy)_2(bpm)PdMe(MeCN)]^{3+}$ which on the one side serves as PRCat (Ru-center) and dimerizes styrene at the Pd-center after a metal-to-ligand charge-transfer (MLCT).^[200–204] In this case however, the reaction is not stereoselective. The catalyst is shown in **Figure 14** as well as an enantiomerically pure Ru(II)-complex ($\Delta-[Ru(menbpy)_3]^{2+}$) that enables coupling of two biaryl-moieties (2-naphthol) in a reaction using $Co(acac)_3$ as stoichiometric oxidant.^[205,206] Although the Ru-complex was used in enantiomerically pure form, (*R*)-BINOL could only be obtained with an *e.r.* = 58:42 as best result.

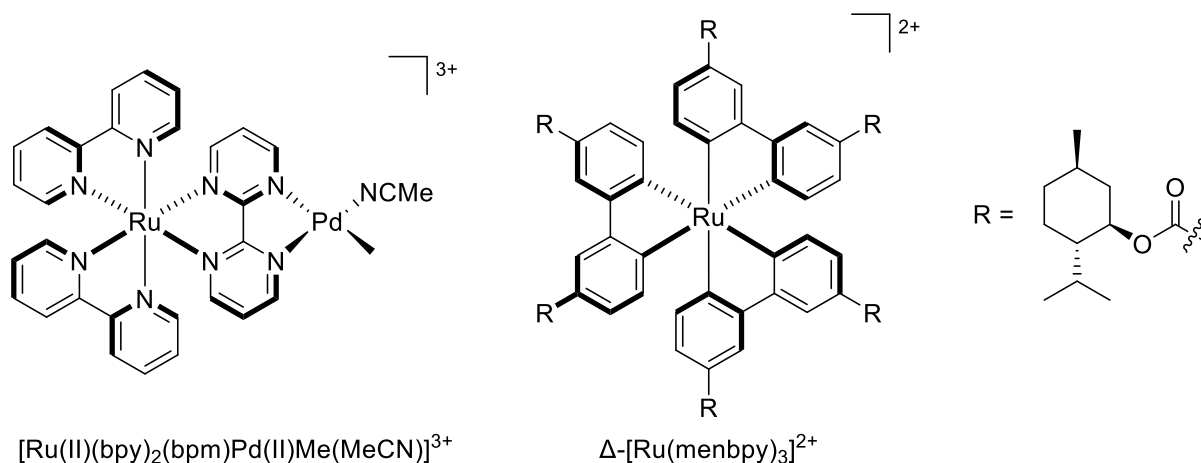
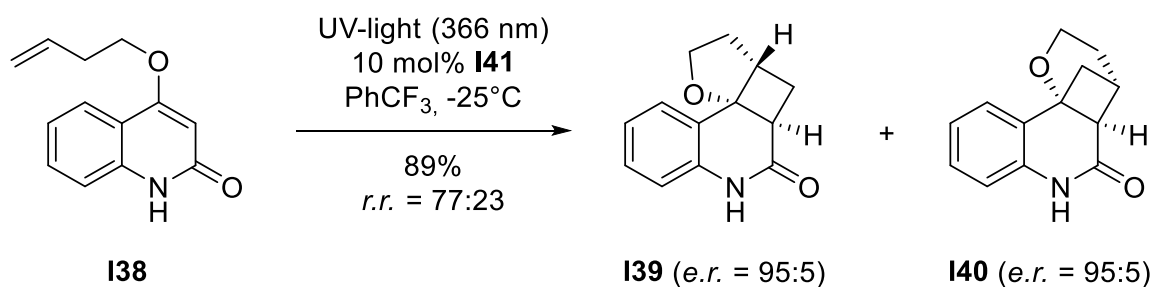


Figure 14: Structures of bimetallic Ru-Pd-complex and enantiomerically pure Ru-PRCat.^[72]

Novel approaches to asymmetric photoredox catalysis by *T. Bach* are the application of chiral *Lewis* and *Brønsted* acid-base adducts that are themselves excitable by light due to attached photosensitizers. Upon stereodefined binding of a prochiral substrate forming a chiral adduct, the attached excited photocatalyst undergoes an intramolecular SET to the bound substrate in close proximity, ensuring a stereoselective reaction due to steric interactions (compare to enzyme substrate binding described in chapter 2.1.2).^[207–211]



Scheme 19: First enantioselective triplet-sensitized [2+2]-photocycloaddition by *Bach*.^[207,210]

For instance, in **Scheme 19** an enantioselective photosensitized [2+2]-cycloaddition catalyzed by xanthone (**I41**) is shown, in which prochiral **I38** is cyclized with high enantioselectivity and mediocre regioselectivity.

However, in these systems the photocycle and the stereoselective organic transformation only occur ‘intramolecularly’ due to the adduct formed (**Figure 15**), although the photosensitizer itself is not involved in the reaction by any immediate (covalent) bond. The triplet energy E_T is transferred from the photosensitizer (UV-irradiation, 366 nm) to the hydrogen bond-attached substrate which then undergoes an intramolecular cyclization. The reaction has to be performed in trifluorotoluene (PhCF_3) at -25°C to achieve best results. Although the enantiomeric purity of the products is quite high, the reaction does not proceed fully regioselectively.^[207,210] This separation into two reactive sites is also true for the other examples given above.

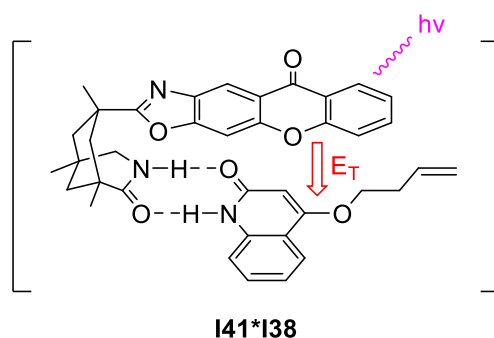


Figure 15: Triplet-energy (E_T) transfer from excited **I41** to bound substrate in the hydrogen bond adduct.^[210]

To summarize, there are only a few dual-functional, stereoselective photocatalysts known today and their regio- and stereoselectivity is still not perfect. In most cases, photoredox catalysts are combined with a second catalyst in a dual-catalysis system – this strategy has proven itself reliable and applicable to many reaction types over the past decades.

3 Special Part

3.1 Task and Objective of this Work

After the recent finding that Cp_2TiCl_2 can be irradiated with green light and be employed as a photoredox catalyst, enabling a new approach to known, well investigated reactions,^[135] the objective of this work was to find possible applications of catalytic systems based on photoexcited titanocenes. In addition, the development of a stereoselective variant, facilitating the use in regio- and diastereodivergent epoxide opening reactions was desirable as the renunciation of until then essential reagents would make the conditions more sustainable and thus meet the requirements of Green Chemistry in a better manner. In a series of screening reactions and evaluating potential applications on not only epoxide opening reactions, but also pinacol couplings and decarboxylations, in combination with various analytical methods and in collaboration with *T. Krebs*, *Z. Zhang*, *T. Hilche*, *M. Leuschner*, *J. Schmidt* and *M. Heinz*, new reaction conditions and substrate structures were investigated. Also, the improvement of established methods aiming for employing less hazardous, cheaper, more sustainable or easily removable reagents played a major role in planning and executing the practical laboratory work underlying this thesis.

In cooperation with the groups of *Prof. R. Flowers* (Bethlehem, PA, USA), *Prof. P. Vöhringer* (Bonn, Germany) and *Prof. S. Grimme* (Bonn, Germany), photochemical investigations and theoretical calculations should be employed to further extend the knowledge and elucidate the mechanism of how titanocenes work when irradiated with visible light and used in new catalytic reactions.

3.2 Applications of the Photoactive Properties of Titanocenes

Soon after the first application of titanocene catalysis merged with photoredox catalysis, described in chapter 2.4 (**Scheme 17**),^[130] Zhang discovered that even without the utilization of an external transition metal-based photoredox catalysts (containing for example Ir or Ru), epoxide opening reactions could successfully be performed. As titanocene dichloride, a bright-red solid, absorbs visible light with two maxima (measured in THF) at 515 nm (green light) and 385 nm (violet light),^[212] irradiation with a suitable light source leads to excitation of an electron from the mainly Cp-ligand centered HOMO (highest occupied molecular orbital) to the mainly titanium-centered LUMO (lowest unoccupied molecular orbital).^[135] Hence, the energy transfer is referred to as ligand-to-metal charge-transfer (LMCT).^[213] In the solid state, Cp_2TiCl_2 exhibits a long-lived LMCT phosphorescence at 77 K of 800 μs .^[214–216] Consequently, this irradiation leads to a weakening of the Ti–Cp-bond. At room temperature, the lifetime of the excited state is massively decreased.^[135]

Irradiation with high energy light can eventually lead to photolysis of the titanocene with loss of one of the Cp-ligands.^[212] Although the absorption maximum in the violet light region is much higher (compare **Figure 16**), reactions are carried out under green light irradiation. This is to prevent or delay photolysis, which can be observed after longer reaction times.^[213,217,218] As the absorbance maximum in the green light region is very broad, no specific wavelength has to be used, so that conventional and commercially available 10 W LEDs are employed.

To avoid the problems resulting from the short lifetime of the excited titanocenes, reductive quenching with a tertiary amine (DIPEA, *N,N*-diisopropylethylamine) leads to formation of catalytically active $\text{Cp}_2\text{Ti(III)Cl}$ and an amino radical cation. This is particularly convenient, as these amino radical cations can also serve as hydrogen atom donors.^[219]

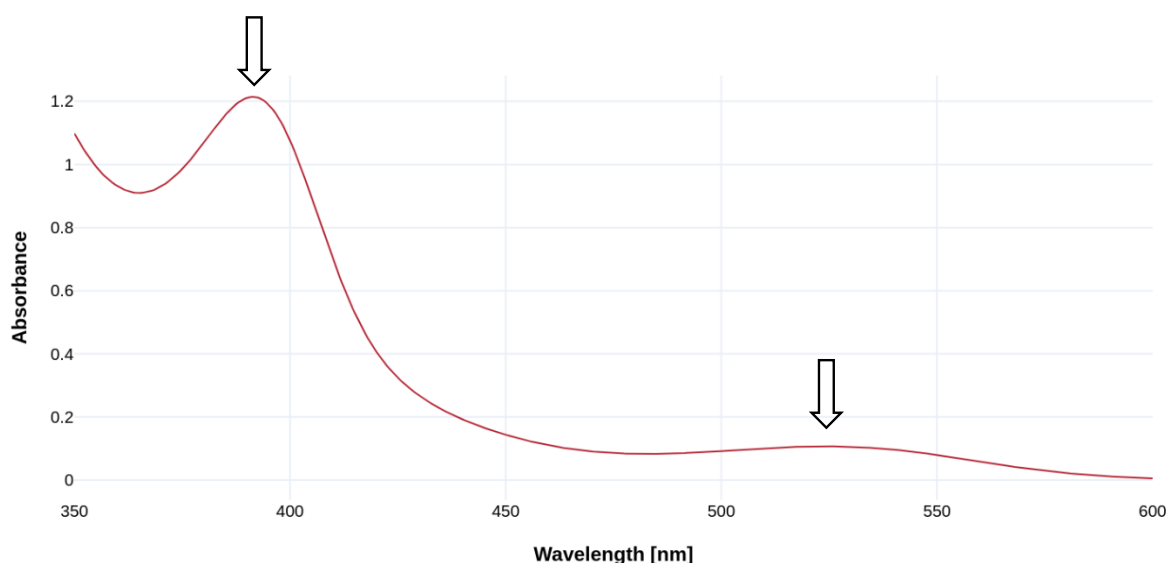
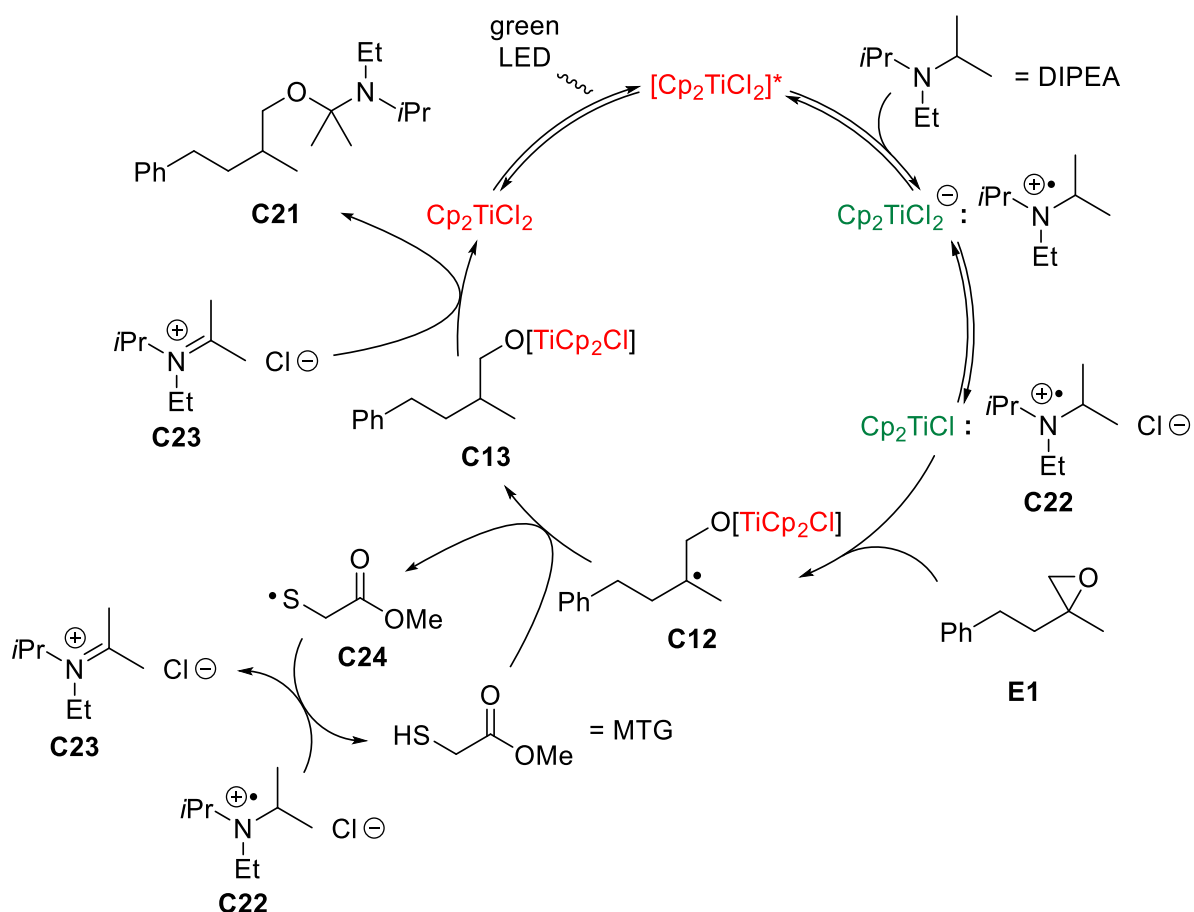


Figure 16: UV-Vis spectrum of Cp_2TiCl_2 in MeCN ($c = 0.5 \mu\text{mol/mL}$). Maxima at 392 nm and 525 nm.

Unfortunately, no direct HAT from this radical to the intermediate β -titanoxy radical formed during the reaction is possible. Hence, a thiol (methyl thioglycolate, MTG) is employed to serve as hydrogen atom transfer catalyst. The proposed catalytic cycle of the titanocene catalyzed epoxide opening under photoredox conditions is depicted in **Scheme 20**.^[135]



Scheme 20: Catalytic cycle of the titanocene catalyzed epoxide opening under photoredox conditions with DIPEA as reductive quencher and MTG as HAT-catalyst.^[135]

Regarding the epoxide, the mechanism only varies in the formation of the hemiaminal **C21**. Alcohol **E2** is liberated in the aqueous work-up (compare to **Scheme 15** and **Scheme 17**). Instead of a protonation of **C13**, the alcohol function of the desired product is protected as a hemiaminal, which is beneficial, as the overall reaction conditions do not tolerate free alcohol, because they can undergo hydrogen-bonding with the thiol (MTG) and thus deactivate it for any HAT reaction.^[73]

The catalytic cycle starts by irradiation of the pre-catalyst Cp_2TiCl_2 with green light. The excited titanocene is reduced upon complex formation with DIPEA, which donates one electron to yield a radical cation. Dissociation of the anionic titanocene complex results in the formation of active Cp_2TiCl and radical cation **C22**. As discussed earlier, **E1** is opened forming β -titanoxy radical **C12** that is reduced by MTG in a hydrogen atom transfer. This results in thiol radical **C24** which

then regenerates MTG by oxidation of amino radical cation **C22** to cationic **C23**. In contrast to the previous reaction conditions, **C23** cleaves the titanium-oxygen bond of **C13** not via protonation but via formation of hemiaminal **C21** under release of Cp_2TiCl_2 .

Control experiments with renunciation of either of the reagents show that the reaction only occurs when DIPEA, MTG and Cp_2TiCl_2 are present.^[73,135] The hemiaminal species **C21** is proposed due to IR investigations of the reaction mixture after removing the solvent but before quenching and aqueous work-up. A comparison with pure **E2** (blue line, alcohol at 3330 cm^{-1}) revealed the lack of the O–H stretching modes in the IR spectrum (red line, **Figure 17**).

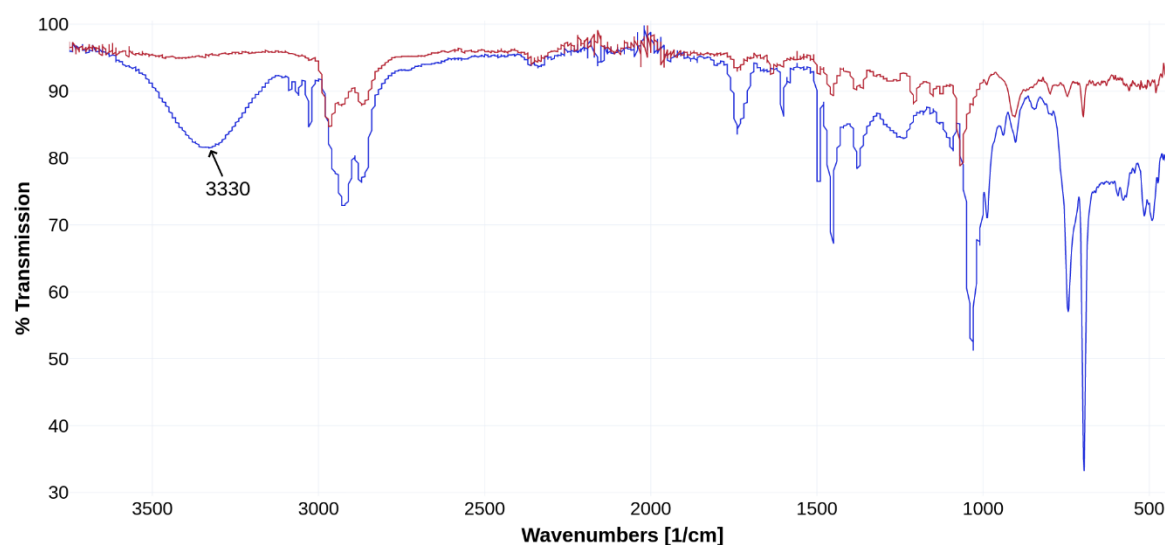
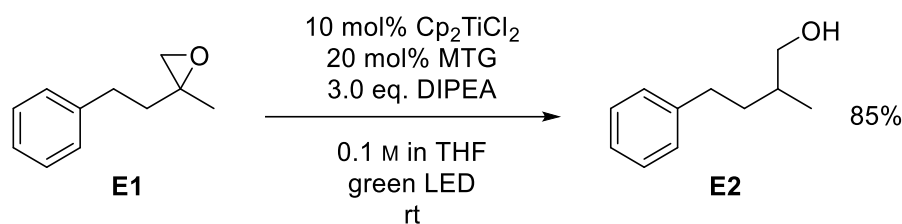


Figure 17: IR spectra of **E2** (blue, O–H stretching modes at 3330 cm^{-1}) and crude reaction mixture (**C21**, red).

The ideal reaction conditions have been examined by *Zhang* and are shown in **Scheme 21**, they consist of 10 mol% Cp_2TiCl_2 , 20 mol% MTG, 3.0 eq. DIPEA and 0.1 M epoxide in THF under irradiation with two green 10 W LEDs at room temperature. *Zhang* evaluated different amines as reductive quenchers, thiols as HAT-catalysts and titanocenes with other anions than chloride. Out of these, only titanocene bromide led to an acceptable, but lower yield (74% vs. 85% with chloride). The reaction can be performed using blue light as well, this however lowers the yield substantially (52%).^[73,135]



Scheme 21: Optimized reaction conditions for the photochemical titanocene catalyzed epoxide opening.^[135]

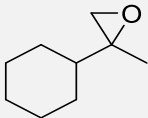
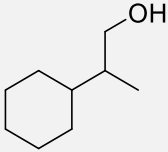
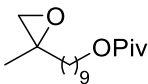
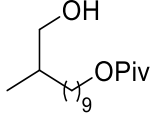
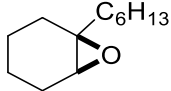
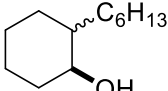
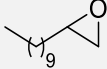
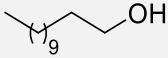
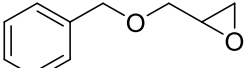
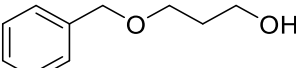
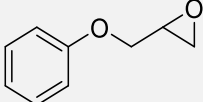
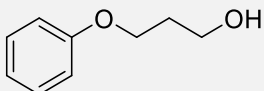
The more rapid catalyst decomposition when higher energy radiation is used is responsible for this. The low yield cannot be rationalized by worse catalyst excitation, as the UV-Vis spectrum shows a high absorption in the energetically higher blue light region (430–490 nm, **Figure 16**), but only by the photolytic decomposition of the catalyst upon irradiation with blue light.

The scope of the photochemical titanocene catalyzed epoxide opening was tested on various 1-monosubstituted, 1,1-disubstituted and 1,1,2-trisubstituted epoxides. A selection of the results following the reaction scheme displayed above (**Scheme 21**) is given in **Table 1**.

Noticeable is the high substrate controlled regioselectivity of the reaction exclusively forming the *anti-Markovnikov* product from most substrates due to the higher stability of secondary or tertiary β -titanoxy radicals formed as intermediates (compare to **C12**, **Scheme 20**). Solely an oxygen atom in β -position to the epoxide as found in **E13** and **E15** results in comparably low yields, as the inductive effect of oxygen destabilizes the desired 1,3-diol-pattern leading to **E14** and **E16**. Preferably, these ‘*Sharpless-type*’ epoxides result in 1,2-diol-products which was verified by theoretical calculations (DFT).^[92,220,221] However for these examples, a primary radical would be formed which is instable and thus the influence of the β -oxygen is hard to determine. The low yields may result from two unfavorable substrate properties in combination with the less stabilized secondary radical formed compared to the tertiary radical from 1,1-disubstituted or 1,1,2-trisubstituted epoxides.

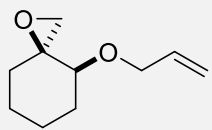
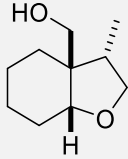
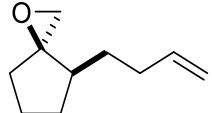
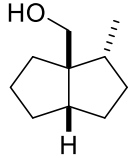
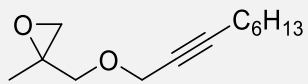
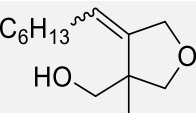
Besides simple opening reactions with subsequent radical reduction, the system was extended by *Zhang* to radical 5-*exo* cyclizations. However, the reaction conditions were modified and instead of MTG, *n*-octyl thioglycolate (OTG) was used in combination with PhSiH_3 as hydrogen atom donor. Application of the original conditions led to unselective reactions with low yields. This is explained by the competing termination of thiyl radical **C24** by addition to the olefin of the cyclization substrates.^[135,222–225] Mechanistically, only the 5-*exo* cyclization of the β -titanoxy radical prior to the radical reduction differs from the mechanism displayed in **Scheme 20**. Generally, 5-*exo* cyclizations are the most prominent radical cyclization reactions with broad application in organic synthesis.^[141,191,226–228]

Table 1: Scope of the photoexcited titanocene catalyzed epoxide opening.

Substrate	Product	Isolated Yield [%]
 E3	 E4	75 ^[a]
 E5	 E6	86 ^[a]
 E7	 E8	76 ^[a] <i>cis:trans</i> = 17:83
 E9	 E10	90 ^[a] <i>cis:trans</i> = 42:58
 E11	 E12	41/35 ^[b] 1-ol:2-ol = 99:1 ^[b]
 E13	 E14	27
 E15	 E16	24

[a] Performed by Zhang.^[135] [b] (*t*BuCp)₂TiCl₂. Conditions: 10 mol% Cp₂TiCl₂, 20 mol% MTG, 3.0 eq. DIPEA, 0.1 M in THF, green LED, rt.

Table 2: Titanocene catalyzed radical 5-exo cyclizations under photoredox conditions.

Substrate	Product	Isolated Yield [%]
 E17	 E18	63 <i>d.r.</i> = 83:17
 E19	 E20	64 <i>d.r.</i> = 99:1
 E21	 E22	72 <i>d.r.</i> = 52:48

Reaction conditions: 10 mol% Cp₂TiCl₂, 20 mol% OTG, 2.5 eq. PhSiH₃, 0.1 M in THF, green LED, rt.^[135]

Examples for titanocene catalyzed radical 5-exo cyclizations under photoredox conditions are shown in **Table 2**.^[73,135] Tetrahydrofuran derivatives **E18** and **E22** can be obtained in acceptable yields as well as fused 5-membered aliphatic carbon ring structures such as **E20**. The diastereoselectivities match the ones typically found for reactions performed with titanocene dichloride reduced with zinc or manganese.^[141,227,228]

With these new results in hand, an expansion and application to other titanocene catalyzed reactions was planned. In addition, the combination with external photocatalysts and various HAT reagents and reductive quenchers promised a broader usability of reactions of these type, especially as there are already many examples reported in the literature.^[130,229–233] By this, regio- and stereoselective reactions under more sustainable reaction conditions and with a greater substrate and product scope were set as final target.

3.3 Expansion to Other Systems

3.3.1 UV-Vis Investigations of Titanocenes

To understand the mechanistic details of the photoexcitation of titanocene dichlorides under visible light irradiation, the absorption properties must be investigated. As these compounds typically show a bright red to orange color, an absorption of complementary green light can be assumed. To verify this, UV-Vis spectroscopy investigations of titanocenes in different solvents were conducted. Generally, titanocene dichlorides exhibit an absorption maximum in the near UV light to violet region of the visible spectrum.^[212,213] Additionally, a second but much lower absorption maximum can be found in the green region, responsible for the visible red color of the compounds.

A selection of absorption maxima of different titanocene dihalides is given in **Table 3**. The influence of the solvent does not drastically change the maxima (≤ 10 nm). For mimicry of the conditions in a reaction solution, DIPEA was added when investigating L-Kagan and Cp*TiCl₃, nevertheless, the influence of the amine for the absorption is neglectable, as no change in color is observed upon addition to the dissolved titanocene.

Table 3: UV-Vis absorptions of selected titanocene dichlorides.

Titanocene	Solvent	Maximum 1 [nm]	Maximum 2 [nm]
Cp ₂ TiCl ₂ ^[a]	THF	385	515
Cp ₂ TiCl ₂	MeCN	392	525
L-Kagan ^[b]	THF	390	525
(MeCp) ₂ TiCl ₂ ^[a]	THF	388	520
(MeCp) ₂ TiCl ₂ ^[a]	MeCN	395	528
Cp*TiCl ₃ ^[c]	toluene	<350	-

MeCp = MeC₅H₄. [a] By Tsai.^[212] [b] Containing 20 eq. DIPEA. [c] Containing 30 eq. DIPEA.

To examine the titanocene dichloride photolysis which occurred in reactions conducted in collaboration with *Heinz* and was visible by color change from red to yellow,^[217] a yellow half-sandwich titanocene Cp*TiCl₃ was also spectroscopically investigated, showing no absorption maximum in the green light region but an increase of absorption towards the UV-region. Reaction details will be given in the following chapters (mainly 3.4), but generally, a catalyst decomposition was observed in unsuccessful reactions after a long reaction time.

The highest visible values for the half-sandwich titanocene can be found for blue-violet light, which matches the complementary color of the compound. *Harrigan* found that photolysis of titanocene dichlorides leads to loss of a Cp-ligand. This supports the experimental results as

well as the fact that irradiation weakens the Ti–Cp bond by excitation of an electron from the Cp-centered HOMO into the Ti-centered LUMO.^[135,213] If the excited titanocene cannot be reductively quenched or transfer the energy towards a suitable acceptor (substrate), the Ti–Cp bond is cleaved.

A second target for UV-Vis investigations were titanocene carboxylate complexes. They were investigated to employ photoexcited titanocenes in decarboxylation reactions. To this end, complexes synthesized by Zhang^[234] were examined dissolved in THF (**Figure 18**). Unfortunately, none of the four complexes possess any absorption maxima in the green light region (**Figure 19**). Generally, the absorption in the visible spectrum is poor. Only carboxylate-chloride complex **T1** has a small absorption maximum at 470 nm (blue light). The compounds themselves are light-orange (**T1**) or light-yellow crystalline solids.^[234,235]

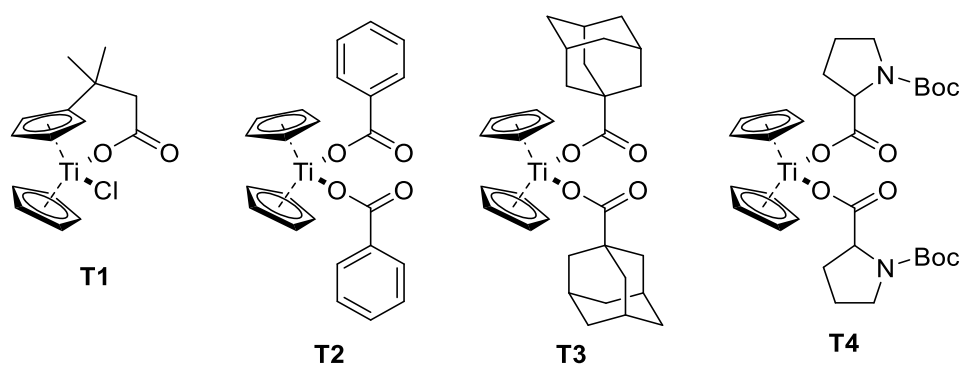


Figure 18: UV-Vis investigated titanocene carboxylate complexes.

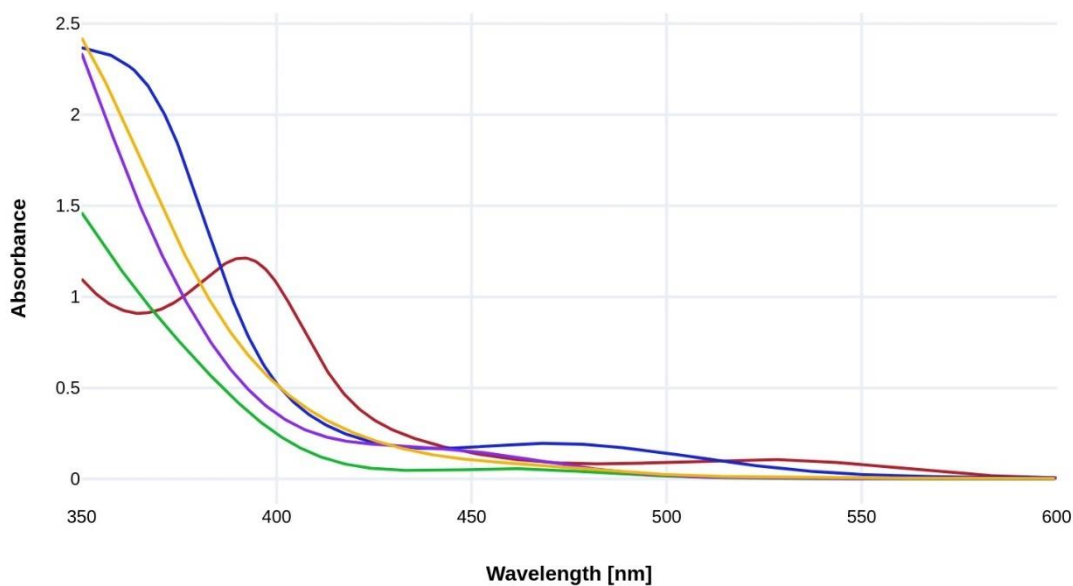
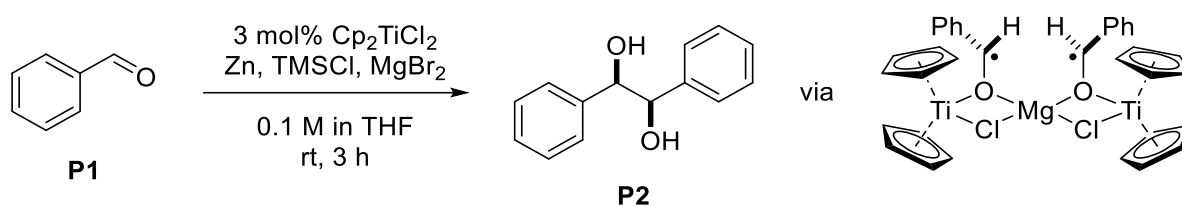


Figure 19: UV-Vis spectra (5 μ m in THF) of Cp₂TiCl₂ (red, 5 μ m in MeCN), **T1** (blue), **T2** (green), **T3** (violet), **T4** (yellow).

3.3.2 Pinacol Couplings

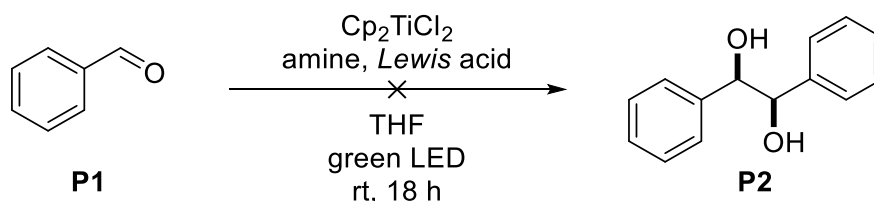
Titanocene catalysts have successfully been employed to convert aldehydes to *syn*-1,2-diols in pinacol coupling reactions.^[129,154,236–239] *Gansäuer* initially used catalytic amounts of Cp_2TiCl_2 with Zn or Mn as reducing agents for active catalyst generation in combination with TMSCl and MgBr_2 as *Lewis* acid. The reaction scheme shows the formation of intermediate ketyl radicals formed by addition of active $\text{Cp}_2\text{Ti(III)Cl}$ catalyst to the respective substrate (**Scheme 22**). Due to complexation of MgBr_2 , a dimeric titanium species ensures a high diastereoselectivity, as a result of steric interactions of the carbonyl's aryl substituent.^[129,154,238]



Scheme 22: Titanocene catalyzed diastereoselective pinacol coupling of benzaldehyde. Conditions: 1.0 eq. Zn, 1.5 eq. TMSCl, 1.0 eq. MgBr_2 , 90% yield, *d.r.* (*syn:anti*) = 95:5.^[154]

The reaction proceeds via single-electron reduction of Cp_2TiCl_2 by Zn and the active catalyst then oxidatively adds to the aldehyde. With MgBr_2 (or alternatively zinc halides), the dimeric complex shown in **Scheme 22** is formed and the titanium alkoxide is scavenged by TMSCl yielding titanocene dichloride and the silyl-protected pinacol product. **P2** is released by acidic work-up (2 M aq. HCl).^[129,154]

Based on this reaction, a potential new catalytic system using a photoexcited titanocene catalyst which is converted to the active Ti(III) species via reductive quenching with a tertiary amine was planned. Mechanistically, the catalyst activation follows the approach depicted in **Scheme 20**. Subsequently, upon binding to the aldehyde, a ketyl radical is formed after a single-electron oxidative addition to the Ti-center. A dimerization of two ketyl radicals yields the pinacol product **P2**. The results of the conducted screening reactions (**Scheme 23**) are given in **Table 4**.



Scheme 23: General reaction conditions for pinacol coupling screening reactions. Conditions: 10 mol% Cp_2TiCl_2 , 3.0 eq. amine, 1.5 eq. TMSCl, 1.0 eq. ZnCl_2 , 0.05 M in THF.

Table 4: Investigated reaction conditions for pinacol coupling of benzaldehyde (**P1**).

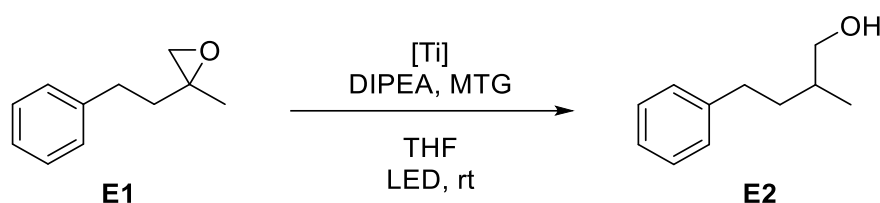
No.	Amine	Lewis acid	LED	Conversion
1	NEt ₃	-	green	-
2	DIPEA	-	green	-
3	NEt ₃	TMSCl	green	-
4	DIPEA	TMSCl	green	-
5	DIPEA	TMSCl, ZnCl ₂	green/blue ^[a]	-
6	DIPEA	ZnCl ₂	green/blue ^[a]	-

[a] 20 h green LED then 20 h blue LED. Conversion monitored by TLC.

Unfortunately, none of the tested reaction conditions showed any conversion of benzaldehyde. The reason for this could potentially be a complex formation of titanocene dichloride with the aldehyde upon ligand exchange, either blocking the approach of the tertiary amine which is crucial to enable the outer-sphere electron transfer to the photoexcited titanocene or changing the absorption properties of the resulting complex to other than the used wavelengths. As Cp₂Ti(III)Cl is generally able to oxidatively add to benzaldehyde, the reaction should proceed, once the ketyl radical is formed. This explanation is supported by the fact that the Ti–O bond is substantially stronger (157 kcal·mol⁻¹^[240]) compared to the Ti–Cl bond (93 kcal·mol⁻¹^[241]) and hence, the ligand exchange is energetically favored. As discussed before, carbonyl ligands do have a huge impact on the UV-Vis absorption spectrum of the respective titanocene complex (see **Figure 19**). Under these circumstances and tested reaction conditions, no pinacol couplings of benzaldehyde by photochemically activated titanocene dichloride could be performed.

3.3.3 Epoxide Openings with Other Titanocenes

Building on the epoxide opening reactions under photochemical conditions published by Gansäuer *et al.*,^[135] the scope of applicable titanocene catalysts should be widened. As the quenching and hydrogen atom transfer system containing DIPEA and MTG had proven to be reliable, epoxide **E1** was reacted with different half-sandwich titanocenes as well as titanocenes containing various non-chloride anions (**Scheme 24**). Matching the UV-Vis properties of Cp*TiCl₃, which show no green region absorbance and a mediocre blue region absorbance, only blue light irradiation leads to the formation of minor product amounts (entries 1 and 2). Interestingly, the addition of ZnCl₂ inhibits the product formation, although the conditions have not been modified otherwise (entry 5). The less electron rich half-sandwich titanocene CpTiCl₃ led to no conversion at all.



Scheme 24: General reaction conditions for photoexcited titanocene catalyzed epoxide opening reactions. Conditions: 10 mol% titanocene catalyst [Ti], 3.0 eq. DIPEA, 20 mol% MTG, 0.05 M in THF.

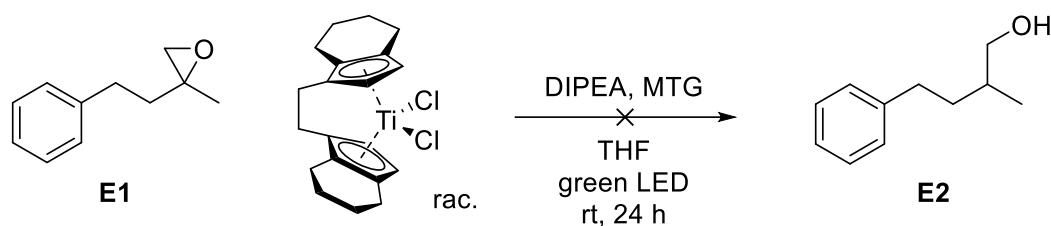
Entries 6–9 show that non-chloride titanocenes cannot reliably form the desired product neither under irradiation with blue nor green LEDs. For Cp₂TiF₂, a bright yellow compound, only complementary blue light has been chosen due to the UV-Vis absorption maximum of 340 nm.^[213] Under similar reaction conditions as in entries 10–12, Cp₂TiCl₂ has given a yield of 85% (entry 13)^[135] and the combined catalyst systems of 5 mol%:5 mol% mixtures of Cp₂TiCl₂/Cp₂Ti(OMs)₂ and Cp₂TiCl₂/Cp₂Ti(TFA)₂ do not improve this result but impair the yield, although some conversion is detectable. This matches the findings of entries 7 and 8, by applying the mesylate and trifluoro acetate catalysts the concentration of potent titanocene dichloride is diminished. However, when only employing 5 mol% of titanocene dichloride, the effective amount is the same as in the mixed examples, but the yield is even lower, about half of what is obtained with 10 mol% of the respective catalyst. This indicates that the non-chloride catalysts can in fact to some extent successfully open epoxide **E1** to give **E2**, but their capability is worse than the originally employed Cp₂TiCl₂.

Table 5: Investigated reaction conditions for epoxide openings of **E1**.

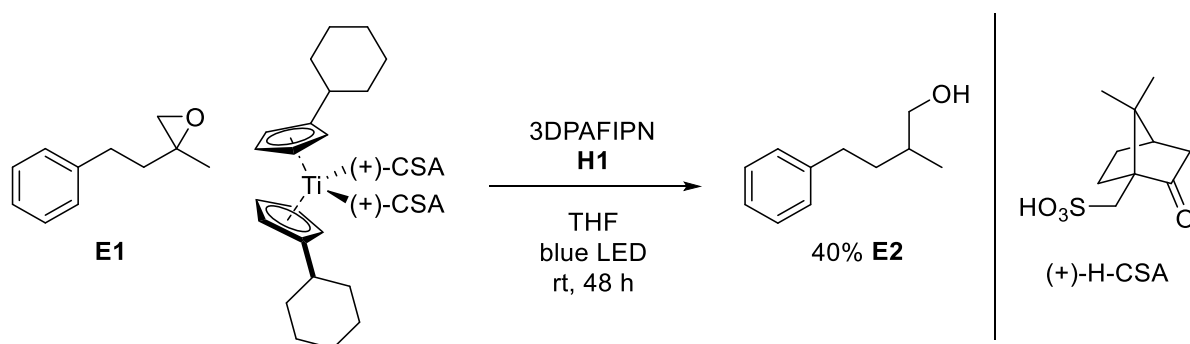
No.	Titanocene	LED	Reaction time [h]	Yield [%]
1	Cp*TiCl ₃	green	90	-
2	Cp*TiCl ₃	blue	90	23 ^[a]
3	CpTiCl ₃	green	70	-
4	CpTiCl ₃	blue	70	-
5 ^[b]	Cp*TiCl ₃	blue	20	-
6	Cp ₂ Ti(OTs) ₂	blue/green ^[c]	40	trace ^[d]
7	Cp ₂ Ti(OMs) ₂	blue/green ^[c]	40	trace ^[d]
8	Cp ₂ Ti(TFA) ₂	blue/green ^[c]	40	trace ^[d]
9	Cp ₂ TiF ₂	blue	90	-
10	Cp ₂ TiCl ₂ / Cp ₂ Ti(OMs) ₂	green	16	57
11	Cp ₂ TiCl ₂ / Cp ₂ Ti(TFA) ₂	green	16	63
12	Cp ₂ TiCl ₂ ^[e]	green	16	38
13	Cp ₂ TiCl ₂	green	48	85 ^[f]

[a] NMR-yield. [b] Addition of 1.0 eq. ZnCl₂. [c] 20 h blue LED then 20 h green LED. [d] Conversion according to TLC. [e] 5 mol% Cp₂TiCl₂. [f] By Zhang.^[135]

A *Brintzinger*-type^[242] titanocene was also tested under the new photochemical conditions. These *ansa*-metallocenes, especially the zirconium complexes, are well-known for their employment in olefin-polymerization reactions, especially the respective zirconocene derivatives.^[243–246] Epoxide **E1** is not opened to the corresponding alcohol (**Scheme 25**). This might be due to a tighter binding pocket on the titanium-center because of the bridged Cp-ligands, so that the epoxide binding is inhibited.



Scheme 25: Photoexcited *Brintzinger*-titanocene catalyzed epoxide opening. Conditions: 10 mol% *rac*-(ebthi)TiCl₂, 3.0 eq. DIPEA, 20 mol% MTG, 0.05 M in THF.



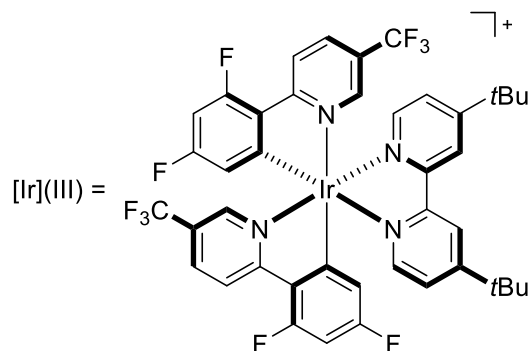
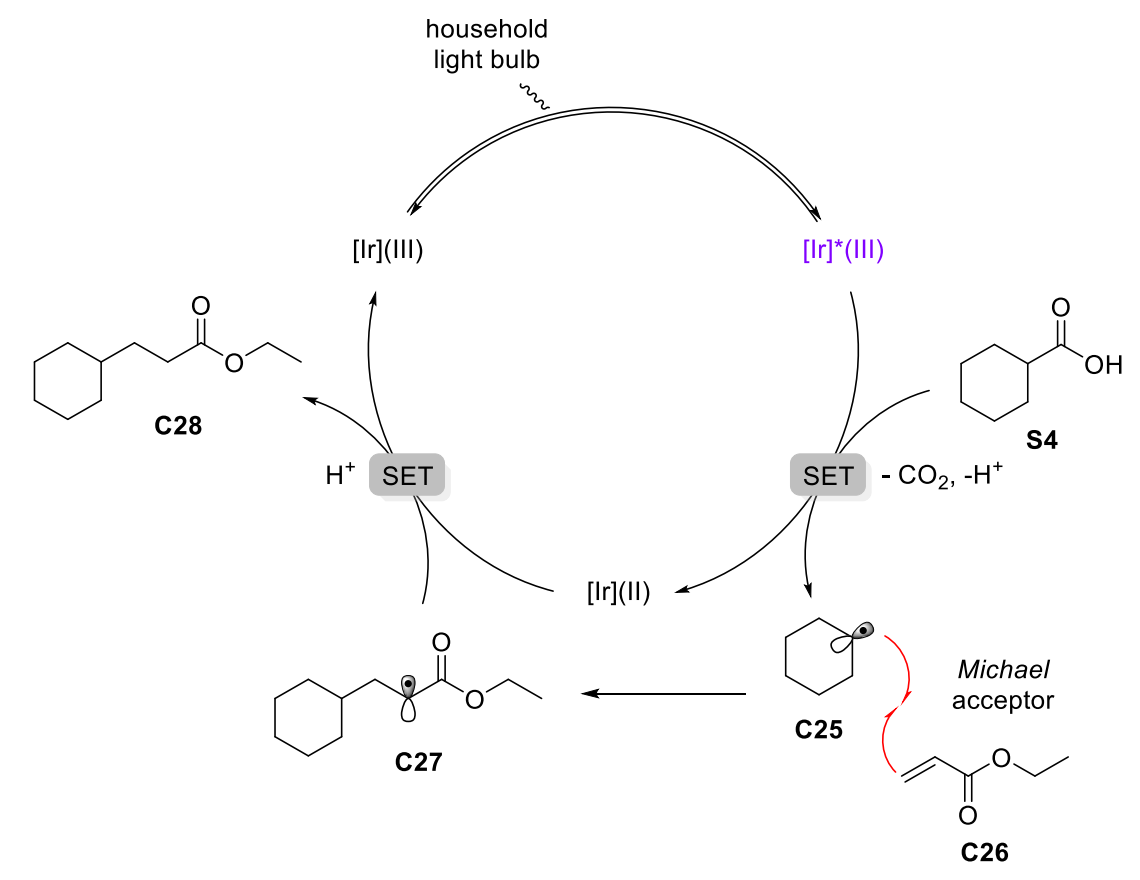
Scheme 26: Epoxide opening applying *cHex*-(+)-CSA titanocene catalyst. Conditions: 10 mol% (cHexCp)₂Ti(CSA)₂, 3 mol% 3DPAFIPN, 2.0 eq. **H1**, 0.05 M in THF.

Besides the given examples with the titanocene acting both as photoredox catalyst and electron transfer catalyst, a new type of chiral titanocenes was tested for epoxide opening reactions applying an external organic photocatalyst (3DPAFIPN) and *Hantzsch* ester (**H1**) as hydrogen donor in a collaboration with *Hilche et al.* (**Scheme 26**).^[247] The epoxide is opened to **E2** in an isolated yield of 40%, which corresponds to about half the yield obtained when employing the classical titanocene dichloride as photoredox catalyst. However, the reaction results are not easily comparable as the catalytic systems differ substantially. Nevertheless, this reaction shows the potential use of CSA-titanocenes in epoxide opening reactions. *Krebs* designed this type of complexes as potential enantiomerically pure non-*ansa* titanocenes for stereoselective reactions. The clue of these titanocenes is their confined or prevented Cp-rotation due to the steric hinderance of the CSA-ligands.^[136,220,248]

3.3.4 Decarboxylations

In recent years, photocatalysis has been employed in decarboxylation reactions of alky and aryl carboxylic acids.^[163,184,186,188,249–252] Decarboxylations also occur in nature. A prime example is the regioselective enzymatic decarboxylation of glutamic acid forming the vital neurotransmitter γ -aminobutyric acid.^[253]

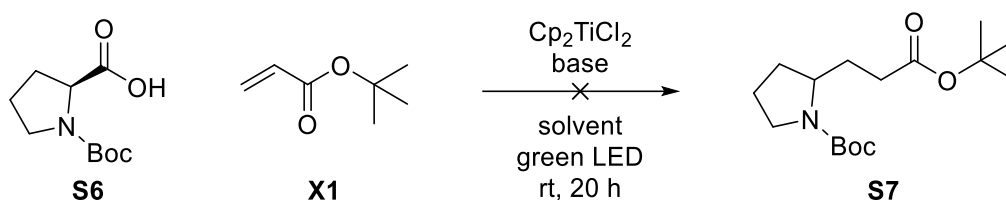
MacMillan et al. developed a method coupling aliphatic radicals made from carboxylic acids to electron deficient *Michael* acceptors such as acrylates after photocatalytic decarboxylation using an iridium photocatalyst.^[252] Their proposed catalytic cycle is shown in **Scheme 27** and exhibits substantial parallels to the single-electron catalysis titanocenes can perform.



Scheme 27: Catalytic cycle of the photochemical decarboxylation with subsequent alkylation by *MacMillan*.^[252]

Table 6: Investigated reaction conditions for decarboxylations of **S4**.

No.	Titanocene	Base	Eq. base	precipitate	Conversion
1	Cp ₂ TiCl ₂	DABCO	0.1	white	-
2	Cp ₂ TiBr ₂	DABCO	0.1	white	-
3	Cp ₂ Ti(TFA) ₂	DABCO	0.1	-	-
4	Cp ₂ Ti(OMs) ₂	DABCO	0.1	white	-
5	Cp ₂ TiCl ₂	DABCO	1.0	white	-
6	Cp ₂ Ti(TFA) ₂	DABCO	1.0	-	-
7	Cp ₂ TiCl ₂	NEt ₃	0.5	-	-
8	Cp ₂ TiCl ₂	collidine	0.5	-	-



Scheme 29: General reaction conditions for photoexcited titanocene catalyzed decarboxylation of **S6**. Conditions: 10 mol% Cp₂TiCl₂, 2.0 eq. **X1**, 0.5 eq. base, 0.05 M in respective solvent. Conversion monitored by TLC.

Table 7: Investigated reaction conditions for decarboxylations of **S6**.

No.	Base	Solvent	Conversion
1	NEt ₃	THF	-
2	collidine	THF	-
3	NEt ₃	DMF	-
4	NEt ₃	DMPU	-
5	NEt ₃	MeCN	-
6	NEt ₃	DME	-

3.4 Arylations

As sketched out in chapter 2.3, atom-economical radical arylations of epoxides enable the transformation of easily accessible and broadly customizable aniline-derived epoxides to indolines. The mechanistic details are given in **Scheme 16** and involve the generation of the active titanocene catalyst by reduction with Mn or Zn metal. As substrates, 1,1-disubstituted epoxides are employed, ensuring the regioselective formation of the *anti-Markovnikov* epoxide opening product.^[139,152] However, this basic arylation does not work well with 1,2-disubstituted epoxides and the reaction cannot be performed in an enantio- or diastereoselective manner. To overcome these drawbacks, a regiodivergent radical arylation has been developed, enabling the diastereo- and enantioselective formation of indoline and tetrahydroquinoline derived products in an atom-economic titanocene catalyzed reaction.^[92,94,149] The general substrate structure for this reaction is shown in **Figure 20** and comprises aniline-derived *syn*-1,2-disubstituted enantiomerically pure epoxides. Their synthesis will be discussed in the following chapter.

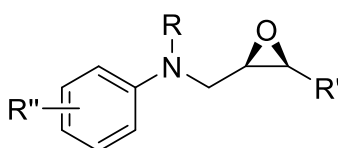
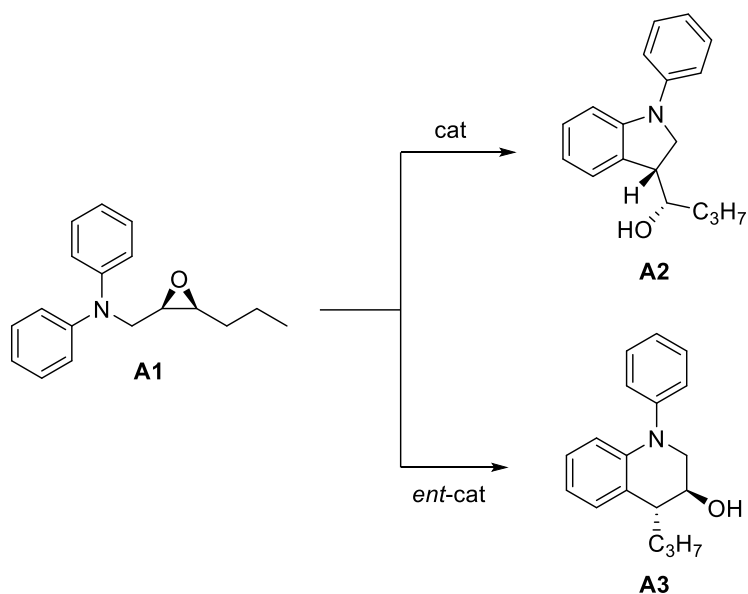


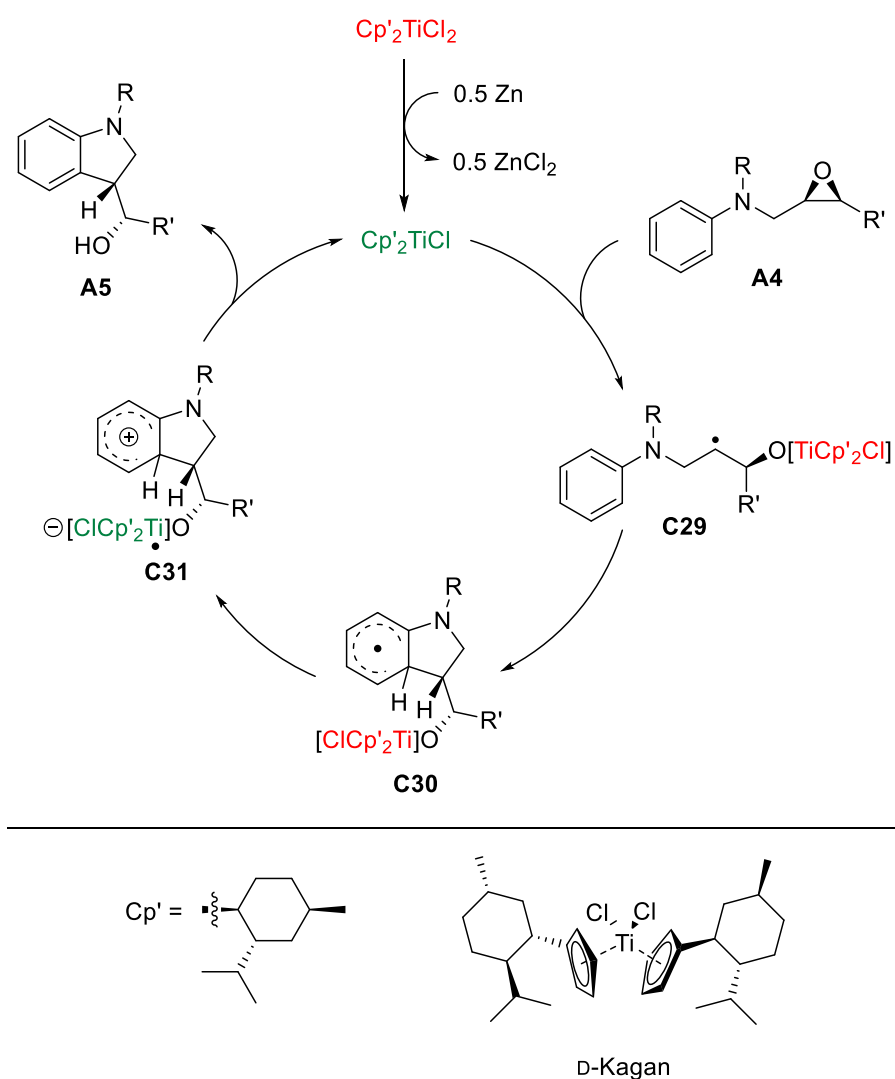
Figure 20: Basic structure of REO-Arylation substrates.^[149]

In contrast to the first reported arylation, the regioselectivity for the epoxide opening does not depend on the *Markovnikov*-rule, as in both possible cases, a secondary β -titanoxy radical would be formed. Because of this, an enantiomerically pure titanocene catalyst is employed, controlling the regioselectivity and thus the product formed in the reaction. Depending on the enantiomer used, an indoline **A2** or tetrahydroquinoline **A3** is obtained as arylation product (**Scheme 30**). The catalytic cycle of the REO-arylation does not substantially vary from the one presented for the radical arylations in chapter 2.3. Most importantly, a derivative of *Kagan's* complex is employed as titanocene catalyst. The cycle is displayed in **Scheme 31** for the formation of indolines from suitable substrate **A4**, the mechanistic steps proceed identically for the formation of the respective tetrahydroquinoline product, apart from the regioselectivity in the epoxide opening.^[149]

The diastereoselectivity of the REO-arylation (compare to **Scheme 30**) is rationalized by the formation of two diastereomeric transition states during the approach of the secondary radical to the arene in intermediate **C29**. Steric repulsion of substituents R and R' as well as *Felkin-Anh*-selectivity^[254,255] disfavor the transition state leading to a *syn*-diastereoisomer, enforcing the *anti*-product **C30** (**A5**) almost exclusively. For THQ formation, a similar explanation is reported, giving the *anti*-THQ-product.^[149]

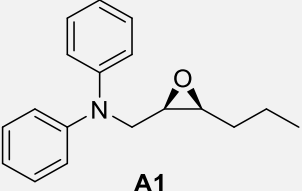
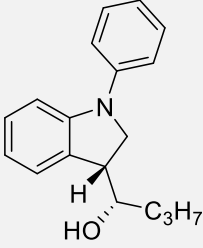
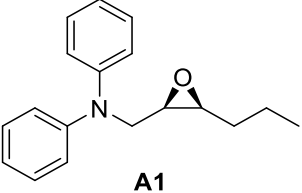
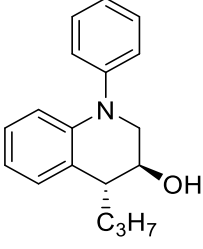
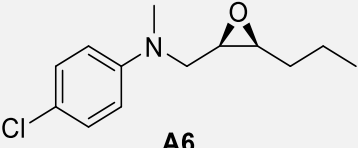
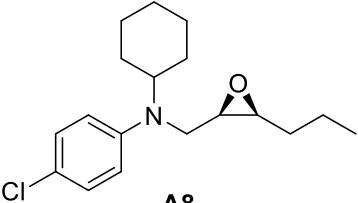
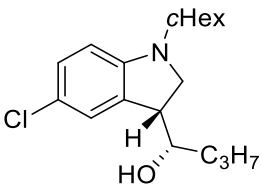
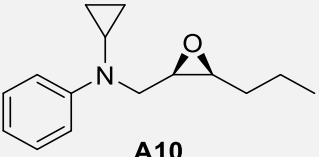
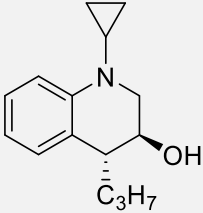


Scheme 30: Concept of product scope for the REO-arylation of epoxide **A1**.^[149]



Scheme 31: Catalytic cycle for the formation of indolines in the REO-arylation.^[149]

Table 8: Selected scope of indoline and THQ synthesis via REO-arylation.

No.	Substrate	Catalyst	Product	Yield [%]
1 ^[a]	 A1	D-Kagan-Cl ₂	 A2 , <i>r.r.</i> = 90:10 <i>d.r.</i> = 92:8	72
2	 A1	L-Kagan-(OTs) ₂	 A3 , <i>r.r.</i> = 94:6 <i>d.r.</i> = 76:24	73
3	 A6	L-Kagan-(OTs) ₂	 A7 , <i>r.r.</i> = >98:<2 <i>d.r.</i> = 94:6	81
4	 A8	D-Kagan-Cl ₂	 A9 , <i>r.r.</i> = 92:8 <i>d.r.</i> = 84:16	57
5	 A10	L-Kagan-(OTs) ₂	 A11 , <i>r.r.</i> = 93:7 <i>d.r.</i> = 88:12	81

Conditions: 7 mol% catalyst, 30 mol% Zn, 30 mol% Lut⁺HCl, 0.2 M in THF, rt, 48 h. *d.r.* of crude products. [a] 5 mol% cat.^[149]

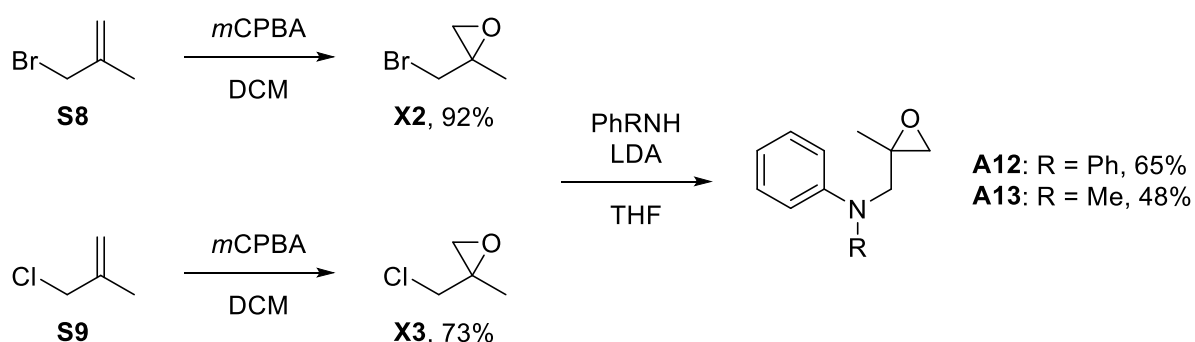
Mühlhaus and Weißbarth investigated the scope and optimal conditions of the REO-arylation for various alkyl- and aryl-substituted substrates. An exemplary selection is presented in **Table 8**.^[149]

Overall, these examples show that the REO-arylation of epoxides is an excellent method for the diastereoselective synthesis of enantiomerically pure indolines and tetrahydroquinolines in good yields. Screening reactions revealed that for the synthesis of the indolines, the chloride-substituted *Kagan's* complex gave the best results (*Kagan-Cl*₂).

For THQ synthesis, the tosylate derivative was employed (*Kagan*-(OTs)₂). Moreover, the indoline products always exhibited a good diastereoisomeric ratio which was generally higher than that for THQs.^[149] The best result was however obtained for the THQ synthesis from epoxide **A6** (entry 3), giving high yield and ideal regio- and diastereoselectivity. Due to this result, epoxide **A6** has been chosen as screening substrate for photocatalytic REO-arylations (chapter 3.4.2).

3.4.1 Arylation Substrate Synthesis

The substrates for the 'conventional' as well as for the REO-arylation can be obtained via reliable, a modular synthesis from commercially available precursors in a few synthetic steps. The synthesis of arylation substrates is shown in **Scheme 32**. Modifications are possible by using functionalized aniline derivatives, as long as their nucleophilicity is high enough to undergo the S_N2-reaction with **X2** or **X3**. For the presented examples, no double-alkylation leading to the respective ammonium salts is observed in the second step, the alkylating agent is employed in a slight excess of 1.2 eq. with regard to the aniline.

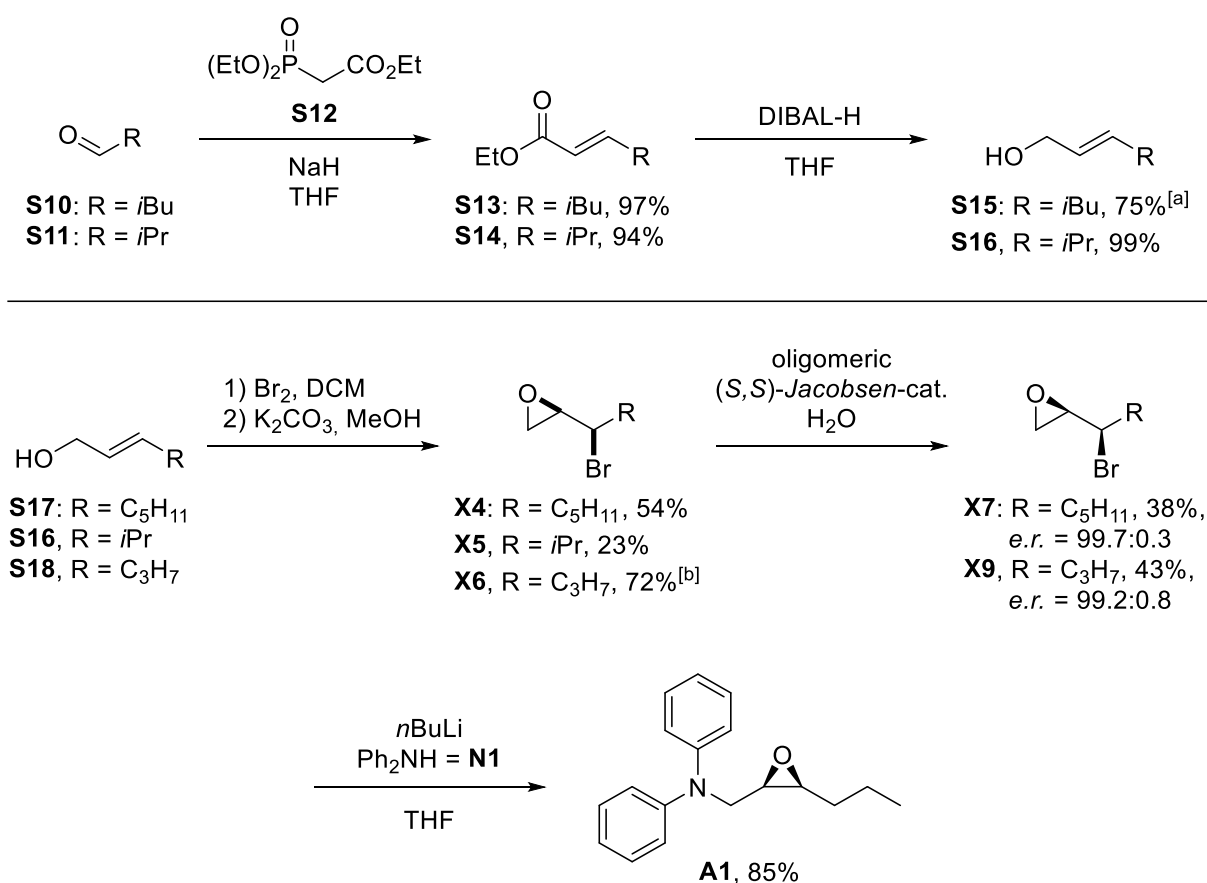


Scheme 32: Synthesis of arylation substrates. **X2** employed in the S_N2-reaction.

For REO-arylation substrates, the synthetic effort is significantly higher, as the substrate has to be made in enantiomerically pure form (**Scheme 33**). This requires a potent method for the preparation of enantiomerically pure epoxides. The hydrolytic kinetic resolution (HKR) by *Jacobsen* using the oligomeric *Jacobsen*-catalyst is employed to resolve the enantiomers of

terminal α -bromo epoxides.^[256–258] The synthetic approach starts from (*E*)-allylic alcohols, which are either commercially available (**S17** and **S18**), or can be made from the corresponding aldehyde via a *Horner-Wadsworth-Emmons*-olefination with subsequent ester reduction by DIBAL-H (**S15** and **S16**) in excellent yields. Upon bromination of the allylic double bond, an α,β -dibromo alcohol is obtained and immediately converted into the respective terminal α -bromo epoxide (**X4** to **X6**) via an intramolecular S_N2 -reaction promoted by stirring with K_2CO_3 in MeOH.^[259,260] The epoxides are resolved in an HKR yielding enantiomerically pure (*e.r.* >99:<1) α -bromo epoxides (**X7** and **X9**). The REO-arylation substrate is obtained after an S_N2 -reaction with a (substituted) aniline derivative (**N1**), opening the terminal epoxide which then undergoes a ring closure losing bromide.

This procedure works well for diaryl- or aryl/alkyl-substituted amines. However, free N–H bonds or common N-protecting groups cannot be used.^[149] Employing various other nucleophiles to establish new REO-substrates was tested in multiple approaches under different reaction conditions, these reactions are discussed in chapter 3.5.1.

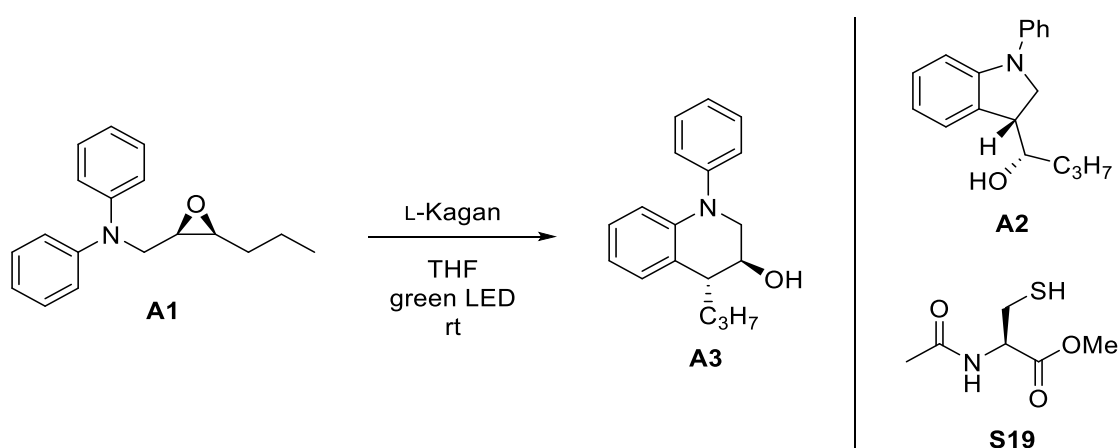


Scheme 33: Modular synthesis of enantiomerically pure REO-arylation substrates.^[149]

[a] Performed by *Heinz*.^[217] [b] Performed by *Weißbarth*.^[220]

3.4.2 Photochemical REO-Arylations

As titanocene catalyzed (REO)-arylations of epoxides are atom economic reactions, meaning that all atoms of the substrate are found in the resulting product, they can be performed without the need for hydrogen atom donors. As Cp_2TiCl_2 can act as both photocatalyst and electron transfer catalyst,^[135] Kagan's complex was assumed to have similar properties due to its nearly identical UV-Vis absorption spectrum. This was tested during a series of screening reactions (**Scheme 34**), the results for the REO-arylations of epoxide **A1** are presented in **Table 9**.



Scheme 34: General THQ synthesis from **A1** in the REO-arylation with indoline **A2** as side-product. Conditions: 10 mol% cat., 0.1 to 1.0 eq. additive if used, 0.05 M in THF.

Table 9: Investigated reaction conditions for REO-arylations of **A1**.

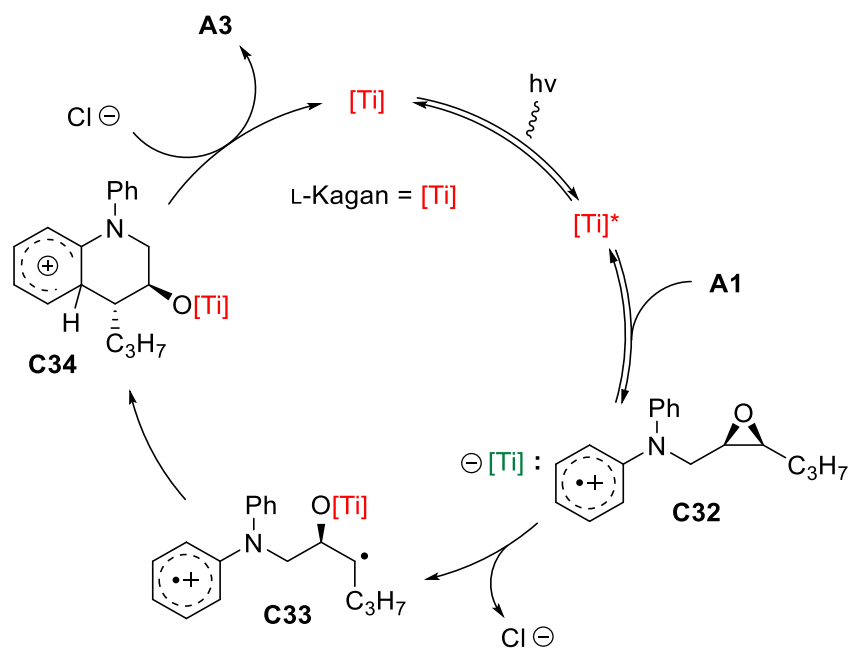
No.	Catalyst	Additive	Temp.	Reaction time	Yield A3:A2 [%]
1 ^[a]	D-Kagan	-	rt	46 h	-
2 ^[b]	L-Kagan	-	rt	46 h	-
3 ^[b]	L-Kagan	MTG ^[c]	65°C	18 h	-
4 ^[b]	L-Kagan	S19 ^[c]	65°C	18 h	-
5	L-Kagan	Ph_3N ^[d]	60°C	4 h	40:23
6	L-Kagan	Ph_3N ^[d]	rt	4 h	13:6
7	L-Kagan	Ph_3N ^[e]	rt	4 h	12:6
8	L-Kagan	(<i>p</i> -MeOPh) Ph_2N ^[e]	rt	4 d	26:11
9	L-Kagan	-	rt	4 d	24:11
10	L-Kagan	3DPAFIPN ^[f]	rt	6 d	14:3

NMR-yield. [a] 0.2 M in THF. [b] 0.8 M in THF. [c] 10 mol%. [d] 1.0 eq. [e] 20 mol%. [f] 3 mol%, blue LED, 0.1 M in THF.

The first attempts basically employed the reported reaction conditions of conventional REO-arylations (entries 1 and 2) under irradiation with green LEDs, performing the reaction at room temperature over 2 days.^[149]

Unfortunately, neither the indoline nor the THQ could be obtained by this method. Higher reaction temperatures in combination with thiols as hydrogen atom transfer catalysts, as used in the photoexcited titanocene catalyzed epoxide openings (chapter 3.2), showed no product formation as well (entries 3 and 4).

A major improvement was achieved when using Ph_3N as additive (entry 5). At 60°C even after a short reaction time of 4 h, 40% of the desired THQ **A3** were yielded. On the other hand, the reaction did not proceed with a good regioselectivity, as additionally 23% of the indoline derivative **A2** were formed. The first approach to explain this finding was that due to the high reaction temperature, the catalyst selectivity was decreased. Hence, the reaction was repeated at room temperature. This led to a drastic decrease in conversion and yield (entry 6). Surprisingly, the ratio of THQ:indoline did not change significantly being 13:6 under these conditions. Decreasing the amount of Ph_3N employed from 1.0 eq. to 0.2 eq. resulted in the same yields (12:6, entry 7).



Scheme 35: Proposed catalytic cycle for the THQ formation via photocatalyzed REO-arylation.

To investigate, whether a more electron rich aryl amine favors the required quenching of the excited titanocene (details in the catalytic cycle, **Scheme 35**) and therefore accelerates the reaction, (*p*-MeOPh) Ph_2N was used. Indeed, the yields could be increased to 26% and 11%, respectively, keeping the ratio of **A3**:**A2** almost fixed (entry 8). However, the reaction was additionally stirred for a much longer reaction time. Thus, the effect of the amine cannot be

unequivocally assessed. Especially interesting in this regard is the reaction described in entry 9, as even without any additive, at a longer reaction time the yields could be increased to 24% and 11%, respectively. Employing 3DPAFIPN as external photoredox catalyst led to poor results, even after an exceptionally long reaction time (entry 10).

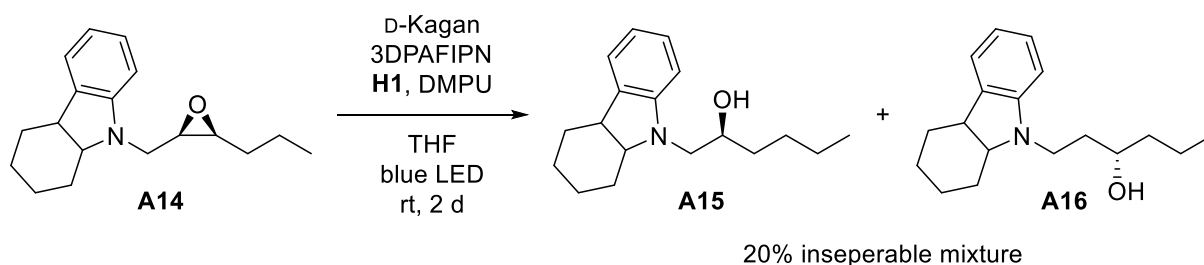
The role of external quenchers has to be evaluated more thoroughly. A possible explanation can be derived from the proposed catalytic cycle of the photochemical REO-arylations, which is displayed in **Scheme 35**.

As the titanocene (*Kagan's* complex) is photochemically excited and then reduced by the aryl amine present (either the substrate or the external quencher), no zinc or manganese is required. In the proposed cycle, **A1** donates an electron to the photoexcited titanocene in close proximity via an outer-sphere electron transfer (OSET). Thereby, radical cation **C32** is generated (mesomeric stabilization over nitrogen and second phenyl omitted for clarity). Upon regioselective reductive epoxide opening, diradical **C33** is obtained, which can undergo radical recombination to give cationic species **C34**. Rearomatization and cleavage of the titanocene by a proton transfer leads to formation of THQ **A3** and liberation of the unexcited catalyst.

This catalytic cycle features some major differences compared to the 'classic' cycle for radical arylations (**Scheme 16** and **Scheme 31**): Apart from catalyst activation, a radical cation is formed from the substrate before the epoxide is opened. This lowers the electron density in the aromatic system and favors a nucleophilic attack to the arene. After generation of the β -titanoxy radical, an intramolecular radical cyclization (recombination) is possible, which is generally a favorable reaction.^[152,261–265] Subsequently, cationic intermediate **C34** is obtained without the slow, rate determining PCET necessary in the 'classic' mechanism. In this new cycle, the catalyst is liberated in the catalytically inactive Ti(IV) form and must be excited again for activation.

When a triaryl amine is added to the reaction mixture as external quencher, radical cation **C32** is not formed, as the electron is transferred from the quencher instead of the arylation substrate. This requires close proximity of excited catalyst and quencher. As this process is assumed to be reversible, the Ti(III) can only open an epoxide, if this is also closely present. Substrate and external quencher compete for the electron transfer. This is why the use of external quenchers does not necessarily increase the yield of the arylation.

Even if the β -titanoxy radical is formed by the reduced titanocene catalyst, the cyclization was much slower compared to the cyclization of displayed diradical cation **C33**. This hypothesis is supported by investigations performed by *Heinz*, as he obtained the 1,2- and 1,3-aminoalcohols instead of the arylation-products when performing reactions with a novel REO-substrate.^[217]

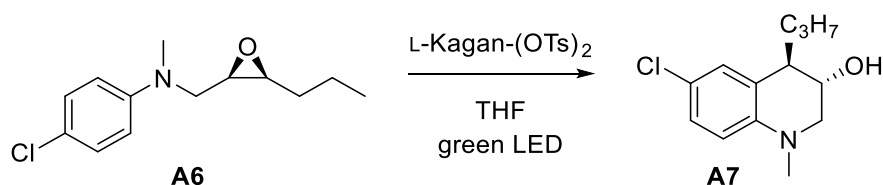


Scheme 36: REO by *Heinz*.^[217] Conditions: 10 mol% D-Kagan, 3 mol% 3DPAFIPN, 2.0 eq. **H1**, 1.5 eq. DMPU, 0.1 M in THF. Isolated yield.

The investigated reaction is depicted in **Scheme 36**. This indicates that the intramolecular arylation does not occur although the β -titanoxy radical must be reduced intermolecularly. In general, the REO-arylation is a slow reaction compared to the conventional arylation, the reaction times vary greatly (48 h versus 30 min).^[139,149]

Heinz also reported catalyst decomposition in his research on photochemical REO-arylations as indicated by a color change of the reaction mixture from dark red to yellow after a few hours of irradiation.^[217] UV-Vis investigations of this decomposition or photolysis process also indicate the loss of one Cp-ligand from the titanocene.^[213] In this case, longer reaction times would not influence the conversion, as the decomposed catalyst is not able to reenter the catalytic cycle. This is supported by the best REO-arylation results obtained (entry 5) in **Table 9**, showing that the conversion is influenced by a high reaction temperature rather than by a long reaction time.

Besides substrate **A1**, the best substrate for the conventional REO-arylations^[149] (**Table 8**) by *Mühlhaus* and *Weißbarth*, **A6**, was also employed under photocatalytic conditions (**Scheme 37**). For this, L-Kagan-(OTs)₂ was chosen as catalyst, as it originally yielded the best results.^[149] The respective reaction results are summarized in **Table 10**.



Scheme 37: General THQ synthesis from **A6** in the REO-arylation. Conditions: 10 mol% cat., 1.0 eq. additive if used, 0.05 M in THF.

Table 10: Investigated reaction conditions for REO-arylations of **A6**.

No.	Catalyst	Additive	Temperature	Reaction time	Yield [%]
1	L-Kagan-(OTs) ₂	-	65°C	24 h	-
2	L-Kagan-(OTs) ₂	-	65°C	72 h	-
3	L-Kagan-(OTs) ₂	-	rt	72 h	-
4	L-Kagan-(OTs) ₂ ^[a]	-	65°C	72 h	-
5	L-Kagan	Ph ₃ N	60°C	16 h	37 ^[b]

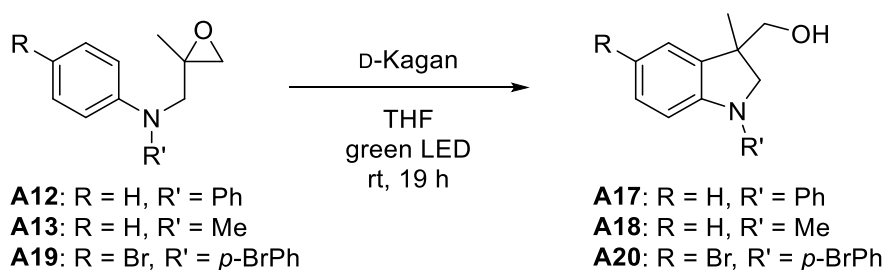
[a] 20 mol% cat. [b] NMR-yield.

It turned out that although L-Kagan-(OTs)₂ catalyzes REO-arylations under the ‘classic’ conditions, its performance in photochemical REO-arylations is much poorer. In fact, no conversion was obtained in any of the investigated reactions, even at elevated temperatures, higher catalyst loading or long reaction times (entries 1 to 4). Surprisingly, the application of L-Kagan in combination with Ph₃N as external quencher led to the formation of 37% of the desired THQ **A7**. At first sight, this contradicts the results presented for the conversion of **A1** (Table 9), in which an external quencher did not increase the yield. However, the electronic properties of **A1** and **A6** vary greatly.

To successfully reductively quench the excited titanocene catalyst, an electron has to be transferred to it in an OSET. This requires a high electron density at the respective quencher, which is given for the two unsubstituted aryl substituents at substrate **A1**. In contrast, **A6** only possesses one aryl substituent, which is in addition less electron rich due to the *para*-chloro substitution. Because of that, **A6** might not be able to act as a reductive quencher and, thus, only Ph₃N meets the required redox potential.^[266,267]

3.4.3 Photochemical Arylations

To further investigate the influence of the substitution pattern of aniline-derived arylation substrates as well as finding suitable titanocene catalysts for photochemical radical arylations, the less complex and fast 'classic' arylation of **A12** and derivatives was chosen (**Scheme 38**). The corresponding reaction results are given in **Table 11**. For the least electron rich substrate **A13**, no product formation could be obtained, even adding electron rich (*p*-MeOPh)₃N did not give any conversion.



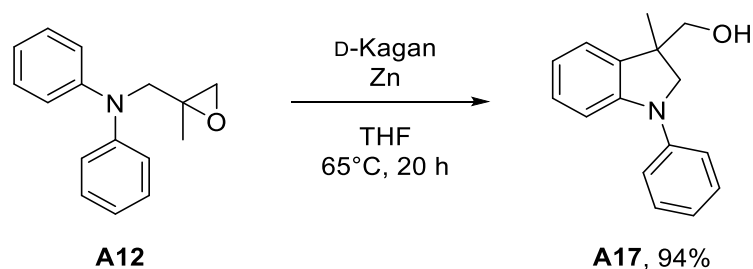
Scheme 38: General indoline synthesis in photochemical arylations. Conditions: 10 mol% D-Kagan, 0.05 M in THF.

Table 11: Investigated reaction conditions for photochemical arylations.

No.	Substrate	Product	Yield [%]
1 ^[a]	A12	A17	93
2	A13	A18	-
3 ^[b]	A13	A18	-
4	A19	A20	53

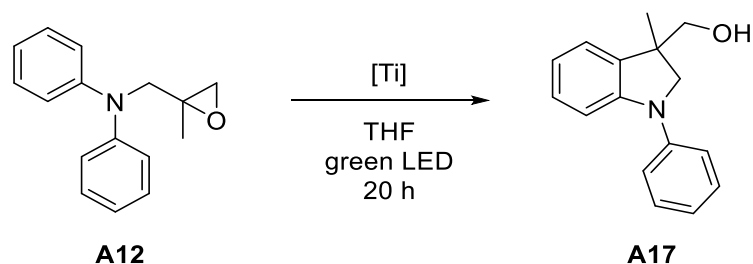
NMR-yield. [a] 20 h. [b] Addition of 1.0 eq. (*p*-MeOPh)₃N.

For the *para*-bromo substituted substrate **A19**, the indoline was formed in 53% yield and the standard substrate **A12** gave almost perfect 93%. These findings indicate that the diphenyl-substituted pattern is best suited for successful photochemical arylations. Employing the classic zinc reduced conditions with D-Kagan at 65°C did not result in a higher product formation, 94% of **A17** was isolated (**Scheme 39**). Using photocatalytic conditions with 3 mol% 3DPAFIPN and blue light irradiation diminishes the yield to 73% (5.5.1.2).



Scheme 39: Classic radical arylation of **A12**. Conditions: 10 mol% D-Kagan, 10 mol% Zn, 0.05 M in THF.

With these results in hand, **A12** was selected for further investigation of suitable titanocenes for the radical arylation (**Scheme 40**). When titanocene dichloride is used as catalyst, 62% of the desired indoline could be isolated (**Table 12**, entry 1). Lower catalyst loading (5 mol%, entry 2) led to major diminution of conversion. Although finding this almost ideal catalytic system with only catalyst, substrate and solvent necessary as reagents in an atom-economic reaction was already a great result, even more spectacular conditions could be found.

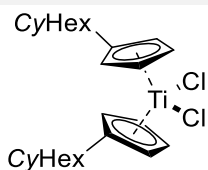
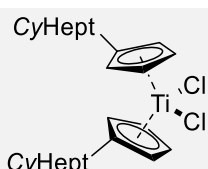
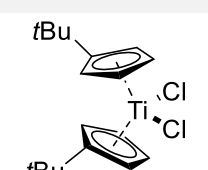
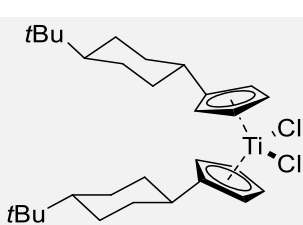
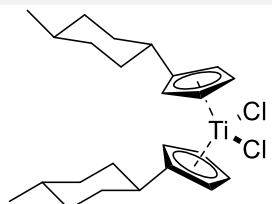


Scheme 40: Photochemical radical arylations of **A12**. Conditions: 10 mol% catalyst, 0.05 M in THF.

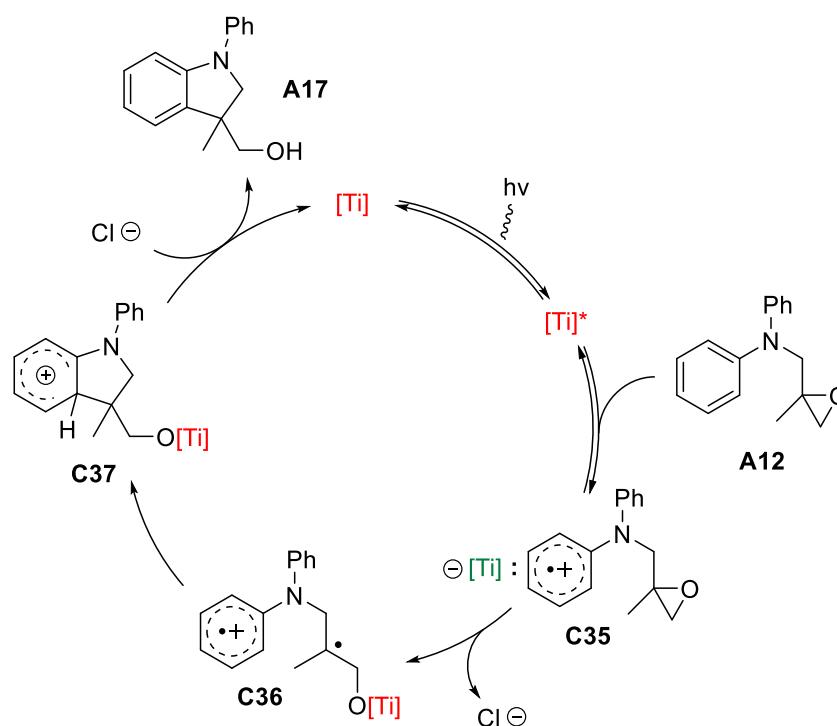
Repeating the reaction with *Kagan's* complex at reflux temperature gave 93% of the desired product (72% isolated), at room temperature 95% of **A17** were obtained (entries 3–5). An elevated reaction temperature does apparently not play a crucial role for this reaction. When $(\text{CyHexCp})_2\text{TiCl}_2$ is used as catalyst at reflux temperature, a minor yield of 62% was isolated. In addition, a series of electron rich titanocenes, structurally similar to *Kagan's* complex, was tested at room temperature to see, whether steric bulk at the Cp-ligand influences the catalyst performance (entries 7–10). Surprisingly, $(\text{CyHeptCp})_2\text{TiCl}_2$ only yielded 63% indoline, whereas the sterically more demanding examples (entries 8–10) resulted in excellent yields of 88–93%. Nevertheless, none of these titanocenes was able to outperform *Kagan's* complex with 95%. Based on this, mainly the electronic influence of the alkyl-substituents on the titanocene define the performance in the arylation reaction. Steric effects are less important with the exception of $(\text{CyHeptCp})_2\text{TiCl}_2$. The proposed catalytic cycle for this photochemical radical arylation is similar to the one suggested for the photochemical REO-arylations. It is shown in **Scheme 41** and starts with the photoexcitation of the respective Ti(IV) precatalyst.

The excited species $[Ti]^*$ is reductively quenched by substrate **A12** via an OSET to give $[Ti(III) : \text{radical cation}]$ complex **C35**. The epoxide is reductively opened by a SET forming the β -titanoxy radical **C36**. Upon radical recombination, cationic intermediate **C37** is generated, from which indoline **A17** and titanocene(IV) precatalyst are liberated. Less electron rich substrates **A13** and **A19** are less potent reductive quenchers for the excited titanocene and therefore, the formation of active $Ti(III)$ catalyst is reduced.

Table 12: Investigated reaction conditions for photochemical arylations.

No.	Catalyst	Temperature	Yield [%]
1	Cp_2TiCl_2	rt	62
2	$Cp_2TiCl_2^{[a]}$	rt	<20 conv.
3	D-Kagan	65°C	93
4	D-Kagan	rt	95
5	L-Kagan	65°C	72 ^[b]
6		65°C	62 ^[b]
7		rt	63
8		rt	91
9		rt	88
10		rt	93

NMR-yield. [a] 5 mol% catalyst. [b] Isolated yield.



Scheme 41: Proposed catalytic cycle for the photocatalyzed radical arylation of **A12**.

In summary, especially alkyl substituted titanocenes, such as *Kagan's* complex, have proven to be useful and efficient photoredox catalysts, especially for photocatalyzed radical arylations of electron rich substrates. Nevertheless, they lack stability in reactions with long irradiation times, as they are prone to photolysis. Because of this, more stable conditions for REO-arylations and modifications to enable conversion of a broader substrate scope will have to be found. However, the given examples make a solid basis for future investigations on this topic.

3.5 REO and DEO Substrates

Regio- or diastereodivergent epoxide opening reactions using *Kagan's* complex as catalyst require either enantiomerically pure *syn*-1,2-epoxides as REO substrates (**Figure 21**) or *pseudo*-racemic mixtures of *syn*-1,2-epoxides for DEO reactions, if another stereocenter with a defined configuration is present in the molecule. If racemic mixtures are employed, the reaction is called a parallel resolution.

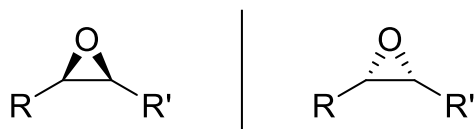


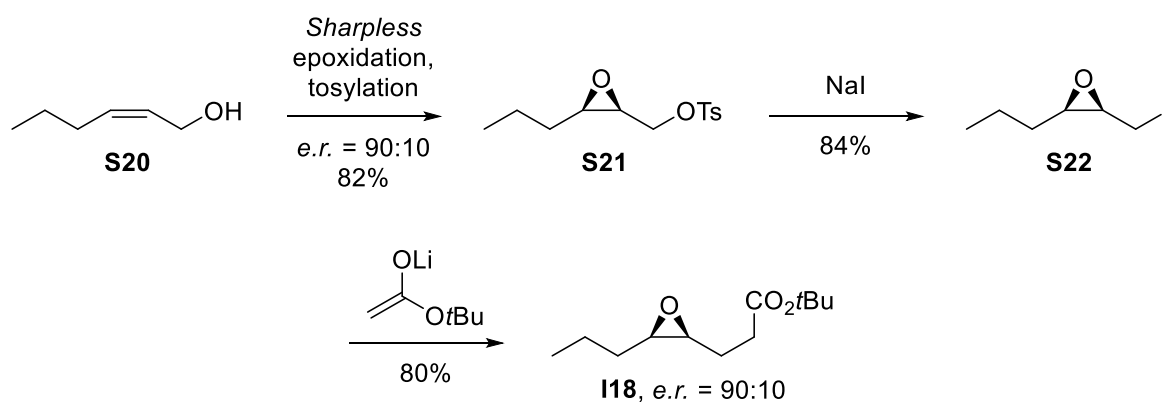
Figure 21: General structure of REO substrates.

Especially the field of REO reactions has been investigated over the past decade by the group of *Gansäuer*, as this reaction type enables stereoselective and reliable access to optically pure compounds in high yield.^[91–94,96,101,110,149,221,268]

Whereas the ideas and concept behind REO and DEO reactions have been explained in chapters 2.2.1 and 2.2.2, the synthesis of suitable substrates has not been elucidated yet. The first idea to synthesize *syn*-1,2-epoxides is an epoxidation of (*Z*)-olefins, in which R equals R'. In this case, a *meso*-epoxide is obtained, which can be used in enantioselective desymmetrization reactions. However, as *meso*-compounds are achiral, technically their desymmetrizations constitute as subclass of the REO as only one substrate reacts.^[96] Desymmetrizations are not a double asymmetric process and thus the enantiomeric ratio of the product solely depends on the catalyst's stereoselectivity.

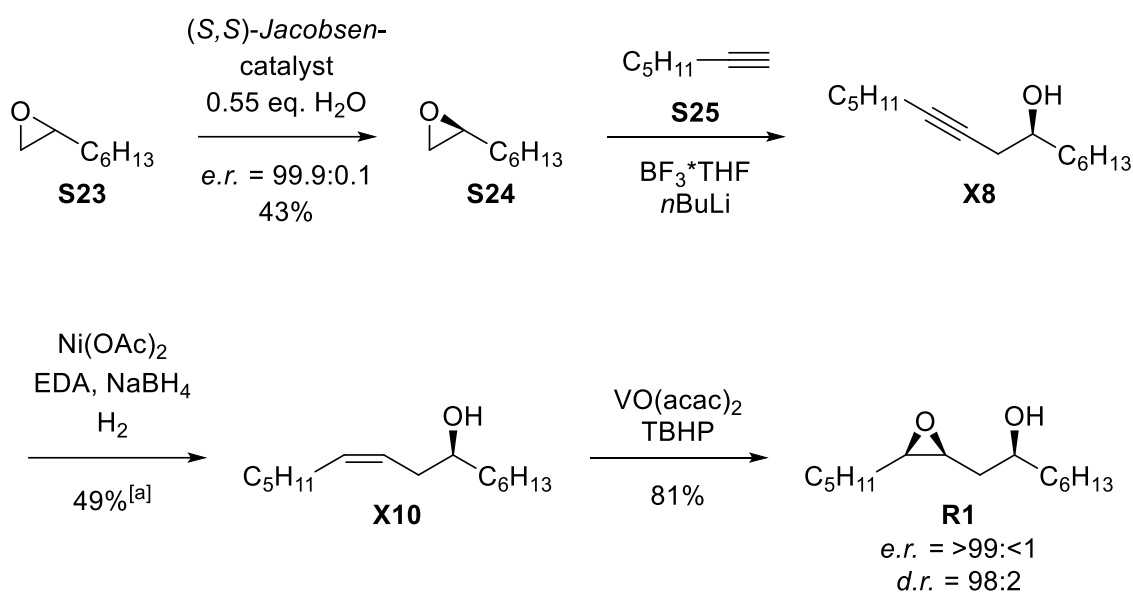
The reaction of a DEO substrate (referred to *pseudo*-racemic mixture for clarity) can be classified as a parallel resolution regarding the epoxide, as both *pseudo*-enantiomers react at a similar rate (**Scheme 11**).^[96] Here, the products are formed as major product of one *pseudo*-enantiomer and minor product of the other. Again, the ratio of the products solely depends on the catalyst's regioselectivity – 90% catalyst regioselectivity results in a product ratio of 90:10 (in case of pure catalyst regiocontrol).

REO substrates are ideally highly enantiomerically enriched or even enantiomerically pure. In this case, the reaction product is formed as the major product of the predominant enantiomer and minor product of the minor enantiomer. This double asymmetric strategy leads to exceptionally high enantiomeric ratios, higher than in the employed substrate (**Scheme 10**).^[96,269] The substrate shown in **Scheme 9** proving the usefulness of the REO was prepared by an asymmetric *Sharpless*-epoxidation in an efficient synthesis with an enantiomeric ratio of 90:10 of the resulting epoxide (**Scheme 42**).^[95]



Scheme 42: Synthesis of first enantiomerically enriched REO substrates by *Gansäuer*.^[95]

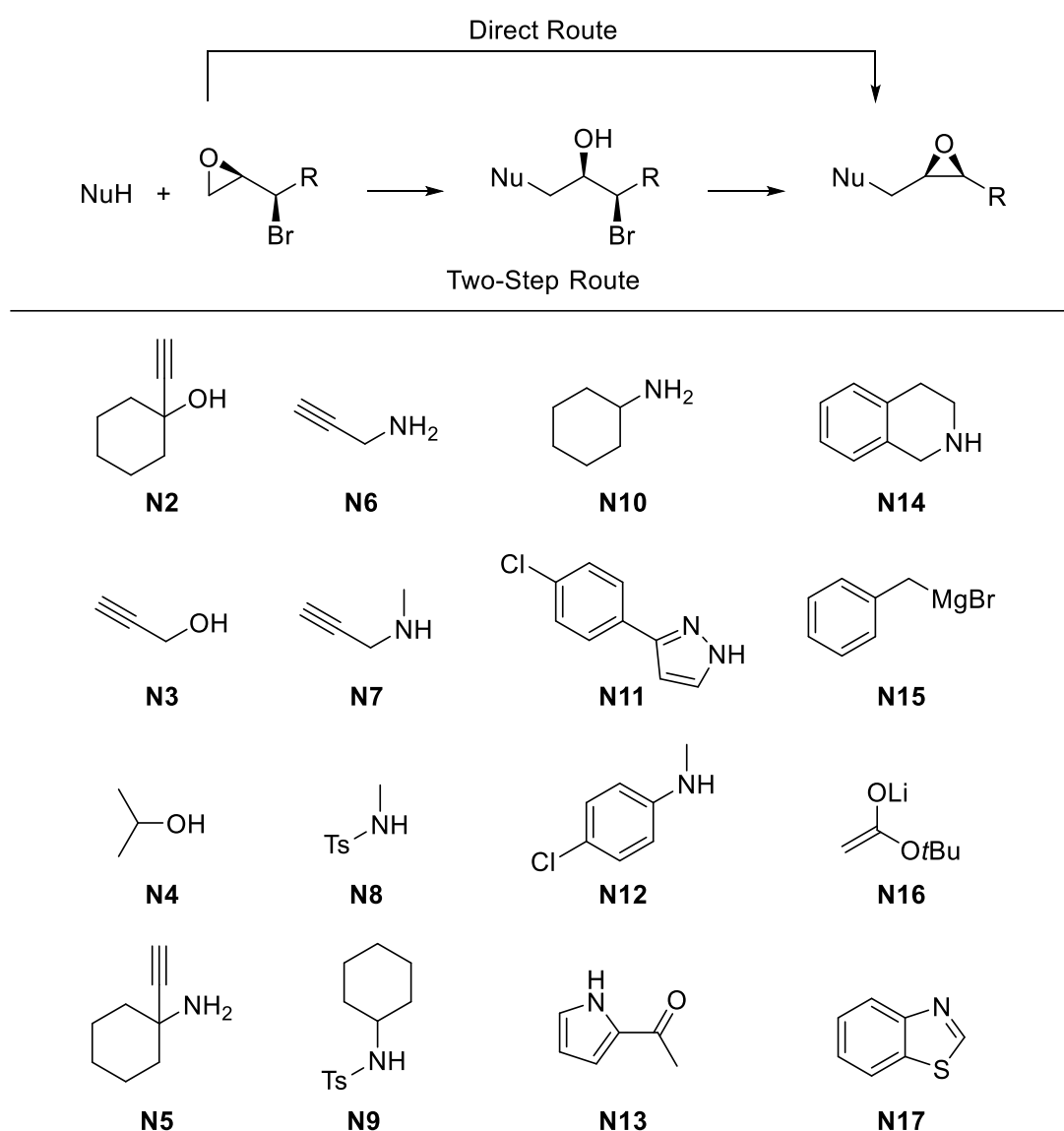
A strategy developed to achieve higher enantiomeric ratios (up to *e.r.* >99:<1) as well as the implementation of a third 'enantiomerically pure' chiral center utilizes the hydrolytic kinetic resolution (HKR) of terminal epoxides by *Jacobsen*.^[110,270–272] The synthetic approach is displayed in **Scheme 43** for a selected exemplary REO substrate **R1** and starts with the mentioned HKR. The maximum yield in this reaction is limited to 45% (for 0.55 eq. of H₂O), epoxide **S23** is cheap and commercially available. **S24** is obtained enantiomerically pure and this stereocenter is set for the following reaction steps including the final product. Alkyne addition and *syn*-reduction^[273,274] yield (*Z*)- β -hydroxy alkene **X10** which is then converted in a *syn*-selective epoxidation with VO(acac)₂ and TBHP.^[275–277] **R1** represents the general structure of an enantio- and diastereomerically pure REO substrate. Overall, the synthetic route is only one step longer than the previously described. It can be synthetically modified by for example alcohol inversion, substitution, or protection.



Scheme 43: Synthetic approach to enantiomerically and diastereomerically pure REO substrates.^[110] [a] Yield over two steps.

3.5.1 Novel REO Substrate Concepts

Besides the presented route, the HKR was used as starting point for a series of testing reactions to synthesize new REO substrates by addition of different nucleophiles. For this, enantiomerically pure α -bromo epoxides were synthesized according to the procedure developed for the formation of REO-arylation substrates (**Scheme 33**). Instead of employing diaryl amines as nucleophiles, various C-, N- and O-nucleophiles were tested for their performance in an S_N2 -reaction with the terminal epoxide (**Scheme 44**). By these methods, REO substrates for the synthesis of enantiomerically pure alcohols and cyclization reactions were prepared in collaboration with *Zhang and Heinz*.^[217,234]



Scheme 44: Strategies for the synthesis of new REO substrates and screened nucleophiles.

REO cyclization substrates require a double or triple bond in δ -position for 5-*exo*-cyclizations or ϵ -position for 6-*exo*-cyclizations regarding the radical formed after reductive epoxide opening according to *Baldwin's* rules.^[278,279] For these, O- and N-nucleophiles containing a terminal alkyne were selected.

The other employed nucleophiles exhibit different steric demands, electronic properties, protecting groups or secondary reactive sites for possible further modifications.

3.5.2 REO and DEO Substrate Synthesis

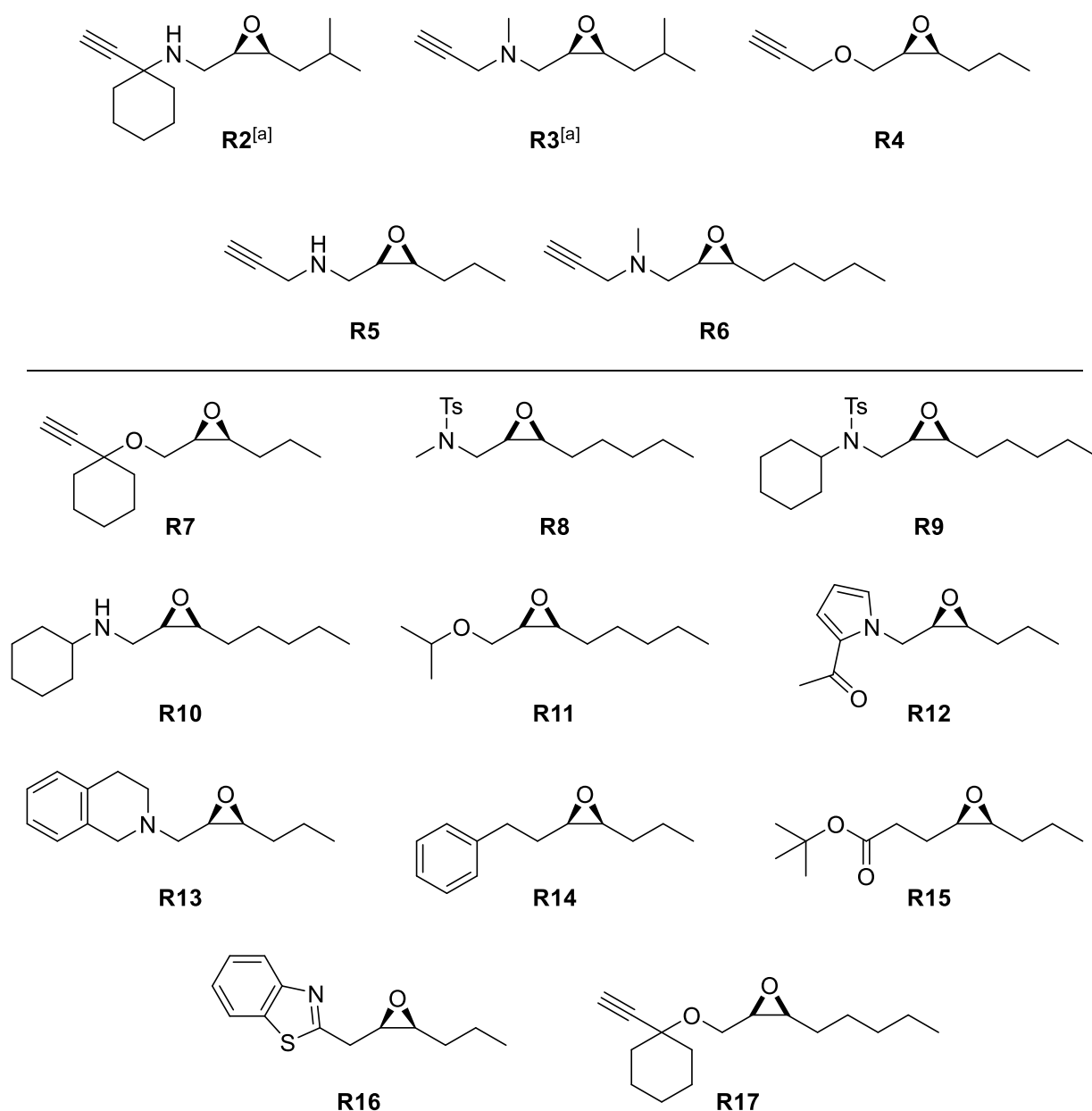
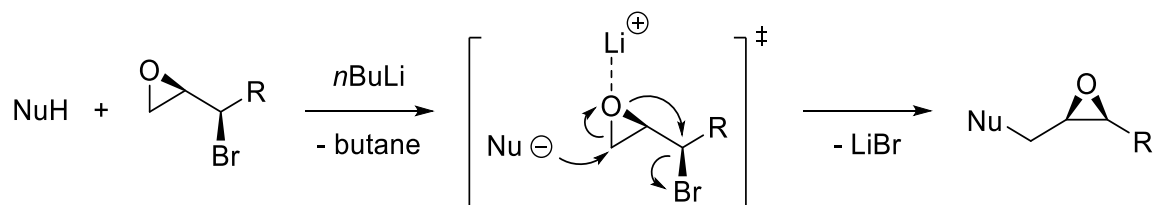


Figure 22: New REO substrates (top) and attempted structures (bottom). [a] Synthesized by Heinz.^[217]

To ensure optical purity of the REO substrates, α -bromo epoxides are converted in an HKR and thus prepared enantiomerically pure. The addition of nucleophiles leads to epoxide opening and subsequent closure, either in one step (direct route, **Scheme 44**) or in two reaction steps with isolation of the intermediate bromo alcohol. The reaction conditions are based on the reported procedures for the synthesis of REO-arylation substrates.^[149]

The REO substrates synthesized in collaboration with *Heinz* during his M.Sc. project are displayed in **Figure 22 (R2–R6)**. Furthermore, unsuccessfully attempted compounds are shown. Some compounds cannot be classified as REO substrates, as they were prepared using racemic α -bromo epoxides. Thus, their epoxide openings are parallel resolutions.

Initial experiments via the direct route were conducted using *n*BuLi as base for deprotonation of the respective nucleophile (**Scheme 45**). This increases the nucleophilicity and in a double S_N2 -reaction, the desired product is obtained. The lithium cation is acting as *Lewis* acid, activating and thus favoring the epoxide opening. The binding must not be too strong, as otherwise the subsequent epoxide formation is hindered and an α -bromo alcohol is formed, which is the case in the two-step approach, but undesired here. The reactions performed under these conditions are listed in **Table 13**.



Scheme 45: Double S_N2 -mechanism in the synthesis of REO substrates from enantiomerically pure α -bromo epoxides.

Table 13: Synthesis of REO substrates via the direct double S_N2 route.

No.	Nucleophile	Epoxide	Reaction time [h]	Yield [%]
1	N2	X4	19	-
2	N10	X4	19	-
3	N4	X4	21	-
4	N13	X9 ^[a]	22	-
5 ^[b]	N14	X9	48	-
6 ^[c]	N16	X9 ^[d]	20	-
7 ^[b]	N17	X9	19	-
8	N1	X9	44	85

Conditions: 1.2 eq. epoxide, 1.05 eq. *n*BuLi, 0.5 M in THF. **N1** = Ph₂NH. [a] 1.1 eq. epoxide. [b] 1.2 eq. *n*BuLi. [c] 0.4 M in THF. [d] 1.0 eq. epoxide.

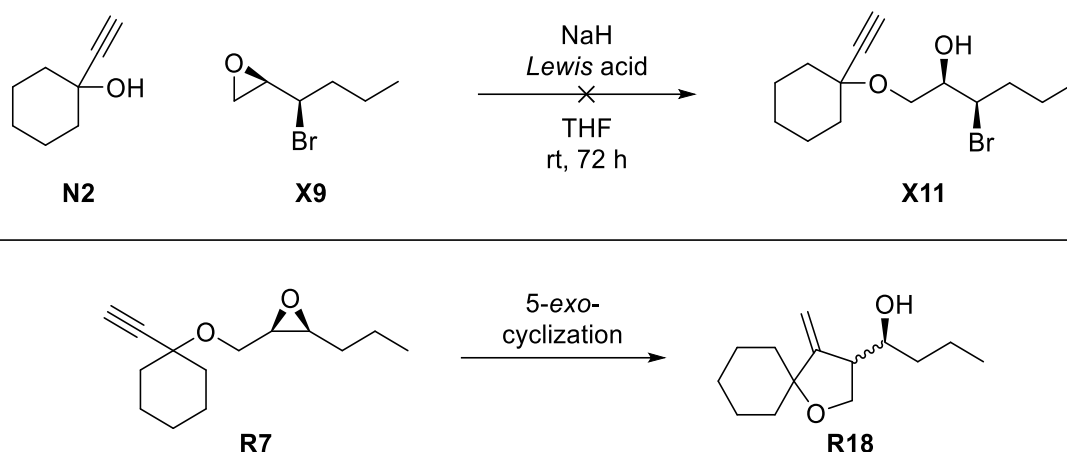
For condition evaluation, racemic epoxide **X4** (compare chapter 3.4.1, **Scheme 33**) has been employed (entries 1–3). Unfortunately, none of the tested nucleophiles was able to successfully perform the epoxide opening. In most cases, unreacted substrates were recovered (entries 1–7). Entry 8 shows that for diaryl amines these reaction conditions can be reliably applied for substrate synthesis.^[149] This suggests that only highly nucleophilic compounds, such as diaryl amides are suitable nucleophiles under these reaction conditions. Steric repulsion should not be limiting the reaction performance, as only **N2** (entry 1) can be considered demanding in this regard.

Furthermore, *n*BuLi is a strong enough base ($pK_b(n\text{BuLi}) = -36$ ^[280,281]) to quantitatively deprotonate alcohols and amines, hence solely the corresponding lithium alcoholates and amides are present in the reaction solution.

As none of the desired products could be synthesized by this approach, screening of different bases for deprotonation and *Lewis* acids for epoxide activation was conducted.

Especially appealing for further investigations was **N2** to obtain **R7** (via **X11**), as the contained spiro-center would render a structurally complex spiro-bicyclic molecule upon radical 5-exo-cyclization (**Scheme 46**). **Table 14** displays the tested reaction conditions. Unfortunately, no epoxide opening could be observed in either of the reactions. This could be explained by the steric demand of **N2**, inhibiting the approach to the terminal epoxide.

In contrast to the lithium alcoholates, sodium binds less strongly to the oxygen, making the alcoholate more nucleophilic. Although **X9** is additionally activated for epoxide opening by *Lewis* acids of different strengths, no S_N2-reaction occurred. The crude NMR-data showed unreacted substrates.^[282]



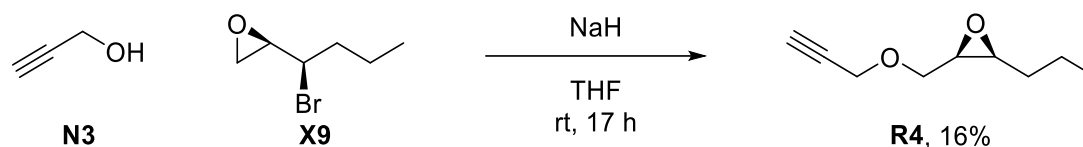
Scheme 46: Two-step route for the synthesis of **R7** and desired 5-*exo*-cyclization.

Table 14: Synthetic approaches to **X11**.

No.	Lewis acid
1 ^[a]	-
2	ZnCl ₂
3	AlCl ₃
4	Yb(OTf) ₃
5	BF ₃ ·OEt ₂
6 ^[b]	AlMe ₃

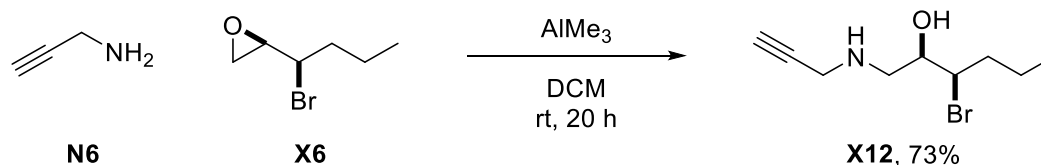
Conditions: 1.2 eq. **X9**, 1.5 eq. NaH, 1.1 eq. Lewis acid, 0.67 M in THF. [a] 16 h. [b] 1.0 eq. AlMe₃, 0.2 M in DCM.

To circumvent steric hinderance by employing a structurally more flexible derivative of **N2**, the corresponding propargylic alcohol **N3** was reacted under the former ineffective reaction conditions (**Scheme 47**). Although not satisfying, 16% of **R4** could be isolated, whereas no opened α -bromo alcohol was formed. This is reasonable, as no additional Lewis acid was used, stabilizing the alcoholate after the first S_N2-reaction and thus leading to the α -bromo alcohol. In addition, the second S_N2-reaction is intramolecular, which is generally faster than intermolecular reactions of the same type.^[283–287]

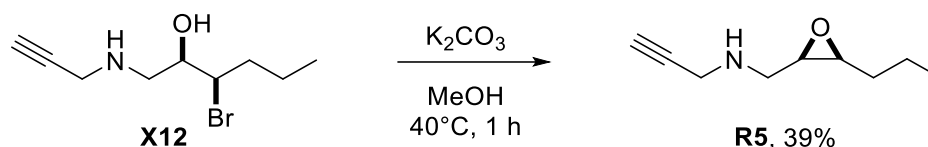


Scheme 47: Preparation of REO-cyclization substrate **R4**. Conditions: 1.2 eq. **X9**, 1.2 eq. NaH, 0.67 M in THF.

Modified reaction conditions^[234] converting the more nucleophilic **N6** by activation with AlMe_3 have been successfully used for the synthesis of **X12** (**Scheme 48**). AlMe_3 acts as *Brønsted* base^[288] upon formation of methane^[289] and additionally as *Lewis* acid for epoxide activation. Trapping the bromo alcohol **X12** is possible due to the Al–O bond formed, inhibiting ring closure. The product is liberated during aqueous work-up in a good yield of 73%. A similar approach for aromatic amines has been used for the synthesis of REO-arylation substrates.^[149] Formation of the desired epoxide is achieved by stirring with K_2CO_3 , promoting the intramolecular $\text{S}_{\text{N}}2$ -reaction to **R5** in 39% isolated yield (**Scheme 49**).

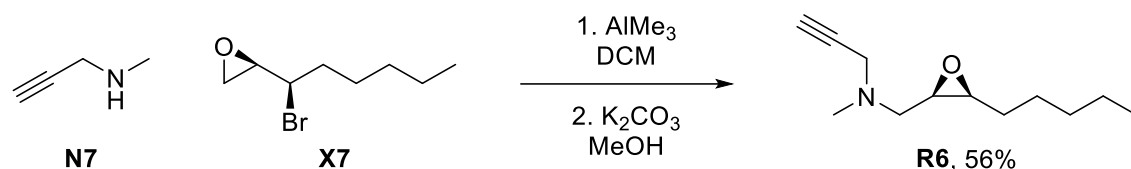


Scheme 48: Application of AlMe_3 as *Lewis* acid and *Brønsted* base^[289] for the conversion of propargyl amine with **X6**. Conditions: 1.2 eq. **X6**, 1.0 eq. AlMe_3 , 0.2 M in DCM.



Scheme 49: Intramolecular epoxidation of **X12** via $\text{S}_{\text{N}}2$ -reaction. Conditions: 2.0 eq. K_2CO_3 , 0.5 M in MeOH.

For testing the performance of the reaction conditions, racemic epoxide **X6** has been used. Consequently, **R5** is no REO substrate, but can be used in a parallel resolution. The same reaction conditions were afterwards employed in the synthesis of REO substrate **R6**. In two reaction steps, the desired compound could be isolated in 56% yield (**Scheme 50**). For the conversion of alkyl substituted primary or propargyl amines, the found reaction conditions rendered a reliable synthetic strategy. By this method, *Heinz* synthesized **R2** and **R3** during his M.Sc. research project (**Figure 22**).^[217]



Scheme 50: Synthesis of REO substrate **R6** via two-step approach with $AlMe_3$. Conditions: 1) 1.2 eq. **X7**, 1.0 eq. $AlMe_3$, 0.2 M in DCM, rt, 20 h; 2) 2.0 eq. K_2CO_3 , 0.5 M in MeOH, 40°C, 1 h.

In addition to the REO-cyclization substrates, a number of further REO substrates for the formation of enantiomerically pure aminols and (di)alcohols was planned. For these, the nucleophiles did not contain any terminal olefin or alkyne.

Starting under mild basic conditions (K_2CO_3), tosyl protected amines **N8** and **N9** (**Scheme 44**) were reacted with epoxide **X4** (**Table 15**). In the latter case, $LiCl$ was employed as *Lewis* acid for epoxide activation. However, these conditions did not lead to any epoxide opening. Pyrazole derivative **N11** did also not react as nucleophile with $AlMe_3$ (entry 3), although S_N2 -reactions at N-1 of the pyrazole ring have been reported for alkylation reactions even under milder conditions.^[290–292]

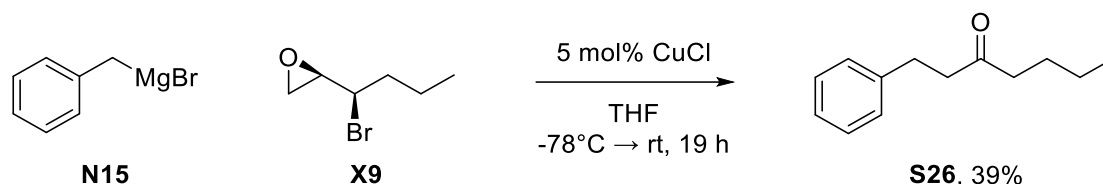
Table 15: Unsuccessful synthetic approaches to new REO substrates.

No.	Nucleophile	Epoxide	Base	<i>Lewis</i> acid	Conversion
1 ^[a]	N8	X4	K_2CO_3	-	-
2 ^[b]	N9	X4	K_2CO_3	$LiCl$	-
3 ^[c]	N11	X7	$AlMe_3$	-	-
4 ^[d]	N11	X9	-	SiO_2	-
5 ^[d]	N12	X9	-	SiO_2	-
6 ^[e]	N15	X9	-	-	-
7 ^[f]	N15	X9	-	$CuCl$	-

Conditions: [a] 1.2 eq. **X4**, 1.5 eq. K_2CO_3 , 1.0 M in DMF, 80°C, 16 h. [b] 1.2 eq. **X4**, 1.5 eq. K_2CO_3 , 0.5 eq. $LiCl$ 1.0 M in DMF, 80°C, 16 h. [c] 1.2 eq. **X7**, 1.0 eq. $AlMe_3$, 0.2 M in DCM, rt, 22 h. [d] 1.0 eq. **X9**, 20 wt% SiO_2 , rt, 3 d. [e] 1.0 eq. **X9**, 0.5 M in THF, -78°C to rt, 19 h. [f] 1.0 eq. **X9**, 5 mol% $CuCl$, 0.5 M in THF, -78°C to rt, 19 h.

Activation of the epoxide by SiO_2 in a solvent-free reaction did not lead to epoxide conversion, either (entry 4). This approach is based on the conditions developed by *Mühlhaus et al.* for the preparation of REO-arylation substrates.^[149] For **N11** and **N12**, the nucleophilicity is apparently insufficient for this kind of reaction. Furthermore, the addition of a *Grignard* reagent **N15** to α -bromo epoxide **X9** was tried. In these cases, the epoxide was converted, but no desired

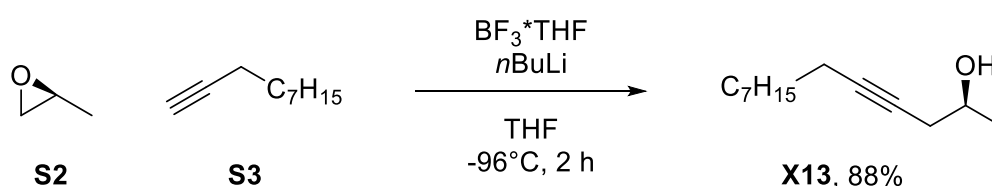
product was formed (entries 6 and 7). Instead, **S26** was isolated in 39% yield for the reaction in entry 7 (**Scheme 51**). The formation of this compound indicates a successful nucleophilic substitution at the terminal epoxide with ring closure and substitution of bromide, but a subsequent loss of MgBr_2 and a *Meinwald*-rearrangement leading to ketone **S26**.



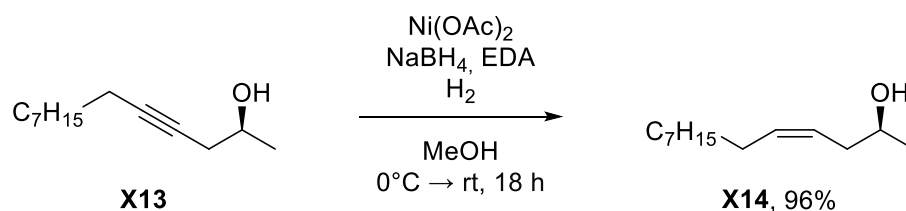
Scheme 51: Observed ketone formation by addition of *Grignard* reagent **N15** to **X9**.

Following the ‘classic’ approach to REO substrates,^[110] multiple new functionalized or silyl-protected compounds have been prepared in collaboration with *Zhang*.^[136,234] One conducted synthesis is displayed in **Scheme 43**.

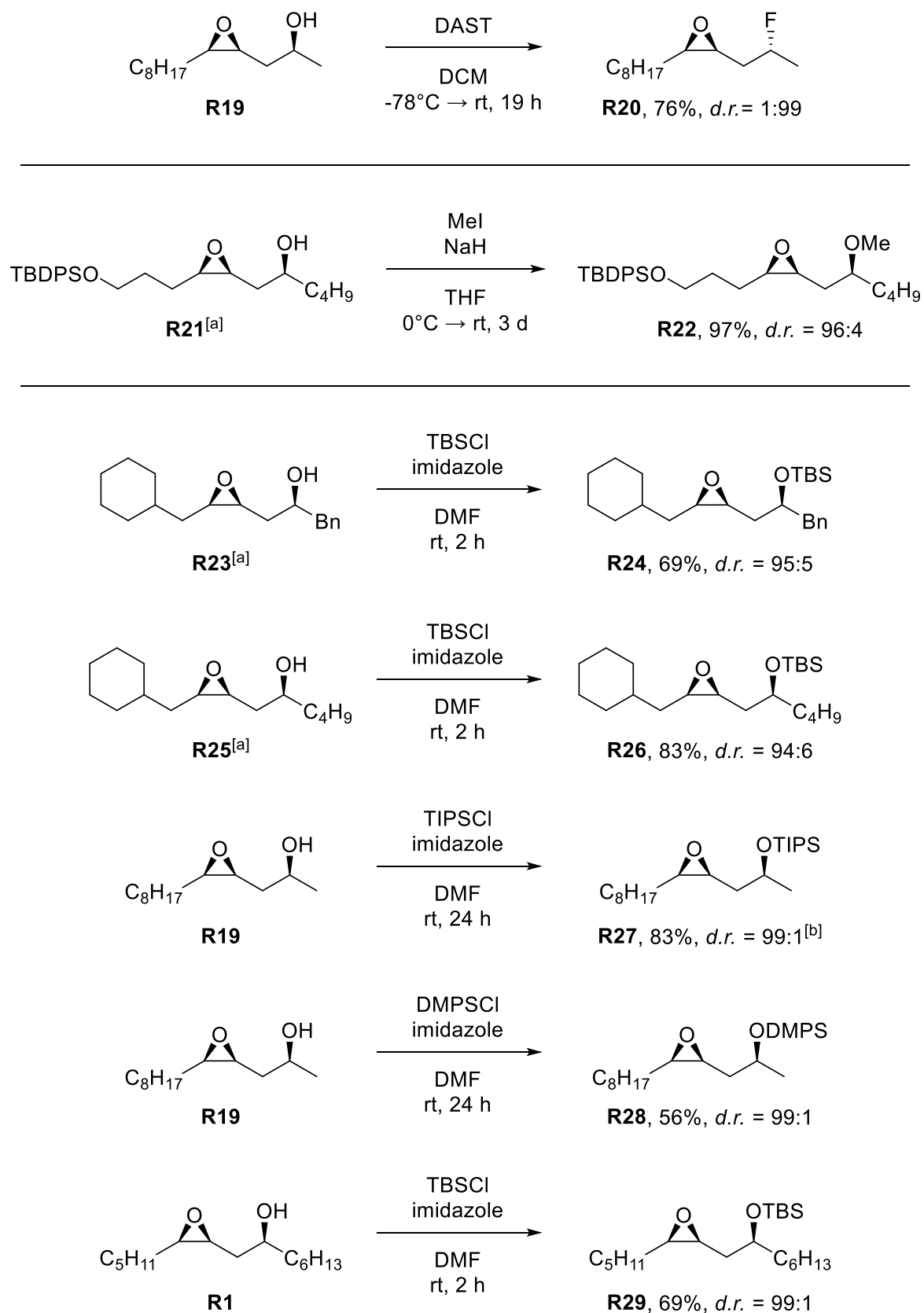
The synthesis was performed according to the procedures developed by *Funken et al.* Alkyne addition to enantiomerically pure terminal epoxide **S2** mediated by BF_3 as strong *Lewis* acid for epoxide activation (**Scheme 52**) set the required enantiomerically pure stereocenter in the REO substrate in an efficient reaction with a good yield of 88%. Subsequently, the homopropargylic alcohol was selectively hydrogenated to give a (*Z*)- β -hydroxy alkene. Employing *in situ* generated P-2 nickel (from $\text{Ni}(\text{OAc})_2$, NaBH_4 and EDA) as a poisoned hydrogenation catalyst under hydrogen gas atmosphere (**Scheme 53**), this reaction proceeded almost quantitatively with an excellent yield of 96%.^[273,274]



Scheme 52: Alkyne addition to enantiomerically pure **S2** (*e.r.* = 98:2). Conditions: 1.0 eq. **S3**, 1.1 eq. $n\text{BuLi}$, 1.0 eq. $\text{BF}_3 \cdot \text{THF}$, 0.63 M in THF.



Scheme 53: Alkyne reduction to (*Z*)- β -hydroxy alkene **X14**. Conditions: 0.25 eq. $\text{Ni}(\text{OAc})_2$, 0.25 eq. NaBH_4 , 0.5 eq. EDA, 0.5 M in MeOH.



Scheme 54: Derivatization of *syn*- β -hydroxy alcohols to substrates for the photochemical REO. Conditions: (fluorination) 1.1 eq. DAST, 0.1 M in DCM; (methylation) 1.94 eq. MeI, 1.46 eq. NaH, 0.3 M in THF; (silylation) 1.2 eq. silyl chloride, 2.5 eq. imidazole, 1.0 M in DMF. [a] Synthesized by Zhang.^[136] [b] Contained inseparable impurity.

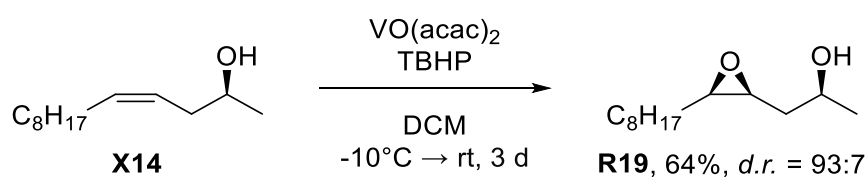
The final REO substrate precursor **R19** is obtained via *syn*-selective epoxidation of the (*Z*)- β -hydroxy alkene with $\text{VO}(\text{acac})_2$ as catalyst,^[275–277] yielding the respective *syn*- β -hydroxy alcohol in moderate yield and good diastereomeric ratio (64%, *d.r.* = 93:7, **Scheme 55**). Under the original reaction conditions using Bu_3SnH as hydrogen atom donor, **R19** could be employed as a REO substrate itself.^[110] However, for the photochemical REO reactions a functionalization, substitution or protection of the free alcohol is necessary. Details on this are given in chapter 3.6.

Because of this, methylation, fluorination and silyl-protection of *syn*- β -hydroxy alcohols were performed to synthesize multiple REO substrates (**Scheme 54**). The diastereomeric ratio of the product did not necessarily resemble the substrate's *d.r.*, as purification by flash column chromatography enables the separation of *syn*- and *anti*-configured compounds.

Fluorination of **R19** with DAST leads to an inversion of configuration at the former hydroxy substituted carbon, as this reaction proceeds via an $\text{S}_{\text{N}}2$ mechanism.^[293,294] By this method, **R20** is obtained in a good yield and diastereomerically pure.

In collaboration with *Krebs*, who synthesized the TBS and TBDPS protected derivatives of **R19**,^[136,248] multiple new silyl-protected REO substrates have been prepared for subsequent investigations under photochemical REO conditions. The protection reactions employing the respective silyl chloride and imidazole for silyl chloride activation in DMF worked well, resulting in good yields and products with excellent diastereomeric ratios. Only DMPSCI did not perform as expected, **R28** could only be obtained in moderate 56% yield.

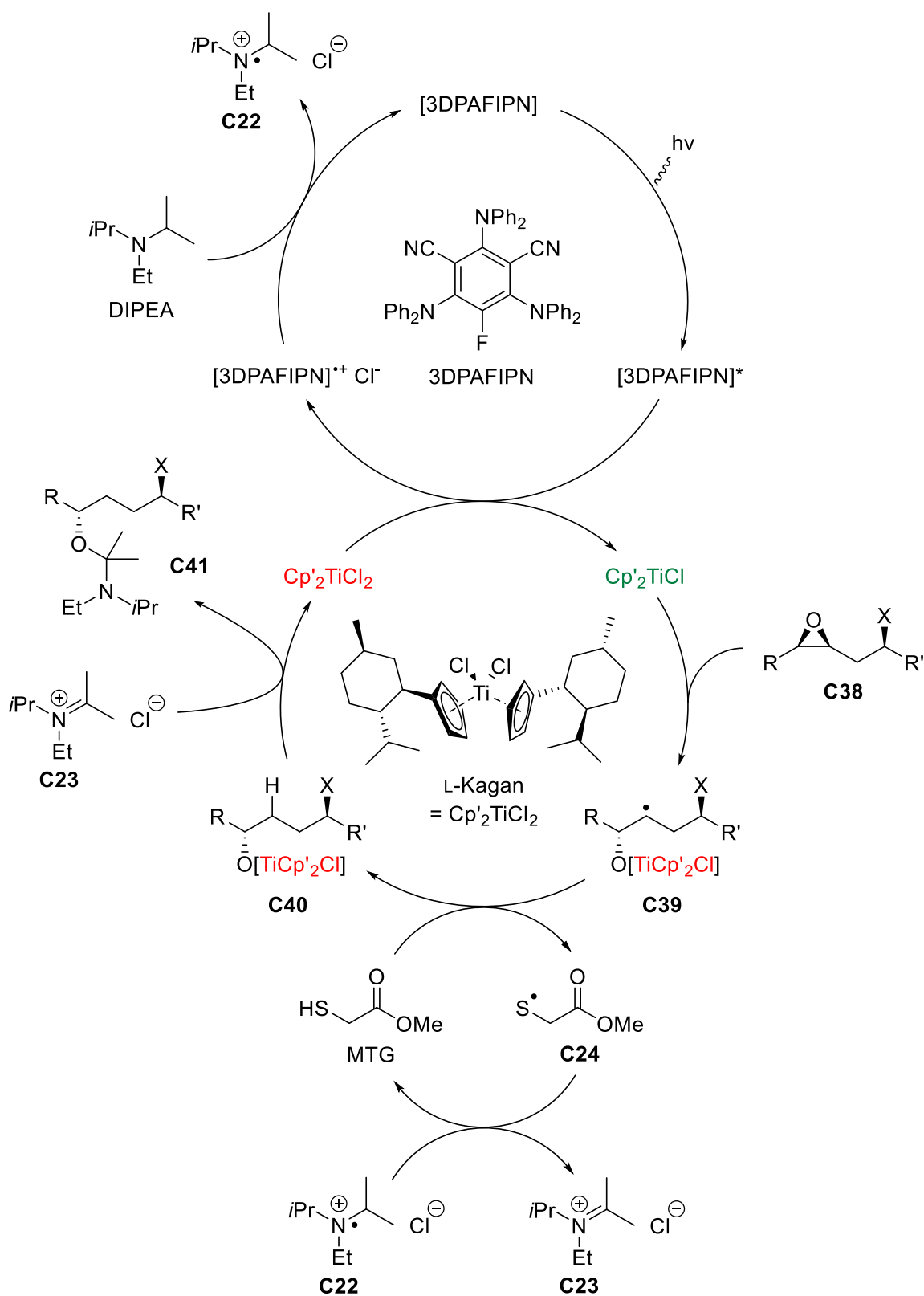
Unfortunately, **R27** could not be employed in a REO reaction, as traces of an inseparable impurity, likely resulting from a side reaction of TIPSCI, contaminated the desired compound.



Scheme 55: *Syn*-selective epoxidation to REO substrate precursor **R19**. Conditions: 5 mol% $\text{VO}(\text{acac})_2$, 1.5 eq. TBHP, 0.1 M in DCM.

3.6 Photochemical REO and DEO Reactions

3.6.1 3DPAFIPN as External Photoredox Catalyst



Scheme 56: Proposed catalytic cycle for the 3DPAFIPN and L-Kagan catalyzed REO reaction.^[73]

Based on the combination of titanocene(III) catalysis with iridium photoredox catalysts, the hydrogen donor and transfer system of the photoexcited titanocene catalysis (DIPEA and MTG) and the REO approach, a new system, merging these with a cheaper, purely organic photoredox catalyst (3DPAFIPN) enabling the conversion of silyl-protected substrates was developed.^[110,130,135]

In **Scheme 56**, the catalytic cycle is shown, highlighting the major advantages of this combined reaction mechanism over the previously used systems. It starts with the excitation of 3DPAFIPN, an easily accessible organic photoredox catalyst, which can be synthesized in a one-step reaction from commercially available starting materials (chapter 5.12.20) that does not contain expensive and unsustainable Ir. Upon irradiation with blue light and consequent excitation, its redox potentials are altered as displayed in **Table 16**.^[164] The excited [3DPAFIPN]* now bears a reduction potential of $E_{1/2}(\text{PRCat}^{*+}/\text{PRCat}^*) = -1.38 \text{ V}$ compared to $E_{1/2}(\text{PRCat}^{*+}/\text{PRCat}) = +1.30 \text{ V}$ in its ground state and thus becomes able to reduce the L-Kagan ($E_{1/2}(\text{Ti}^{\text{IV}}/\text{Ti}^{\text{III}}) = -0.89 \text{ V}$ (in THF versus SCE)^[148,295]) as a strong reductant. The photocatalytic cycle is completed by reduction of [3DPAFIPN]⁺⁺ with DIPEA ($E_{1/2}(\text{DIPEA}^{*+}/\text{DIPEA}) +0.90 \text{ V}$ (in THF versus SCE)^[296,297]).

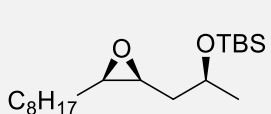
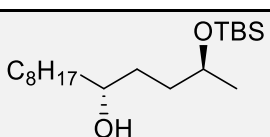
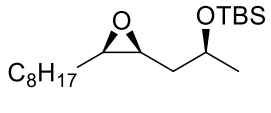
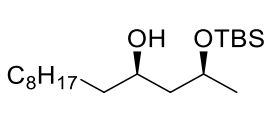
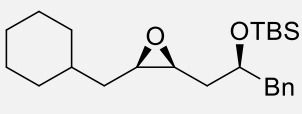
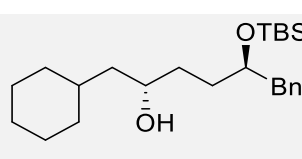
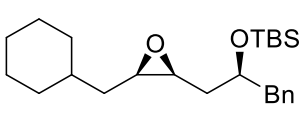
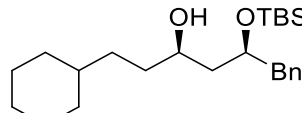
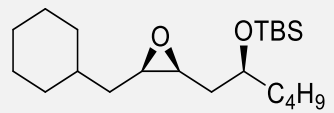
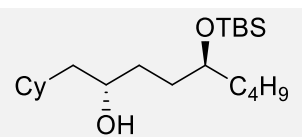
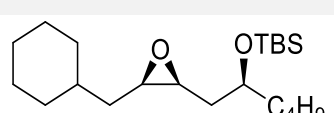
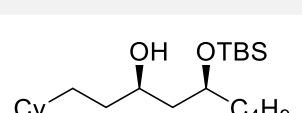
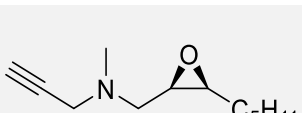
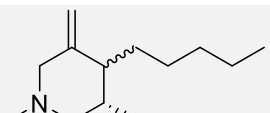
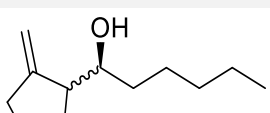
Table 16: Ground state and excited state redox potentials $E_{1/2}$ of 3DPAFIPN.

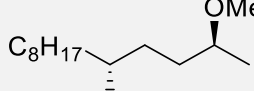
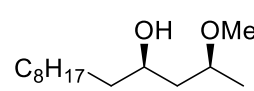
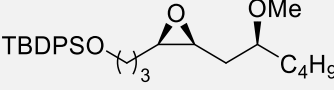
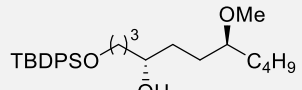
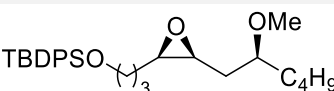
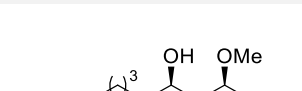
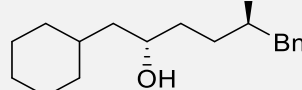
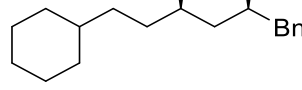
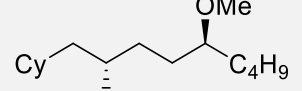
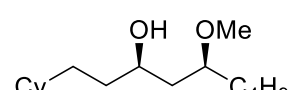
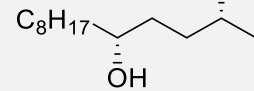
3DPAFIPN	PRCat	PRCat*
PRCat ⁺⁺	+1.30	-1.38
PRCat ⁻	-1.59	+1.09

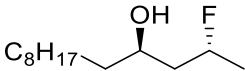
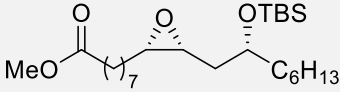
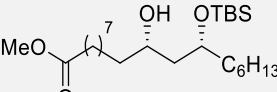
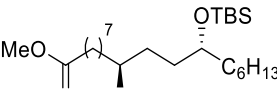
All values denoted in V versus SCE in MeCN.^[164,298]

The titanocene cycle and the hydrogen atom transfer cycle proceed identical to the one discussed in **Scheme 20** with the only difference in titanocene reduction and the employed substrate. As the regioselectivity in the epoxide opening to intermediate **C39** is mainly catalyst controlled, the stereocenter and substituent in β -position do not have a substantial influence on the outcome. This is proven by the application of sterically demanding TBS-protection groups. **Table 17** shows the conducted REO reactions with the new, merged system.

Table 17: REO reactions using 3DPAFIPN as catalyst.

No.	Substrate	Cat.	Product	r.r.	d.r.	Yield ^[a]
1	 R30^[b]	L	 R31	9:91	1:99	71
2	 R30^[b]	D	 R41^[b]	96:4	99:1	61
3	 R24	L	 R33	20:80	1:99	30
4	 R24	D	 R35	92:8	99:1	39
5	 R26	L	 R35	15:85	1:99	59
6	 R26	D	 R36	94:6	99:1	78
7	 R6	L	 R37	-	-	-
8	 R6	D	 R38	-	-	-

9		L		4:96	1:99	72
	R42^[c]		R43^[c]			
10		D		94:6	99:1	70
	R42^[c]		R44^[c]			
11		L		2:98	1:99	75
	R45^[c]		R46^[c]			
12		D		91:9	99:1	72
	R45^[c]		R47^[c]			
13		L		8:92	1:99	70
	R48^[c]		R49^[c]			
14		D		96:4	99:1	69
	R48^[c]		R50^[c]			
15		L		9:91	1:99	73
	R51^[c]		R52^[c]			
16		D		94:6	99:1	70
	R51^[c]		R53^[c]			
17		L		92:8	99:1	70
	R54^[c]		R55^[c]			

18		D		5:95	1:99	72
	R54^[c]		R56^[c]			
19		L		89:11	99:1	61
	R57^[b]		R58^[b]			
20		D		6:94	1:99	36
	R57^[b]		R59^[b]			

Conditions: 10 mol% L- or D-Kagan, 3 mol% 3DPAFIPN, 3.0 eq. DIPEA, 20 mol% MTG, 0.1 M in THF, blue LED, rt, 4 d. *r.r.* denoted as 1,3:1,4. *d.r.* denoted as *syn:anti*. [a] Isolated yield of the displayed REO product in %. [b] Synthesized by *Krebs*.^[248] [c] Synthesized by *Zhang*.^[234]

The reactions were performed in collaboration with *Krebs* and *Zhang*.^[234,248] Overall, the applied method is reliable for the preparation of diastereomerically and enantiomerically pure 1,3- and 1,4-diol-derived molecules from methylated, fluorinated or silyl-protected enantiomerically pure substrates.

Especially the tolerance against silyl ethers in the reaction is an important advantage compared to the original REO-conditions, in which this was not observed.^[102,299] *Funken* proposed that steric hinderance inhibits binding of the titanocene catalyst to the epoxide moiety. However, this could not be verified as even more bulky TBDPS-protection groups in combination with large supramolecular chloride-binders have also been successfully employed in REO reactions, details on that can be found in chapter 3.6.3. On the downside, free alcohol groups are not tolerated under the photochemical reaction conditions. Due to the hemiaminal formation, this functional group arising from the epoxide is not present in the reaction mixture, although being the final reaction product, as it is only liberated during aqueous work-up.

For all successfully performed reactions, the diastereomeric ratio of the obtained product is 99:1 or 1:99, respectively. This can be explained by the double asymmetric mechanism in the REO reaction (**Scheme 10**).^[269,300,301] Starting from an enantiomerically pure and diastereomerically enriched (typically >95:<5) substrate, the ‘wrong’ regioselectivity in the epoxide opening leads to the formation of a constitutional isomer – hence a separation is possible via flash column chromatography. This is reflected in the regioisomeric ratio, which is usually higher than 90:10 in favor of the desired regioisomer (except for entries 3 and 5), although the minor substrate diastereoisomer is mainly converted to the ‘wrong’ regioisomer as well. Because of this, the product’s diastereoisomer cannot be detected by ¹³C-NMR

spectroscopy (<1%). The products are obtained diastereomerically pure. As the non-reacting stereocenter has been set in enantiomerically pure manner by an HKR during substrate synthesis, the final REO product is also enantiomerically pure.

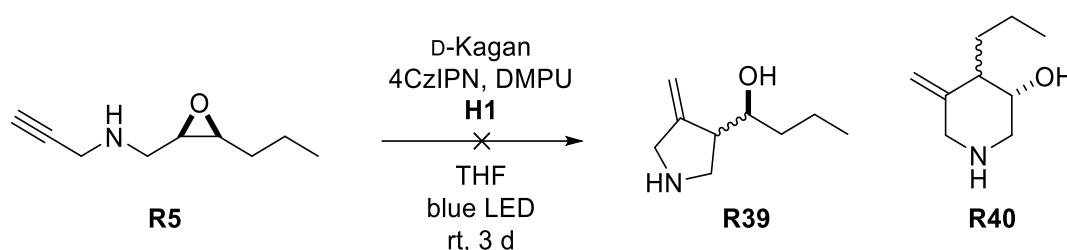
Besides this great stereoselectivity, the reactions can be carried out in good yields, typically around 70%, which is a good result considering the high number of stereo- and regioisomers possible. Exceptions of these yields are entries 3 and 4, in which sterically demanding **R24** was converted. This is true for both catalyst enantiomers used. The substrate's structure bears phenyl- and cyclohexyl-substituents in close proximity to the epoxide center. In contrast to the alkyl-chains present in most other substrates, which can rotate to diminish steric interactions with the catalyst, the rotation of the cyclohexyl-, OTBS- or benzyl-substituents does not suffice to avoid repulsion. In addition, the presence of a benzylic position in the substrate might disturb the hydrogen transfer cycle, as hydrogen atoms originating from this position can quench the required thiyl radical **C24** (Scheme 56). It was found by Zhang that benzyl-protection groups at the alcohol-center are not tolerated under the reaction conditions used.^[234] However, this influence, if present at all, is minor compared to the steric influence, as **R48** can be converted in good yields (entries 13 and 14).

The only other major exception from high yields for the formation of diol-derivatives is the REO of **R57** with D-Kagan (entry 20). As the reaction with the catalyst's enantiomer proceeds as expected, showing the ricinolate's ability to rotate the terminal alkyl-chain and thus avoid steric inhibition, this cannot explain the poor result. It is more likely that a 'human mistake' during work-up or purification is the origin of the low yield of 36%, as *r.r.* and *d.r.* indicate no trouble originating from the reaction itself.

In previous investigations of the REO, it has also been discussed, whether the substrates bear an influence on the regioselectivity of the reaction.^[102,299] As stated above, the REO is mainly catalyst-controlled, meaning that the structure of the substrate does not affect the *r.r.* in the opening. A substrate-specific favoring of the formation of 1,4-diol-derivatives could not be observed in the performed reactions displayed in Table 17. It has been argued that the differences in size of the epoxide's substituents (alkyl-chain > CH(OR)Me) benefit the 1,4-opening and create a *matched-case* scenario, in which both substrate and catalyst favor this regioisomer.^[102] This could not be verified with the REO reactions conducted under photochemical conditions. As many substrates do not possess the 'classic' shape of the REO substrates (compare **R54**) with two substituents which differ substantially in size, this could explain the lack of the substrate's influence. Moreover, a better reaction performance when using *anti*-substrates as for example **R54** compared to *syn*-substrates, which has been previously reported,^[102] could not be observed.

Noteworthy in the presented REO reactions are entries 7 and 8 as here, a REO cyclization was attempted. Unfortunately, neither of the catalyst's enantiomers yielded any of the desired

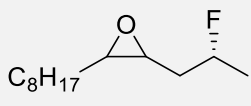
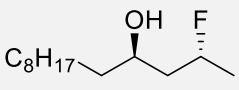
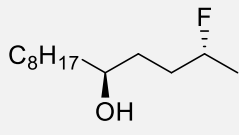
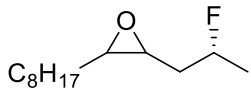
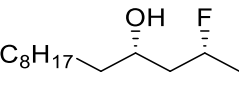
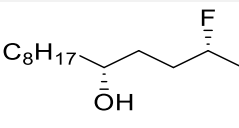
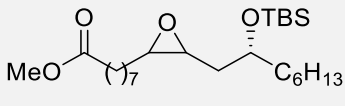
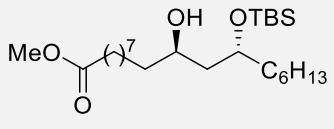
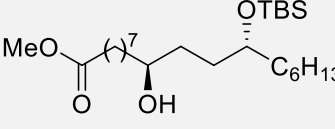
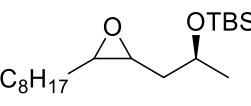
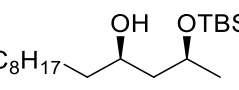
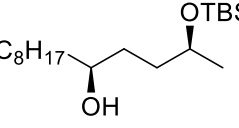
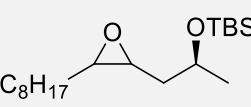
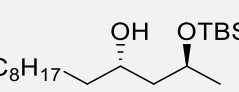
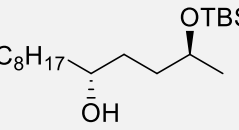
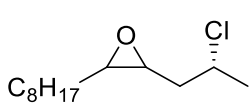
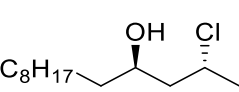
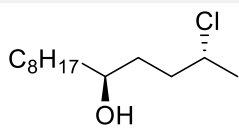
5-*exo*- or 6-*endo*-cyclization products. Reactions of this type have been reported for the photochemical non-regiodivergent epoxide openings.^[135] Possible competing reactions are the HAT to the β -titanoxy radical or radical trapping by either active titanocene catalyst or thiyl radical.^[149,217] In a parallel resolution, racemic epoxide **R5** was also tested for its ability to undergo these types of cyclization reactions (**Scheme 57**). Here, 4CzIPN was used as photoredox catalyst, which has similar redox potentials as the previously employed 3DPAFIPN,^[164] in combination with *Hantzsch* ester **H1** as hydrogen atom donor (HAD). Again, no conversion was observed in these cyclizations, as before for the REO cyclizations.

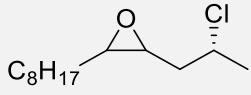
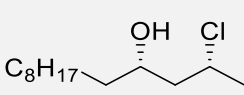
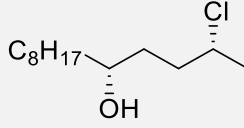
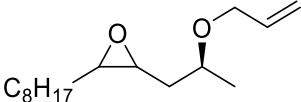


Scheme 57: Attempted photochemical parallel resolution of **R5**. Conditions: 10 mol% D-Kagan, 2.5 mol% 4CzIPN, 1.5 eq. DMPU, 2.0 eq. **H1**, 0.1 M in THF.

Table 18: DEO reactions using 3DPAFIPN as catalyst.

No.	Substrate/Cat.	1,3-Product	1,4-Product
1			
	D1	D7	D8
	$d.r. = 62:38$		
	D-cat., $r.r. = 57:43$ ^[a,b]	34%, $d.r. = 96:4$	26%, $d.r. = 81:19$
	D-cat., $r.r. = 62:38$ ^[a]	46%, $d.r. = 95:5$	33%, $d.r. = 82:18$
2			
	D1	D9	D10
	$d.r. = 62:38$	15%	31%
	L-cat., $r.r. = 32:68$ ^[b]	$d.r. = 18:82$	$d.r. = 7:93$

3	 D2 <i>d.r.</i> = 32:68 D-cat., <i>r.r.</i> = 67:33	 D11 49% <i>d.r.</i> = 1:99	 D12 31% <i>d.r.</i> = 16:84
4	 D2 <i>d.r.</i> = 32:68 L-cat., <i>r.r.</i> = 33:67	 D13 30% <i>d.r.</i> = 89:11	 D14 53% <i>d.r.</i> = 93:7
5	 D3 <i>d.r.</i> = 60:40 D-cat., <i>r.r.</i> = 38:62	 D15 27% <i>d.r.</i> = 12:88	 D16 51% <i>d.r.</i> = 8:92
6	 D4 <i>d.r.</i> = 68:32 D-cat., <i>r.r.</i> = 67:33	 R41 57% <i>d.r.</i> = 99:1	 D17 28% <i>d.r.</i> = 90:10
7	 D4 <i>d.r.</i> = 68:32 L-cat., <i>r.r.</i> = 32:68	 D18 26% <i>d.r.</i> = 14:86	 R31 49% <i>d.r.</i> = 7:93
8	 D5 <i>d.r.</i> = 40:60 D-cat., <i>r.r.</i> = 33:67 ^[c]	 D19 47% <i>d.r.</i> = 28:72	 D20 29% <i>d.r.</i> = 40:60

9	 D5 <i>d.r.</i> = 40:60 L-cat., <i>r.r.</i> = 33:67 ^[c]	 D21 27% <i>d.r.</i> = 62:38	 D22 36% <i>d.r.</i> = 75:25
10	 D6 <i>d.r.</i> = 70:30 D-cat.	-	-

Conditions: 10 mol% L- or D-Kagan, 3 mol% 3DPAFIPN, 3.0 eq. DIPEA, 20 mol% MTG, 0.1 M in THF, blue LED, rt, 4 d. *r.r.* denoted as 1,3:1,4 and determined from crude ¹³C-NMR. *d.r.* denoted as *syn:anti*. Isolated yields. [a] 7 d. [b] Addition of 1.5 eq. DMPU. [c] 5 d.

Following the same reaction mechanism and catalytic cycle and thus reaction conditions as the REO reactions (**Scheme 56**), DEO reactions have been conducted with various substrates for the parallel synthesis of one 1,3- and one 1,4-diol in one reaction. The two regioisomeric products either both exhibit *syn*- or *anti*-configuration depending on the substrate configuration. This is due to the double asymmetric conversion of a *pseudo*-racemic substrate mixture; the concept is depicted in **Scheme 11** and the resulting main reaction products are shown in **Scheme 12** for every possible substrate configuration. The regioisomeric ratio of the reaction resembles the diastereomeric ratio of the employed substrate. Generally, the major of the two reaction products is obtained in a high *d.r.*, whereas the minor product has a lower *d.r.*, while still being diastereomerically enriched. This can also be deduced from the theoretical calculation of the DEO reactions in **Scheme 11**.

In **Table 18** the reaction results of the photochemical DEO reactions are listed, which have been performed under the same reaction conditions as the REOs presented before. Due to the substrate's lower *d.r.*, the products have a lower *d.r.* compared to the REO products, as well, as absolutely speaking more of the minor diastereomer is converted to the 'wrong' product.

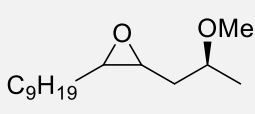
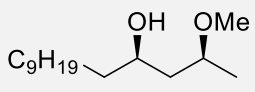
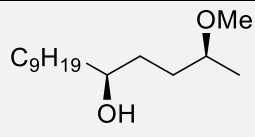
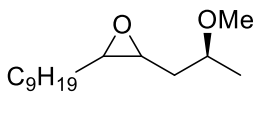
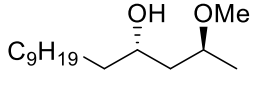
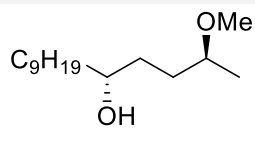
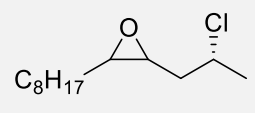
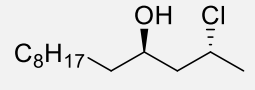
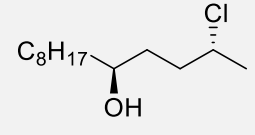
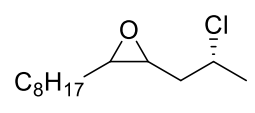
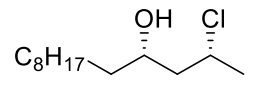
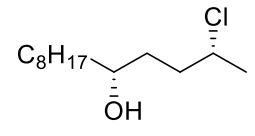
The major advantage of the DEO approach is however that two separable regioisomers are obtained in one single reaction, making this an interesting strategy for diversity oriented synthesis (compare chapter 2.2.3).^[102,108,109] Additionally, all four diastereoisomers of the desired products can be obtained in two DEO reactions. In contrast to that, four REO reactions would be necessary and require elaborate and multi-step substrate modification.

The initial DEO reactions tested contained 1.5 eq. of DMPU, as in previous photochemical studies this has been suggested to improve the yield.^[234] Comparing the two conditions described in entry 1, it is clear to see that for the DEO, this is not true. Omitting the DMPU increased the yield by about one third while keeping the *d.r.* fixed. Combining the enantiomeric catalyst and DMPU (entry 2) also led to poor yields for the respective products. Typically, the combined yields in the DEO reactions reached 70-80%. Sterically demanding substrates **D3** and **D4** bearing TBS protection groups were successfully converted under the described reaction conditions (entries 5–7).

Allyl substituted substrate **D6** (entry 10) was employed without any conversion, the substrate could be recovered in pure form from the reaction mixture almost quantitatively.

An unexpected result was obtained when reacting chloro epoxide **D5** with either of the catalyst enantiomers (entries 8 and 9). With the isolated yields of the desired products and the *r.r.* being in line with the other DEO results, the diastereomeric ratios were very poor. With a *d.r.* = 75:25 for **D22** being the highest ratio received, for product **D20**, only a value of 40:60 was obtained. This is not explainable with the mechanism discussed earlier, as for this the catalyst selectivity must be exceptionally poor. When compared to DEO conditions employing Bu₃SnH as HAD performed by Adamietz (**Table 19**),^[103] which yield comparable yields and *d.r.s* for other substrates (entries 1 and 2), chloro epoxide **D5** gave bad *d.r.s* for the respective products under these conditions as well, matching the ones found under photochemical conditions. Why this is the case remains unclear. Possibly the chloro-substitution of the β-hydroxy epoxide during the synthesis of **D5** does not proceed exclusively according to an S_N2-mechanism, so that the *d.r.* = 40:60 does not solely resemble the structures shown, but also the respective enantiomers.

Table 19: Selected DEO reactions using Bu₃SnH as HAD by Adamietz.

No.	Substrate/Cat.	1,3-Product	1,4-Product
1	 D1 <i>d.r.</i> = 62:38 D-cat., <i>r.r.</i> = 58:42	 D7 48% <i>d.r.</i> = 98:2	 D8 40% <i>d.r.</i> = 85:15
2	 D1 <i>d.r.</i> = 62:38 L-cat., <i>r.r.</i> = 24:76	 D9 16% <i>d.r.</i> = 15:85	 D10 44% <i>d.r.</i> = 6:94
3	 D5 <i>d.r.</i> = 40:60 D-cat., <i>r.r.</i> = 62:38	 D19 46% <i>d.r.</i> = 31:69	 D20 28% <i>d.r.</i> = 35:65
4	 D5 <i>d.r.</i> = 40:60 L-cat., <i>r.r.</i> = 50:50	 D21 40% <i>d.r.</i> = 59:41	 D22 40% <i>d.r.</i> = 73:27

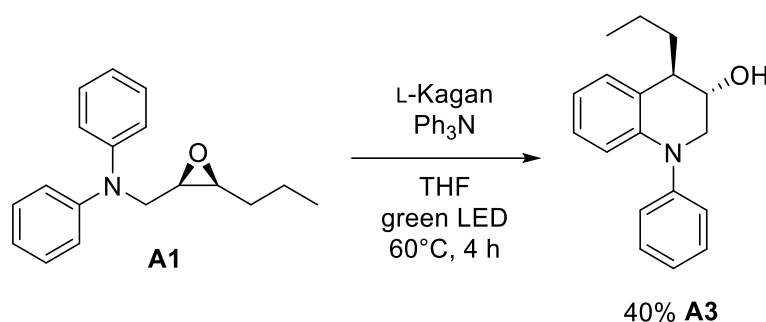
Conditions: 10 mol% L- or D-Kagan, 1.5 eq. Mn, 1.5 eq. Lut*HCl, 2.2 eq. Bu₃SnH, 0.17 M in THF, rt, 3 d. *r.r.* denoted as 1,3:1,4 and determined from crude ¹³C-NMR. *d.r.* denoted as *syn:anti*. Isolated yields.^[103]

Summarizing, the photochemical DEO reaction conditions surpass the 'classic' conditions with Bu₃SnH in terms of sustainability and are also an improvement regarding the substrate scope, as silyl-protected β-hydroxy epoxides can be reliably converted to *syn*- and *anti*-1,3- and 1,4-diol-derivatives.

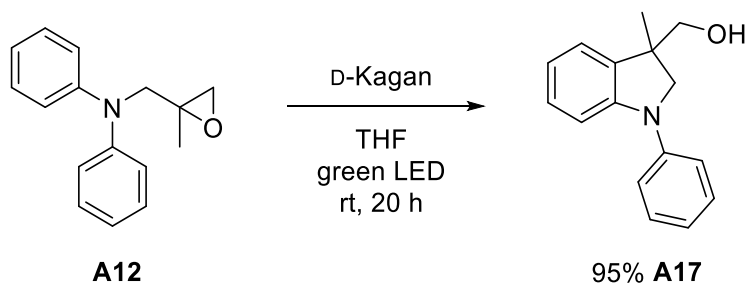
3.6.2 Enantiomerically Pure Titanocenes as Photoredox Catalysts

The final goal of the development of photochemical reaction conditions employing titanocenes as photoredox catalysts and electron transfer catalysts simultaneously was the utilization of enantiomerically pure titanocenes such as *Kagan's* complex in REO reactions.

Considering the results achieved in the (REO)-arylations (chapters 3.4.2 and 3.4.3), the first steps towards this goal have already been made. The best result for the REO-arylations was obtained for the THQ-synthesis starting from **A1** in combination with Ph₃N as reductive quencher with a yield of 40% (**Scheme 58**) and for the arylations it was the formation of indoline **A17** in 95% yield at room temperature (**Scheme 59**).

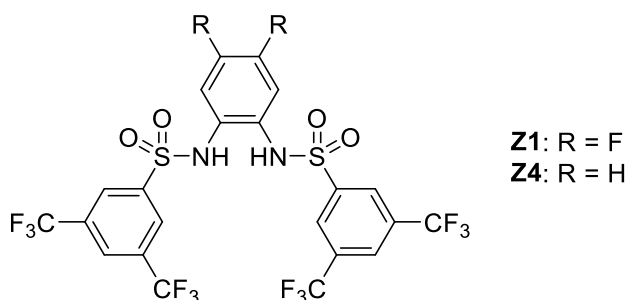
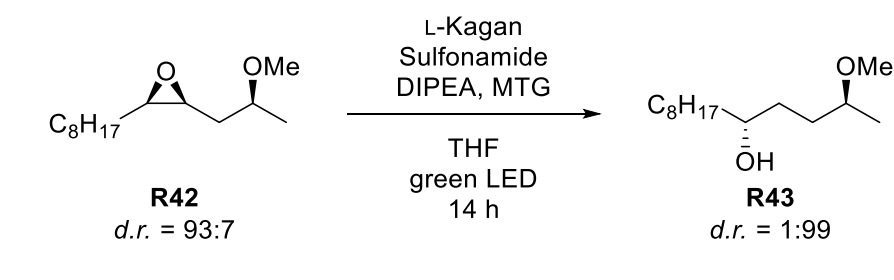


Scheme 58: Best performance of L-Kagan as photoredox catalyst in a REO-arylation from Table 9. Conditions: 10 mol% L-Kagan, 1.0 eq. Ph₃N, 0.05 M in THF.



Scheme 59: Best performance of D-Kagan as photoredox catalyst in an arylation reaction from Table 11. Conditions: 10 mol% D-Kagan, 0.05 M in THF.

To improve the performance of *Kagan's* complex as photoredox catalyst, *Zhang* investigated an elevated catalyst loading of 15 mol% in combination with employing sulfonamides as supramolecular chloride-binders (**Scheme 60**).^[136,234] This approach has previously been studied for the electrochemical activation of titanocenes (compare chapter 2.3).^[131,150] The results of the testing reactions conducted with **Z1** and **Z4** compared to a reference reaction without sulfonamide at different temperatures are presented in **Table 20**. The reaction conditions were based on the ones found for the photochemical REOs with external photoredox catalyst.



Scheme 60: Screening reaction for the performance of sulfonamides as chloride-acceptors in photochemical REO reactions. Conditions: 15 mol% L-Kagan, 15 mol% sulfonamide, 2.0 eq. DIPEA, 20 mol% MTG, 0.17 M in THF.^[136]

Table 20: Results for the performance of sulfonamides in REO of **R42** to **R43**.

No.	Sulfonamide	T [°C]	Yield [%]
1	-	60	65
2	Z4	60	85
3	Z4	45	<20 ^[a]
4	Z1	45	85
5 ^[b]	Z1	25	43

[a] Conversion.^[136] [b] By *Krebs*.^[248]

The reference reaction (entry 1) gave an isolated yield of 65% for the desired 1,4-diol **R43** at an elevated reaction temperature of 60°C. Upon addition of **Z4**, the yield could be increased to 85% under the same conditions. At lower temperatures (45°C, entry 3), the conversion of the reaction decreased drastically. Exchanging the sulfonamide for the less electron rich derivative **Z1**, an isolated yield of 85% could be obtained even at 45°C. Performing the reaction at room temperature with **Z1** decreases the yield to 43% (entry 5).^[248] Other chloride-acceptors such as squaramides or ureas and their respective sulfur analogues (**Figure 12**) led to worse yields and were thus not studied further.^[234] Because of this, the following REO reactions employing sulfonamides were conducted under the optimized reaction conditions with **Z1** at 45°C.

To answer the question on how sulfonamides benefit the performance of the photochemical REO, *Hilche et al.* investigated the stabilization of activated Cp_2TiCl with **Z4** by structural and energetic DFT calculations.^[150] Deducted from their results, the proposed complexation of $[\text{Cp}_2\text{TiCl} : \text{Z1}]$ is shown in **Figure 23**. Besides their role as chloride-acceptors, sulfonamides are able to stabilize Ti(III) centers by coordination with one of the sulfur-bound oxygen atoms. Thereby, the electron density at the titanium center is increased and the vacant coordination site is occupied.

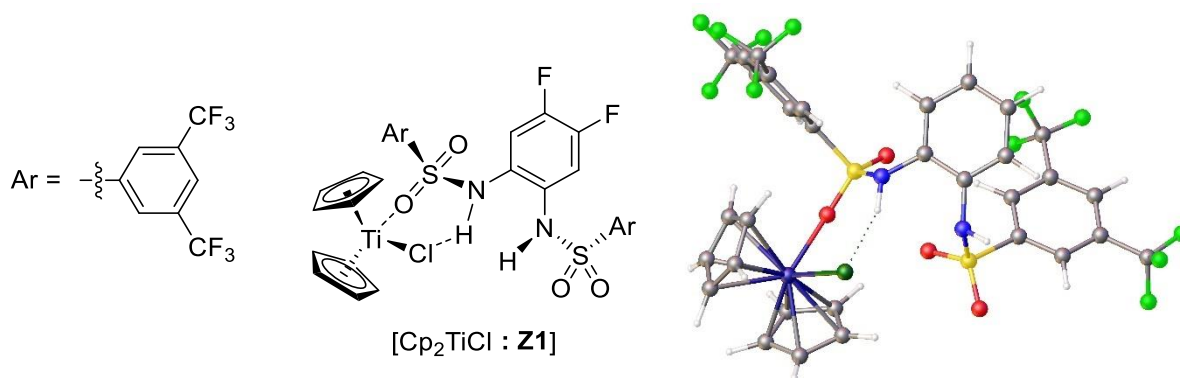


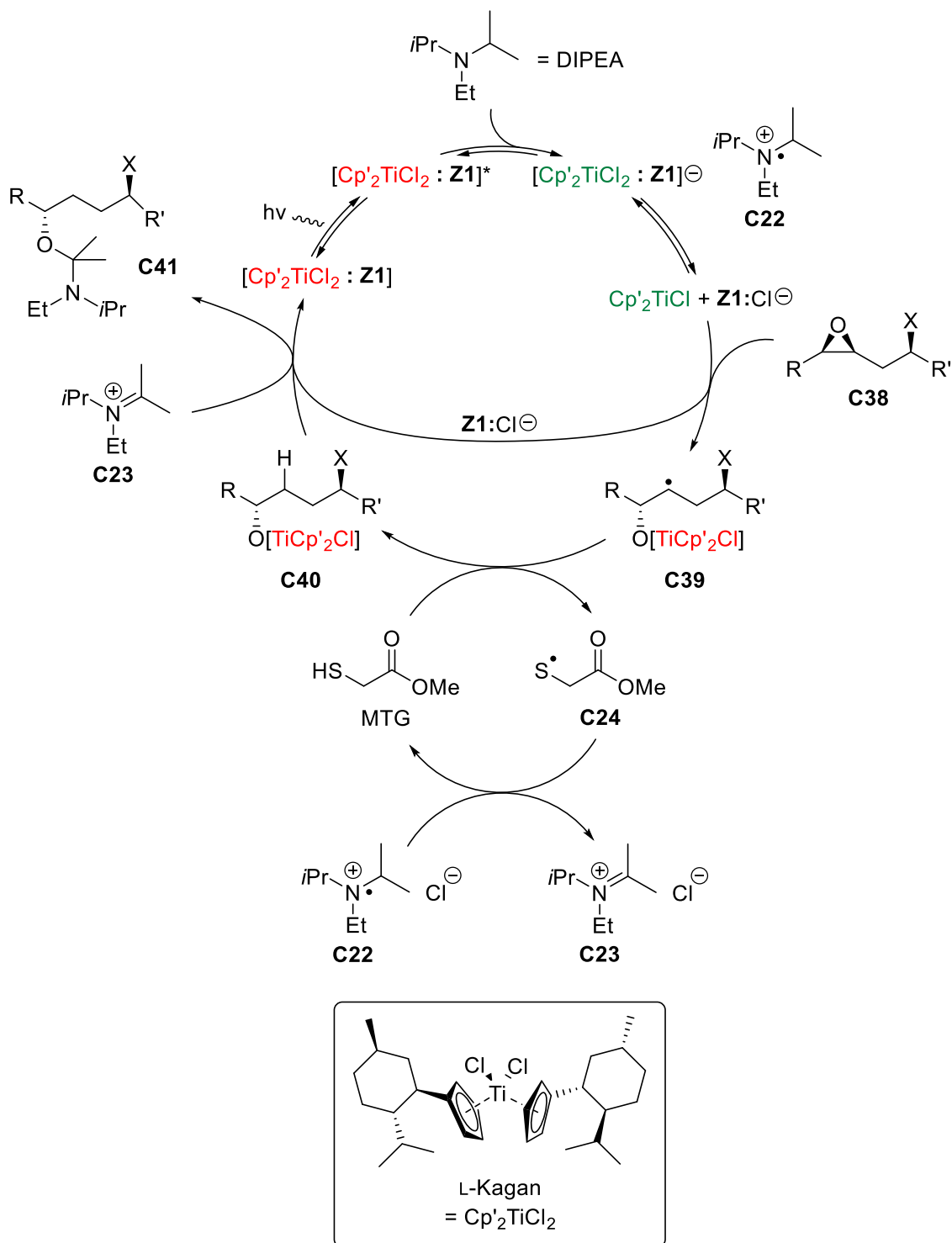
Figure 23: Proposed stabilization by supramolecular binding of **Z1** to $\text{Cp}_2\text{Ti(III)Cl}$ (left) based on DFT calculations for comparable $[\text{Cp}_2\text{TiCl} : \text{Z4}]$ (right).^[150]

Upon this stabilization, the sulfonamide enables the formation of a resting state of the active catalyst, comparable to the role of Coll^*HCl in the original titanocene catalyzed epoxide openings (**Scheme 15**). This could be visually observed by the color of the reaction mixture. While catalyst decomposition led to a color change from titanocene-red to yellow, when employing sulfonamides in the reaction, this change did not happen.

Hence, the sulfonamide occupying the vacant coordination site at the titanium, no complexation with THF, as known for other chloride-acceptors, is occurring. Whereas more electron rich **Z4** forms a complex in the same manner as displayed, more electron deficient **Z1** turned out to form a stabilized, yet more reactive complex with Cp_2TiCl . Thus, the reaction temperature could be decreased by 15°C. Regarding the stereoselectivity this is an advantage, as higher reaction temperatures generally decrease the reaction time but on the flip side also decrease the selectivity, as the reaction can proceed via multiple pathways resulting in the formation of undesired byproducts.^[302–305]

The proposed catalytic cycle for the photochemical REO with **Z1** is depicted in **Scheme 61**.^[136] Starting at the inactive titanocene, it forms a complex with sulfonamide **Z1**. This is irradiated with green light and the excited complex is reductively quenched by DIPEA in an OSET, forming the DIPEA radical cation and a Ti(III) species with one of **Z1**'s N–H groups binding one chloride-ion.^[150]

Loss of this ion renders the previously described stabilized complex, from which the active titanocene can undergo the single-electron reductive epoxide opening with REO substrate **C38**. The subsequent reaction steps proceed as for the REO with 3DPAFIPN (**Scheme 56**), until hemiaminal **C41** and the titanocene precatalyst are liberated, while the latter is immediately complexed by **Z1**.^[136]

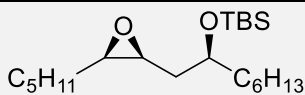
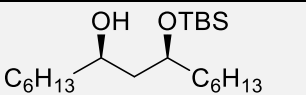
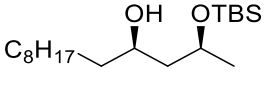
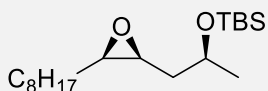
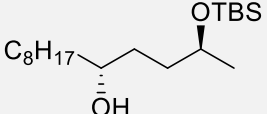
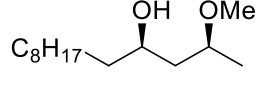
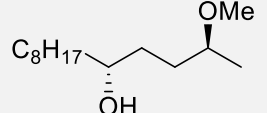
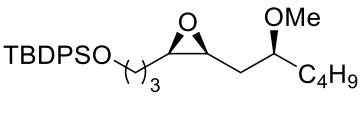
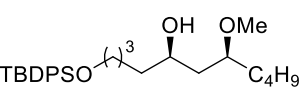
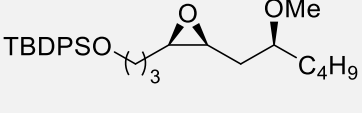
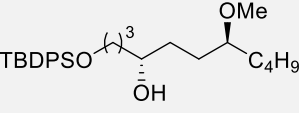


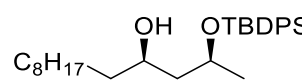
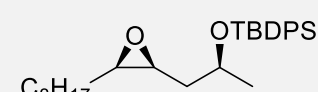
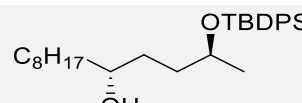
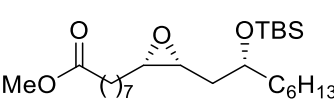
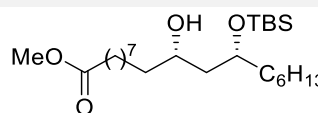
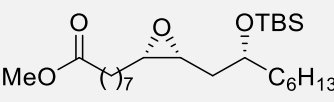
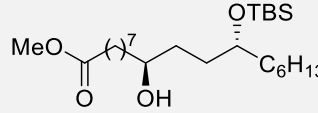
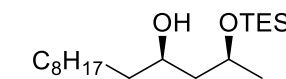
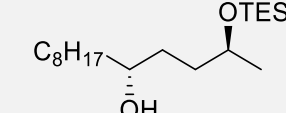
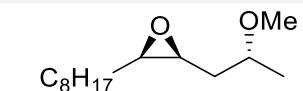
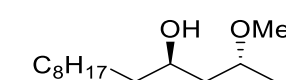
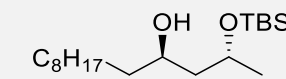
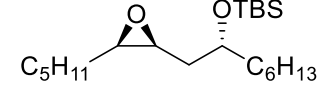
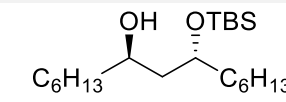
Scheme 61: Proposed catalytic cycle of the sulfonamide assisted photochemical REO.^[136]

3.6.3 Application of Sulfonamides in REO Reactions

Employing the optimized reaction conditions developed for the REO reactions with sulfonamide **Z1**, many differently functionalized substrates containing methoxy substitution as well as silyl-protecting groups of different size and stability were reacted to the corresponding 1,3-*syn*- and 1,4-*anti*-diol-based structures. Substrates exhibiting an *anti*-configuration led to the respective 1,3-*anti*-product. The REO reaction results are displayed in **Table 21**. By this method, enantiomerically and diastereomerically pure products were obtained.

Table 21: REO reactions with sulfonamide **Z1** at 45°C.

No.	Substrate	Cat.	Product	<i>r.r.</i>	<i>d.r.</i>	Yield ^[a]
1	 R29	D	 R60	94:6	99:1	77
2	 R30^[b]	D	 R41	94:6	99:1	73
3	 R30	L	 R31	7:93	1:99	69
4	 R42	D	 R44	90:10	99:1	66
5	 R42^[c]	L	 R43	7:93	1:99	85
6	 R45	D	 R47	94:6	99:1	70
7	 R45	L	 R46	6:94	1:99	78

8		D		90:10	99:1	74
	R61		R62			
9		L		10:90	1:99	72
	R61		R63			
10		L		91:9	99:1	74
	R57		R58			
11		D		8:92	1:99	68
	R57		D16			
12		D		93:7	98:2	73
	R65^[b]		R66			
13		L		7:93	1:99	70
	R65		R67			
14		D		90:10	1:99	72
	R68^[b]		R69			
15		D		94:6	1:99	76
	R70^[b]		ent-D18			
16		D		95:5	1:99	78
	R71^[b]		R72			

Conditions: 15 mol% L- or D-Kagan, 15 mol% **Z1**, 3.0 eq. DIPEA, 20 mol% MTG, 0.17 M in THF, green LED, 45°C, 16 h. *r.r.* denoted as 1,3:1,4 and determined from crude ¹³C-NMR. *d.r.* denoted as *syn:anti*. [a] Isolated yield of the displayed REO product in %. [b] Performed by *Krebs*. [c] Performed by *Zhang*.^[136]

Overall, the performed reactions show a high regioselectivity of the catalyst with a range of 90:10 to 95:5. Due to the double asymmetric mechanism, starting with an enantiomerically pure and diastereomerically enriched (*d.r.* >90:<10) substrate, the products are obtained as single enantiomers and diastereomers. This is especially appealing for mono-silyl-protected diol **R60** obtained in entry 1, as the structure resembles a *pseudo-meso* compound not accessible in enantiomerically pure form by desymmetrization of the respective *meso*-diol, as the two alcohol functions cannot be distinguished in this achiral molecule by any known catalyst.

Generally, the REO approach provides a reliable method for the preparation of mono-silyl-protected, stereodefined and optically pure diols in good yields. Major advantages are the formation of a hemiaminal in the reaction mixture rather than the free alcohol and the mildly basic reaction conditions, which prevent any silyl-migration and therefore minimize the formation of byproducts.^[306–308] Solely **R67** showed unwanted silyl-migration. However, this did not occur in the reaction itself (proven by crude ¹³C-NMR), but in the acidic CDCl₃ after purification – in CD₂Cl₂ this was not observed. Furthermore, it is worth mentioning that silyl-protecting groups were not tolerated at all under the classic REO conditions employing Bu₃SnH.^[102,110,299]

Previously it was assumed that sterically demanding substituents at the β-hydroxy position inhibit the REO due to hinderance of the approach of the catalyst to the epoxide. Among other reasons this was used to explain why silylated substrates cannot be employed.^[299] The examples given in **Table 21** indicate that this is not the case here, as crowded molecules such as in entries 10 and 11 or large silyl groups as in entries 8 and 9 could be successfully converted in good results without deviation from sterically less demanding substrates. Considering the catalytic cycle (**Scheme 61**) and the complexation of the titanocene with **Z1** (**Figure 23**), the reaction results show that this complex mechanism involving the interaction of multiple large molecules in close proximity works well despite the steric demand of the respective participants. However, the chloride-abstraction by **Z1** also diminishes the competition of chloride and epoxide for binding to the titanium center. In this case, the inhibition by chloride-coordination is prevented and the sterically more demanding epoxide can approach successfully.

The main drawback of the new REO conditions is the intolerance towards free alcohols in the substrates. Because of that, the free diols can only be obtained by deprotection from silyl-protected derivatives, which results in two additional reaction steps (protection and deprotection) and the resulting generation of waste.

Regarding sustainability, the use of toxic,^[309] hard to remove Bu₃SnH as well as Lut*HCl and Mn can be avoided – only DIPEA is employed in over-stoichiometric amounts (**Figure 24**).^[136]

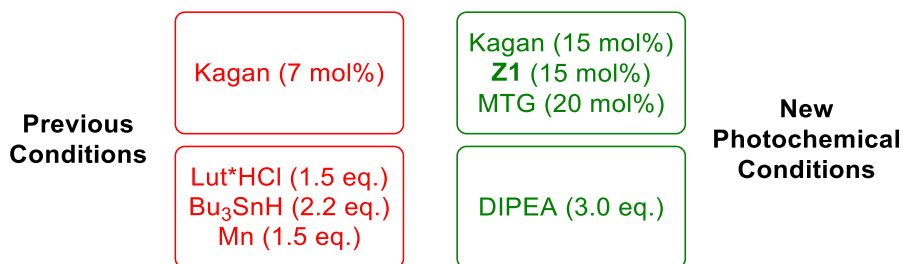


Figure 24: Comparison of required REO reagents, catalytic (top) and stoichiometric (bottom).^[110,136]

3.6.4 Silyl-protected 1,3-Diols

Complex, biologically active molecules such as Chivosazol A (**Figure 25**) often bear discrete, stereodefined polyol patterns which pose a major challenge to synthetic chemists in the laboratory preparation. For chivosazol A, the synthesis involves multiple aldol reactions in combination with employing TBS-protection groups, especially in the preparation of the right hand triol-fragment.^[310,311]

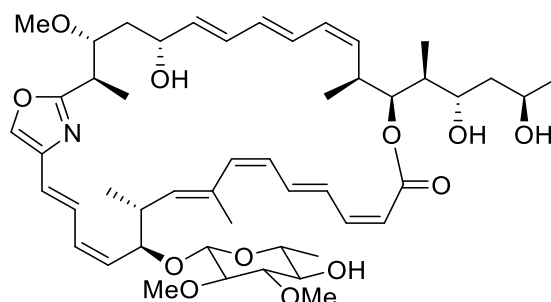
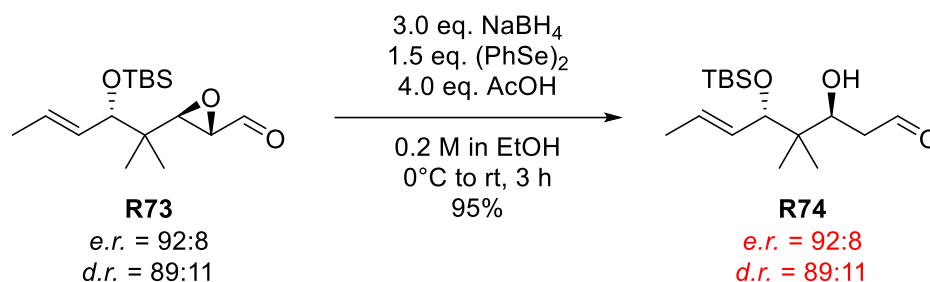


Figure 25: Structure of chivosazol A.^[117]

Generally, 1,3-diol-moieties are often prepared by aldol reactions with subsequent reduction using either *Narasaka-Prasad* conditions ($n\text{Bu}_3\text{B}$, NaBH_4) for the synthesis of 1,3-*syn*-diols or *Evans-Saksena* or *Evans-Tishchenko* conditions ($\text{Me}_4\text{NHB}(\text{OAc})_3$ or aldehyde/ SmI_2) for 1,3-*anti*-diols.^[312–320] A disadvantage of this approach is the necessity of the free neighboring β -alcohol in the reduction for chelate complexation of the hydrogen-directing reagent, so that afterwards an unprotected 1,3-diol is obtained. Often, a subsequent regioselective protection is not possible.

Obviously, other routes to obtain enantiomerically enriched silyl-protected secondary 1,3-diols are known.^[315,321] *Kretschmer et al.* describe a reductive regioselective epoxide opening of an (*E*)- α,β -epoxy aldehyde mediated by an organoselenium compound (**Scheme 62**).^[322] In contrast to the previously described methods using an enantiomerically pure catalyst (*Kagan's*

complex), this reaction is purely substrate-controlled in stereochemistry, the product is not enriched further in neither enantiomeric nor diastereomeric ratio.



Scheme 62: Organoselenium-mediated regioselective epoxide opening.^[315,322]

Because of this, the *e.r.* obtained in the synthesis of **R73** by an asymmetric *Mukaiyama* aldol reaction of 92:8 is also present in the product.^[323,324] The *d.r.* is set by a *Sharpless* epoxidation of the corresponding (*E*)-allylic alcohol.^[325–327] The downsides of this approach are the lack of a double asymmetric reaction increasing the product's *d.r.*, as well as the over-stoichiometric use of the employed reagents (NaBH₄, (PhSe)₂). Product **R74** can thus only be referred to as enantiomerically and diastereomerically enriched.

By the photochemical REO, the synthesis of enantiomerically and diastereomerically pure, regioselectively silyl-protected diols in *syn*- and *anti*-configuration is possible. Gratifyingly, a REO of substrate **R45** (**Table 21**) allows the distinction between three alcohol functions. Additionally, the preparation of *pseudo-meso* or *pseudo-C*₂-symmetrical TBS-protected secondary 1,3-diols is achievable (**Figure 26**), making unselective, low yield desymmetrization reactions superfluent.^[328]

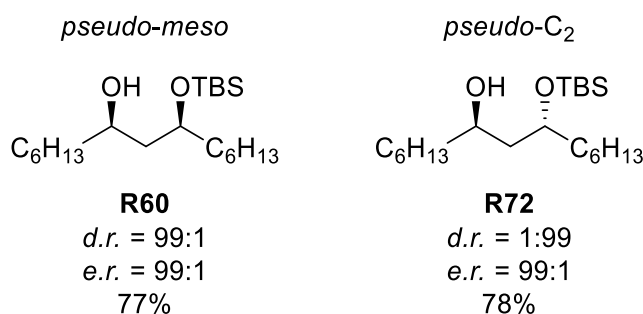
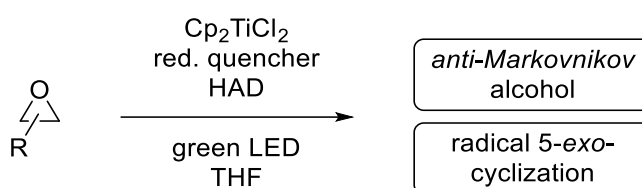


Figure 26: Enantio- and diastereomerically pure *pseudo*-symmetrical secondary 1,3-diols obtained by the photochemical REO.^[136]

4 Summary and Outlook

After it was discovered that Cp_2TiCl_2 can act as photoredox catalyst in epoxide opening reactions with suitable reductive quenchers, hydrogen atom donors and hydrogen atom transfer catalysts, in addition to its previously known role as electron transfer catalyst (**Scheme 63**), the question of applicability to other reaction types, in which titanocenes are known to act as catalysts, arose.

UV/Vis-investigations of the bright-red compound revealed an absorption maximum in the near UV region of the spectrum (392 nm), as well as a smaller absorption maximum in the visible green light region (525 nm), which was successfully used for excitation.



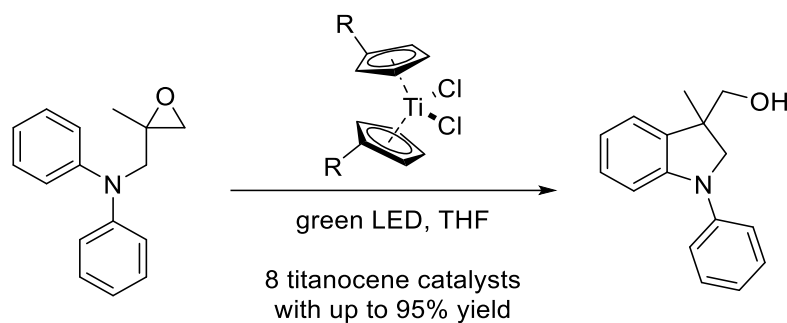
Scheme 63: Titanocene dichloride as photoredox catalyst in epoxide openings and 5-exo-cyclizations.

As titanocenes can be employed in pinacol coupling reactions, these were investigated under the newly discovered conditions with green light irradiation. Unfortunately, the crucial radical intermediates were not generated under the photochemical conditions and, thus, these reactions could not be successfully performed.

Regarding epoxide openings, other titanocenes than Cp_2TiCl_2 were tested for their performance in these well-known reactions. They revealed some promising results, however, none of them could match or surpass the performance of titanocene dichloride.

Currently, *Gansäuer et al.* are investigating the iodide, isothiocyanate and camphor sulfonate derivatives and although the reaction mechanism might differ due to the titanocene's photo-properties, especially the iodide seems to be a promising candidate for future reactions.

Radical arylations of epoxides are another attractive reaction type employing titanocenes as photoredox and electron transfer catalyst. The substrates are readily available by efficient, established procedures and can thus be synthesized with customized substitution patterns. The same holds true for REO-arylation substrates, which can be obtained in enantiomerically pure form. Whereas REO-arylations could not be conducted with photoexcited enantiomerically pure titanocenes (*Kagan's* complexes), as catalyst decomposition was faster than conversion, a new reaction mechanism was found for radical arylations. In an ideal scenario only the titanocene catalyst, substrate and solvent are used (**Scheme 64**).



Scheme 64: Highly sustainable, atom-economic radical arylation of epoxides with substituted titanocenes under photoredox conditions. R = H or (cyclo)alkyl, substituent sizes from R = H to (tBu)CyHex.

This system could be employed for multiple substituted titanocene catalysts with excellent reaction results but is so far unfortunately limited to a single specific substrate used for catalyst screening. Nevertheless, these results are remarkable regarding the steric and electronic properties of the titanocenes, as the conversion of electron-rich substrates generally requires an electron-deficient catalyst. Due to the new photochemical reaction mechanism, this demand is circumvented. Further condition screening including the application of titanocene diiodide as catalyst or ionic liquids as solvents is currently investigated to extend the substrate scope.

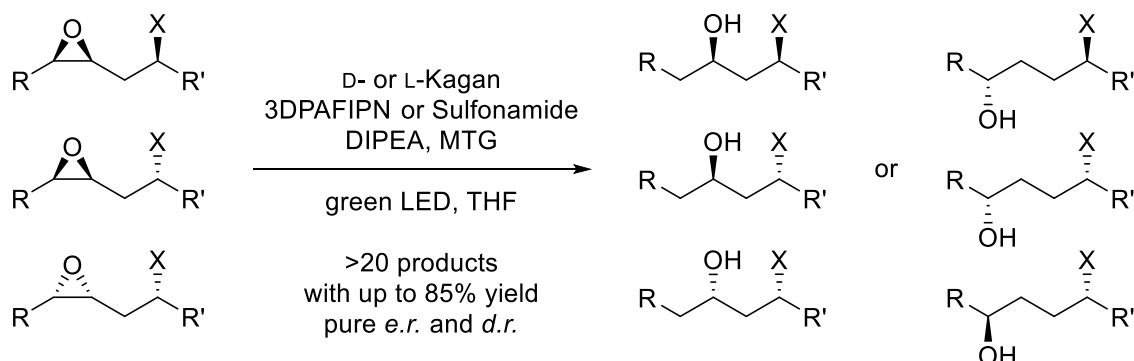
For regio- and diastereodivergent epoxide openings, new substrate structures based on the established synthesis from (di)aryl amines and enantiomerically pure α -bromo epoxides were synthesized in collaboration with *M. Heinz* during his M.Sc. project. Especially for (di)alkyl amines, reliable and reproduceable reaction conditions could be found.

To improve the 'classic' unsustainable reaction conditions for REO reactions of β -substituted *syn*-epoxides using toxic Bu_3SnH and other over-stoichiometric additives, a new synthetic pathway was established. Employing an external organic photoredox catalyst (3DPAFIPN), REOs with good yields and excellent diastereomeric and enantiomeric purity of the obtained 1,3- and 1,4-diol-derivatives could be performed (**Scheme 65**). Especially the high functional group tolerance allows the use of various silyl-protecting groups commonly established in organic synthesis. This is a huge improvement regarding the substrate scope. Gratifyingly, due to the reaction mechanism, a silyl-migration in the reaction mixture is impossible, as the alcohol obtained is initially 'protected' as hemiaminal, and only released upon aqueous work-up – another valuable benefit of the photochemical reaction conditions.

In DEO reactions, two regioisomers with opposite configuration could be synthesized in a single reaction in diastereomerically enriched forms, making this reaction a suitable method for diversity-oriented synthesis of diol-derived molecules. The reaction products could be readily separated via flash column chromatography in good overall yields. Once again,

previous reaction conditions were much less sustainable, employing toxic organotin reagents and using over-stoichiometric amounts of additives.

Together with *T. Krebs*, the advantages in photochemical titanocene catalyzed epoxide openings and the new REO reaction conditions were merged. *Kagan's* complex as enantiomerically pure titanocene was successfully used as the first chiral titanocene serving as both photoredox and electron transfer catalyst in REO reactions. By the aid of catalytic amounts of sulfonamides, catalyst photolysis could be prevented and catalyst activation was facilitated by chloride-abstraction. With the sulfonamides, the required reaction times could be substantially decreased compared to the previous conditions and the reactions reliably resulted in good yields and diastereo- and enantiomerically pure 1,3- and 1,4-diol-derivatives (**Scheme 65**). Moreover, (sterically demanding) silyl-protecting groups were tolerated under these reaction conditions for the first time. Thus, the selectively mono-protected diols could be obtained as products, which are valuable and useful structures in natural product or pharmaceutical drug synthesis and difficult to prepare otherwise.



Scheme 65: General overview of photochemical REOs. R/R' = alkyl or alcohol/ester-substituted alkyl. X = F, OMe, OTBS or other silyl-protecting group.

Overall, the photochemical approach to titanocene catalyzed epoxide openings diminishes the amount of over-stoichiometric, toxic, and waste-generating additives and reagents by replacing them with catalysts and less hazardous chemicals. Therefore, the new reactions meet the requirements of Green Chemistry, enabling more sustainable, yet equally or even more efficient stereoselective syntheses. Moreover, the substrate scope could be substantially increased. Ideally, future investigations will lead to reaction conditions for photochemical REO-arylations and the elucidation of hidden mechanistic details of the photocatalytic reactions.

5 Experimental Part

5.1 General Information

All reactions containing air or moisture sensitive reagents or products were performed in heat-dried glassware under argon atmosphere using *Schlenk* technique. Liquid reagents and dry solvents were transferred via argon flushed syringes or transfer cannulas through septa.

Commercially available chemicals from *Sigma Aldrich*, *ChemPur*, *Alfa Aesar*, *Acros Organics*, *abcr*, *TCI Chemicals*, *Fluorochem* and *Merck* were used without purification as obtained unless stated otherwise.

5.1.1 Instruments and Analytics

5.1.1.1 Chromatography

All reactions were monitored by TLC (thin layer chromatography) on *Merck* silica gel 60 F₂₅₄ plates using UV light as visualizing agent (if applicable) and/or a solution of ammonium molybdate tetrahydrate (25 g/L) and Ce(SO₄)₂*4 H₂O (10 g/L) in 10% aqueous solution of H₂SO₄ followed by heating as developing agent. The reaction products were purified by flash column chromatography on *Merck* silica gel 60 or *Merck* aluminum oxide neutral. The solvent mixtures used as eluent are denoted in the respective reaction information.

5.1.1.2 NMR-Spectroscopy

¹H-, ¹³C-, and ¹⁹F-NMR spectra were recorded on a *Bruker* Avance I 500 MHz (base frequency 499.13 MHz), *Bruker* Avance III HD 500 MHz (base frequency 500.13 MHz) or *Bruker* Avance I 400 MHz (base frequency 400.13 MHz) instrument at room temperature. Chemical shifts (δ) are denoted in ppm and were calibrated by using residual undeuterated solvent signals as internal reference for ¹H-NMR (CDCl₃: 7.26 ppm; C₆D₆: 7.16 ppm and CD₂Cl₂: 5.32 ppm) and the central signal of the deuterated solvent as internal standard for ¹³C-NMR (CDCl₃: 77.2 ppm; C₆D₆: 128.1 ppm and CD₂Cl₂: 54.0 ppm).^[329] H,H-coupling constants (*J*) are reported in Hz.

Unless stated otherwise, the regioisomeric and diastereoisomeric ratio of the products were determined by ¹³C-NMR spectroscopy.^[330] The regioisomeric ratio was determined from the crude reaction mixture after work-up and the diastereoisomeric ratio was determined from the purified compounds.

5.1.1.3 IR-Spectroscopy

IR spectra were recorded on a *Nicolet ATR-IR 380* spectrometer by *Thermo Electron*. Wavenumbers were rounded to 0 or 5 and denoted in cm^{-1} .

5.1.1.4 High Resolution Mass Spectrometry

Electron spray ionization (ESI) measurements were performed on a time-of-flight spectrometer *microTOF-Q* by *Bruker Daltonic* with a collision energy of 8.0 eV. Atmospheric-pressure chemical ionization (APCI) measurements were performed on an *Orbitrap XL* spectrometer. Electron ionization (EI) measurements were performed on sector field mass analyzers *MAT 90* and *MAT 95 XL* by *Thermo Finnigan*.

5.1.1.5 High Performance Liquid Chromatography

Analytical chiral HPLC was measured on a *Knauer Azura HPG* device using *Chiralpak IH-U* 1.6 μm columns with a flow rate of 0.85 mL/min and *n*-hexane/isopropanol or *n*-heptane/isopropanol mixtures as eluent.

5.1.1.6 Polarimetry

$[\alpha]_{\text{D}}^{20}$ (specific optical rotation at 20°C) values of the purified products were measured on a circular polarimeter *MCP150* by *Anton Paar* with a concentration of 10 g/L. The respective solvent used is denoted in the substance information.

5.1.1.7 LED Lamps

The LED light sources were *Eurolite LED IP FL-10 Outdoor LEDs* (10 W).

5.1.1.8 Melting Points

Melting points (mp) were measured on a *DigiMelt MPA 160* by *SRS*.

5.1.1.9 UV/Vis-Spectroscopy

UV/Vis spectra were recorded on a *Perkin Elmer UV/Vis* spectrometer *Lambda 18*. The concentration of the UV/Vis-active compound was set to approximately 5 $\mu\text{mol/mL}$.

5.1.2 Solvents

The solvents used in air and moisture sensitive reactions were either purchased in bottles under inert atmosphere or dried according to the following protocols.

Acetonitrile (MeCN)	Purchased from <i>Thermo Fisher Scientific</i> as extra dry solvent and used without further drying.
Dichloromethane (DCM)	Obtained from <i>M. Braun</i> MB SPS 800 solvent drying system under an argon stream.
Diisopropylamine (DIPEA)	Purchased from <i>TCI Chemicals</i> as GC grade solvent. Pre-dried over CaH ₂ and distilled under argon atmosphere, stored over 3Å molecular sieves under argon.
Dimethoxyethane (DME)	Purchased from <i>Thermo Fisher Scientific</i> as extra dry solvent and used without further drying.
<i>N,N'</i> -Dimethylpropyleneurea (DMPU)	Purchased from <i>Thermo Fisher Scientific</i> as extra dry solvent and used without further drying.
Methylthioglycolate (MTG)	Purchased from <i>TCI Chemicals</i> as GC grade solvent. Distilled under argon atmosphere, stored over 3Å molecular sieves under argon.
Pyridine	Obtained from <i>M. Braun</i> MB SPS 800 solvent drying system under an argon stream.
Tetrahydrofuran (THF)	Either obtained from <i>M. Braun</i> MB SPS 800 solvent drying system under an argon stream, or pre-dried over potassium hydroxide, refluxed over sodium/benzophenone and distilled under argon before use.

5.2 General Procedures

5.2.1 Opening of Terminal Epoxides (**GP1**)

The titanocene-catalyst (10 mol%) is placed in a heat-dried *Schlenk* tube and evacuated for 30 min. Under argon, epoxide (1.0 eq.), DIPEA (3.0 eq.) MTG (20 mol%) and THF (10 mL, 0.05 M) are added. The *Schlenk* tube is placed in a reactor and the reaction is stirred at room temperature under irradiation with LEDs. After the reaction is finished, the reaction mixture is diluted with Et₂O and quenched using phosphate buffer. The layers are separated, and the aqueous layer is extracted with Et₂O (3x). After drying over MgSO₄, the solvent is removed under reduced pressure. The crude product is purified by flash column chromatography (SiO₂, CH/EA).

5.2.2 Pinacol Coupling of Benzaldehyde (**GP2**)

Cp₂TiCl₂ (10 mol%) is placed in a heat-dried *Schlenk* tube under argon. Benzaldehyde (1.0 eq.), amine (3.0 eq.), TMSCl (1.5 eq.) and THF (10 mL, 0.05 M) are added, and the reaction mixture is stirred at room temperature under irradiation with green LEDs overnight. The reaction conversion is monitored by TLC.

5.2.3 Radical Arylation of Epoxides (**GP3**)

In a heat-dried *Schlenk* tube titanocene catalyst (10 mol%) is placed and evacuated for 30 min. Under argon atmosphere, dry THF (0.05 M) and epoxide (1.0 eq.) are added, the reaction mixture is stirred overnight at the respective temperature under irradiation with green light. After completion, the reaction mixture is diluted with Et₂O. The layers are separated, the aqueous layer is extracted with Et₂O (3x), the combined organic phases are dried over MgSO₄ and the solvent is evaporated. The yield is determined by ¹H-NMR data evaluation of the crude product with an internal standard (DMT).

5.2.4 Bromination-Epoxidation of (*E*)-Allylic Alcohols (**GP4**)

The synthesis is performed according to the literature.^[149] Under ambient conditions a solution of the (*E*)-allylic alcohol (1.0 eq.) in DCM (0.5 M) is cooled to -78°C. Over a period of 1 h, Br₂ (1.0 eq., dissolved in pre-cooled DCM, about 20% of the solvent) is added via a dropping funnel while the reaction mixture is stirred at -78°C. The reaction is quenched by addition of sat. aq. Na₂S₂O₃ solution (until the solution is pale-yellow). After warming up to room temperature, about 75% of the solvent is removed under reduced pressure, the phases are separated, and the aqueous phase is extracted with DCM (2x). The combined organic layers are dried over MgSO₄, and the solvent is removed under reduced pressure. The crude product is used without further purification. It is then dissolved in MeOH (0.5 M) and finely ground K₂CO₃ (2.0 eq.) is added. The mixture is stirred for 3 h until the conversion is complete (monitor by TLC). 75% of the solvent is removed under reduced pressure and the residue is diluted with EA (0.5 M). K₂CO₃ is removed via vacuum filtration and the solvent is evaporated. The crude product is purified by flash column chromatography (SiO₂, CH/EA) or distillation.

5.2.5 Nucleophilic Substitution on α -Bromo Epoxides (**GP5**)

The reaction is performed in a heat-dried *Schlenk* flask under argon atmosphere. The respective nucleophile (1.0 eq.) is dissolved in dry THF and the solution is cooled to 0°C, sodium hydride (60% dispersion in mineral oil, 1.5 eq.) or *n*BuLi (2.5 M solution in hexane, 1.5 eq.) is added and the solution is stirred for 1 h. After the α -bromo epoxide (1.2 eq.) and the respective *Lewis* acid (1.1 eq.) are added, the reaction mixture is stirred at room temperature. It is diluted with Et₂O and washed with water and brine. The combined organic phases are dried over MgSO₄, and the solvent is removed under reduced pressure. The crude product is purified by flash column chromatography (SiO₂, CH/EA).

5.2.6 Silyl Protection of β -Epoxy Alcohols (GP6)

Imidazole (2.5 eq.) is placed in a *Schlenk* flask and evacuated for 30 min. Under argon, DMF (1.0 M) is added. Subsequently, the β -epoxy alcohol (1.0 eq.) and corresponding silyl chloride (1.2 eq.) are added, and the reaction mixture is stirred for 2 h at room temperature. The mixture is diluted with Et₂O (0.5 M) followed by slow addition of saturated aqueous solution of NaHCO₃. The layers are separated, and the organic layer is washed 3x with saturated aqueous solution of NaHCO₃ and 3x with H₂O. After drying over MgSO₄ the solvent is removed under reduced pressure and the crude product is purified by flash column chromatography.

5.2.7 Addition of Terminal Alkynes to Terminal Epoxides (GP7)

To a solution of terminal alkyne (1.2 eq.) in dry THF (0.6 M), *n*BuLi (2.5 M in hexane, 1.2 eq.) is added at -96°C. The solution is stirred for 1 h. BF₃·THF (1.0 eq.) and the terminal epoxide (1.0 eq.) are added dropwise simultaneously. The reaction is stirred for 2h while the reaction temperature has to be kept between -96°C and -78°C. After addition of saturated aqueous NaHCO₃ solution, the mixture is warmed up to room temperature. The layers are separated, and the aqueous phase extracted with Et₂O. The combined organic phases are dried over MgSO₄, and the solvent is removed under reduced pressure. The crude product is purified by flash column chromatography.

5.2.8 Reduction of Homopropargylic Alcohols to (*Z*)-Homoallylic Alcohols (GP8)

To a solution of Ni(OAc)₂·4H₂O (0.25 eq.) in MeOH (0.2 M), NaBH₄ (0.25 eq.) is added at 0°C. The solution is warmed up to room temperature and ethylene diamine (EDA, 0.5 eq.) and alkyne (1.0 eq.) are added. The reaction mixture is stirred vigorously overnight (if not stated otherwise) under hydrogen atmosphere. The solvent is removed under reduced pressure and the residue is dissolved in Et₂O and filtered through a silica plug. The solvent is removed, and the crude product is used without further purification.

The residue of P-2 nickel is **immediately** reacted with 3 M aq. HCl until a complete color change from black to green is observed. P-2 nickel might spontaneously ignite under air.

5.2.9 Diastereoselective Epoxidation of (*Z*)-Homoallylic Alcohols (**GP9**)

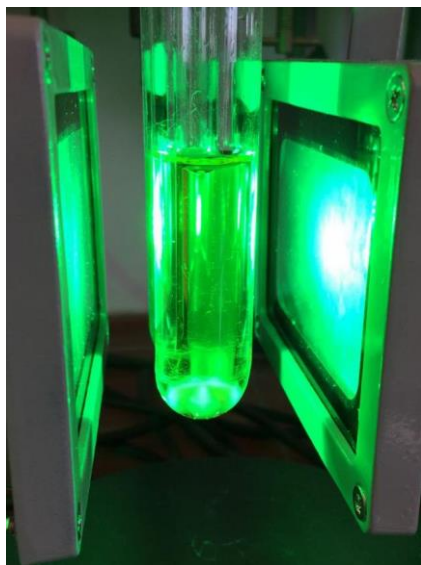
To a solution of (*Z*)-homoallylic alcohol (1.0 eq.) in DCM (0.1 M), VO(acac)₂ (5 mol%) is added. At 0°C TBHP (5.5 M solution in decane, 1.5 eq.) is added. The reaction is warmed up to room temperature and stirred overnight. The reaction mixture is treated with saturated aqueous NaHSO₃ solution, the layers are separated, and the organic layer is washed with water and brine. The organic phase is dried over MgSO₄, and the solvents are removed under reduced pressure. The crude product is purified by flash column chromatography to yield the corresponding *syn*-β-epoxy alcohol.

5.2.10 Methylation of β-Epoxy Alcohols (**GP10**)

To a solution of a β-epoxy alcohol (1.0 eq.) in THF (0.3 M), NaH (60% in mineral oil, 1.5 eq.) is added at 0°C. The suspension is stirred for 30 min until gas evolution ceased and MeI (3.0 eq.) is added. The reaction mixture is stirred overnight at room temperature. Saturated aqueous Na₂S₂O₃ solution is added, and the mixture is extracted with Et₂O, washed with brine and dried over MgSO₄. The solvent is removed under reduced pressure and the crude product is purified by flash column chromatography.

5.2.11 REO and DEO Reactions with Organic Photocatalysts (**GP11**)

The reaction is performed in a heat-dried *Schlenk* tube under argon atmosphere. *Kagan's* complex (10 mol%) and 3DPAFIPN (3 mol%) and epoxide (1.0 eq., if solid) are placed in the tube and evacuated for 30 min. After flushing with argon, THF (0.1 M) and epoxide (if liquid) are added, followed by DIPEA (3.0 eq.) and MTG (20 mol%). The reaction is stirred under irradiation with blue light at room temperature. After the reaction is finished, 5 mL of phosphate buffer solution and 5 mL of Et₂O are added. The reaction is stirred for 10 min, afterwards the phases are separated, and the aqueous layer is extracted with Et₂O (3x). The combined organic phase is dried over MgSO₄, and the solvent is removed under reduced pressure. The crude product is purified by flash column chromatography (SiO₂, CH/EA). The regioisomeric ratio (*r.r.* 1,3:1,4) is determined from the crude ¹³C-NMR spectrum, the diastereoisomeric ratio (*d.r. syn:anti*) is determined from the ¹³C-NMR spectrum of the purified product.

5.2.12 REO Reactions with Sulfonamides (**GP12**)

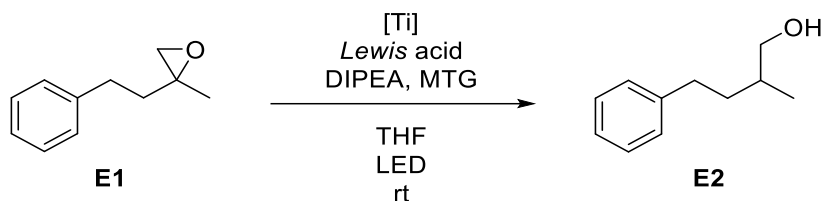
In a heat-dried *Schlenk* tube *Kagan's* complex (15 mol%) and sulfonamide **Z1** (15 mol%) are added and evacuated for 30 min. Under argon atmosphere, REO substrate (1.0 eq.), dry THF (0.17 M), DIPEA (3.0 eq.) and MTG (20 mol%) are subsequently added. The *Schlenk* tube is placed in a reactor and the reaction is stirred at 45°C under irradiation with green LEDs. After the reaction is finished, the reaction mixture is diluted with Et₂O and quenched using aqueous phosphate buffer. The layers are separated, and the aqueous layer is extracted with Et₂O (3x). After drying over MgSO₄ the solvent is removed under reduced pressure. For determination of the regioisomeric ratio (*r.r.*) a ¹³C-NMR spectrum of the crude product is recorded. The crude product is purified by flash column chromatography (CH/EA 95:5, if not denoted otherwise). The diastereoisomeric ratio (*d.r.*) is determined from the ¹³C-NMR spectrum of the pure product.^[136]

5.2.13 Decarboxylation and Acrylate Addition of Carboxylic Acids (**GP13**)

In a heat-dried *Schlenk* tube, titanocene catalyst (10 mol%), carboxylic acid (1.0 eq.) and base (10 mol%, 0.5 eq. or 1.0 eq.) are placed under argon atmosphere. *tert*-butyl acrylate (2.0 eq.) and dry THF (0.05 M) are added, and the reaction mixture is stirred at room temperature under irradiation with green light for 20 h. The reaction conversion is monitored by TLC.

5.3 Photoexcited Titanocene Catalyzed Epoxide Openings

5.3.1 Opening of 2-methyl-2-phenethyloxirane

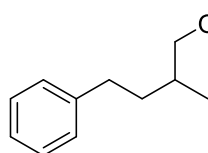


5.3.1.1

According to **GP1** 2-methyl-2-phenethyloxirane (**E1**, 1.0 eq., 0.50 mmol, 81.1 mg), Cp^*TiCl_3 (10 mol%, 0.05 mmol, 14.5 mg), DIPEA (3.0 eq., 1.50 mmol, 0.26 mL) and MTG (20 mol%, 0.10 mmol, 9 μL) are reacted in THF (10 mL) at room temperature under irradiation with green LEDs for 90 h. According to TLC, no conversion is observed.

5.3.1.2

According to **GP1** 2-methyl-2-phenethyloxirane (**E1**, 1.0 eq., 0.50 mmol, 81.1 mg), Cp^*TiCl_3 (10 mol%, 0.05 mmol, 14.5 mg), DIPEA (3.0 eq., 1.50 mmol, 0.26 mL) and MTG (20 mol%, 0.10 mmol, 9 μL) are reacted in THF (10 mL) at room temperature under irradiation with blue LEDs for 90 h. After work-up, the yield of **E2** is determined by $^1\text{H-NMR}$ data evaluation of the crude product with an internal standard (TMB) to be 23% (0.12 mmol).



E2: $\text{C}_{11}\text{H}_{16}\text{O}$; **MW** = 164.25 g/mol; $^1\text{H-NMR}$ (400 MHz, CDCl_3) δ [ppm] 7.32 – 7.25 (m, 2H), 7.22 – 7.16 (m, 3H), 3.58 – 3.44 (m, 2H), 2.76 – 2.56 (m, 2H), 1.83 – 1.62 (m, 2H), 1.51 – 1.40 (m, 1H), 1.38 (s, 1H), 1.00 (d, $J = 6.7$ Hz, 3H).

The analytical data is in agreement with the literature.^[125,132,156]

5.3.1.3

According to **GP1** 2-methyl-2-phenethyloxirane (**E1**, 1.0 eq., 0.50 mmol, 81.1 mg), CpTiCl_3 (10 mol%, 0.05 mmol, 11.0 mg), DIPEA (3.0 eq., 1.50 mmol, 0.26 mL) and MTG (20 mol%, 0.10 mmol, 9 μL) are reacted in THF (10 mL) at room temperature under irradiation with green LEDs for 70 h. According to TLC, no conversion is observed.

5.3.1.4

According to **GP1** 2-methyl-2-phenethyloxirane (**E1**, 1.0 eq., 0.50 mmol, 81.1 mg), CpTiCl_3 (10 mol%, 0.05 mmol, 11.0 mg), DIPEA (3.0 eq., 1.50 mmol, 0.26 mL) and MTG (20 mol%, 0.10 mmol, 9 μL) are reacted in THF (10 mL) at room temperature under irradiation with blue LEDs for 70 h. According to TLC, no conversion is observed.

5.3.1.5

According to **GP1** 2-methyl-2-phenethyloxirane (**E1**, 1.0 eq., 0.50 mmol, 81.1 mg), Cp^*TiCl_3 (10 mol%, 0.05 mmol, 14.5 mg), DIPEA (3.0 eq., 1.50 mmol, 0.26 mL), MTG (20 mol%, 0.10 mmol, 9 μL) and ZnCl_2 (1.0 M solution in THF, 1.0 eq., 0.50 mmol, 0.5 mL) are reacted in THF (10 mL) at room temperature under irradiation with blue LEDs for 20 h and subsequently with green LEDs for 20 h. According to TLC, no conversion is observed.

5.3.1.6

According to **GP1** 2-methyl-2-phenethyloxirane (**E1**, 1.0 eq., 0.50 mmol, 81.1 mg), $\text{Cp}_2\text{Ti}(\text{OTf})_2$ (10 mol%, 0.05 mmol, 26.0 mg), DIPEA (3.0 eq., 1.50 mmol, 0.26 mL) and MTG (20 mol%, 0.10 mmol, 9 μL) are reacted in THF (10 mL) at room temperature under irradiation with blue LEDs for 20 h and subsequently with green LEDs for 20 h. According to TLC, low conversion is observed, the product is not isolated.

5.3.1.7

According to **GP1** 2-methyl-2-phenethyloxirane (**E1**, 1.0 eq., 0.50 mmol, 81.1 mg), $\text{Cp}_2\text{Ti}(\text{OMe})_2$ (10 mol%, 0.05 mmol, 18.4 mg), DIPEA (3.0 eq., 1.50 mmol, 0.26 mL) and MTG (20 mol%, 0.10 mmol, 9 μL) are reacted in THF (10 mL) at room temperature under irradiation with blue LEDs for 20 h and subsequently with green LEDs for 20 h. According to TLC, low conversion is observed, the product is not isolated.

5.3.1.8

According to **GP1** 2-methyl-2-phenethyloxirane (**E1**, 1.0 eq., 0.50 mmol, 81.1 mg), $\text{Cp}_2\text{Ti}(\text{TFA})_2$ (10 mol%, 0.05 mmol, 20.2 mg), DIPEA (3.0 eq., 1.50 mmol, 0.26 mL) and MTG (20 mol%, 0.10 mmol, 9 μL) are reacted in THF (10 mL) at room temperature under irradiation with blue LEDs for 20 h and subsequently with green LEDs for 20 h. According to TLC, low conversion is observed, the product is not isolated.

5.3.1.9

According to **GP1** 2-methyl-2-phenethyloxirane (**E1**, 1.0 eq., 0.50 mmol, 81.1 mg), Cp_2TiF_2 (10 mol%, 0.05 mmol, 10.8 mg), DIPEA (3.0 eq., 1.50 mmol, 0.26 mL) and MTG (20 mol%, 0.10 mmol, 9 μL) are reacted in THF (10 mL) at room temperature under irradiation with blue LEDs for 90 h. According to TLC, no conversion is observed.

5.3.1.10

According to **GP1** 2-methyl-2-phenethyloxirane (**E1**, 1.0 eq., 0.50 mmol, 81.1 mg), Cp_2TiCl_2 (5 mol%, 0.025 mmol, 6.2 mg), $\text{Cp}_2\text{Ti}(\text{OMs})_2$ (5 mol%, 0.025 mmol, 9.2 mg), DIPEA (3.0 eq., 1.50 mmol, 0.26 mL) and MTG (20 mol%, 0.10 mmol, 9 μL) are reacted in THF (10 mL) at room temperature under irradiation with green LEDs for 16 h. After purification, **E2** (0.29 mmol, 47 mg, 57%) is obtained as a colorless oil.

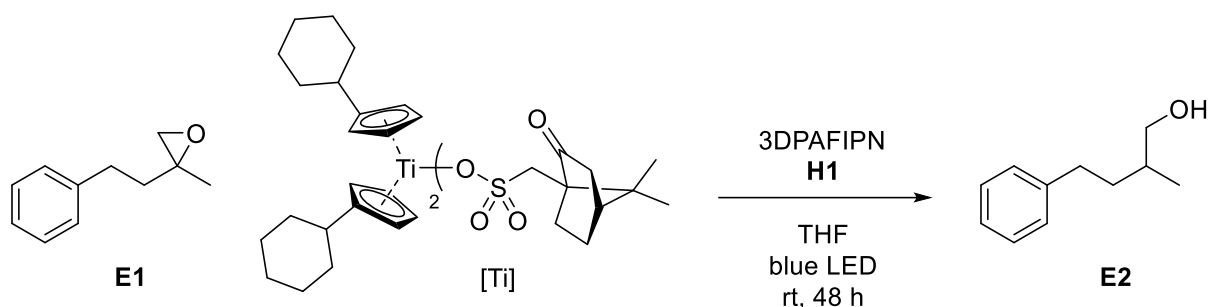
5.3.1.11

According to **GP1** 2-methyl-2-phenethyloxirane (**E1**, 1.0 eq., 0.50 mmol, 81.1 mg), Cp_2TiCl_2 (5 mol%, 0.025 mmol, 6.2 mg), $\text{Cp}_2\text{Ti}(\text{TFA})_2$ (5 mol%, 0.025 mmol, 10.1 mg), DIPEA (3.0 eq., 1.50 mmol, 0.26 mL) and MTG (20 mol%, 0.10 mmol, 9 μL) are reacted in THF (10 mL) at room temperature under irradiation with green LEDs for 16 h. After purification, **E2** (0.32 mmol, 52 mg, 63%) is obtained as a colorless oil.

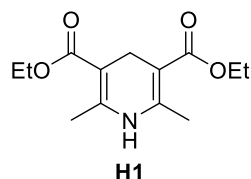
5.3.1.12

According to **GP1** 2-methyl-2-phenethyloxirane (**E1**, 1.0 eq., 0.50 mmol, 81.1 mg), Cp_2TiCl_2 (5 mol%, 0.025 mmol, 6.2 mg), DIPEA (3.0 eq., 1.50 mmol, 0.26 mL) and MTG (20 mol%, 0.10 mmol, 9 μL) are reacted in THF (10 mL) at room temperature under irradiation with green LEDs for 16 h. After purification, **E2** (0.19 mmol, 31 mg, 38%) is obtained as a colorless oil.

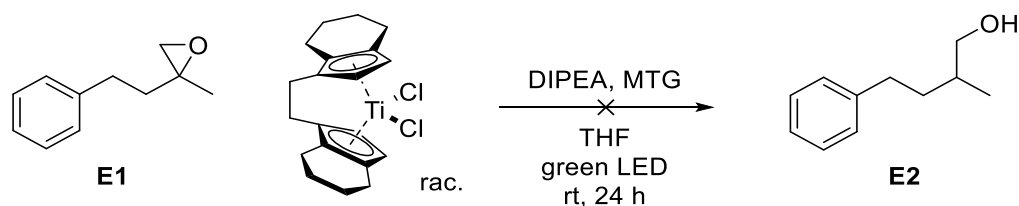
5.3.1.13



In a heat-dried *Schlenk* tube under argon atmosphere, 2-methyl-2-phenethyloxirane **E1** (1.0 eq., 0.50 mmol, 81.1 mg), **[Ti]** ((+)-CSA, 10 mol%, 0.05 mmol, 40.3 mg), 3DPAFIPN (3 mol%, 12.5 μ mol, 8.0 mg), **H1** (2.0 eq., 1.0 mmol, 253.3 mg) are dissolved in dry THF (0.05 M, 10 mL) and the reaction mixture is stirred under irradiation with blue light at room temperature for 48 h. The solvent is removed under reduced pressure and the crude product is purified by flash column chromatography (SiO₂, CH/EA 4:1). **E2** is obtained as a colorless oil (0.20 mmol, 32.9 mg, 40%).



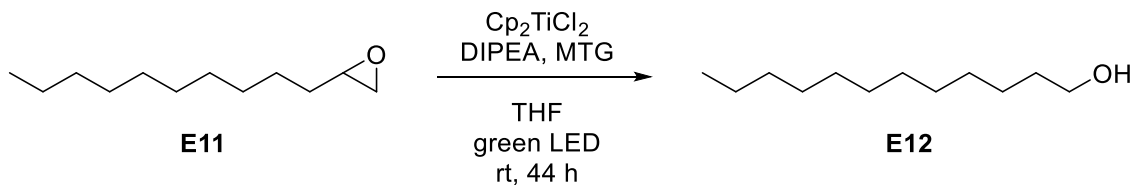
5.3.1.14



According to **GP1** 2-methyl-2-phenethyloxirane **E1** (1.0 eq., 0.50 mmol, 81.1 mg), racemic titanocene catalyst (*rac*-(*ebthi*)TiCl₂, 10 mol%, 0.05 mmol, 19.2 mg), DIPEA (3.0 eq., 1.50 mmol, 0.26 mL) and MTG (20 mol%, 0.10 mmol, 9 μ L) are reacted in THF (10 mL) at room temperature under irradiation with green LEDs for 24 h. According to TLC, no conversion is observed.

5.3.2 Opening of 2-decyloxirane

5.3.2.1



According to **GP1** 2-decyloxirane (**E11**, 1.0 eq., 0.50 mmol, 92.2 mg), Cp_2TiCl_2 (10 mol%, 0.05 mmol, 12.5 mg), DIPEA (3.0 eq., 1.50 mmol, 0.26 mL) and MTG (20 mol%, 0.10 mmol, 9 μL) are reacted in THF (5 mL) at room temperature under irradiation with green LEDs for 44 h. After work-up, the yield is determined by $^1\text{H-NMR}$ data evaluation of the crude product with an internal standard (TMB). Dodecan-1-ol (**E12**, 0.21 mmol, 41%) is obtained.

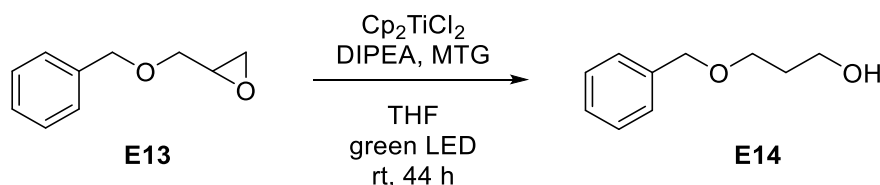
E12: $\text{C}_{12}\text{H}_{26}\text{O}$; **MW** = 186.34 g/mol; $^1\text{H-NMR}$ (400 MHz, CDCl_3) δ [ppm] 3.64 (q, J = 6.1 Hz, 2H), 1.63 – 1.51 (m, 2H), 1.38 – 1.16 (m, 18H), 0.88 (t, J = 6.8 Hz, 3H).

The analytical data is in agreement with the literature.^[331]

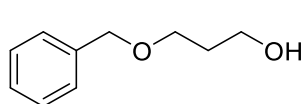
5.3.2.2

According to **GP1** 2-decyloxirane (**E11**, 1.0 eq., 0.50 mmol, 92.2 mg), $(t\text{BuCp})_2\text{TiCl}_2$ (10 mol%, 0.05 mmol, 18.1 mg), DIPEA (3.0 eq., 1.50 mmol, 0.26 mL) and MTG (20 mol%, 0.10 mmol, 9 μL) are reacted in THF (10 mL) at 50°C under irradiation with green LEDs for 24 h. After work-up, the yield is determined by $^1\text{H-NMR}$ data evaluation of the crude product with an internal standard (CH_2Br_2). Dodecan-1-ol (**E12**, 0.18 mmol, 35%, 1-ol:2-ol = 99:1) is obtained.

5.3.3 Opening of 2-((benzyloxy)methyl)oxirane



According to **GP1** 2-((benzyloxy)methyl)oxirane (**E13**, 1.0 eq., 0.50 mmol, 82.1 mg), Cp_2TiCl_2 (10 mol%, 0.05 mmol, 12.5 mg), DIPEA (3.0 eq., 1.50 mmol, 0.26 mL) and MTG (20 mol%, 0.10 mmol, 9 μL) are reacted in THF (5 mL) at room temperature under irradiation with green LEDs for 44 h. After work-up, the yield is determined by $^1\text{H-NMR}$ data evaluation of the crude product with an internal standard (TMB). 3-(benzyloxy)propan-1-ol (**E14**, 0.13 mmol, 27%) is obtained.

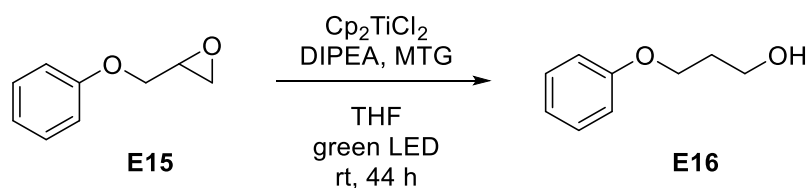


E14: C₁₀H₁₄O₂; **MW** = 166.22 g/mol; **¹H-NMR** (400 MHz, CDCl₃) δ [ppm] 7.37 – 7.27 (m, 5H), 4.53 (s, 2H), 3.79 (td, *J* = 5.6, 5.6 Hz, 2H), 3.67 (t, *J* = 5.6 Hz, 2H), 2.25 (s, 1H), 1.87 (tt, *J* = 5.6, 5.6

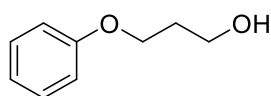
Hz, 2H).

The analytical data is in agreement with the literature.^[332,333]

5.3.4 Opening of 2-(phenoxy)methyl)oxirane



According to **GP1** 2-(phenoxy)methyl)oxirane (**E15**, 1.0 eq., 0.50 mmol, 75.1 mg), Cp₂TiCl₂ (10 mol%, 0.05 mmol, 12.5 mg), DIPEA (3.0 eq., 1.50 mmol, 0.26 mL) and MTG (20 mol%, 0.10 mmol, 9 μL) are reacted in THF (5 mL) at room temperature under irradiation with green LEDs for 44 h. After work-up, the yield is determined by ¹H-NMR data evaluation of the crude product with an internal standard (TMB). 3-phenoxypropan-1-ol (**E16**, 0.12 mmol, 24%) is obtained.

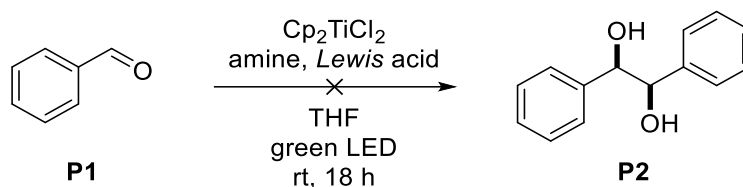


E16: C₉H₁₂O₂; **MW** = 152.19 g/mol; **¹H-NMR** (400 MHz, CDCl₃) δ [ppm] 7.31 – 7.22 (m, 2H), 6.97 – 6.84 (m, 3H), 4.08 (t, *J* = 6.0 Hz, 2H), 3.81 (t, *J* = 6.0 Hz, 2H), 2.00 (dt, *J* = 6.0 Hz, 2H).

The analytical data is in agreement with the literature.^[334]

5.4 Pinacol Couplings

5.4.1 Pinacol Coupling of Benzaldehyde



5.4.1.1

According to **GP2** benzaldehyde (**P1**, 1.0 eq., 0.50 mmol, 50.5 μL), Cp_2TiCl_2 (10 mol%, 0.05 mmol, 12.5 mg) and triethylamine (3.0 eq., 1.50 mmol, 0.21 mL) are reacted in THF (10 mL) under irradiation with green light for 18 h. According to TLC, no conversion is observed.

5.4.1.2

According to **GP2** benzaldehyde (**P1**, 1.0 eq., 0.50 mmol, 50.5 μL), Cp_2TiCl_2 (10 mol%, 0.05 mmol, 12.5 mg) and DIPEA (3.0 eq., 1.50 mmol, 0.26 mL) are reacted in THF (10 mL) under irradiation with green light for 18 h. According to TLC, no conversion is observed.

5.4.1.3

According to **GP2** benzaldehyde (**P1**, 1.0 eq., 0.50 mmol, 50.5 μL), Cp_2TiCl_2 (10 mol%, 0.05 mmol, 12.5 mg), triethylamine (3.0 eq., 1.50 mmol, 0.21 mL) and TMSCl (1.5 eq., 0.75 mmol, 0.10 mL) are reacted in THF (10 mL) under irradiation with green light for 18 h. According to TLC, no conversion is observed.

5.4.1.4

According to **GP2** benzaldehyde (**P1**, 1.0 eq., 0.50 mmol, 50.5 μL), Cp_2TiCl_2 (10 mol%, 0.05 mmol, 12.5 mg), DIPEA (3.0 eq., 1.50 mmol, 0.26 mL) and TMSCl (1.5 eq., 0.75 mmol, 0.10 mL) are reacted in THF (10 mL) under irradiation with green light for 18 h. According to TLC, no conversion is observed.

5.4.1.5

According to **GP2** benzaldehyde (**P1**, 1.0 eq., 0.50 mmol, 50.5 μL), Cp_2TiCl_2 (10 mol%, 0.05 mmol, 12.5 mg), DIPEA (3.0 eq., 1.50 mmol, 0.26 mL) TMSCl (1.5 eq., 0.75 mmol, 0.10 mL) and ZnCl_2 (1.0 M solution in THF, 1.0 eq., 0.50 mmol, 0.5 mL) are reacted in THF (10 mL) under irradiation with green LEDs for 20 h and subsequently with blue LEDs for 20 h. According to TLC, no conversion is observed.

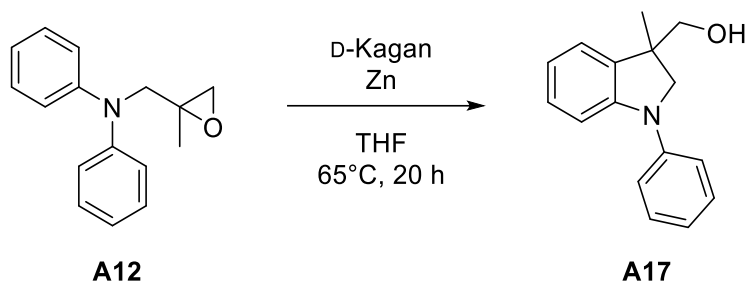
5.4.1.6

According to **GP2** benzaldehyde (**P1**, 1.0 eq., 0.50 mmol, 50.5 μ L), Cp_2TiCl_2 (10 mol%, 0.05 mmol, 12.5 mg), DIPEA (3.0 eq., 1.50 mmol, 0.26 mL) and ZnCl_2 (1.0 M solution in THF, 1.0 eq., 0.50 mmol, 0.5 mL) are reacted in THF (10 mL) under irradiation with green LEDs for 20 h and subsequently with blue LEDs for 20 h. According to TLC, no conversion is observed.

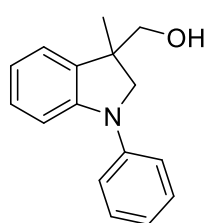
5.5 Radical Arylations and REO-Arylations of Epoxides

5.5.1 Arylations of *N*-((2-methyloxiran-2-yl)methyl)-*N*-phenylaniline

5.5.1.1



In a heat-dried *Schlenk* tube, Zn (10 mol%, 0.05 mmol, 3.3 mg) and D-Kagan (10 mol%, 0.05 mmol, 26.3 mg) are placed and evacuated for 30 min. Under argon atmosphere, dry THF (0.05 M, 10 mL) and **A12** (1.0 eq., 0.5 mmol, 119.7 mg) are added, the reaction mixture is heated to 65°C and stirred overnight. It is quenched by the addition of sat. aq. NH₄Cl solution and diluted with Et₂O. The layers are separated, the aqueous layer is extracted with Et₂O (3x) and the combined organic phases are dried over MgSO₄ and the solvent is evaporated. The yield of **A17** is determined by ¹H-NMR data evaluation of the crude product with an internal standard (DMT) to be 94% (0.47 mmol).

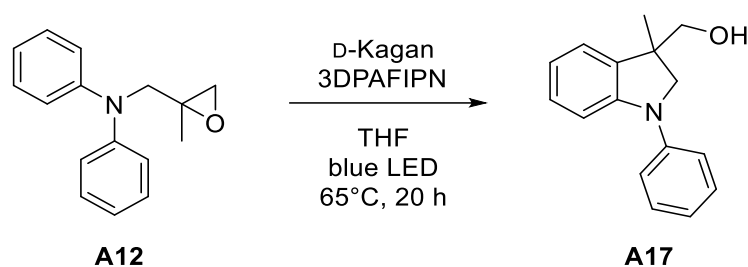


A17: C₁₆H₁₇NO; MW = 239.32 g/mol; ¹H-NMR (500 MHz, C₆D₆) δ [ppm] 7.23 – 7.19 (m, 2H), 7.18 – 7.16 (m, 1H), 7.14 – 7.11 (m, 2H), 7.03 (ddd, *J* = 8.0, 7.4, 1.4 Hz, 1H), 6.94 (ddd, *J* = 7.4, 1.4, 0.6 Hz, 1H), 6.90 (tt, *J* = 7.3, 1.2 Hz, 1H), 6.76 (td, *J* = 7.4, 0.9 Hz, 1H), 3.63 (d, *J* = 9.3 Hz, 1H), 3.30 (dd, *J* = 9.9, 3.2 Hz, 2H), 3.22 (d, *J* = 10.6 Hz, 1H), 1.15 (s, 3H), 0.99 (s, 1H);

¹³C-NMR (126 MHz, C₆D₆) δ [ppm] 147.1, 144.4, 136.3, 129.5, 128.3, 123.6, 121.2, 119.4, 118.0, 108.9, 68.9, 61.8, 45.5, 22.1.

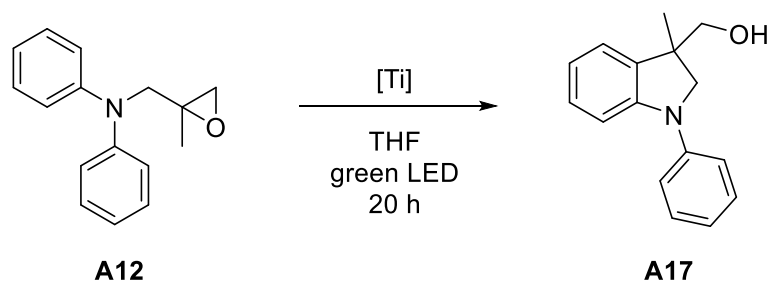
The analytical data is in agreement with the literature.^[139]

5.5.1.2



In a heat-dried *Schlenk* tube, 3DPAFIPN (3 mol%, 0.015 mmol, 10.0 mg) and D-Kagan (10 mol%, 0.05 mmol, 26.3 mg) are placed and evacuated for 30 min. Under argon atmosphere, dry THF (0.05 M, 10 mL) and **A12** (1.0 eq., 0.5 mmol, 119.7 mg) are added, the reaction mixture is heated to 65°C and stirred overnight under irradiation with blue light. After completion, the reaction mixture is diluted with Et₂O. The layers are separated, the aqueous layer is extracted with Et₂O (3x) and the combined organic phases are dried over MgSO₄ and the solvent is evaporated. The yield of **A17** is determined by ¹H-NMR data evaluation of the crude product with an internal standard (DMT) to be 73% (0.37 mmol).

5.5.1.3



According to **GP3**, D-Kagan (10 mol%, 0.05 mmol, 26.3 mg) and **A12** (1.0 eq., 0.5 mmol, 119.7 mg) are reacted in dry THF (0.05 M, 10 mL) at 65°C under irradiation with green light for 20 h. **A17** (0.47 mmol, 93%) is obtained (¹H-NMR-yield).

5.5.1.4

According to **GP3**, D-Kagan (10 mol%, 0.05 mmol, 26.3 mg) and **A12** (1.0 eq., 0.5 mmol, 119.7 mg) are reacted in dry THF (0.05 M, 10 mL) at room temperature under irradiation with green light for 20 h. **A17** (0.47 mmol, 93%) is obtained (¹H-NMR-yield).

5.5.1.5

According to **GP3**, Cp₂TiCl₂ (10 mol%, 0.05 mmol, 12.5 mg) and **A12** (1.0 eq., 0.5 mmol, 119.7 mg) are reacted in dry THF (0.05 M, 10 mL) at room temperature under irradiation with green light for 20 h. **A17** (0.31 mmol, 62%) is obtained (¹H-NMR-yield).

5.5.1.6

According to **GP3**, Cp_2TiCl_2 (5 mol%, 0.025 mmol, 6.2 mg) and **A12** (1.0 eq., 0.5 mmol, 119.7 mg) are reacted in dry THF (0.05 M, 10 mL) at room temperature under irradiation with green light for 20 h. According to TLC, the conversion is low (<20%), no work-up is done.

5.5.1.7

According to **GP3**, L-Kagan (10 mol%, 0.05 mmol, 26.3 mg) and **A12** (1.0 eq., 0.5 mmol, 119.7 mg) are reacted in dry THF (0.05 M, 10 mL) at 65°C under irradiation with green light for 20 h. After purification by flash column chromatography (SiO_2 , CH/EA 6:1) **A17** is obtained as a colorless oil (0.46 mmol, 86.5 mg, 72%).

5.5.1.8

According to **GP3**, $(\text{CyHexCp})_2\text{TiCl}_2$ (10 mol%, 0.05 mmol, 20.7 mg) and **A12** (1.0 eq., 0.5 mmol, 119.7 mg) are reacted in dry THF (0.05 M, 10 mL) at 65°C under irradiation with green light for 20 h. After purification by flash column chromatography (SiO_2 , CH/EA 6:1) **A17** is obtained as a colorless oil (0.31 mmol, 73.9 mg, 62%).

5.5.1.9

According to **GP3**, D-Kagan (10 mol%, 0.05 mmol, 26.3 mg) and **A12** (1.0 eq., 0.5 mmol, 119.7 mg) are reacted in dry THF (0.05 M, 10 mL) at room temperature under irradiation with green light for 20 h. **A17** (0.47 mmol, 95%) is obtained ($^1\text{H-NMR}$ -yield).

5.5.1.10

According to **GP3**, $(t\text{BuCp})_2\text{TiCl}_2$ (10 mol%, 0.05 mmol, 18.1 mg) and **A12** (1.0 eq., 0.5 mmol, 119.7 mg) are reacted in dry THF (0.05 M, 10 mL) at room temperature under irradiation with green light for 20 h. **A17** (0.46 mmol, 91%) is obtained ($^1\text{H-NMR}$ -yield).

5.5.1.11

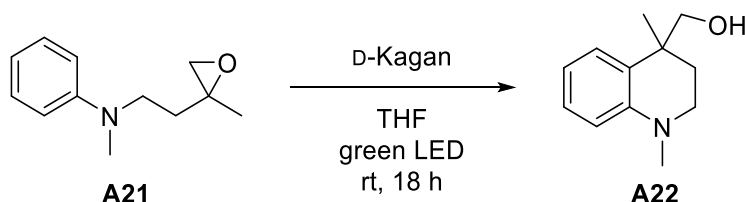
According to **GP3**, $(4-t\text{BuCyHexCp})_2\text{TiCl}_2$ (10 mol%, 0.05 mmol, 26.3 mg) and **A12** (1.0 eq., 0.5 mmol, 119.7 mg) are reacted in dry THF (0.05 M, 10 mL) at room temperature under irradiation with green light for 20 h. **A17** (0.44 mmol, 88%) is obtained ($^1\text{H-NMR}$ -yield).

5.5.1.12

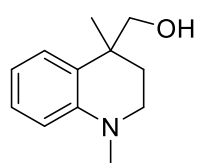
According to **GP3**, (CyHeptCp)₂TiCl₂ (10 mol%, 0.05 mmol, 22.1 mg) and **A12** (1.0 eq., 0.5 mmol, 119.7 mg) are reacted in dry THF (0.05 M, 10 mL) at room temperature under irradiation with green light for 20 h. **A17** (0.31 mmol, 63%) is obtained (¹H-NMR-yield).

5.5.1.13

According to **GP3**, (4-MeCyHexCp)₂TiCl₂ (10 mol%, 0.05 mmol, 22.1 mg) and **A12** (1.0 eq., 0.5 mmol, 119.7 mg) are reacted in dry THF (0.05 M, 10 mL) at room temperature under irradiation with green light for 20 h. **A17** (0.46 mmol, 93%) is obtained (¹H-NMR-yield).

5.5.2 Arylation of *N*-methyl-*N*-(2-(2-methyloxiran-2-yl)ethyl)aniline

According to **GP3** *N*-methyl-*N*-(2-(2-methyloxiran-2-yl)ethyl)aniline (**A21**, 1.0 eq., 0.50 mmol, 95.6 mg) and D-Kagan (10 mol%, 0.05 mmol, 26.3 mg) are reacted in THF (0.05 M, 10 mL) at room temperature under irradiation with green LEDs overnight. After work-up, the yield is determined by ¹H-NMR data evaluation of the crude product with an internal standard (DMT). (1,4-dimethyl-1,2,3,4-tetrahydroquinolin-4-yl)methanol **A22** (0.11 mmol, 22%) is obtained with a total conversion of 66% of the substrate.



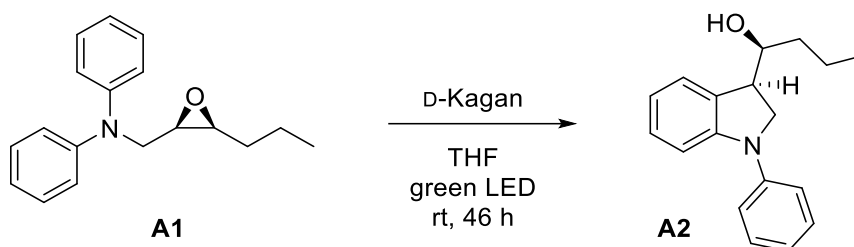
A22: C₁₂H₁₇NO; MW = 191.27 g/mol; ¹H-NMR (500 MHz, C₆D₆) δ [ppm] 7.13 (ddd, *J* = 8.4, 7.3, 1.6 Hz, 1H), 7.08 (dd, *J* = 7.7, 1.6 Hz, 1H), 6.74 (td, *J* = 7.4, 1.2 Hz, 1H), 6.53 (dd, *J* = 8.3, 1.2 Hz, 1H), 3.52 (d, *J* = 10.8 Hz, 1H), 3.30 (d, *J* = 10.8 Hz, 1H), 2.91 (ddd, *J* = 11.3, 8.6, 4.0 Hz, 1H), 2.77 (ddd, *J* = 11.4,

7.1, 4.2 Hz, 1H), 2.50 (s, 3H), 1.98 (ddd, *J* = 13.2, 7.1, 4.0 Hz, 1H), 1.46 (ddd, *J* = 13.1, 8.5, 4.2 Hz, 1H), 1.12 (s, 3H).

The analytical data is in agreement with the literature.^[335]

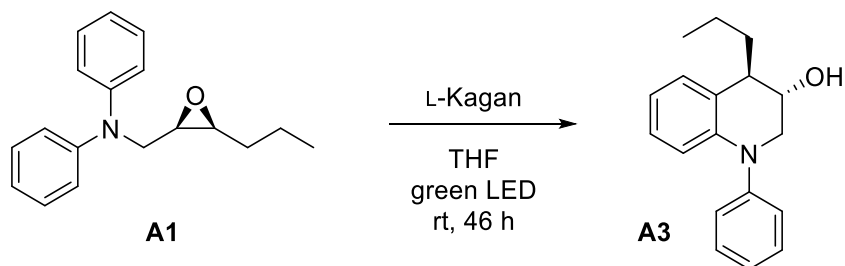
5.5.3 REO-Arylations of *N*-phenyl-*N*-(((2*R*,3*S*)-3-propyloxiran-2-yl)methyl)aniline

5.5.3.1



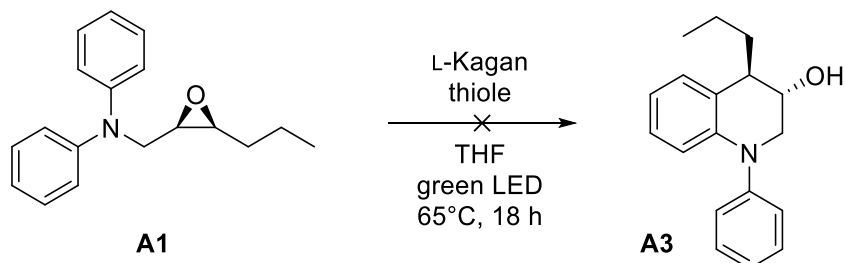
According to **GP3**, D-Kagan (10 mol%, 0.05 mmol, 26.3 mg) and **A1** (1.0 eq., 0.5 mmol, 133.7 mg) are reacted in dry THF (0.2 M, 2.5 mL) at room temperature under irradiation with green light for 46 h. According to TLC, the conversion is low. According to the crude $^1\text{H-NMR}$ data^[149], a mixture of substrate, desired product **A2** and its THQ-derivative **A3** are obtained. The product is not isolated.

5.5.3.2



According to **GP3**, L-Kagan (10 mol%, 0.05 mmol, 26.3 mg) and **A1** (1.0 eq., 0.5 mmol, 133.7 mg) are reacted in dry THF (0.2 M, 2.5 mL) at room temperature under irradiation with green light for 46 h. According to TLC, the conversion is low. According to the crude $^1\text{H-NMR}$ data^[149], a mixture of substrate, desired product **A3** and its indoline-derivative **A2** are obtained. The product is not isolated.

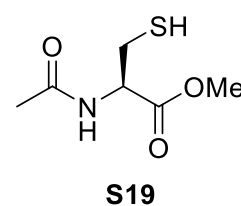
5.5.3.3



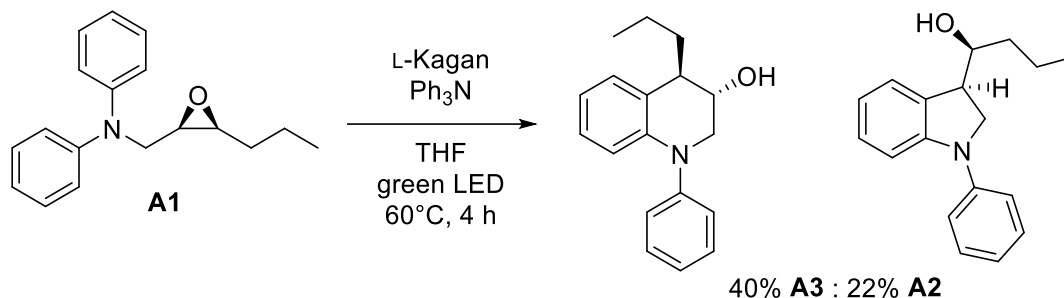
According to **GP3**, L-Kagan (10 mol%, 0.025 mmol, 13.1 mg), **A1** (1.0 eq., 0.25 mmol, 66.8 mg) and MTG (10 mol%, 0.025 mmol, 2 μL) are reacted in dry THF (0.08 M, 3 mL) at 65°C under irradiation with green light for 18 h. According to the crude $^1\text{H-NMR}$ data, no desired product **A3** is obtained.

5.5.3.4

According to **GP3**, L-Kagan (10 mol%, 0.025 mmol, 13.1 mg), **A1** (1.0 eq., 0.25 mmol, 66.8 mg) and thiol **S19** (10 mol%, 0.025 mmol, 4.4 mg) are reacted in dry THF (0.08 M, 3 mL) at 65°C under irradiation with green light for 18 h. According to the crude ¹H-NMR data, no desired product **A3** is obtained.



5.5.3.5



According to **GP3**, L-Kagan (10 mol%, 0.05 mmol, 26.3 mg), **A1** (1.0 eq., 0.5 mmol, 133.7 mg) and Ph₃N (1.0 eq., 0.5 mmol, 122.7 mg) are reacted in dry THF (0.05 M, 10 mL) at 60°C under irradiation with green light for 4 h. According to the crude ¹H-NMR data, 62% of the substrate is converted to 40% of the desired **A3** and 22% of **A2**.

5.5.3.6

According to **GP3**, L-Kagan (10 mol%, 0.05 mmol, 26.3 mg), **A1** (1.0 eq., 0.5 mmol, 133.7 mg) and Ph₃N (1.0 eq., 0.5 mmol, 122.7 mg) are reacted in dry THF (0.05 M, 10 mL) at room temperature under irradiation with green light for 4 h. According to the crude ¹H-NMR data, 19% of the substrate is converted to 13% of the desired **A3** and 6% of **A2**.

5.5.3.7

According to **GP3**, L-Kagan (10 mol%, 0.05 mmol, 26.3 mg), **A1** (1.0 eq., 0.5 mmol, 133.7 mg) and Ph₃N (20 mol%, 0.1 mmol, 24.5 mg) are reacted in dry THF (0.05 M, 10 mL) at room temperature under irradiation with green light for 4 h. According to the crude ¹H-NMR data, 18% of the substrate is converted to 12% of the desired **A3** and 6% of **A2**.

5.5.3.8

According to **GP3**, L-Kagan (10 mol%, 0.05 mmol, 26.3 mg), **A1** (1.0 eq., 0.5 mmol, 133.7 mg) and (*p*-MeOPh)₂N (20 mol%, 0.1 mmol, 33.5 mg) are reacted in dry THF (0.05 M, 10 mL) at room temperature under irradiation with green light for 4 d. According to the crude ¹H-NMR data, 37% of the substrate is converted to 26% of the desired **A3** and 11% of **A2**.

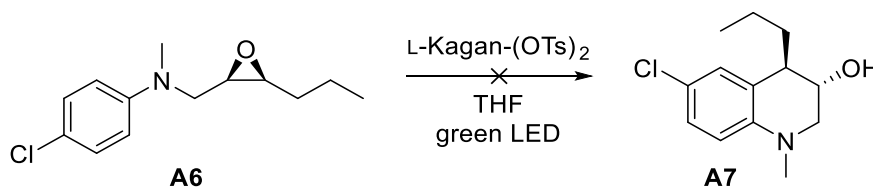
5.5.3.9

According to **GP3**, L-Kagan (10 mol%, 0.05 mmol, 26.3 mg) and **A1** (1.0 eq., 0.5 mmol, 133.7 mg) are reacted in dry THF (0.05 M, 10 mL) at room temperature under irradiation with green light for 4 d. According to the crude $^1\text{H-NMR}$ data, 35% of the substrate is converted to 24% of the desired **A3** and 11% of **A2**.

5.5.3.10

According to **GP3**, L-Kagan (10 mol%, 0.025 mmol, 13.1 mg), 3DPAFIPN (3 mol%, 7.5 μmol , 5.0 mg) and **A1** (1.0 eq., 0.25 mmol, 66.8 mg) are reacted in dry THF (0.1 M, 2.5 mL) at room temperature under irradiation with blue light for 6 d. According to the crude $^1\text{H-NMR}$ data, 14% of the desired **A3** and 3% of **A2** are obtained.

5.5.4 REO-Arylations of 4-chloro-*N*-methyl-*N*-(((2*R*,3*S*)-3-propyloxiran-2-yl)methyl)aniline



5.5.4.1

According to **GP3**, L-Kagan-(OTs)₂ (10 mol%, 0.05 mmol, 39.9 mg) and **A6** (synthesized by *Heinz*,^[217] 1.0 eq., 0.5 mmol, 119.9 mg) are reacted in dry THF (0.05 M, 10 mL) at 65°C under irradiation with green light for 24 h. According to the crude $^1\text{H-NMR}$ data, no desired product **A7** is obtained.

5.5.4.2

According to **GP3**, L-Kagan-(OTs)₂ (10 mol%, 0.05 mmol, 39.9 mg) and **A6** (1.0 eq., 0.5 mmol, 119.9 mg) are reacted in dry THF (0.05 M, 10 mL) at 65°C under irradiation with green light for 72 h. According to the crude $^1\text{H-NMR}$ data, no desired product **A7** is obtained.

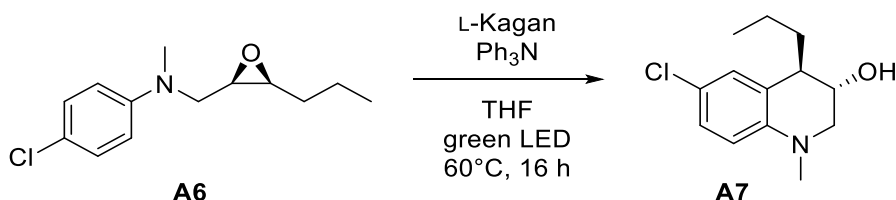
5.5.4.3

According to **GP3**, L-Kagan-(OTs)₂ (10 mol%, 0.05 mmol, 39.9 mg) and **A6** (1.0 eq., 0.5 mmol, 119.9 mg) are reacted in dry THF (0.05 M, 10 mL) at room temperature under irradiation with green light for 72 h. According to the crude $^1\text{H-NMR}$ data, no desired product **A7** is obtained.

5.5.4.4

According to **GP3**, L-Kagan-(OTs)₂ (20 mol%, 0.10 mmol, 79.7 mg) and **A6** (1.0 eq., 0.5 mmol, 119.9 mg) are reacted in dry THF (0.05 M, 10 mL) at 65°C under irradiation with green light for 72 h. According to the crude ¹H-NMR data, no desired product **A7** is obtained.

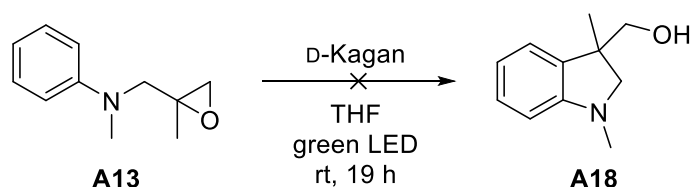
5.5.4.5



According to **GP3**, L-Kagan (10 mol%, 0.05 mmol, 26.3 mg), **A6** (1.0 eq., 0.5 mmol, 119.9 mg) and Ph₃N (1.0 eq., 0.5 mmol, 122.7 mg) are reacted in dry THF (0.05 M, 10 mL) at 60°C under irradiation with green light overnight. According to the crude ¹H-NMR data, **A7** (0.19 mmol, 37%) is obtained with 63% of the substrate unconverted.

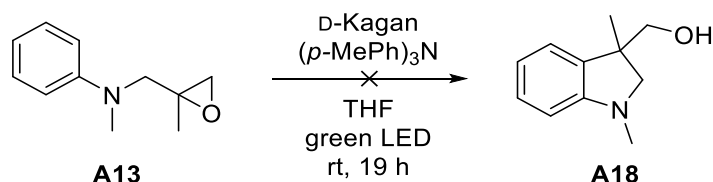
5.5.5 Arylations of *N*-methyl-*N*-((2-methyloxiran-2-yl)methyl)aniline

5.5.5.1



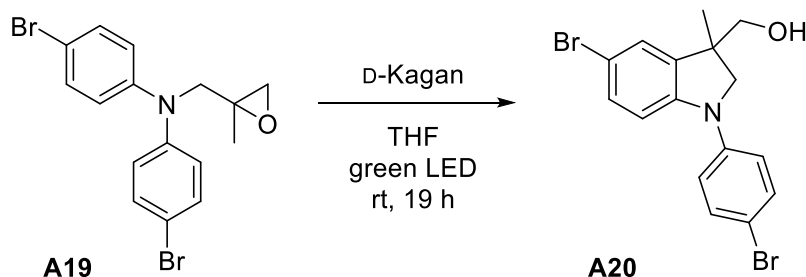
According to **GP3**, D-Kagan (10 mol%, 0.05 mmol, 26.3 mg) and **A13** (1.0 eq., 0.5 mmol, 88.6 mg) are reacted in dry THF (0.05 M, 10 mL) at room temperature under irradiation with green light for 19 h. According to TLC, no conversion is observed.

5.5.5.2

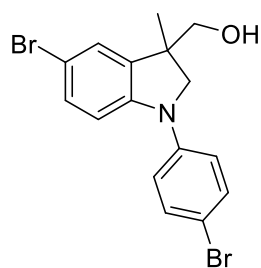


According to **GP3**, D-Kagan (10 mol%, 0.05 mmol, 26.3 mg), **A13** (1.0 eq., 0.5 mmol, 88.6 mg) and (*p*-MePh)₃N (0.5 eq., 0.25 mmol, 71.6 mg) are reacted in dry THF (0.05 M, 10 mL) at room temperature under irradiation with green light for 19 h. According to TLC, no conversion is observed.

5.5.6 Arylations of 4-bromo-*N*-(4-bromophenyl)-*N*-((2-methyloxiran-2-yl)methyl)aniline



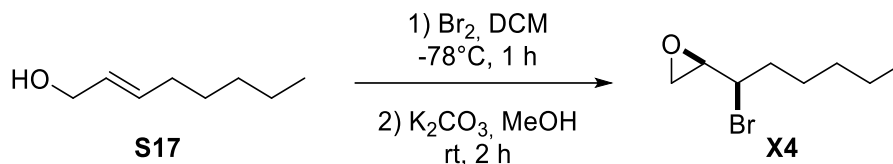
According to **GP3**, D-Kagan (10 mol%, 0.032 mmol, 16.6 mg) and **A19** (1.0 eq., 0.32 mmol, 124.6 mg) are reacted in dry THF (0.05 M, 6.4 mL) at room temperature under irradiation with green light for 19 h. (5-bromo-1-(4-bromophenyl)-3-methylindolin-3-yl)methanol (**A20**, 0.17 mmol, 53%) is obtained (¹H-NMR-yield).



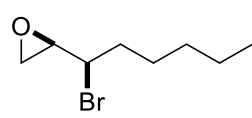
A20: C₁₆H₁₅Br₂NO; MW = 397.11 g/mol; ¹H-NMR (400 MHz, C₆D₆) δ [ppm] 7.27 – 7.21 (m, 2H), 7.15 – 7.08 (m, 2H), 6.64 – 6.55 (m, 3H), 3.35 (d, *J* = 9.4 Hz, 1H), 3.06 (dd, *J* = 10.6, 4.7 Hz, 1H), 3.01 – 2.94 (m, 2H), 0.93 (s, 3H); ¹³C-NMR (101 MHz, CDCl₃) δ [ppm] 145.4, 142.7, 139.1, 132.4, 130.9, 127.0, 119.3, 113.6, 111.3, 110.1, 68.4, 61.8, 45.5, 22.0.

The analytical data is in agreement with the literature.^[336]

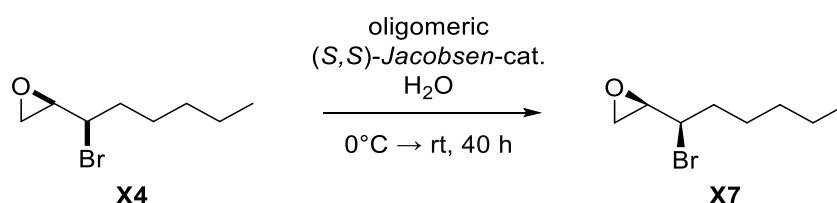
5.6 REO Substrate Syntheses

5.6.1 Synthesis of Enantiomerically pure α -Bromo Epoxides5.6.1.1 Synthesis of *syn*-2-(1-bromohexyl)oxirane

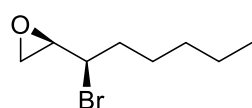
According to **GP4** (*E*)-oct-2-en-1-ol (**S17**, 1.0 eq., 250 mmol, 37.7 mL) is reacted with Br₂ (1.0 eq., 250 mmol, 12.8 mL) in DCM (0.5 M, 500 mL) for 1 h and subsequently with K₂CO₃ (2.0 eq., 500 mmol, 69.1 g) in MeOH (0.5 M, 500 mL) for 2 h. After purification by distillation (100°C, 10 mbar), **X4** is obtained as a colorless oil (134.5 mmol, 27.86 g, 54%).

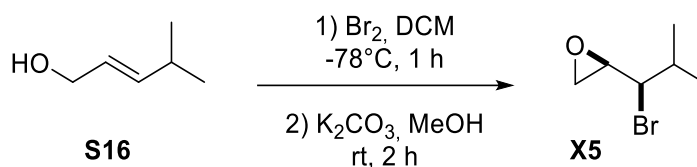
 **X4**: C₈H₁₅BrO; **MW** = 207.11 g/mol; **¹H-NMR** (500 MHz, CDCl₃) δ [ppm] 3.69 – 3.63 (m, 1H), 3.20 (ddd, J = 7.6, 3.9, 2.5 Hz, 1H), 2.96 (dd, J = 4.8, 3.8 Hz, 1H), 2.73 (dd, J = 4.8, 2.5 Hz, 1H), 1.94 – 1.80 (m, 2H), 1.59 – 1.49 (m, 1H), 1.47 – 1.38 (m, 1H), 1.35 – 1.25 (m, 4H), 0.89 (t, J = 7.0 Hz, 3H); **¹³C-NMR** (126 MHz, CDCl₃) δ [ppm] 56.2, 55.8, 49.0, 35.1, 31.3, 27.1, 22.5, 14.1.

The analytical data is in agreement with the literature.^[149]

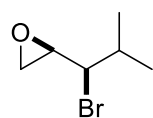
5.6.1.2 Synthesis of (*R*)-2-((*R*)-1-bromohexyl)oxirane

The reaction is performed under ambient conditions. In a round bottom flask, oligomeric (*S,S*)-*Jacobsen*-catalyst (0.2 mg/mmol, 14.6 mg) is added to the racemic epoxide **X4** (1.0 eq., 74.9 mmol, 15.52 g) and the mixture is cooled to 0°C. Water (0.55 eq., 41.2 mmol, 0.74 mL) is added and the reaction is stirred vigorously while warming to room temperature for 40 h. The crude product is purified by flash column chromatography (SiO₂, CH/EA 30:1). **X7** (28.3 mmol, 5.86 g, 38%) is obtained as a colorless oil.

 **X7**: C₈H₁₅BrO; **MW** = 207.11 g/mol.
e.r. = 99.7:0.3.

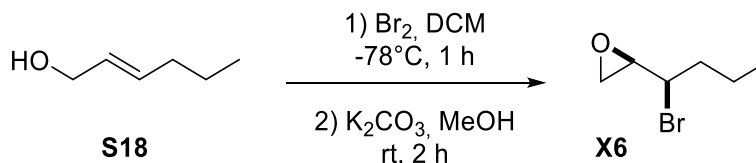
5.6.1.3 Synthesis of *syn*-2-(1-bromo-2-methylpropyl)oxirane

According to **GP4** (*E*)-4-methylpent-2-en-1-ol (**S16**, 1.0 eq., 92.7 mmol, 9.28 g) is reacted with Br₂ (1.0 eq., 92.7 mmol, 4.75 mL) in DCM (1 M, 100 mL) for 1 h and subsequently with K₂CO₃ (2.0 eq., 185.4 mmol, 25.6 g) in MeOH (0.5 M, 180 mL) for 2 h. After purification by distillation (100°C, 10 mbar), **X5** is obtained as a colorless oil (21.7 mmol, 3.88 g, 23%).

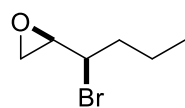


X5: C₆H₁₁BrO; **MW** = 179.06 g/mol; **¹H-NMR** (400 MHz, CDCl₃) δ [ppm] 3.47 (dd, *J* = 8.6, 5.5 Hz, 1H), 3.21 (ddd, *J* = 8.5, 3.8, 2.5 Hz, 1H), 3.02 (dd, *J* = 4.9, 3.8 Hz, 1H), 2.74 (dd, *J* = 4.9, 2.5 Hz, 1H), 2.06 (pd, *J* = 6.7, 5.5 Hz, 1H), 1.10 (dd, *J* = 9.1, 6.7 Hz, 6H).

The analytical data is in agreement with the literature.^[102]

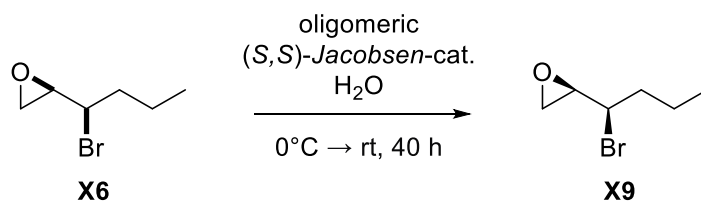
5.6.1.4 Synthesis of *syn*-2-(1-bromobutyl)oxirane

According to **GP4** (*E*)-hex-2-en-1-ol (**S18**, 1.0 eq., 250 mmol, 29.7 g) is reacted with Br₂ (1.0 eq., 250 mmol, 12.8 mL) in DCM (0.5 M, 500 mL) for 1 h and subsequently with K₂CO₃ (2.0 eq., 500 mmol, 69.1 g) in MeOH (0.5 M, 500 mL) for 2 h. After purification by flash column chromatography (SiO₂, CH/EA 30:1), **X6** is obtained as a colorless oil (111.2 mmol, 19.91 g, 44%).

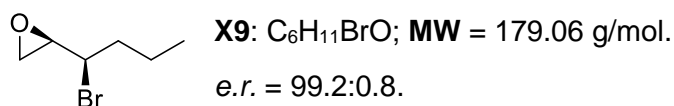


X6: C₆H₁₁BrO; **MW** = 179.06 g/mol; **¹H-NMR** (400 MHz, CDCl₃) δ [ppm] 3.68 (td, *J* = 7.6, 6.6 Hz, 1H), 3.21 (ddd, *J* = 7.6, 3.9, 2.5 Hz, 1H), 2.97 (dd, *J* = 4.8, 3.9 Hz, 1H), 2.74 (dd, *J* = 4.8, 2.5 Hz, 1H), 1.90 – 1.82 (m, 2H), 1.65 – 1.43 (m, 2H), 0.94 (t, *J* = 7.4 Hz, 3H).

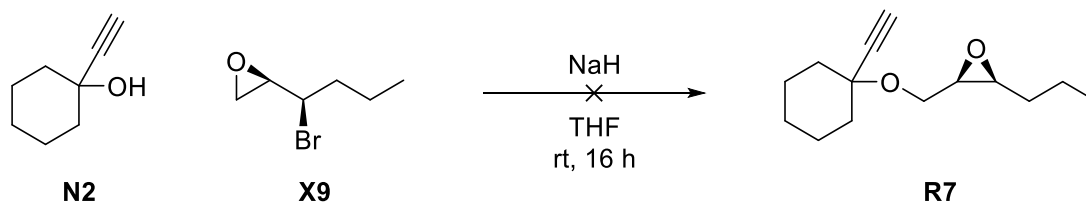
The analytical data is in agreement with the literature.^[149]

5.6.1.5 Synthesis of (*R*)-2-((*R*)-1-bromobutyl)oxirane

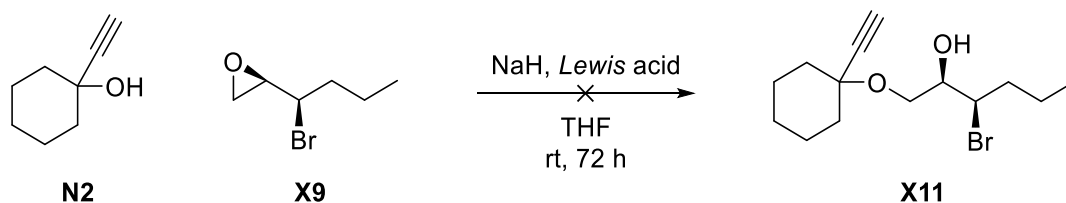
The reaction is performed under ambient conditions. In a round bottom flask, oligomeric (*S,S*)-*Jacobsen*-catalyst (0.2 mg/mmol, 46.4 mg) is added to the racemic epoxide **X6** (1.0 eq., 232.7 mmol, 41.67 g) and the mixture is cooled to 0°C. Water (0.55 eq., 121.0 mmol, 2.18 mL) is added and the reaction is stirred vigorously while warming to room temperature for 40 h. The crude product is purified by flash column chromatography (SiO₂, CH/EA 30:1). **X9** (99.12 mmol, 17.75 g, 43%) is obtained as a colorless oil.



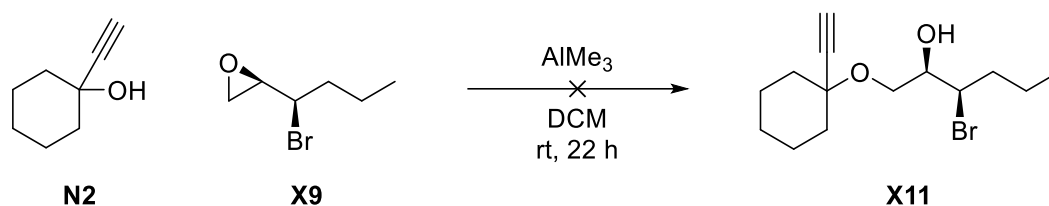
5.6.2 REO Substrates for Cyclizations

5.6.2.1 Synthesis of (2*R*,3*S*)-2-(((1-ethynylcyclohexyl)oxy)methyl)-3-propyloxirane

In a heat-dried *Schlenk* flask 1-ethynylcyclohexan-1-ol (**N2**, 1.0 eq., 1.0 mmol, 124 mg) is dissolved in dry THF (1.5 mL) under argon atmosphere. The solution is cooled to 0°C, sodium hydride (60% dispersion in mineral oil, 1.5 eq., 1.5 mmol, 60 mg) is added and the solution is stirred for 1 h. After (*R*)-2-((*R*)-1-bromobutyl)oxirane (**X9**, 1.2 eq., 1.2 mmol, 215 mg) is added, the reaction mixture is stirred at room temperature overnight. According to TLC, no conversion is observed.

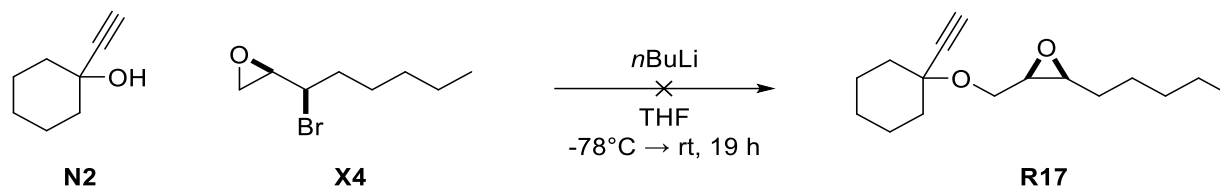
5.6.2.2 Synthesis of (2*R*,3*R*)-3-bromo-1-((1-ethynylcyclohexyl)oxy)hexan-2-ol

- I) According to **GP5** 1-ethynylcyclohexan-1-ol (**N2**, 1.0 eq., 1.0 mmol, 124 mg) is reacted with (*R*)-2-((*R*)-1-bromobutyl)oxirane (**X9**, 1.2 eq., 1.2 mmol, 215 mg), sodium hydride (60% dispersion in mineral oil, 1.5 eq., 1.5 mmol, 60 mg) and ZnCl₂ (1.1 eq., 1.1 mmol, 150 mg) in dry THF (1.5 mL) for 72 h. According to TLC, no conversion is observed.
- II) According to **GP5** 1-ethynylcyclohexan-1-ol (**N2**, 1.0 eq., 1.0 mmol, 124 mg) is reacted with (*R*)-2-((*R*)-1-bromobutyl)oxirane (**X9**, 1.2 eq., 1.2 mmol, 215 mg), sodium hydride (60% dispersion in mineral oil, 1.5 eq., 1.5 mmol, 60 mg) and AlCl₃ (1.1 eq., 1.1 mmol, 147 mg) in dry THF (1.5 mL) for 72 h. According to TLC, no conversion is observed.
- III) According to **GP5** 1-ethynylcyclohexan-1-ol (**N2**, 1.0 eq., 1.0 mmol, 124 mg) is reacted with (*R*)-2-((*R*)-1-bromobutyl)oxirane (**X9**, 1.2 eq., 1.2 mmol, 215 mg), sodium hydride (60% dispersion in mineral oil, 1.5 eq., 1.5 mmol, 60 mg) and Yb(OTf)₃ (1.1 eq., 1.1 mmol, 682mg) in dry THF (1.5 mL) for 72 h. According to TLC, no conversion is observed.
- IV) According to **GP5** 1-ethynylcyclohexan-1-ol (**N2**, 1.0 eq., 1.0 mmol, 124 mg) is reacted with (*R*)-2-((*R*)-1-bromobutyl)oxirane (**X9**, 1.2 eq., 1.2 mmol, 215 mg), sodium hydride (60% dispersion in mineral oil, 1.5 eq., 1.5 mmol, 60 mg) and BF₃·OEt₂ (1.1 eq., 1.1 mmol, 0.14 mL) in dry THF (1.5 mL) for 72 h. According to TLC, no conversion is observed.

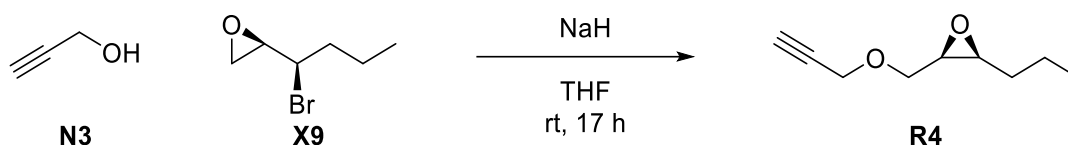


- V) In a heat-dried *Schlenk* flask, 1-ethynylcyclohexan-1-ol (**N2**, 1.0 eq., 8.0 mmol, 993 mg) is dissolved in dry DCM (0.2 M, 40 mL) under argon atmosphere. AlMe_3 (2.0 M solution in toluene, 1.0 eq., 8.0 mmol, 4.0 mL) is added and the solution is stirred for 1 h (caution, gas evolution). **X9** (1.2 eq., 9.6 mmol, 1.72 g) is added and the reaction is stirred at room temperature for 20 h. It is quenched by the addition of *i*PrOH, then H_2O and the solution is concentrated under reduced pressure. According to TLC, no conversion is observed.

5.6.2.3 Synthesis of (2*R*,3*S*)-2-(((1-ethynylcyclohexyl)oxy)methyl)-3-pentylloxirane



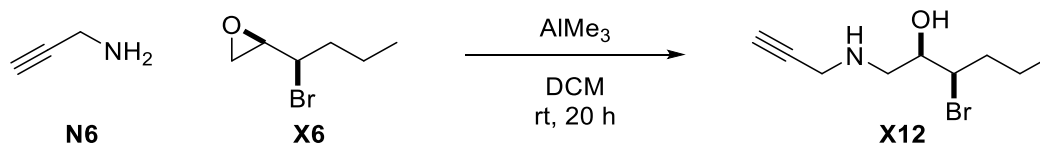
In a heat-dried *Schlenk* flask, 1-ethynylcyclohexan-1-ol (**N2**, 1.0 eq., 5.0 mmol, 621 mg) is dissolved in dry THF (0.5 M, 10 mL) under argon atmosphere and cooled to -78°C . *n*BuLi (2.5 M solution in hexane, 1.05 eq., 5.25 mmol, 2.1 mL) is added dropwise and the solution is stirred at -78°C for 30 min. **X4** (1.2 eq., 6.0 mmol, 1.24 g) is added, the mixture is warmed up to room temperature and stirred overnight. It is quenched by the addition of sat. aq. NH_4Cl solution (10 mL). According to TLC, no conversion is observed.

5.6.2.4 Synthesis of (2*R*,3*S*)-2-((prop-2-yn-1-yloxy)methyl)-3-propyloxirane

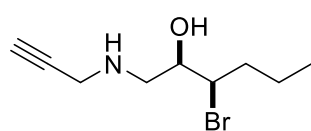
In a heat-dried *Schlenk* flask prop-2-yn-1-ol (**N3**, 1.0 eq., 1.0 mmol, 58 μ L) is dissolved in dry THF (1.5 mL) under argon atmosphere. The solution is cooled to 0°C, sodium hydride (60% dispersion in mineral oil, 1.2 eq., 1.2 mmol, 47 mg) is added and the solution is stirred for 1 h. After (*R*)-2-((*R*)-1-bromobutyl)oxirane (**X9**, 1.2 eq., 1.2 mmol, 215 mg) is added, the reaction mixture is stirred at room temperature overnight. It is diluted with Et₂O, then washed with water and brine and the layers are separated. The combined organic phases are dried over MgSO₄, and the solvent is removed under reduced pressure. The crude product is purified by flash column chromatography (SiO₂, CH/EA 10:1). **R4** is obtained as a colorless oil (0.16 mmol, 26 mg, 16%).

R4: C₉H₁₄O₂; MW = 154.21 g/mol; ¹H-NMR (500 MHz, CDCl₃) δ [ppm] 4.25 (dd, *J* = 15.8, 2.4 Hz, 1H), 4.18 (dd, *J* = 15.8, 2.4 Hz, 1H), 3.77 (dd, *J* = 10.9, 4.4 Hz, 1H), 3.56 (dd, *J* = 10.9, 6.5 Hz, 1H), 3.15 (dt, *J* = 6.5, 4.4 Hz, 1H), 3.02 – 2.95 (m, 1H), 2.45 (t, *J* = 2.4 Hz, 1H), 1.57 – 1.44 (m, 4H), 0.99 – 0.95 (m, 3H); ¹³C-NMR (126 MHz, CDCl₃) δ [ppm] 79.4, 74.9, 68.1, 58.5, 56.2, 54.9, 30.1, 20.1, 14.1; HRMS (ESI) *m/z* calcd. for [M+Na]⁺ 177.0886, found 177.0884.

Due to the low amount of product, no IR spectrum is measured.

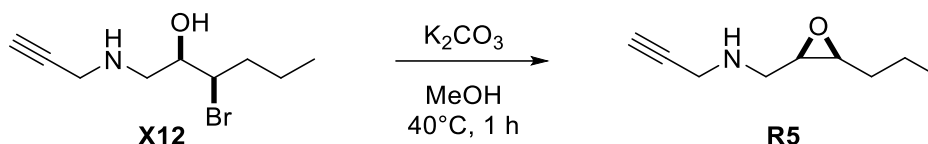
5.6.2.5 Synthesis of (2*R*,3*R*)-3-bromo-1-(prop-2-yn-1-ylamino)hexan-2-ol

In a heat-dried *Schlenk* flask, prop-2-yn-1-amine (**N6**, 1.0 eq., 10.0 mmol, 0.64 mL) is dissolved in dry DCM (0.2 M, 50 mL) under argon atmosphere. AlMe₃ (2.0 M solution in toluene, 1.0 eq., 10.0 mmol, 5.0 mL) is added and the solution is stirred for 1 h (caution, gas evolution). **X6** (1.2 eq., 12.0 mmol, 2.15 g) is added and the reaction is stirred at room temperature for 20 h. It is quenched by the addition of *i*PrOH, then H₂O and the solution is concentrated under reduced pressure. The layers are separated, and the aqueous layer is extracted with DCM. The combined organic phases are washed with water and brine and dried over MgSO₄. The solvent is evaporated, and the crude product is purified by flash column chromatography (SiO₂, CH/EA 2:1). **X12** (7.27 mmol, 1.70 g, 73%) is obtained as a pale-yellow oil.

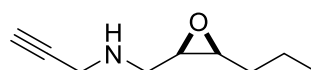


X12: C₉H₁₆BrNO; **MW** = 234.14 g/mol; **¹H-NMR** (500 MHz, C₆D₆) δ [ppm] 3.92 (ddd, *J* = 9.8, 4.2, 3.4 Hz, 1H), 3.50 (ddd, *J* = 7.1, 5.2, 3.4 Hz, 1H), 3.10 (d, *J* = 2.5 Hz, 2H), 2.68 (d, *J* = 2.4 Hz, 1H), 2.67 (s, 1H), 2.56 (s, 2H), 1.94 (t, *J* = 2.4 Hz, 1H), 1.83 (dtd, *J* = 14.5, 9.9, 4.8 Hz, 1H), 1.71 (dddd, *J* = 14.2, 10.0, 6.1, 4.2 Hz, 1H), 1.59 – 1.46 (m, 1H), 1.31 (dddd, *J* = 13.4, 9.9, 7.4, 6.1 Hz, 1H), 0.78 (t, *J* = 7.4 Hz, 3H); **¹³C-NMR** (126 MHz, C₆D₆) δ [ppm] 81.9, 72.3, 72.2, 61.5, 52.4, 38.2, 37.4, 21.4, 13.6; **IR** [cm⁻¹] $\tilde{\nu}_{\max}$ 3225, 2955, 2870, 1395, 1115, 815, 705, 525; **HRMS** (EI) *m/z* calcd. for [M+H]⁺ 234.0488, found 234.0489.

5.6.2.6 Synthesis of *N*-(((2*R*,3*S*)-3-propyloxiran-2-yl)methyl)prop-2-yn-1-amine



The bromo-alcohol **X12** (1.0 eq., 7.2 mmol, 1.69 g) is dissolved in MeOH (0.5 M, 15 mL) and freshly ground K₂CO₃ (2.0 eq., 14.4 mmol, 1.99 g) is added. The reaction mixture is stirred at 40°C for 1 h. It is then cooled to room temperature and an excess of Et₂O is added. The K₂CO₃ is removed by filtration over a plug of *Celite*[®], and the solvent is removed under reduced pressure. The crude product is purified by flash column chromatography (SiO₂, CH/EA 3:2). **R5** is obtained as a pale-yellow oil (2.83 mmol, 433 mg, 39%).

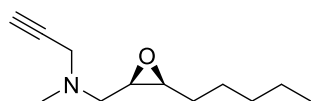


R5: C₉H₁₅NO; **MW** = 153.23 g/mol; **¹H-NMR** (400 MHz, CDCl₃) δ [ppm] 3.49 (d, *J* = 2.4 Hz, 2H), 3.08 (dt, *J* = 7.3, 4.3 Hz, 1H), 2.99 – 2.90 (m, 2H), 2.79 (dd, *J* = 12.7, 7.3 Hz, 1H), 2.23 (t, *J* = 2.4 Hz, 1H), 1.89 (s, 1H), 1.57 – 1.45 (m, 4H), 1.01 – 0.92 (m, 3H); **¹³C-NMR** (126 MHz, CDCl₃) δ [ppm] 81.8, 71.9, 56.7, 56.0, 46.9, 38.3, 30.1, 20.1, 14.1; **IR** [cm⁻¹] $\tilde{\nu}_{\max}$ 3285, 2960, 2930, 2875, 1460, 1115, 765, 645; **HRMS** (ESI) *m/z* calcd. for [M+H]⁺ 154.1226, found 154.1227.

5.6.2.7 Synthesis of *N*-(((2*R*,3*S*)-3-hexyloxiran-2-yl)methyl)-*N*-methylprop-2-yn-1-amine

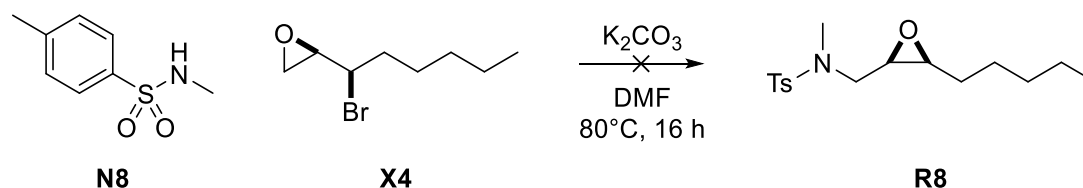
In a heat-dried *Schlenk* flask, **N7** (1.0 eq., 10.0 mmol, 0.85 mL) is dissolved in dry DCM (0.2 M, 50 mL) under argon atmosphere. AlMe_3 (2.0 M solution in toluene, 1.0 eq., 10.0 mmol, 5.0 mL) is added and the solution is stirred for 1 h (caution, gas evolution). **X7** (1.2 eq., 12.0 mmol, 2.49 g) is added and the reaction is stirred at room temperature for 20 h. It is quenched by the addition of *i*PrOH, then H_2O and the solution is concentrated under reduced pressure. The layers are separated, and the aqueous layer is extracted with DCM. The combined organic phases are washed with water and brine and dried over MgSO_4 . The solvent is evaporated, and the crude product is used without further purification.

It is dissolved in MeOH (0.5 M, 20 mL) and freshly ground K_2CO_3 (2.0 eq., 14.4 mmol, 1.99 g) is added. The reaction mixture is stirred at 40°C for 1 h. It is then cooled to room temperature and an excess of Et_2O is added. The K_2CO_3 is removed by filtration over a plug of *Celite*[®], and the solvent is removed under reduced pressure. The crude product is purified by flash column chromatography (SiO_2 , CH/Ea 1:1). **R6** is obtained as a colorless oil (5.58 mmol, 1.09 g, 56%).

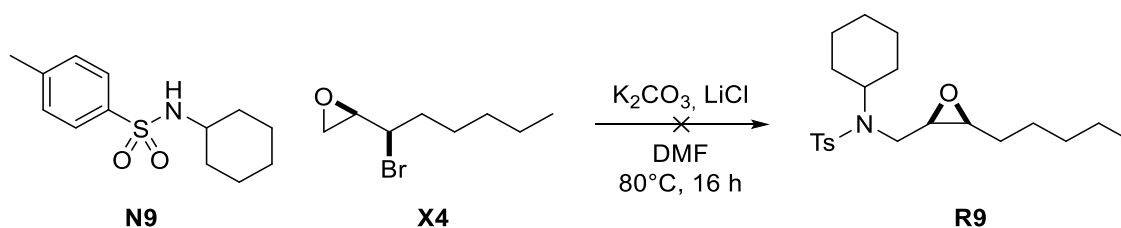


R6: $\text{C}_{12}\text{H}_{21}\text{NO}$; MW = 195.31 g/mol; $^1\text{H-NMR}$ (500 MHz, CDCl_3) δ [ppm] 3.45 (d, $J = 2.9$ Hz, 2H), 3.09 (dt, $J = 7.8, 4.0$ Hz, 1H), 2.98 – 2.90 (m, 1H), 2.82 (dt, $J = 13.4, 4.3$ Hz, 1H), 2.48 (ddd, $J = 13.3, 7.0, 3.2$ Hz, 1H), 2.43 (d, $J = 3.4$ Hz, 3H), 2.26 (q, $J = 2.5$ Hz, 1H), 1.62 – 1.26 (m, 8H), 0.94 – 0.85 (m, 3H); $^{13}\text{C-NMR}$ (126 MHz, CDCl_3) δ [ppm] 78.4, 73.7, 56.2, 55.4, 54.3, 46.3, 42.2, 31.8, 28.2, 26.5, 22.7, 14.1; IR [cm^{-1}] $\tilde{\nu}_{\text{max}}$ 3310, 2955, 2925, 2860, 1735, 1455, 1035, 840, 650, 625; HRMS (APCI) m/z calcd. for $[\text{M}+\text{H}]^+$ 196.1696, found 196.1698; $[\alpha]_{\text{D}}^{20}$ (CHCl_3) = -4.7° .

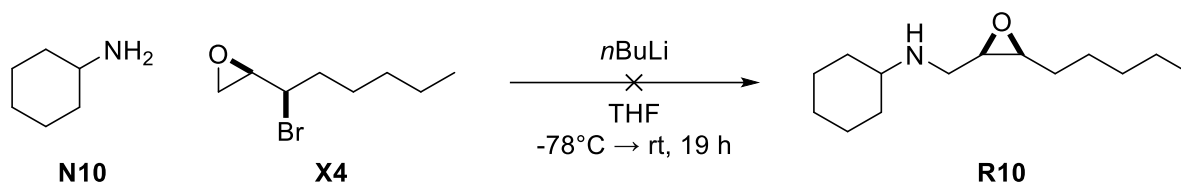
5.6.3 Other REO Substrates

5.6.3.1 Synthesis of *N*,4-dimethyl-*N*-(((2*R*,3*S*)-3-pentyloxiran-2-yl)methyl)benzenesulfonamide

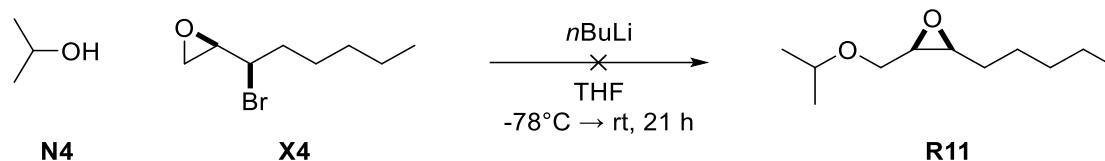
The reaction is performed under ambient conditions. *N*,4-dimethylbenzenesulfonamide (**N8**, 1.0 eq., 10.0 mmol, 1.85 g) and **X4** (1.2 eq., 12.0 mmol, 2.49 g) are dissolved in DMF (1.0 M, 10 mL). Finely ground K_2CO_3 (1.5 eq., 15.0 mmol, 2.07 g) is added and the reaction is stirred at 80°C overnight. It is diluted with Et_2O (10 mL) and the mixture is washed with water (5x) and brine. The layers are separated, the combined organic layers are dried over MgSO_4 , and the solvent is removed under reduced pressure. No desired **R8** can be detected in the crude $^1\text{H-NMR}$ spectrum.

5.6.3.2 Synthesis of *N*-cyclohexyl-4-methyl-*N*-(((2*R*,3*S*)-3-pentyloxiran-2-yl)methyl)benzenesulfonamide

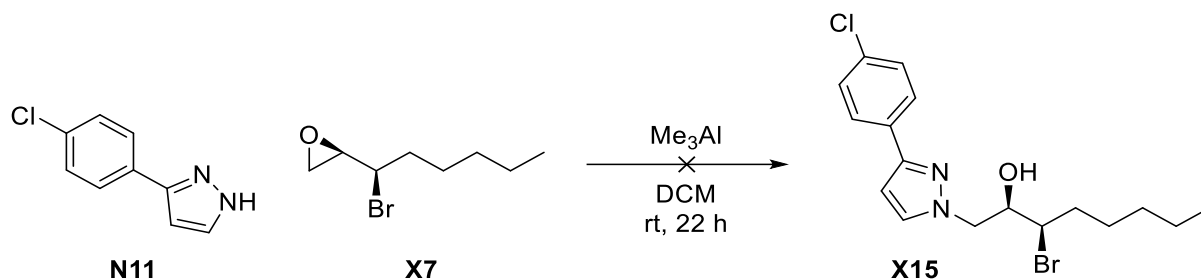
The reaction is performed under ambient conditions. **N9** (1.0 eq., 10.0 mmol, 2.53 g) and **X4** (1.2 eq., 12.0 mmol, 2.49 g) are dissolved in DMF (1.0 M, 10 mL). Finely ground K_2CO_3 (1.5 eq., 15.0 mmol, 2.07 g) and LiCl (0.5 eq., 5.0 mmol, 0.21 g) are added and the reaction is stirred at 80°C overnight. It is diluted with Et_2O (10 mL) and the mixture is washed with water (5x) and brine. The layers are separated, the combined organic layers are dried over MgSO_4 , and the solvent is removed under reduced pressure. No desired **R9** can be detected in the crude $^1\text{H-NMR}$ spectrum.

5.6.3.3 Synthesis of *N*-(((2*R*,3*S*)-3-pentylloxiran-2-yl)methyl)cyclohexanamine

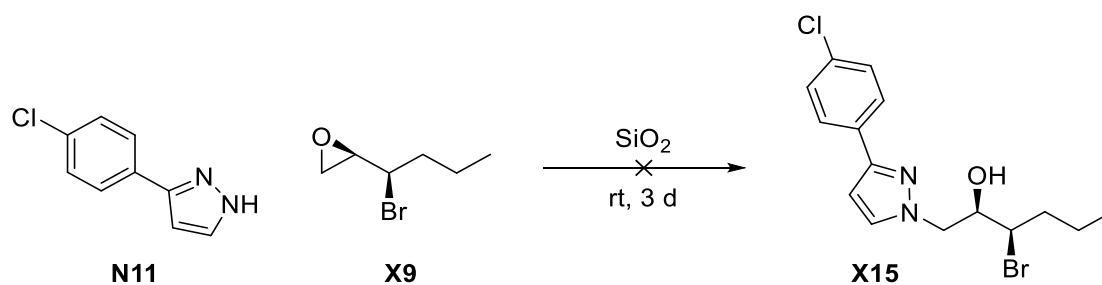
In a heat-dried *Schlenk* flask, cyclohexanamine (**N10**, 1.0 eq., 10.0 mmol, 1.15 mL) is dissolved in dry THF (0.5 M, 20 mL) under argon atmosphere and cooled to -78°C . *n*BuLi (2.5 M solution in hexane, 1.05 eq., 10.5 mmol, 4.2 mL) is added dropwise and the solution is stirred at -78°C for 30 min. **X4** (1.2 eq., 12.0 mmol, 2.49 g) is added, the mixture is warmed up to room temperature and stirred overnight. It is quenched by the addition of sat. aq. NH_4Cl solution (20 mL), the layers are separated, and the aq. layer is extracted with Et_2O (3x). The combined organic phases are washed with water and brine, dried over MgSO_4 and the solvent is removed under reduced pressure. No desired **R10** can be detected in the crude $^1\text{H-NMR}$ spectrum.

5.6.3.4 Synthesis of (2*R*,3*S*)-2-(isopropoxymethyl)-3-pentylloxirane

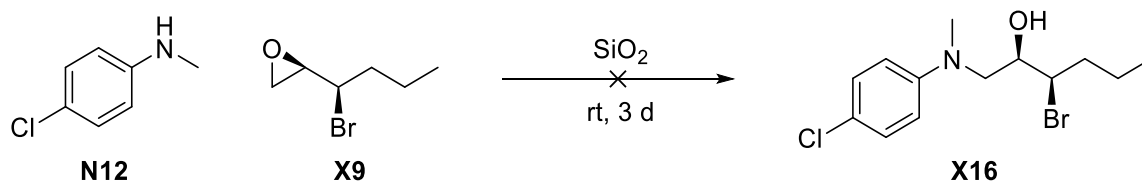
In a heat-dried *Schlenk* flask, isopropanol (**N4**, 1.0 eq., 5.0 mmol, 382 μL) is dissolved in dry THF (0.5 M, 10 mL) under argon atmosphere and cooled to -78°C . *n*BuLi (2.5 M solution in hexane, 1.05 eq., 5.25 mmol, 2.1 mL) is added dropwise and the solution is stirred at -78°C for 30 min. **X4** (1.2 eq., 6.0 mmol, 1.24 g) is added, the mixture is warmed up to room temperature and stirred overnight. It is quenched by the addition of sat. aq. NH_4Cl solution (10 mL). According to TLC, no conversion is observed.

5.6.3.5 Synthesis of (2*R*,3*R*)-3-bromo-1-(3-(4-chlorophenyl)-1*H*-pyrazol-1-yl)octan-2-ol

In a heat-dried *Schlenk* flask, **N11** (1.0 eq., 4.0 mmol, 715 mg) is dissolved in dry DCM (0.2 M, 20 mL) under argon atmosphere. AlMe_3 (2.0 M solution in toluene, 1.0 eq., 4.0 mmol, 2.0 mL) is added and the solution is stirred for 1 h (caution, gas evolution). **X7** (1.2 eq., 4.8 mmol, 994 mg) is added and the reaction is stirred at room temperature for 22 h. It is quenched by the addition of *i*PrOH, then H_2O . According to TLC, no conversion is observed.

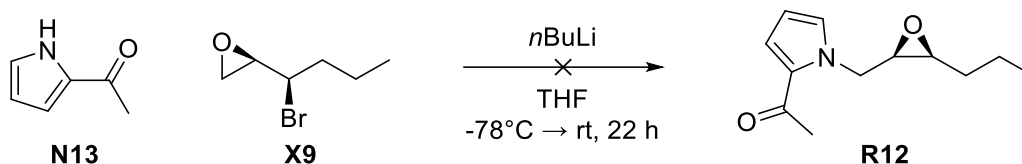
5.6.3.6 Synthesis of (2*R*,3*R*)-3-bromo-1-(3-(4-chlorophenyl)-1*H*-pyrazol-1-yl)hexan-2-ol

The reaction is performed under ambient conditions. **N11** (1.0 eq., 2.0 mmol, 357 mg) and **X9** (1.0 eq., 2.0 mmol, 358 mg) are placed in a tightly closable flask and SiO_2 (20 wt%, 72 mg) is added. The reaction mixture is stirred at room temperature for 3 d. It is diluted with DCM (5 mL) and stirred for 30 min before filtering off the solid. According to TLC, no conversion is observed.

5.6.3.7 Synthesis of (2*R*,3*R*)-3-bromo-1-((4-chlorophenyl)(methyl)amino)hexan-2-ol

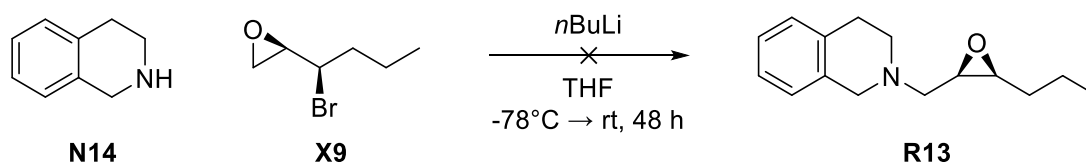
The reaction is performed under ambient conditions. **N12** (1.0 eq., 10.0 mmol, 1.42 g) and **X9** (1.0 eq., 10.0 mmol, 1.79 g) are placed in a tightly closed flask and SiO_2 (20 wt%, 642 mg) is added. The reaction mixture is stirred at room temperature for 3 d. It is diluted with DCM (5 mL) and stirred for 30 min before filtering off the solid. According to TLC, no conversion is observed.

5.6.3.8 Synthesis of 1-((2*R*,3*S*)-3-propyloxiran-2-yl)methyl)-1*H*-pyrrol-2-yl)ethan-1-one

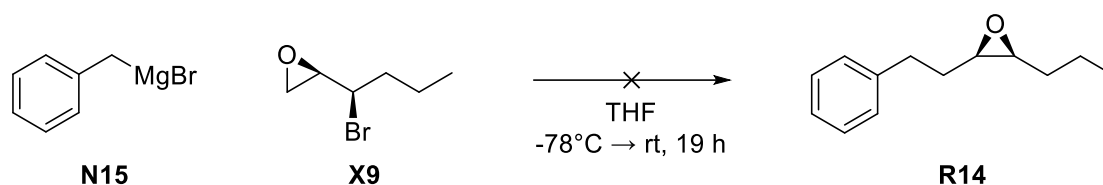


In a heat-dried *Schlenk* flask, 1-((1*H*-pyrrol-2-yl)ethan-1-one (**N13**, 1.0 eq., 1.68 mmol, 183 mg) is dissolved in dry THF (0.5 M, 5 mL) under argon atmosphere and cooled to -78°C. *n*BuLi (2.5 M solution in hexane, 1.05 eq., 1.76 mmol, 0.71 mL) is added dropwise and the solution is stirred at -78°C for 30 min. **X9** (1.1 eq., 1.85 mmol, 324 mg) is added, the mixture is warmed up to room temperature and stirred overnight. It is quenched by the addition of sat. aq. NH₄Cl solution (20 mL), the layers are separated, and the aq. layer is extracted with EA (3x). The combined organic phases are washed with water and brine, dried over MgSO₄ and the solvent is removed under reduced pressure. No desired **R12** can be detected in the crude ¹H-NMR spectrum.

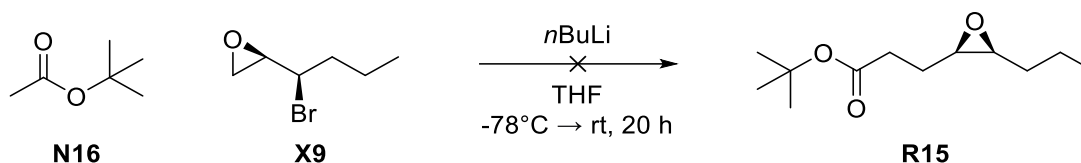
5.6.3.9 Synthesis of 2-(((2*R*,3*S*)-3-propyloxiran-2-yl)methyl)-1,2,3,4-tetrahydroisoquinoline



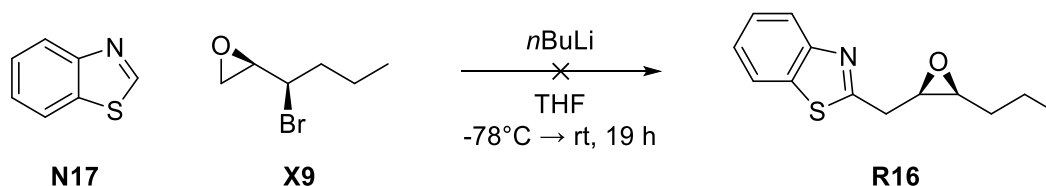
In a heat-dried *Schlenk* flask, 1,2,3,4-tetrahydroisoquinoline (**N14**, 1.0 eq., 7.0 mmol, 932 mg) is dissolved in dry THF (0.5 M, 15 mL) under argon atmosphere and cooled to -78°C. *n*BuLi (2.5 M solution in hexane, 1.2 eq., 8.4 mmol, 3.36 mL) is added dropwise and the solution is stirred at -78°C for 30 min. **X9** (1.2 eq., 8.4 mmol, 1.50 g) is added, the mixture is warmed up to room temperature and stirred for 48 h. It is quenched by the addition of sat. aq. NH₄Cl solution (20 mL), the layers are separated, and the aq. layer is extracted with EA (3x). The combined organic phases are washed with water and brine, dried over MgSO₄ and the solvent is removed under reduced pressure. The desired product **R13** can be detected in the crude ¹H-NMR spectrum as well as in the HRMS data (HRMS (ESI) *m/z* calcd. for [M+H]⁺ 232.1691, found 232.1692). After purification by flash column chromatography (SiO₂, CH/EA 10:1), the product cannot be isolated (decomposition).

5.6.3.10 Synthesis of (2*R*,3*S*)-2-phenethyl-3-propyloxirane

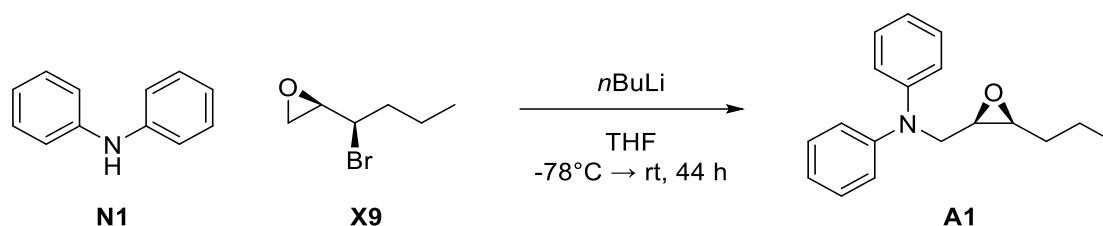
- I) The reaction is performed in heat-dried glassware under argon atmosphere. **X9** (1.0 eq., 3.0 mmol, 537 mg) is dissolved in dry THF (0.5 M, 6 mL) and the solution is cooled to -78°C. **N15** (0.52 M solution in THF, 1.0 eq., 3.0 mmol, 5.77 mL) is added over 30 min. The reaction mixture is stirred overnight while warming to room temperature. It is diluted with Et₂O and quenched by the addition of aq. HCl (2 M). The layers are separated, the organic phase is washed with water and dried over MgSO₄. The solvent is removed under reduced pressure. According to crude ¹H-NMR data no **R14** is formed.
- II) The reaction is performed in heat-dried glassware under argon atmosphere. CuCl (5 mol%, 0.15 mmol, 14.6 mg) is placed in a *Schlenk* flask and evacuated for 30 min, then flushed with argon. **X9** (1.0 eq., 3.0 mmol, 537 mg) is added and dissolved in dry THF (0.5 M, 6 mL) and the solution is cooled to -78°C. **N15** (0.52 M solution in THF, 1.0 eq., 3.0 mmol, 5.77 mL) is added over 30 min. The reaction mixture is stirred overnight while warming to room temperature. It is diluted with Et₂O and quenched by the addition of aq. HCl (2 M). The layers are separated, the organic phase is washed with water and dried over MgSO₄. The solvent is removed under reduced pressure. According to crude ¹H-NMR data no **R14** is formed. 1-Phenylheptan-3-one (1.17 mmol, 39%) is isolated after purification by flash column chromatography.^[337]

5.6.3.11 Synthesis of *tert*-butyl 3-((2*R*,3*S*)-3-propyloxiran-2-yl)propanoate

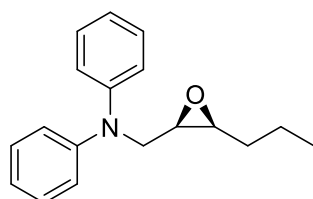
The reaction is performed in a heat-dried *Schlenk* flask under argon atmosphere. *tert*-butyl acetate (**N16**, 1.05 eq., 10.5 mmol, 1.42 mL) is dissolved in dry THF (0.4 M, 20 mL) and cooled to -78°C, *n*BuLi (2.5 M solution in hexane, 1.05 eq., 10.5 mmol, 4.20 mL) is slowly added and the solution is stirred for 30 min. The epoxide **X9** (1.0 eq., 10.0 mmol, 1.79 g) is dissolved in THF (5 mL) and the solution is slowly added to the reaction mixture. The reaction is stirred while warming up to room temperature overnight. It is quenched by the addition of sat. aq. NH₄Cl solution and Et₂O (20 mL) is added. The phases are separated, the aqueous layer is extracted with EA. The combined organic layers are dried over MgSO₄ and the solvent is removed under reduced pressure. According to crude ¹H-NMR data no **R15** is formed.

5.6.3.12 Synthesis of 2-(((2*R*,3*S*)-3-propyloxiran-2-yl)methyl)benzo[*d*]thiazole

The reaction is performed in a heat-dried *Schlenk* flask under argon atmosphere. Benzo[*d*]thiazole (**N17**, 1.2 eq., 3.6 mmol, 393 μL) is dissolved in dry THF (0.5 M, 6 mL) and cooled to -78°C, *n*BuLi (2.5 M solution in hexane, 1.2 eq., 3.6 mmol, 1.44 mL) is slowly added and the solution is stirred for 30 min. **X9** (1.0 eq., 3.0 mmol, 573 mg) is slowly added to the reaction mixture. The reaction is stirred while warming up to room temperature overnight. It is quenched by the addition of sat. aq. NH₄Cl solution. According to TLC, no conversion is observed.

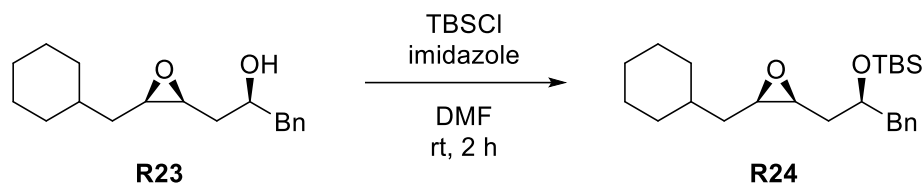
5.6.3.13 Synthesis of *N*-phenyl-*N*-(((2*R*,3*S*)-3-propyloxiran-2-yl)methyl)aniline

The reaction is performed according to the literature.^[149] In a heat-dried *Schlenk* flask under argon atmosphere, diphenylamine (**N1**, 1.0 eq., 6.7 mmol, 1.13 g) is dissolved in dry THF (0.5 M, 13 mL) and cooled to -78°C . *n*BuLi (2.5 M solution in hexane, 1.2 eq., 8.04 mmol, 3.22 mL) is slowly added and the solution is stirred for 30 min. **X9** (1.2 eq., 8.04 mmol, 1.44 g) is slowly added to the reaction mixture. The reaction is stirred while warming up to room temperature overnight. It is quenched by the addition of sat. aq. NH_4Cl solution. The phases are separated, and the aqueous layer is extracted with Et_2O (3x). The combined organic layers are washed with water and brine and dried over MgSO_4 . The solvent is removed under reduced pressure. The crude product is purified by flash column chromatography (SiO_2 , CH/EA 30:1). **A1** is obtained as a colorless oil (5.69 mmol, 1.52 g, 85%).



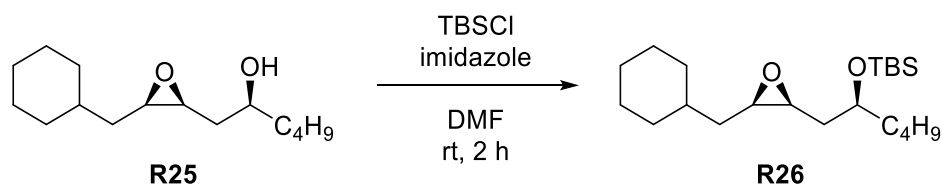
A1: $\text{C}_{18}\text{H}_{21}\text{NO}$; **MW** = 267.37 g/mol; **$^1\text{H-NMR}$** (500 MHz, CDCl_3) δ [ppm] 7.31 – 7.27 (m, 4H), 7.09 – 7.05 (m, 4H), 6.98 (tt, $J = 7.4, 1.1$ Hz, 2H), 3.96 (dd, $J = 15.7, 4.5$ Hz, 1H), 3.80 (dd, $J = 15.7, 5.3$ Hz, 1H), 3.22 (dt, $J = 5.4, 4.4$ Hz, 1H), 2.96 (ddd, $J = 6.8, 5.1, 4.1$ Hz, 1H), 1.54 – 1.35 (m, 4H), 0.97 – 0.92 (m, 3H); **$^{13}\text{C-NMR}$** (126 MHz, CDCl_3) δ [ppm] 148.0, 129.5, 121.9, 121.3, 57.1, 55.0, 51.1, 30.2, 20.1, 14.1.

The analytical data is in agreement with the literature.^[149]

5.6.4 Silylation of β -Epoxy Alcohols5.6.4.1 Synthesis of *tert*-butyl(((*S*)-1-((2*S*,3*R*)-3-(cyclohexylmethyl)oxiran-2-yl)-3-phenylpropan-2-yl)oxy)dimethylsilane

According to **GP6** epoxy alcohol **R23** (1.0 eq., 3.43 mmol, 942 mg, *d.r.* = 94:6) is reacted with imidazole (2.5 eq., 8.58 mmol, 584 mg) and TBSCl (1.2 eq., 4.12 mmol, 621 mg) in DMF (1.0 M, 3.5 mL) at room temperature for 2 h. After purification, **R24** is obtained as a colorless oil (2.36 mmol, 918 mg, 69%, *d.r.* = 95:5).

R24: C₂₄H₄₀O₂Si; MW = 388.67 g/mol; ¹H-NMR (400 MHz, CDCl₃) δ [ppm] 7.30 – 7.24 (m, 2H), 7.22 – 7.17 (m, 3H), 4.06 – 3.98 (m, 1H), 3.14 (dt, *J* = 7.1, 4.7 Hz, 1H), 2.96 (ddd, *J* = 6.6, 5.7, 4.3 Hz, 1H), 2.89 – 2.78 (m, 2H), 1.80 – 1.59 (m, 7H), 1.50 – 1.38 (m, 1H), 1.32 – 1.09 (m, 5H), 1.02 – 0.88 (m, 2H), 0.86 (s, 9H), -0.03 (s, 3H), -0.18 (s, 3H); ¹³C-NMR (101 MHz, CDCl₃) δ [ppm] 139.1, 130.0, 128.3, 126.3, 72.4, 55.2, 53.7, 44.1, 36.3, 35.5, 35.1, 33.7, 33.4, 26.6, 26.4, 26.4, 26.0, 18.2, -4.7, -4.9; IR [cm⁻¹] $\tilde{\nu}_{\max}$ 2925, 2855, 1255, 810, 775, 700; HRMS (APCI) *m/z* calcd. for [M+H]⁺ 389.2870, found 389.2867; [α]_D²⁰ (DCM) = -12.6°.

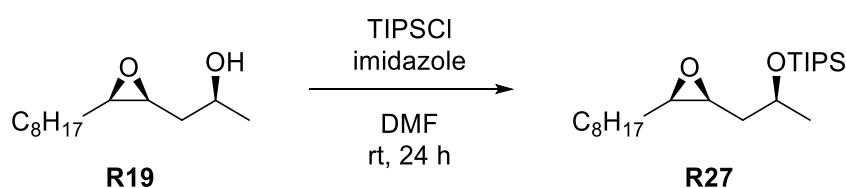
5.6.4.2 Synthesis of *tert*-butyl(((*S*)-1-((2*S*,3*R*)-3-(cyclohexylmethyl)oxiran-2-yl)hexan-2-yl)oxy)dimethylsilane

According to **GP6** epoxy alcohol **R25** (1.0 eq., 4.39 mmol, 1.06 g, *d.r.* = 92:8) is reacted with imidazole (2.5 eq., 11.0 mmol, 748 mg) and TBSCl (1.2 eq., 5.27 mmol, 795 mg) in DMF (1.0 M, 4.5 mL) at room temperature for 2 h. After purification, **R26** is obtained as a colorless oil (3.64 mmol, 1.29 g, 83%, *d.r.* = 94:6).

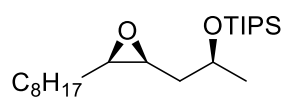


R26: C₂₁H₄₂O₂Si; **MW** = 354.65 g/mol; **¹H-NMR** (500 MHz, CDCl₃) δ [ppm] 3.83 (p, *J* = 5.8 Hz, 1H), 3.05 (ddd, *J* = 6.8, 5.1, 4.3 Hz, 1H), 2.95 (ddd, *J* = 6.9, 5.2, 4.3 Hz, 1H), 1.83 – 1.10 (m, 21H), 0.91 – 0.88 (m, 12H), 0.06 (s, 3H), 0.05 (s, 3H); **¹³C-NMR** (126 MHz, CDCl₃) δ [ppm] 70.7, 55.3, 53.9, 37.0, 36.3, 35.6, 33.8, 33.5, 27.8, 26.6, 26.4, 26.4, 26.0, 22.9, 18.2, 14.2, -4.3; **IR** [cm⁻¹] $\tilde{\nu}_{\max}$ 2925, 2855, 1255, 1055, 835, 775; **HRMS** (APCI) *m/z* calcd. for [M+H]⁺ 355.3027, found 355.3022; **[α]_D²⁰** (DCM) = -1.1°.

5.6.4.3 Synthesis of triisopropyl(((S)-1-((2S,3R)-3-octyloxiran-2-yl)propan-2-yl)oxy)silane

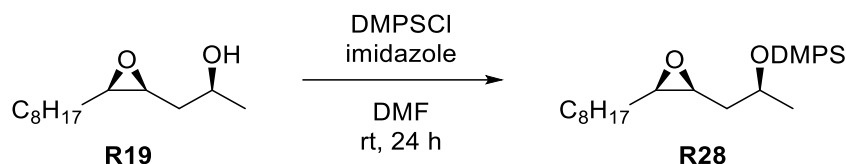


According to **GP6** epoxy alcohol **R19** (1.0 eq., 10.0 mmol, 2.14 g, *d.r.* = 93:7) is reacted with imidazole (2.5 eq., 25.0 mmol, 1.70 g) and TIPSCI (1.2 eq., 12.0 mmol, 2.55 mL) in DMF (1.0 M, 10 mL) at room temperature for 24 h. After purification, **R27** is obtained as a colorless oil (8.30 mmol, 3.08 g, 83%, *d.r.* = 99:1). Traces of an unidentified compound could not be separated by flash column chromatography.

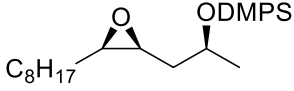


R27: C₂₂H₄₆O₂Si; **MW** = 370.69 g/mol; **¹H-NMR** (500 MHz, CDCl₃) δ [ppm] 4.16 (pd, *J* = 6.2, 4.7 Hz, 1H), 3.08 (dt, *J* = 7.2, 4.6 Hz, 1H), 2.90 (td, *J* = 5.8, 4.2 Hz, 1H), 1.70 (qdd, *J* = 14.0, 6.9, 4.7 Hz, 2H), 1.53 – 1.22 (m, 16H), 1.12 – 1.01 (m, 22H), 0.88 (t, *J* = 6.8 Hz, 3H); **¹³C-NMR** (126 MHz, CDCl₃) δ [ppm] 66.9, 56.7, 54.0, 37.9, 32.0, 29.7, 29.7, 29.4, 28.2, 27.1, 26.7, 23.8, 22.8, 18.3, 18.2, 14.2, 12.6; **IR** [cm⁻¹] $\tilde{\nu}_{\max}$ 2925, 2865, 1465, 1130, 1090, 1000, 880, 675; **HRMS** (ESI) *m/z* calcd. for [M+H]⁺ 371.3340, found 371.3340; **[α]_D²⁰** (CHCl₃) = -3.1°.

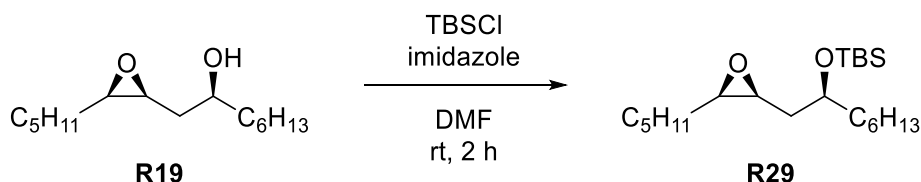
5.6.4.4 Synthesis of dimethyl(((S)-1-((2S,3R)-3-octyloxiran-2-yl)propan-2-yl)oxy)(phenyl)silane



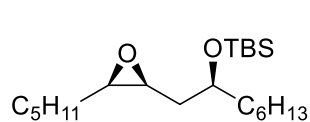
According to **GP6** epoxy alcohol **R19** (1.0 eq., 10.0 mmol, 2.14 g, *d.r.* = 93:7) is reacted with imidazole (2.5 eq., 25.0 mmol, 1.70 g) and DMPSCI (1.2 eq., 12.0 mmol, 2.01 mL) in DMF (1.0 M, 10 mL) at room temperature for 24 h. After purification, **R28** is obtained as a colorless oil (5.59 mmol, 1.95 g, 56%, *d.r.* = 99:1).

 **R28**: $\text{C}_{21}\text{H}_{36}\text{O}_2\text{Si}$; **MW** = 348.60 g/mol; **$^1\text{H-NMR}$** (500 MHz, CDCl_3) δ [ppm] 7.62 – 7.57 (m, 2H), 7.40 – 7.34 (m, 3H), 4.01 (ddd, J = 6.1, 6.1, 6.1 Hz, 1H), 2.98 (ddd, J = 6.8, 5.6, 4.2 Hz, 1H), 2.81 (q, J = 5.7 Hz, 1H), 1.73 – 1.65 (m, 1H), 1.64 – 1.56 (m, 1H), 1.48 – 1.24 (m, 14H), 1.21 (d, J = 6.2 Hz, 3H), 0.89 (t, J = 6.8 Hz, 3H), 0.40 (s, 6H); **$^{13}\text{C-NMR}$** (126 MHz, CDCl_3) δ [ppm] 138.2, 133.7, 129.7, 127.9, 67.2, 56.7, 54.2, 37.5, 32.0, 29.7, 29.7, 29.4, 28.1, 26.7, 23.7, 22.8, 14.2, -1.1, -1.1; **IR** [cm^{-1}] $\tilde{\nu}_{\text{max}}$ 2925, 1250, 1115, 1090, 785, 700; **HRMS** (ESI) m/z calcd. for $[\text{M}+\text{Na}]^+$ 371.2377, found 371.2376; **$[\alpha]_{\text{D}}^{20}$** (CHCl_3) = +0.8°.

5.6.4.5 Synthesis of tert-butyl(dimethyl(((S)-1-((2S,3R)-3-pentyloxiran-2-yl)octan-2-yl)oxy)silane



According to **GP6** epoxy alcohol **R19** (1.0 eq., 2.0 mmol, 484 mg, *d.r.* = 98:2) is reacted with imidazole (2.5 eq., 5.0 mmol, 340 mg) and TBSCl (1.2 eq., 2.4 mmol, 361 mg) in DMF (1.0 M, 2 mL) at room temperature for 2 h. After purification, **R29** is obtained as a colorless oil (1.37 mmol, 488 mg, 69%, *d.r.* = 99:1).

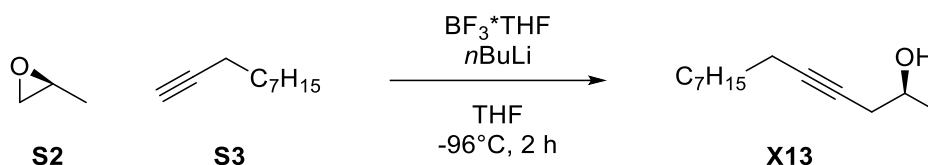


R29: C₂₁H₄₄O₂Si; **MW** = 356.67 g/mol; **¹H-NMR** (500 MHz, CDCl₃) δ [ppm] 3.83 (p, *J* = 5.9 Hz, 1H), 3.06 (td, *J* = 5.9, 4.3 Hz, 1H), 2.89 (q, *J* = 5.6 Hz, 1H), 1.66 (td, *J* = 5.8, 2.6 Hz, 2H), 1.57 (s, 1H), 1.55 – 1.24 (m, 17H), 0.93 – 0.85 (m, 15H), 0.06 (s, 3H), 0.05 (s, 3H); **¹³C-NMR** (126 MHz, CDCl₃) δ [ppm] 37.4, 35.5, 32.0, 31.9, 29.6, 28.1, 26.5, 26.0, 25.6, 22.8, 22.7, 18.2, 14.2, 14.1, -4.3, -4.4; **IR** [cm⁻¹] $\tilde{\nu}_{\max}$ 2955, 2930, 2860, 1255, 1070, 835, 775; **HRMS** (EI) *m/z* calcd. for [M-C₄H₉]⁺ 299.2401, found 299.2410; **[α]_D²⁰** (DCM) = -2.4°.

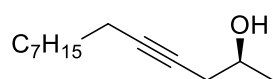
The analytical data is in agreement with the literature.^[136]

5.6.5 Alkyne Addition to Terminal Epoxides

5.6.5.1 Synthesis of (*S*)-tridec-4-yn-2-ol

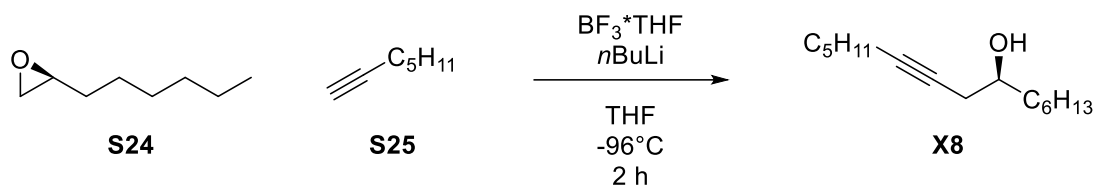


According to **GP7**, 1-decyne **S3** (1.2 eq., 138.4 mmol, 25.0 mL), (*S*)-2-methyloxirane **S2** (1.0 eq., 115.4 mmol, 8.1 mL, *e.r.* = 98:2), BF₃*THF (1.0 eq., 115.4 mmol, 12.7 mL) and *n*BuLi (2.5 M solution in hexane, 1.1 eq., 126.9 mmol, 50.8 mL) are reacted in THF (0.63 M, 220 mL) at -96°C for 2 h. **X13** is obtained as a colorless oil (20.03 g, 102.0 mmol, 88%) without further purification.

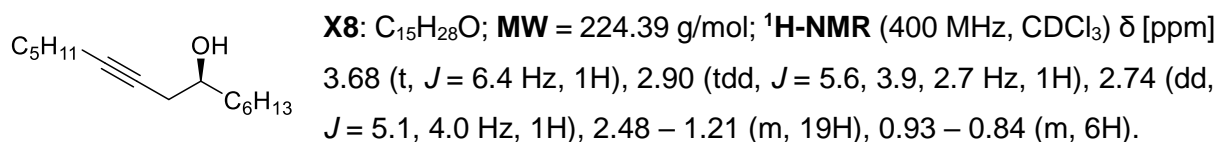


X13: C₁₃H₂₄O; **MW** = 196.33 g/mol; **¹H-NMR** (400 MHz, CDCl₃) δ [ppm] 3.90 (ddd, *J* = 6.3, 6.3, 4.9 Hz, 1H), 2.35 (dt, *J* = 4.9, 2.4 Hz, 1H), 2.29 (dt, *J* = 6.7, 2.3 Hz, 1H), 2.17 (tt, *J* = 7.1, 2.4 Hz, 2H), 1.92 (s, 1H), 1.57 – 1.20 (m, 15H), 0.92 – 0.80 (m, 3H); **¹³C-NMR** (101 MHz, CDCl₃) δ [ppm] 83.5, 76.2, 66.7, 32.0, 29.6, 29.3, 29.2, 29.1, 29.0, 22.8, 22.3, 18.9, 14.2.

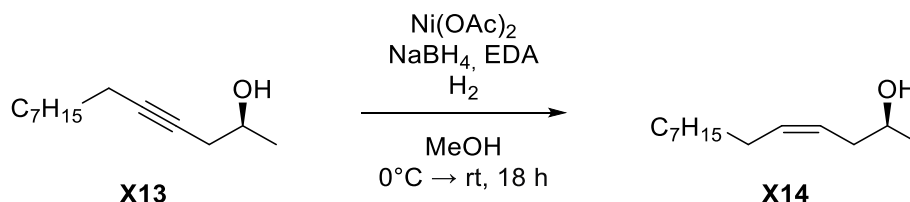
The analytical data is in agreement with the literature.^[110,299]

5.6.5.2 Synthesis of (*S*)-pentadec-9-yn-7-ol

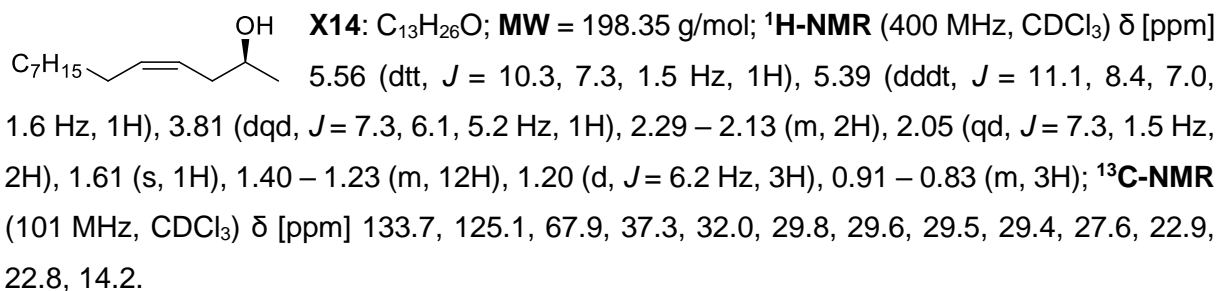
According to **GP7**, 1-heptyne **S25** (1.2 eq., 30.0 mmol, 3.94 mL), (*S*)-2-hexyloxirane **S24** (1.0 eq., 25.0 mmol, 3.21 g, *e.r.* = 99:1), $\text{BF}_3 \cdot \text{THF}$ (1.0 eq., 25.0 mmol, 2.75 mL) and *n*BuLi (2.5 M solution in hexane, 1.1 eq., 27.5 mmol, 11.0 mL) are reacted in THF (0.63 M, 40 mL) at -96°C for 2 h. **X8** is obtained as a colorless oil and used without further purification (see 5.6.6.2 for yield).



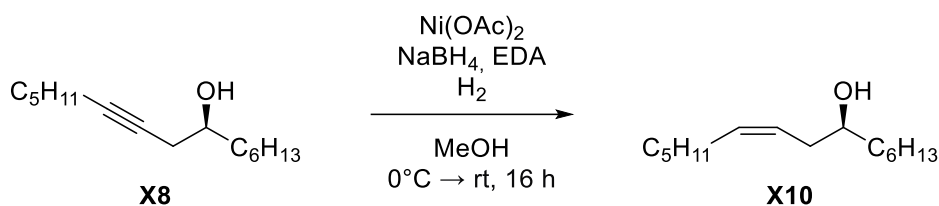
The analytical data is in agreement with the literature.^[338]

5.6.6 Reduction of β -Hydroxy Alkynes to (*Z*)-Alkenes5.6.6.1 Synthesis of (*S,Z*)-tridec-4-en-2-ol

According to **GP8**, (*S*)-tridec-4-yn-2-ol **X13** (1.0 eq., 102.0 mmol, 20.0 g), Ni(OAc)_2 (0.25 eq., 28.0 mmol, 4.95 g), NaBH_4 (0.25 eq., 28.0 mmol, 1.06 g) and EDA (0.5 eq., 56.0 mmol, 3.74 mL) are reacted in MeOH (0.5 M, 220 mL) at room temperature for 18 h. **X14** is obtained as a colorless oil (19.35 g, 97.6 mmol, 96%) without further purification.



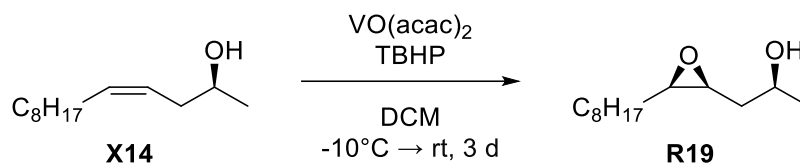
The analytical data is in agreement with the literature.^[110,299]

5.6.6.2 Synthesis of (*S,Z*)-pentadec-9-en-7-ol

According to **GP8**, (*S*)-pentadec-9-yn-7-ol **X8** (1.0 eq., 25.0 mmol, 5.61 g), Ni(OAc)₂ (0.25 eq., 6.25 mmol, 1.10 g), NaBH₄ (0.25 eq., 6.25 mmol, 236 mg) and EDA (0.5 eq., 12.5 mmol, 0.83 mL) are reacted in MeOH (0.5 M, 50 mL) at room temperature for 16 h. **X10** is obtained as a colorless oil (2.78 g, 12.28 mmol, 49% over two steps) without further purification.

X10: C₁₅H₃₀O; MW = 226.40 g/mol; ¹H-NMR (400 MHz, CDCl₃) δ [ppm] 5.61 – 5.52 (m, 1H), 5.40 (dt, *J* = 10.7, 7.4, 1.6 Hz, 1H), 3.62 (qt, *J* = 5.9, 3.7 Hz, 1H), 2.21 (ddd, *J* = 7.8, 6.2, 1.5 Hz, 2H), 2.05 (qd, *J* = 7.2, 1.6 Hz, 2H), 1.65 – 1.20 (m, 17H), 0.93 – 0.85 (m, 6H); ¹³C-NMR (101 MHz, CDCl₃) δ [ppm] 133.7, 125.2, 71.7, 37.0, 35.5, 32.0, 31.7, 29.5, 27.5, 25.9, 22.8, 22.7, 14.2.

The analytical data is in agreement with the literature.^[339]

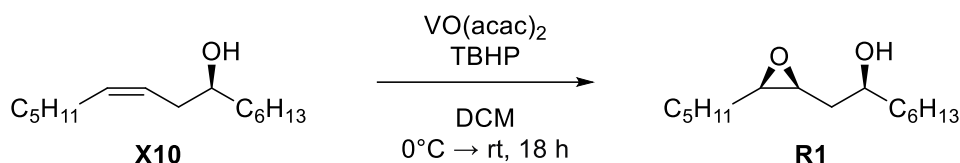
5.6.7 Syn-selective Epoxidation of (*Z*)-β-Hydroxy Alkenes5.6.7.1 Synthesis of (*S*)-1-((2*S*,3*R*)-3-octyloxiran-2-yl)propan-2-ol

According to **GP9**, (*S,Z*)-tridec-4-en-2-ol **X14** (1.0 eq., 97.5 mmol, 19.35 g), VO(acac)₂ (5 mol%, 4.88 mmol, 1.29 g) and TBHP (5.5 M solution in decane, 1.5 eq., 146.3 mmol, 26.6 mL) are reacted in DCM (0.1 M, 1000 mL) at room temperature for 3 d. After purification, **R19** is obtained as a colorless oil (13.32 g, 62.2 mmol, 64%, *d.r.* = 93:7).

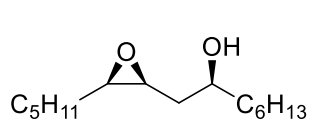
R19: C₁₃H₂₆O₂; MW = 214.35 g/mol; ¹H-NMR (400 MHz, CDCl₃) δ [ppm] 4.12 (dq, *J* = 8.3, 6.2, 3.9 Hz, 1H), 3.13 – 3.07 (m, 1H), 2.95 – 2.88 (m, 1H), 2.30 (s, 1H), 1.78 (dt, *J* = 14.3, 4.0 Hz, 1H), 1.58 – 1.21 (m, 18H), 0.91 – 0.85 (m, 3H); ¹³C-NMR (126 MHz, CDCl₃) δ [ppm] 67.2, 56.5, 55.5, 36.5, 32.0, 29.6, 29.6, 29.3, 28.1, 26.6, 23.6, 22.8, 14.2.

The analytical data is in agreement with the literature.^[110,299]

5.6.7.2 Synthesis of (S)-1-((2S,3R)-3-pentylloxiran-2-yl)octan-2-ol



According to **GP9**, (S,Z)-pentadec-9-en-7-ol **X10** (1.0 eq., 12.28 mmol, 2.78 g), VO(acac)₂ (5 mol%, 0.614 mmol, 163.8 mg) and TBHP (5.5 M solution in decane, 1.5 eq., 18.42 mmol, 3.35 mL) are reacted in DCM (0.1 M, 120 mL) at room temperature for 18 h. After purification, **R1** is obtained as a colorless oil (2.40 g, 9.89 mmol, 81%, *d.r.* = 98:2).

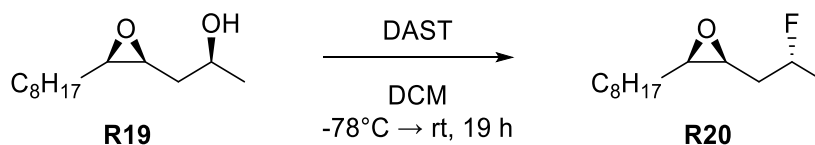


R1: C₁₅H₃₀O₂; MW = 242.40 g/mol; **¹H-NMR** (500 MHz, CDCl₃) δ [ppm] 3.91 (dtd, *J* = 10.8, 5.3, 2.9 Hz, 1H), 3.12 (dt, *J* = 8.5, 4.3 Hz, 1H), 2.92 (td, *J* = 6.1, 4.3 Hz, 1H), 2.26 (d, *J* = 2.9 Hz, 1H), 1.80 (dt, *J* = 14.4, 3.8 Hz, 1H), 1.57 – 1.24 (m, 19H), 0.92 – 0.85 (m, 6H); **¹³C-NMR** (126 MHz, CDCl₃) δ [ppm] 71.1, 56.5, 55.6, 37.6, 34.9, 32.0, 31.8, 29.4, 28.0, 26.3, 25.6, 22.7, 22.7, 14.2, 14.1; **IR** [cm⁻¹] $\tilde{\nu}_{\text{max}}$ 3425, 2955, 2925, 2855, 1465, 1050, 840, 725; **HRMS** (ESI) *m/z* calcd. for [M+Na]⁺ 265.2138, found 265.2142; [α]_D²⁰ (DCM) = -3.6°.

The analytical data is in agreement with the literature.^[136]

5.6.8 Fluorination of β-Epoxy Alcohols

5.6.8.1 Synthesis of (2S,3R)-2-((R)-2-fluoropropyl)-3-octyloxirane



The synthesis is performed according to the literature.^[299] In a heat-dried *Schlenk* flask under argon atmosphere, **R19** (1.0 eq., 5.0 mmol, 1.07 g, *d.r.* = 99:1) is dissolved in DCM (0.1 M, 50 mL) and cooled to -78°C. Dropwise, DAST (1.1 eq., 5.5 mmol, 0.73 mL) is added and the reaction is stirred while warming to room temperature for 19 h. It is quenched by the addition of EA (50 mL) and sat. aq. NH₄Cl solution (25 mL). The phases are separated, and the aqueous layer is extracted with EA (3x). The combined organic layers are washed with water and brine, dried over MgSO₄ and the solvent is evaporated. The crude product is purified by flash column chromatography (SiO₂, CH/EA 4:1). The product **R20** is obtained as a colorless oil (3.82 mmol, 827 mg, 76%, *d.r.* = 1:99).

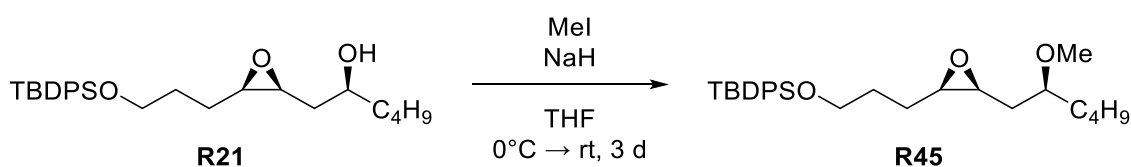


R20: C₁₃H₂₅FO; **MW** = 216.34 g/mol; **¹H-NMR** (400 MHz, CDCl₃) δ [ppm] 4.98 – 4.77 (m, 1H), 3.09 (dt, *J* = 7.7, 4.3 Hz, 1H), 2.96 (td, *J* = 5.9, 4.3 Hz, 1H), 1.94 (tdd, *J* = 14.7, 8.7, 4.3 Hz, 1H), 1.70 – 1.54 (m, 1H), 1.54 – 1.18 (m, 17H), 0.92 – 0.82 (m, 3H); **¹³C-NMR** (101 MHz, CDCl₃) δ [ppm] 89.0 (d, *J* = 165.9 Hz), 57.2, 53.7 (d, *J* = 5.6 Hz), 35.8 (d, *J* = 20.7 Hz), 32.0, 29.7, 29.4, 28.1, 26.6, 22.8, 21.6 (d, *J* = 22.3 Hz), 14.2; **[α]_D²⁰** (CHCl₃) = -20.7°.

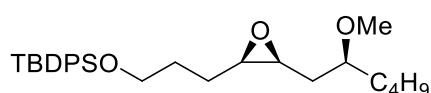
The analytical data is in agreement with the literature.^[299]

5.6.9 Methylation of β-Epoxy Alcohols

5.6.9.1 Synthesis of tert-butyl(3-((2*R*,3*S*)-3-((*S*)-2-methoxyhexyl)oxiran-2-yl)propoxy)diphenylsilane



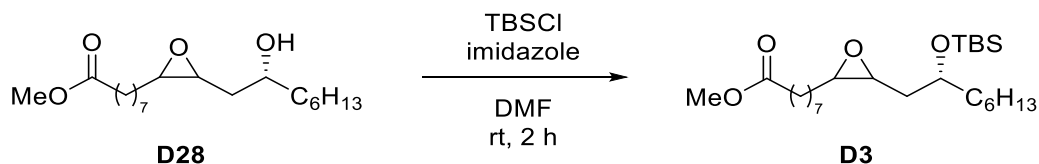
According to **GP10**, **R21** (1.0 eq., 7.22 mmol, 3.18 g) is reacted with MeI (1.94 eq., 14.0 mmol, 0.87 mL) and NaH (60% dispersion in mineral oil, 1.46 eq., 10.5 mmol, 420 mg) in dry THF (0.3 M, 21 mL) at room temperature for 3 d. After purification, **R45** is obtained as a pale-yellow oil (7.00 mmol, 3.15 g, 97%, *d.r.* = 96:4).



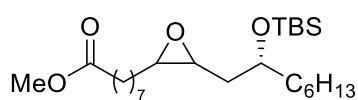
R45: C₂₈H₄₂O₃Si; **MW** = 454.73 g/mol; **¹H-NMR** (500 MHz, CDCl₃) δ [ppm] 7.67 (dt, *J* = 6.6, 1.6 Hz, 4H), 7.44 – 7.36 (m, 6H), 3.72 (ddt, *J* = 10.3, 10.3, 6.1 Hz, 2H), 3.40 – 3.30 (m, 4H), 3.03 (dt, *J* = 6.8, 4.7 Hz, 1H), 2.92 (ddd, *J* = 6.8, 5.6, 4.3 Hz, 1H), 1.80 – 1.50 (m, 8H), 1.40 – 1.28 (m, 4H), 1.05 (s, 9H), 0.93 – 0.89 (m, 3H); **¹³C-NMR** (126 MHz, CDCl₃) δ [ppm] 135.7, 135.7, 134.0, 134.0, 129.7, 127.8, 79.5, 63.6, 56.7, 56.5, 54.3, 33.6, 31.8, 29.7, 27.7, 27.0, 24.8, 23.0, 19.4, 14.2; **IR** [cm⁻¹] $\tilde{\nu}_{\max}$ 2930, 2860, 1430, 1090, 825, 740, 700, 500; **HRMS** (APCI) *m/z* calcd. for [M+H]⁺ 455.2976, found 455.2976; **[α]_D²⁰** (DCM) = -5.5°.

The analytical data is in agreement with the literature.^[136]

5.7 DEO Substrate Syntheses

5.7.1 Synthesis of methyl 8-(3-((*R*)-2-((*tert*-butyldimethylsilyl)oxy)octyl)oxiran-2-yl)octanoate

According to **GP6** epoxy alcohol **D28** (1.0 eq., 5.0 mmol, 1.64 g, *d.r.* = 60:40) is reacted with imidazole (2.5 eq., 12.5 mmol, 851 mg) and TBSCl (1.2 eq., 6.0 eq., 904 mg) in DMF (1.0 M, 5 mL) at room temperature for 2 h. After purification, **D3** is obtained as a colorless oil (4.56 mmol, 2.02 g, 91%, *d.r.* = 60:40).



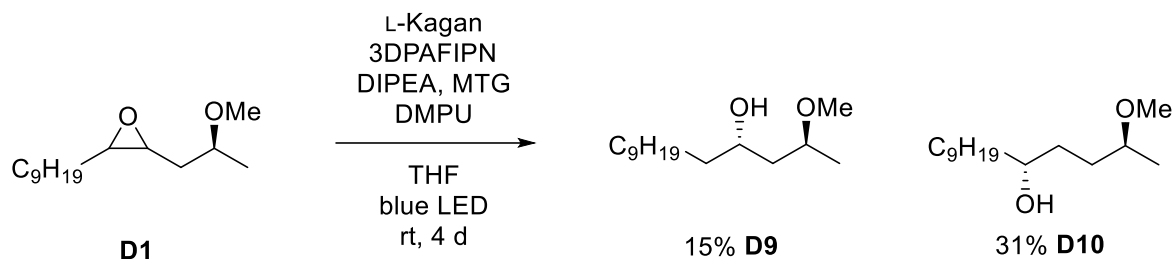
D3: $\text{C}_{25}\text{H}_{50}\text{O}_4\text{Si}$; **MW** = 442.76 g/mol; **$^1\text{H-NMR}$** (500 MHz, CDCl_3) δ [ppm] 3.89 – 3.79 (m, 1H), 3.66 (s, 3H), 3.08 – 3.02 (m, 1H), 2.94 – 2.85 (m, 1H), 2.30 (t, $J = 7.5$ Hz, 2H), 1.69 – 1.24 (m, 24H), 0.91 – 0.85 (m, 12H), 0.08 – 0.03 (m, 6H); **$^{13}\text{C-NMR}$** (126 MHz, CDCl_3) δ [ppm] 174.4, 70.6, 57.5, 54.8, 51.6, 38.2, 35.4, 34.2, 32.0, 29.6, 29.6, 29.5, 29.3, 28.3, 26.7, 26.0, 25.6, 25.1, 22.8, 18.2, 14.2, -4.3, -4.4.

The analytical data is in agreement with the literature.^[340]

5.8 Diastereodivergent Epoxide Openings

5.8.1 Opening of 2-((S)-2-methoxypropyl)-3-nonyloxirane

5.8.1.1



According to **GP11**, **D1** (1.0 eq., 0.5 mmol, 121.2 mg, *d.r.* = 62:38) is reacted with L-Kagan (10 mol%, 0.05 mmol, 26.3 mg), 3DPAFIPN (3 mol%, 0.015 μmol , 10.0 mg), DIPEA (3.0 eq., 1.5 mmol, 0.26 mL), DMPU (1.5 eq., 0.75 mmol, 91 μL) and MTG (20 mol%, 0.1 mmol, 9 μL) in THF (0.1 M, 5 mL) under irradiation with blue light at room temperature for 4 days. After purification, **D9** (18.0 mg, 0.074 mmol, 15%, *d.r.* = 18:82) and **D10** (38.0 mg, 0.155 mmol, 31%, *d.r.* = 7:93) are obtained as colorless oils. *r.r.* (1,3:1,4) = 32:68.

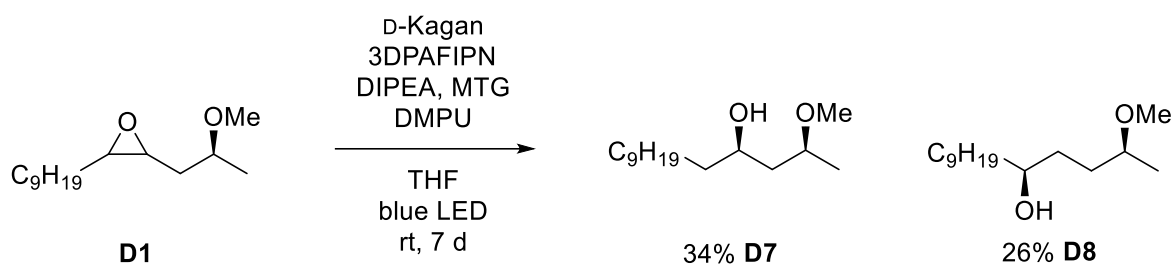
D9: $\text{C}_{15}\text{H}_{32}\text{O}_2$; **MW** = 244.42 g/mol; **$^1\text{H-NMR}$** (500 MHz, CDCl_3) δ [ppm] 3.87 (dtd, J = 7.8, 4.7, 2.5 Hz, 1H), 3.66 (pd, J = 6.4, 3.7 Hz, 1H), 3.34 (s, 3H), 1.66 – 1.53 (m, 2H), 1.52 – 1.22 (m, 20H), 1.19 (d, J = 6.2 Hz, 2H), 0.87 (t, J = 6.9 Hz, 3H); **$^{13}\text{C-NMR}$** (126 MHz, CDCl_3) δ [ppm] 75.1, 68.9, 56.3, 42.5, 37.8, 32.1, 29.9, 29.8, 29.8, 29.8, 29.5, 25.9, 22.8, 18.8, 14.3.

The analytical data is in agreement with the literature.^[110]

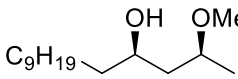
D10: $\text{C}_{15}\text{H}_{32}\text{O}_2$; **MW** = 244.42 g/mol; **$^1\text{H-NMR}$** (500 MHz, CDCl_3) δ [ppm] 3.56 (ddt, J = 6.3, 4.7, 2.7 Hz, 1H), 3.37 – 3.29 (m, 4H), 2.19 (s, 1H), 1.58 (qdd, J = 9.6, 6.0, 1.9 Hz, 3H), 1.48 – 1.37 (m, 4H), 1.35 – 1.19 (m, 13H), 1.14 (d, J = 6.1 Hz, 3H), 0.87 (t, J = 6.8 Hz, 3H); **$^{13}\text{C-NMR}$** (126 MHz, CDCl_3) δ [ppm] 77.1, 71.8, 56.1, 37.7, 33.4, 32.6, 32.0, 29.9, 29.8, 29.7, 29.5, 25.9, 22.8, 19.0, 14.2.

The analytical data is in agreement with the literature.^[110]

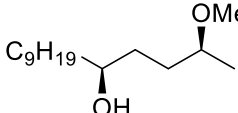
5.8.1.2



According to **GP11**, **D1** (1.0 eq., 0.5 mmol, 121.2 mg, *d.r.* = 62:38) is reacted with D-Kagan (10 mol%, 0.05 mmol, 26.3 mg), 3DPAFIPN (3 mol%, 0.015 μmol , 10.0 mg), DIPEA (3.0 eq., 1.5 mmol, 0.26 mL), DMPU (1.5 eq., 0.75 mmol, 91 μL) and MTG (20 mol%, 0.1 mmol, 9 μL) in THF (0.1 M, 5 mL) under irradiation with blue light at room temperature for 7 days. After purification, **D7** (42.0 mg, 0.172 mmol, 34%, *d.r.* = 96:4) and **D8** (32.0 mg, 0.131 mmol, 26%, *d.r.* = 81:19) are obtained as colorless oils. *r.r.* (1,3:1,4) = 57:43.

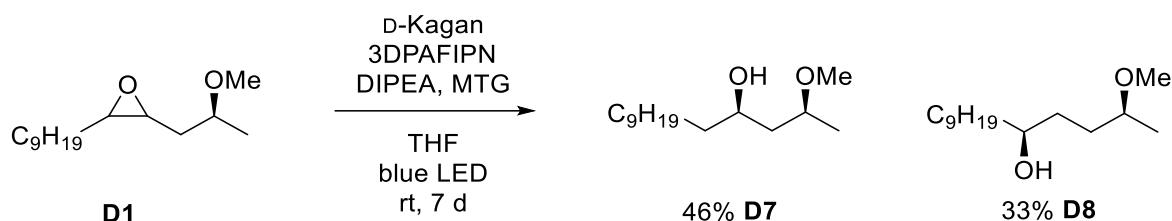

D7: $\text{C}_{15}\text{H}_{32}\text{O}_2$; **MW** = 244.42 g/mol; **$^1\text{H-NMR}$** (400 MHz, CDCl_3) δ [ppm] 3.81 – 3.72 (m, 1H), 3.62 – 3.52 (m, 1H), 3.35 (s, 3H), 1.56 – 1.21 (m, 21H), 1.16 (d, J = 6.1 Hz, 3H), 0.90 – 0.84 (m, 3H); **$^{13}\text{C-NMR}$** (101 MHz, CDCl_3) δ [ppm] 78.6, 72.1, 55.9, 43.8, 37.9, 32.1, 29.9, 29.8, 29.8, 29.8, 29.5, 25.6, 22.8, 19.3, 14.3.

The analytical data is in agreement with the literature.^[110]


D8: $\text{C}_{15}\text{H}_{32}\text{O}_2$; **MW** = 244.42 g/mol; **$^1\text{H-NMR}$** (400 MHz, CDCl_3) δ [ppm] 3.61 – 3.52 (m, 1H), 3.33 (s, 4H), 2.16 (s, 1H), 1.65 – 1.21 (m, 20H), 1.15 (d, J = 6.1 Hz, 3H), 0.91 – 0.84 (m, 3H).; **$^{13}\text{C-NMR}$** (101 MHz, CDCl_3) δ [ppm] 77.4, 72.2, 56.1, 37.8, 33.8, 33.2, 32.1, 29.9, 29.8, 29.7, 29.5, 25.9, 22.8, 19.0, 14.3.

The analytical data is in agreement with the literature.^[110]

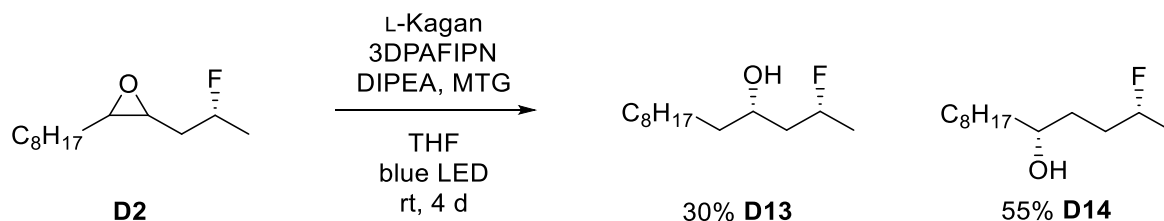
5.8.1.3



According to **GP11**, **D1** (1.0 eq., 0.5 mmol, 121.2 mg, *d.r.* = 62:38) is reacted with D-Kagan (10 mol%, 0.05 mmol, 26.3 mg), 3DPAFIPN (3 mol%, 0.015 μ mol, 10.0 mg), DIPEA (3.0 eq., 1.5 mmol, 0.26 mL), DMPU (1.5 eq., 0.75 mmol, 91 μ L) and MTG (20 mol%, 0.1 mmol, 9 μ L) in THF (0.1 M, 5 mL) under irradiation with blue light at room temperature for 7 days. After purification, **D7** (56.0 mg, 0.230 mmol, 46%, *d.r.* = 95:5) and **D8** (40.0 mg, 0.163 mmol, 33%, *d.r.* = 82:18) are obtained as colorless oils. *r.r.* (1,3:1,4) = 62:38.

5.8.2 Opening of 2-((*R*)-2-fluoropropyl)-3-octyloxirane

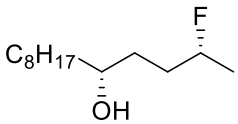
5.8.2.1



According to **GP11**, **D2** (1.0 eq., 0.5 mmol, 108.2 mg, *d.r.* = 32:68) is reacted with L-Kagan (10 mol%, 0.05 mmol, 26.3 mg), 3DPAFIPN (3 mol%, 0.015 μ mol, 10.0 mg), DIPEA (3.0 eq., 1.5 mmol, 0.26 mL) and MTG (20 mol%, 0.1 mmol, 9 μ L) in THF (0.1 M, 5 mL) under irradiation with blue light at room temperature for 4 days. After purification, **D13** (32.9 mg, 0.151 mmol, 30%, *d.r.* = 89:11) and **D14** (60.0 mg, 0.275 mmol, 55%, *d.r.* = 96:4, containing 4% **D11** (1,3-*anti*)) are obtained as colorless solids. *r.r.* (1,3:1,4) = 33:67.

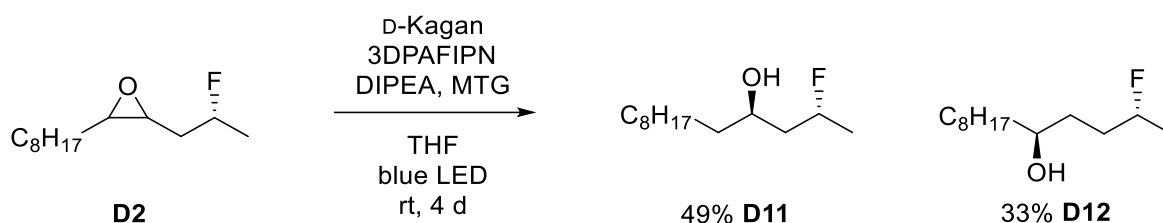
D13: $C_{13}H_{27}FO$; **MW** = 218.36 g/mol; 1H -NMR (500 MHz, $CDCl_3$) δ [ppm] 4.89 (dtdd, J = 49.4, 8.3, 4.4, 2.0 Hz, 1H), 3.84 – 3.78 (m, 1H), 1.88 – 1.23 (m, 22H), 0.88 (t, J = 6.9 Hz, 3H); ^{13}C -NMR (126 MHz, $CDCl_3$) δ [ppm] 91.2 (d, J = 161.6 Hz), 70.4 (d, J = 4.1 Hz), 44.3 (d, J = 18.7 Hz), 37.7, 32.0, 29.8, 29.8, 29.7, 29.5, 25.6, 22.8, 21.6 (d, J = 22.6 Hz), 14.3; ^{19}F -NMR (470 MHz, $CDCl_3$) δ [ppm] -172.4; **IR** [cm^{-1}] $\tilde{\nu}_{max}$ 3385, 2925, 2855, 1460, 1385, 1130, 1050, 925, 825, 720, 520, 460; **HRMS** (ESI) m/z calcd. for $[M+H]^+$ 219.2119, found 219.2118; $[\alpha]_D^{20}$ (DCM) = -7.5°.

The analytical data is in agreement with the literature.^[103]

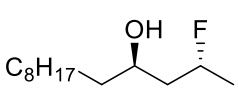

D14: C₁₃H₂₇FO; **MW** = 218.36 g/mol; **¹H-NMR** (500 MHz, CDCl₃) δ [ppm] 4.77 – 4.60 (m, 1H), 3.65 – 3.58 (m, 1H), 1.89 – 1.18 (m, 22H), 0.87 (t, *J* = 6.9 Hz, 3H); **¹³C-NMR** (126 MHz, CDCl₃) δ [ppm] 91.0 (d, *J* = 164.3 Hz), 71.6, 37.7, 33.0 (d, *J* = 20.8 Hz), 32.7 (d, *J* = 4.1 Hz), 32.0, 29.8, 29.7, 29.4, 25.8, 22.8, 21.1 (d, *J* = 22.8 Hz), 14.2; **¹⁹F-NMR** (470 MHz, CDCl₃) δ [ppm] -172.7; **IR** [cm⁻¹] $\tilde{\nu}_{\max}$ 3335, 2950, 2920, 2850, 1470, 1385, 1135, 1055, 885, 820, 540, 440; **HRMS** (ESI) *m/z* calcd. for [M+H]⁺ 219.2119, found 219.2120; **[α]_D²⁰** (DCM) = -10.0°.

The analytical data is in agreement with the literature.^[110]

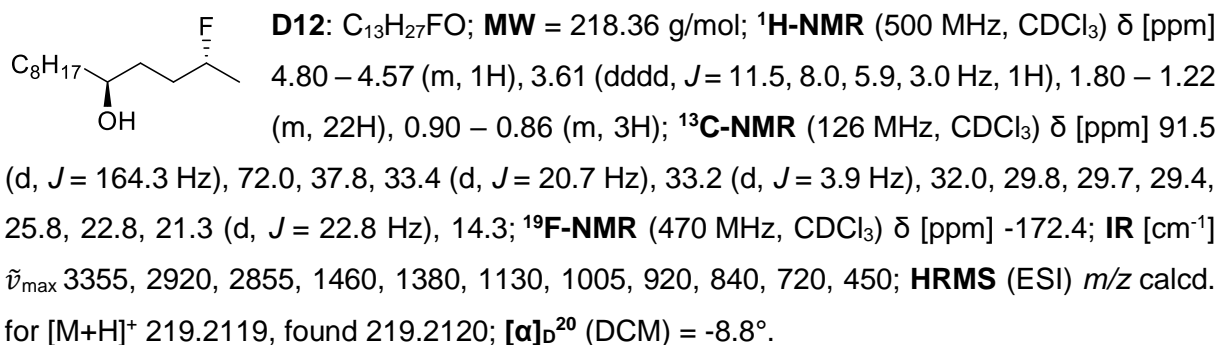
5.8.2.2



According to **GP11**, **D2** (1.0 eq., 0.5 mmol, 108.2 mg, *d.r.* = 32:68) is reacted with D-Kagan (10 mol%, 0.05 mmol, 26.3 mg), 3DPAFIPN (3 mol%, 0.015 μmol, 10.0 mg), DIPEA (3.0 eq., 1.5 mmol, 0.26 mL) and MTG (20 mol%, 0.1 mmol, 9 μL) in THF (0.1 M, 5 mL) under irradiation with blue light at room temperature for 4 days. After purification, **D11** (53.9 mg, 0.247 mmol, 49%, *d.r.* = 3:97) and **D12** (37.2 mg, 0.164 mmol, 33%, *d.r.* = 16:84, containing 7% **D13** (1,3-*syn*)) are obtained as colorless solids. *r.r.* (1,3:1,4) = 67:33.


D11: C₁₃H₂₇FO; **MW** = 218.36 g/mol; **¹H-NMR** (500 MHz, CDCl₃) δ [ppm] 4.96 (ddtd, *J* = 49.5, 12.8, 6.3, 3.1 Hz, 1H), 3.86 (dddd, *J* = 9.8, 7.2, 4.7, 2.5 Hz, 1H), 1.82 – 1.20 (m, 22H), 0.88 (t, *J* = 6.9 Hz, 3H); **¹³C-NMR** (126 MHz, CDCl₃) δ [ppm] 88.5 (d, *J* = 162.7 Hz), 68.2 (d, *J* = 2.9 Hz), 44.5 (d, *J* = 19.9 Hz), 38.1, 32.0, 29.8, 29.7, 29.7, 29.5, 25.7, 22.8, 21.6 (d, *J* = 22.5 Hz), 14.3; **¹⁹F-NMR** (470 MHz, CDCl₃) δ [ppm] -175.5; **IR** [cm⁻¹] $\tilde{\nu}_{\max}$ 3345, 2955, 2920, 2875, 2850, 1470, 1390, 1130, 1130, 1045, 920, 815, 720, 650, 470; **HRMS** (ESI) *m/z* calcd. for [M+H]⁺ 219.2119, found 219.2117; **[α]_D²⁰** (DCM) = -20.7°.

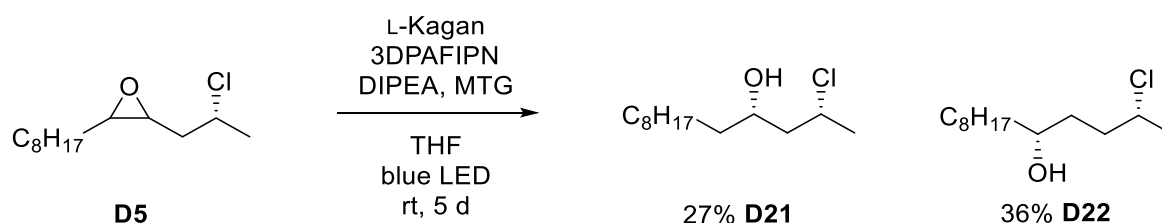
The analytical data is in agreement with the literature.^[110]



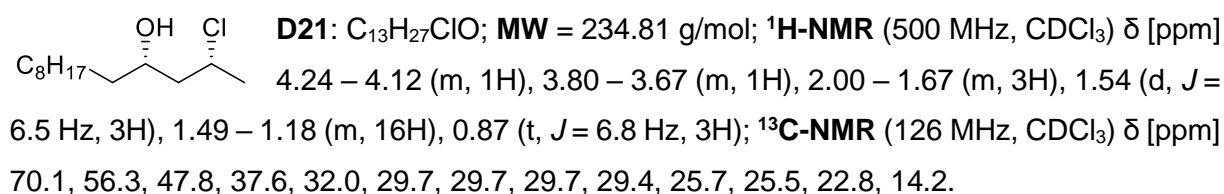
The analytical data is in agreement with the literature.^[103]

5.8.3 Opening of 2-((*R*)-2-chloropropyl)-3-octyloxirane

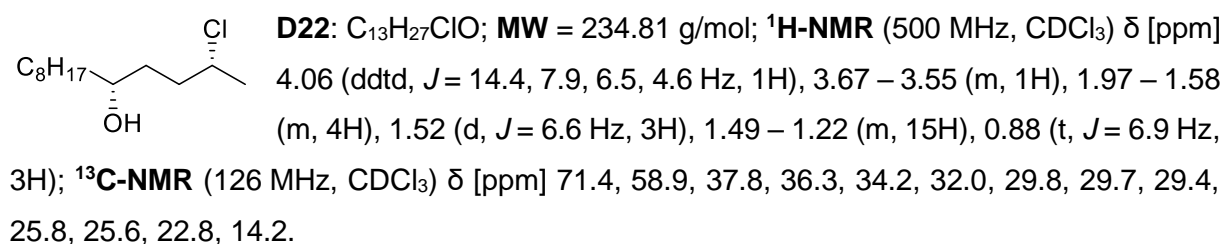
5.8.3.1



According to **GP11**, **D5** (1.0 eq., 0.5 mmol, 116.4 mg, *d.r.* = 40:60) is reacted with L-Kagan (10 mol%, 0.05 mmol, 26.3 mg), 3DPAFIPN (3 mol%, 0.015 μmol, 10.0 mg), DIPEA (3.0 eq., 1.5 mmol, 0.26 mL) and MTG (20 mol%, 0.1 mmol, 9 μL) in THF (0.1 M, 5 mL) under irradiation with blue light at room temperature for 5 days. After purification, **D21** (32.0 mg, 0.136 mmol, 27%, *d.r.* = 62:38) and **D22** (41.8 mg, 0.178 mmol, 36%, *d.r.* = 75:25) are obtained as yellow oils. *r.r.* (1,3:1,4) = 43:57.

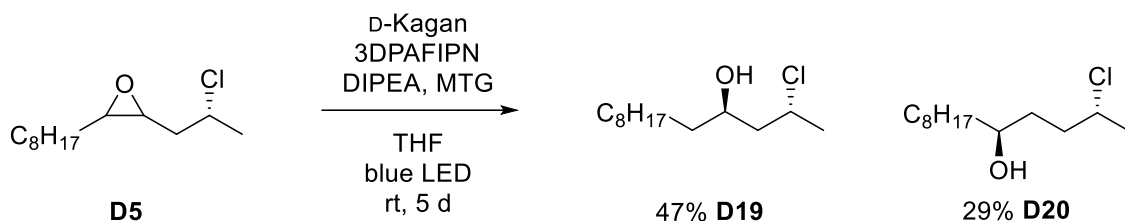


The analytical data is in agreement with the literature.^[103]



The analytical data is in agreement with the literature.^[110]

5.8.3.2



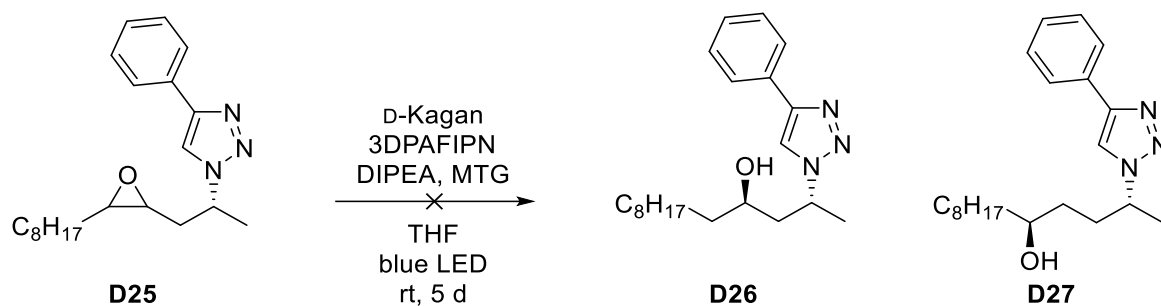
According to **GP11**, **D5** (1.0 eq., 0.5 mmol, 116.4 mg, *d.r.* = 40:60) is reacted with D-Kagan (10 mol%, 0.05 mmol, 26.3 mg), 3DPAFIPN (3 mol%, 0.015 μ mol, 10.0 mg), DIPEA (3.0 eq., 1.5 mmol, 0.26 mL) and MTG (20 mol%, 0.1 mmol, 9 μ L) in THF (0.1 M, 5 mL) under irradiation with blue light at room temperature for 5 days. After purification, **D19** (54.8 mg, 0.233 mmol, 47%, *d.r.* = 28:72) and **D20** (34.6 mg, 0.147 mmol, 29%, *d.r.* = 40:60) are obtained as yellow oils. *r.r.* (1,3:1,4) = 62:38.

D19: $C_{13}H_{27}ClO$; **MW** = 234.81 g/mol; **1H -NMR** (400 MHz, $CDCl_3$) δ [ppm] 4.37 – 4.28 (m, 1H), 3.90 (tdd, J = 8.7, 6.1, 3.8 Hz, 1H), 1.85 – 1.66 (m, 3H), 1.54 (dd, J = 6.5, 0.8 Hz, 3H), 1.50 – 1.21 (m, 16H), 0.90 – 0.83 (m, 3H); **^{13}C -NMR** (101 MHz, $CDCl_3$) δ [ppm] 69.1, 56.1, 47.7, 37.9, 32.0, 29.7, 29.7, 29.7, 29.4, 26.1, 25.7, 22.8, 14.2.

The analytical data is in agreement with the literature.^[110]

D20: $C_{13}H_{27}ClO$; **MW** = 234.81 g/mol; **1H -NMR** (400 MHz, $CDCl_3$) δ [ppm] 4.05 (ddqd, J = 11.1, 8.2, 6.5, 4.7 Hz, 1H), 3.60 (dddd, J = 12.0, 8.4, 5.7, 4.7 Hz, 1H), 1.99 – 1.56 (m, 3H), 1.52 (d, J = 6.6 Hz, 3H), 1.49 – 1.21 (m, 16H), 0.90 – 0.83 (m, 3H); **^{13}C -NMR** (126 MHz, $CDCl_3$) δ [ppm] 71.9, 59.4, 37.8, 36.9, 34.7, 32.0, 29.8, 29.7, 29.4, 25.7, 25.6, 22.8, 14.2.

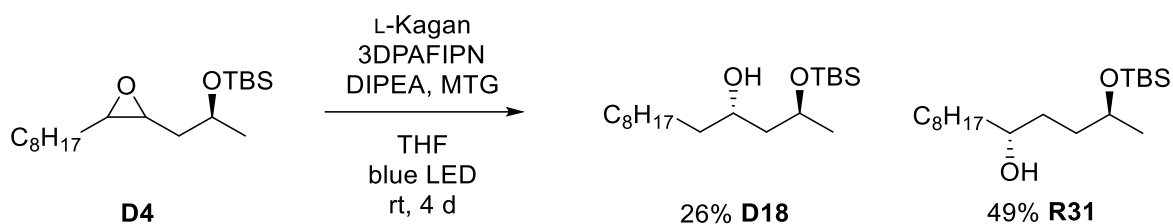
The analytical data is in agreement with the literature.^[103]

5.8.4 Opening of 2-((*R*)-2-(4-phenyl-1*H*-1,2,3-triazol-1-yl)propyl)-3-octyloxirane

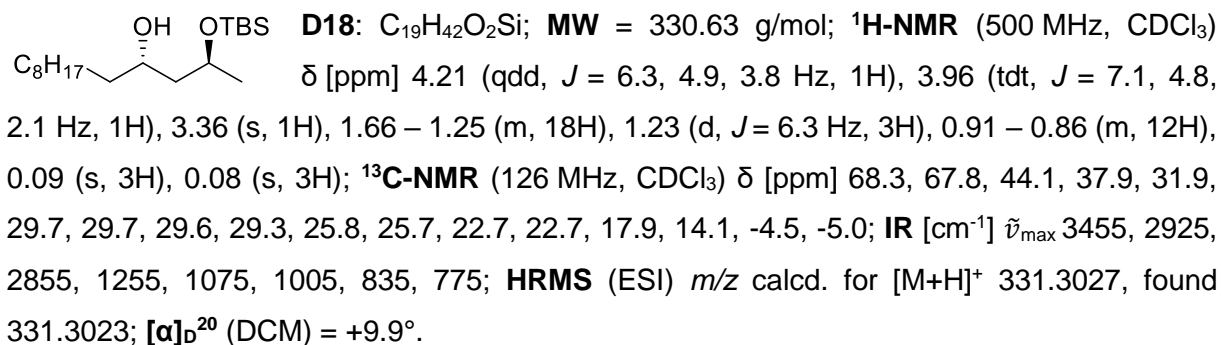
According to **GP11**, **D25** (1.0 eq., 0.5 mmol, 170.8 mg, *d.r.* = 32:68) is reacted with D-Kagan (10 mol%, 0.05 mmol, 26.3 mg), 3DPAFIPN (3 mol%, 0.015 μmol , 10.0 mg), DIPEA (3.0 eq., 1.5 mmol, 0.26 mL) and MTG (20 mol%, 0.1 mmol, 9 μL) in THF (0.1 M, 5 mL) under irradiation with blue light at room temperature for 5 days. According to TLC, no conversion is observed.

5.8.5 Opening of *tert*-butyldimethyl(((*S*)-1-(3-octyloxiran-2-yl)propan-2-yl)oxy)silane

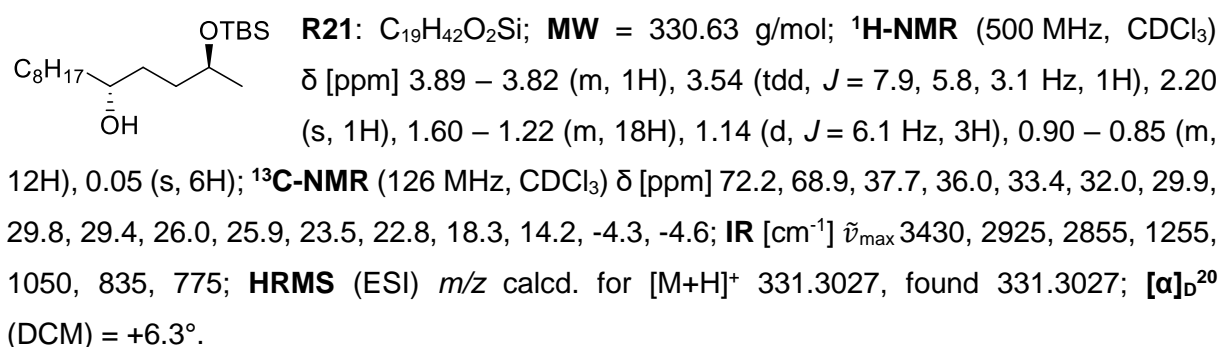
5.8.5.1



According to **GP11**, **D4** (1.0 eq., 0.5 mmol, 108.2 mg, *d.r.* = 68:32) is reacted with L-Kagan (10 mol%, 0.05 mmol, 26.3 mg), 3DPAFIPN (3 mol%, 0.015 μmol , 10.0 mg), DIPEA (3.0 eq., 1.5 mmol, 0.26 mL) and MTG (20 mol%, 0.1 mmol, 9 μL) in THF (0.1 M, 5 mL) under irradiation with blue light at room temperature for 4 days. After purification, **D18** (42.3 mg, 0.140 mmol, 26%, *d.r.* = 14:86) and **R31** (80.4 mg, 0.243 mmol, 49%, *d.r.* = 7:93) are obtained as pale-yellow oils. *r.r.* (1,3:1,4) = 32:68.

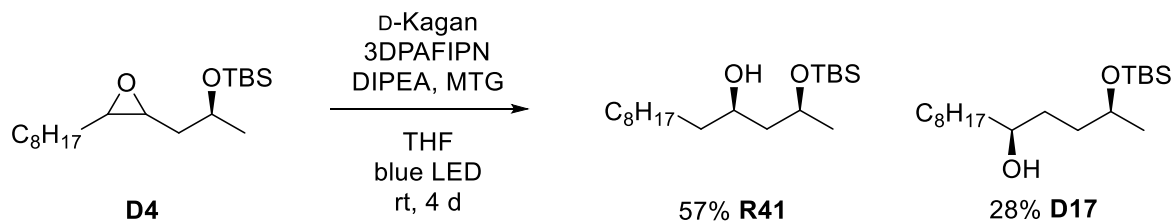

D18: C₁₉H₄₂O₂Si; **MW** = 330.63 g/mol; **¹H-NMR** (500 MHz, CDCl₃) δ [ppm] 4.21 (qdd, *J* = 6.3, 4.9, 3.8 Hz, 1H), 3.96 (tdt, *J* = 7.1, 4.8, 2.1 Hz, 1H), 3.36 (s, 1H), 1.66 – 1.25 (m, 18H), 1.23 (d, *J* = 6.3 Hz, 3H), 0.91 – 0.86 (m, 12H), 0.09 (s, 3H), 0.08 (s, 3H); **¹³C-NMR** (126 MHz, CDCl₃) δ [ppm] 68.3, 67.8, 44.1, 37.9, 31.9, 29.7, 29.7, 29.6, 29.3, 25.8, 25.7, 22.7, 22.7, 17.9, 14.1, -4.5, -5.0; **IR** [cm⁻¹] $\tilde{\nu}_{\max}$ 3455, 2925, 2855, 1255, 1075, 1005, 835, 775; **HRMS** (ESI) *m/z* calcd. for [M+H]⁺ 331.3027, found 331.3023; **[α]_D²⁰** (DCM) = +9.9°.

The analytical data is in agreement with the literature.^[136]

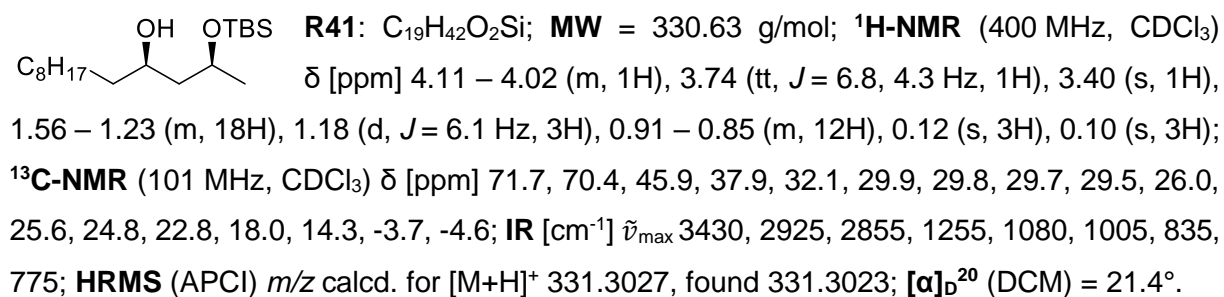

R21: C₁₉H₄₂O₂Si; **MW** = 330.63 g/mol; **¹H-NMR** (500 MHz, CDCl₃) δ [ppm] 3.89 – 3.82 (m, 1H), 3.54 (tdt, *J* = 7.9, 5.8, 3.1 Hz, 1H), 2.20 (s, 1H), 1.60 – 1.22 (m, 18H), 1.14 (d, *J* = 6.1 Hz, 3H), 0.90 – 0.85 (m, 12H), 0.05 (s, 6H); **¹³C-NMR** (126 MHz, CDCl₃) δ [ppm] 72.2, 68.9, 37.7, 36.0, 33.4, 32.0, 29.9, 29.8, 29.4, 26.0, 25.9, 23.5, 22.8, 18.3, 14.2, -4.3, -4.6; **IR** [cm⁻¹] $\tilde{\nu}_{\max}$ 3430, 2925, 2855, 1255, 1050, 835, 775; **HRMS** (ESI) *m/z* calcd. for [M+H]⁺ 331.3027, found 331.3027; **[α]_D²⁰** (DCM) = +6.3°.

The analytical data is in agreement with the literature.^[136]

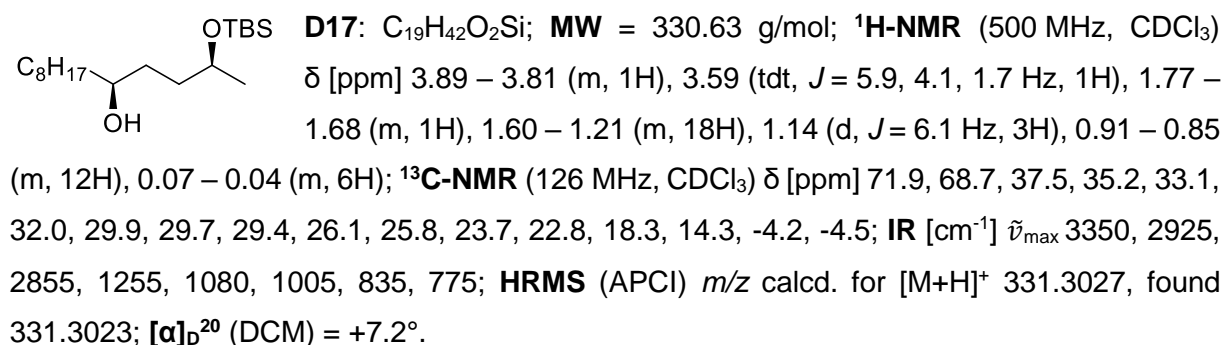
5.8.5.2



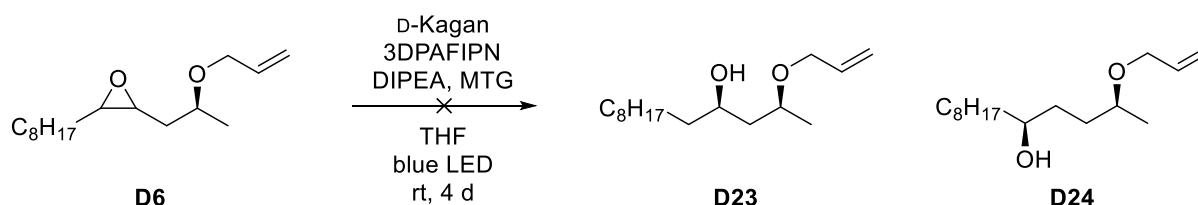
According to **GP11**, **D4** (1.0 eq., 0.5 mmol, 108.2 mg, *d.r.* = 68:32) is reacted with D-Kagan (10 mol%, 0.05 mmol, 26.3 mg), 3DPAFIPN (3 mol%, 0.015 μmol, 10.0 mg), DIPEA (3.0 eq., 1.5 mmol, 0.26 mL) and MTG (20 mol%, 0.1 mmol, 9 μL) in THF (0.1 M, 5 mL) under irradiation with blue light at room temperature for 4 days. After purification, **R41** (91.4 mg, 0.285 mmol, 57%, *d.r.* = 99:1) and **D17** (46.7 mg, 0.141 mmol, 28%, *d.r.* = 90:10) are obtained as colorless oils. *r.r.* (1,3:1,4) = 67:33.


R41: C₁₉H₄₂O₂Si; **MW** = 330.63 g/mol; **¹H-NMR** (400 MHz, CDCl₃) δ [ppm] 4.11 – 4.02 (m, 1H), 3.74 (tt, *J* = 6.8, 4.3 Hz, 1H), 3.40 (s, 1H), 1.56 – 1.23 (m, 18H), 1.18 (d, *J* = 6.1 Hz, 3H), 0.91 – 0.85 (m, 12H), 0.12 (s, 3H), 0.10 (s, 3H); **¹³C-NMR** (101 MHz, CDCl₃) δ [ppm] 71.7, 70.4, 45.9, 37.9, 32.1, 29.9, 29.8, 29.7, 29.5, 26.0, 25.6, 24.8, 22.8, 18.0, 14.3, -3.7, -4.6; **IR** [cm⁻¹] $\tilde{\nu}_{\max}$ 3430, 2925, 2855, 1255, 1080, 1005, 835, 775; **HRMS** (APCI) *m/z* calcd. for [M+H]⁺ 331.3027, found 331.3023; **[α]_D²⁰** (DCM) = 21.4°.

The analytical data is in agreement with the literature.^[136]

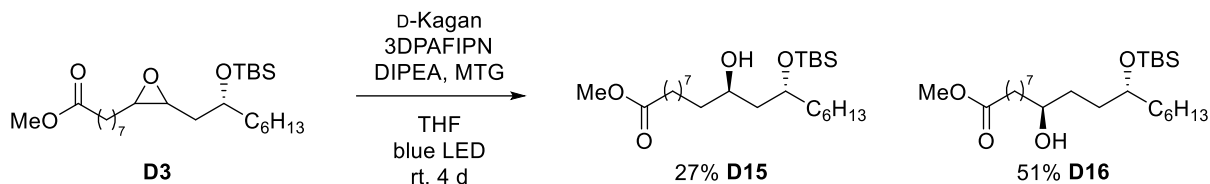

D17: C₁₉H₄₂O₂Si; **MW** = 330.63 g/mol; **¹H-NMR** (500 MHz, CDCl₃) δ [ppm] 3.89 – 3.81 (m, 1H), 3.59 (tdt, *J* = 5.9, 4.1, 1.7 Hz, 1H), 1.77 – 1.68 (m, 1H), 1.60 – 1.21 (m, 18H), 1.14 (d, *J* = 6.1 Hz, 3H), 0.91 – 0.85 (m, 12H), 0.07 – 0.04 (m, 6H); **¹³C-NMR** (126 MHz, CDCl₃) δ [ppm] 71.9, 68.7, 37.5, 35.2, 33.1, 32.0, 29.9, 29.7, 29.4, 26.1, 25.8, 23.7, 22.8, 18.3, 14.3, -4.2, -4.5; **IR** [cm⁻¹] $\tilde{\nu}_{\max}$ 3350, 2925, 2855, 1255, 1080, 1005, 835, 775; **HRMS** (APCI) *m/z* calcd. for [M+H]⁺ 331.3027, found 331.3023; **[α]_D²⁰** (DCM) = +7.2°.

5.8.6 Opening of 2-((S)-2-(allyloxy)propyl)-3-octyloxirane



According to **GP11**, **D6** (1.0 eq., 0.5 mmol, 127.2 mg, *d.r.* = 70:30) is reacted with D-Kagan (10 mol%, 0.05 mmol, 26.3 mg), 3DPAFIPN (3 mol%, 0.015 μmol, 10.0 mg), DIPEA (3.0 eq., 1.5 mmol, 0.26 mL) and MTG (20 mol%, 0.1 mmol, 9 μL) in THF (0.1 M, 5 mL) under irradiation with blue light at room temperature for 4 days. According to TLC, no conversion is observed.

5.8.7 Opening of methyl 8-(3-((*R*)-2-((*tert*-butyldimethylsilyl)oxy)octyl)oxiran-2-yl)octanoate



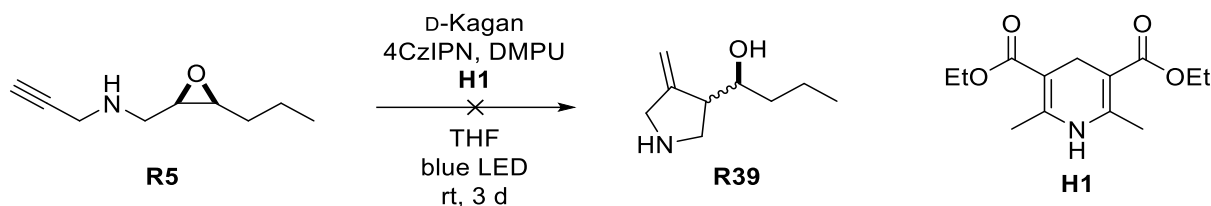
According to **GP11**, **D3** (1.0 eq., 0.5 mmol, 221.4 mg, *d.r.* = 60:40) is reacted with D-Kagan (10 mol%, 0.05 mmol, 26.3 mg), 3DPAFIPN (3 mol%, 0.015 μmol , 10.0 mg), DIPEA (3.0 eq., 1.5 mmol, 0.26 mL) and MTG (20 mol%, 0.1 mmol, 9 μL) in THF (0.1 M, 5 mL) under irradiation with blue light at room temperature for 4 days. After purification, **D15** (61.0 mg, 0.137 mmol, 27%, *d.r.* = 12:88) and **D16** (112.8 mg, 0.254 mmol, 51%, *d.r.* = 8:92) are obtained as pale-yellow oils. *r.r.* (1,3:1,4) = 38:62.

D15: $\text{C}_{25}\text{H}_{52}\text{O}_4\text{Si}$; **MW** = 444.77 g/mol; **¹H-NMR** (500 MHz, CDCl_3) δ [ppm] 4.01 – 3.86 (m, 2H), 3.65 (s, 3H), 2.29 (t, J = 7.5 Hz, 2H), 1.64 – 1.22 (m, 27H), 0.91 – 0.86 (m, 12H), 0.09 (s, 3H), 0.07 (s, 3H); **¹³C-NMR** (126 MHz, CDCl_3) δ [ppm] 174.4, 72.2, 68.4, 51.6, 41.4, 38.2, 36.2, 34.2, 31.9, 29.8, 29.6, 29.5, 29.3, 29.3, 26.0, 25.7, 25.1, 22.7, 18.1, 14.2, -4.4, -4.6; **IR** [cm^{-1}] $\tilde{\nu}_{\text{max}}$ 3455, 2930, 2855, 1740, 1255, 1070, 835, 775; **HRMS** (ESI) m/z calcd. for $[\text{M}+\text{H}]^+$ 445.3708, found 445.3705; **$[\alpha]_{\text{D}}^{20}$** (DCM) = -8.3°.

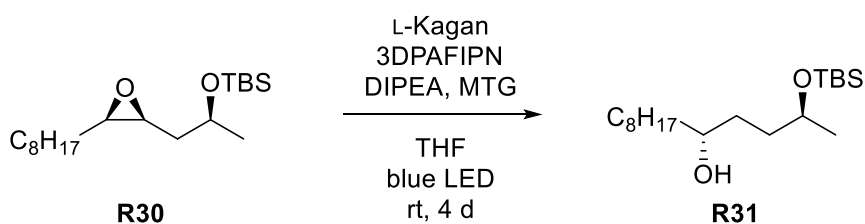
D16: $\text{C}_{25}\text{H}_{52}\text{O}_4\text{Si}$; **MW** = 444.77 g/mol; **¹H-NMR** (500 MHz, CDCl_3) δ [ppm] 3.69 (td, J = 5.8, 4.1 Hz, 1H), 3.65 (s, 3H), 3.52 (tdd, J = 7.6, 5.7, 3.1 Hz, 1H), 2.29 (t, J = 7.5 Hz, 2H), 1.66 – 1.19 (m, 27H), 0.91 – 0.85 (m, 12H), 0.05 (s, 3H), 0.05 (s, 3H); **¹³C-NMR** (126 MHz, CDCl_3) δ [ppm] 174.4, 72.6, 72.2, 51.6, 37.7, 36.7, 34.2, 33.4, 33.0, 32.0, 29.6, 29.6, 29.4, 29.2, 26.0, 25.8, 25.6, 25.1, 22.8, 18.3, 14.2, -4.3; **IR** [cm^{-1}] $\tilde{\nu}_{\text{max}}$ 3430, 2930, 2855, 1740, 1255, 1045, 835, 775; **HRMS** (ESI) m/z calcd. for $[\text{M}+\text{H}]^+$ 445.3708, found 445.3708; **$[\alpha]_{\text{D}}^{20}$** (DCM) = -1.2°.

The analytical data is in agreement with the literature.^[136]

5.9 Regiodivergent Epoxide Openings with Organic Photocatalysts

5.9.1 Opening of *N*-(((2*R*,3*S*)-3-propyloxiran-2-yl)methyl)prop-2-yn-1-amine

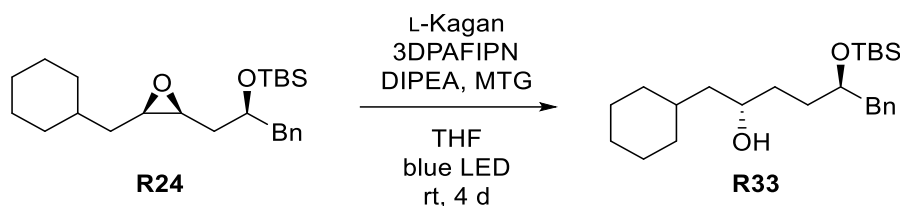
The reaction is performed in a heat-dried *Schlenk* tube under argon atmosphere. D-Kagan (10 mol%, 0.025 mmol, 13.1 mg) and 4CzIPN (2.5 mol%, 6.25 μ mol, 4.9 mg) are placed in the tube and evacuated for 30 min. After flushing with argon, THF (0.1 M, 2.5 mL) and epoxide **R5** (1.0 eq., 0.25 mmol, 38.3 mg) are added, followed by *Hantzsch* ester (**H1**, 2.0 eq., 0.5 mmol, 126.7 mg) and DMPU (1.5 eq., 0.75 mmol, 45 μ L). The reaction is stirred under irradiation with blue light at room temperature for 3 d. After the reaction is finished, 2 mL of phosphate buffer solution and 2 mL of Et₂O are added. The reaction is stirred for 10 min, afterwards the phases are separated, and the aqueous layer is extracted with Et₂O (3x). The combined organic phase is dried over MgSO₄, filtered, and the solvent is removed under reduced pressure. No product can be isolated and the ¹H-NMR data show decomposition of the substrate and product. Only *Hantzsch* ester (**H1**) can be isolated.

5.9.2 Opening of *tert*-butyldimethyl(((*S*)-1-((2*S*,3*R*)-3-octyloxiran-2-yl)propan-2-yl)oxy)silane

According to **GP11** L-Kagan (10 mol%, 0.05 mmol, 26.3 mg), **R30** (1.0 eq., 0.5 mmol, 164.3 mg), 3DPAFIPN (3 mol%, 0.015 μ mol, 10.0 mg), DIPEA (3.0 eq., 1.5 mmol, 0.26 mL) and MTG (20 mol%, 0.1 mmol, 9 μ L) are reacted in THF (0.1 M, 5 mL) under irradiation with blue light at room temperature for 4 days. After purification, **R31** (117.5 mg, 0.355 mmol, 71%, *d.r.* = 1:99) is obtained as a colorless oil. *r.r.* (1,3:1,4) = 9:91.

5.9.3 Opening of *tert*-butyl(((*S*)-1-((2*S*,3*R*)-3-(cyclohexylmethyl)oxiran-2-yl)-3-phenylpropan-2-yl)oxy)dimethylsilane

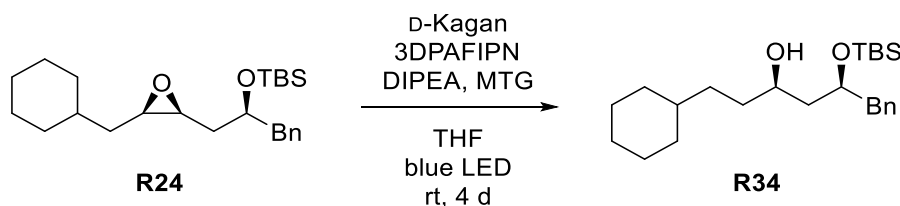
5.9.3.1



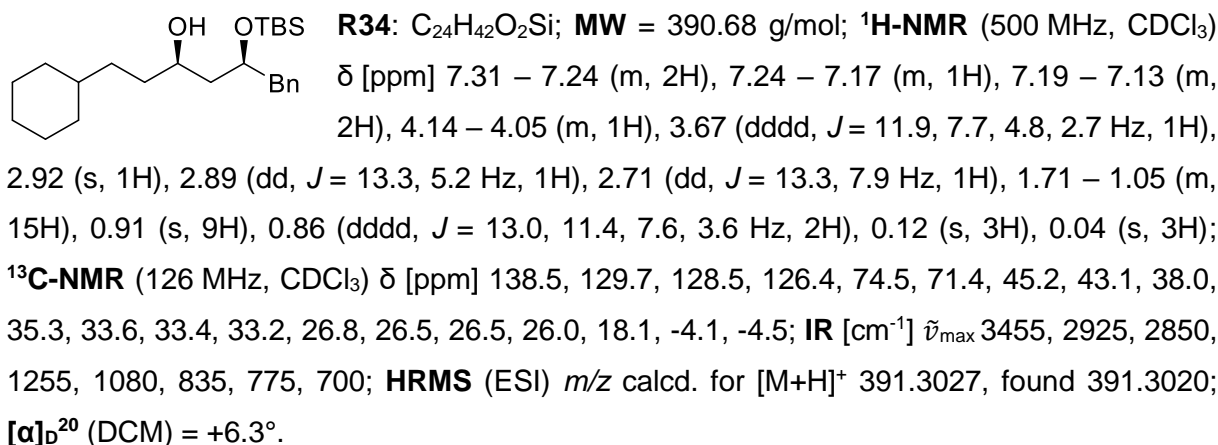
According to **GP11** L-Kagan (10 mol%, 0.05 mmol, 26.3 mg), **R24** (1.0 eq., 0.5 mmol, 194.3 mg), 3DPAFIPN (3 mol%, 0.015 μmol , 10.0 mg), DIPEA (3.0 eq., 1.5 mmol, 0.26 mL) and MTG (20 mol%, 0.1 mmol, 9 μL) are reacted in THF (0.1 M, 5 mL) under irradiation with blue light at room temperature for 4 days. After purification, **R33** (57.7 mg, 0.148 mmol, 30%, *d.r.* = 1:99) is obtained as a pale-yellow oil. *r.r.* (1,3:1,4) = 20:80.

R33: $\text{C}_{24}\text{H}_{42}\text{O}_2\text{Si}$; **MW** = 390.68 g/mol; **$^1\text{H-NMR}$** (400 MHz, CDCl_3) δ [ppm] 7.28 (ddt, $J = 7.0, 5.9, 1.0$ Hz, 2H), 7.23 – 7.16 (m, 3H), 3.93 (tt, $J = 6.5, 4.6$ Hz, 1H), 3.71 – 3.63 (m, 1H), 2.86 – 2.71 (m, 2H), 2.13 (s, 1H), 1.84 – 1.10 (m, 14H), 0.88 (s, 12H), -0.00 (s, 3H), -0.16 (s, 3H); **$^{13}\text{C-NMR}$** (101 MHz, CDCl_3) δ [ppm] 139.3, 129.8, 128.3, 126.2, 74.0, 69.5, 45.6, 43.5, 34.3, 33.6, 33.4, 33.1, 26.8, 26.5, 26.4, 26.0, 18.2, -4.6, -4.8; **IR** [cm^{-1}] $\tilde{\nu}_{\text{max}}$ 3360, 2925, 2855, 1255, 1085, 1045, 835, 775, 695; **HRMS** (ESI) m/z calcd. for $[\text{M}+\text{H}]^+$ 391.3027, found 391.3027; **$[\alpha]_{\text{D}}^{20}$** (DCM) = -1.8° .

5.9.3.2

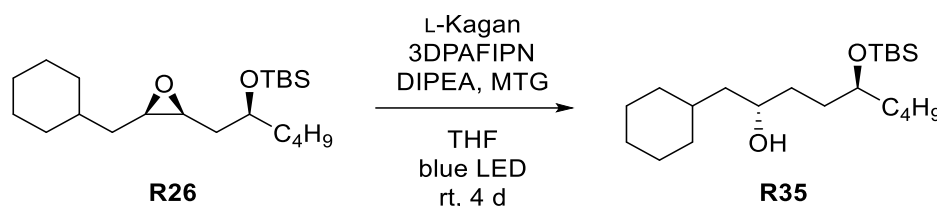


According to **GP11** D-Kagan (10 mol%, 0.05 mmol, 26.3 mg), **R24** (1.0 eq., 0.5 mmol, 194.3 mg), 3DPAFIPN (3 mol%, 0.015 μmol , 10.0 mg), DIPEA (3.0 eq., 1.5 mmol, 0.26 mL) and MTG (20 mol%, 0.1 mmol, 9 μL) are reacted in THF (0.1 M, 5 mL) under irradiation with blue light at room temperature for 4 days. After purification, **R34** (74.9 mg, 0.192 mmol, 39%, *d.r.* = 99:1) is obtained as a pale-yellow oil. *r.r.* (1,3:1,4) = 92:8.

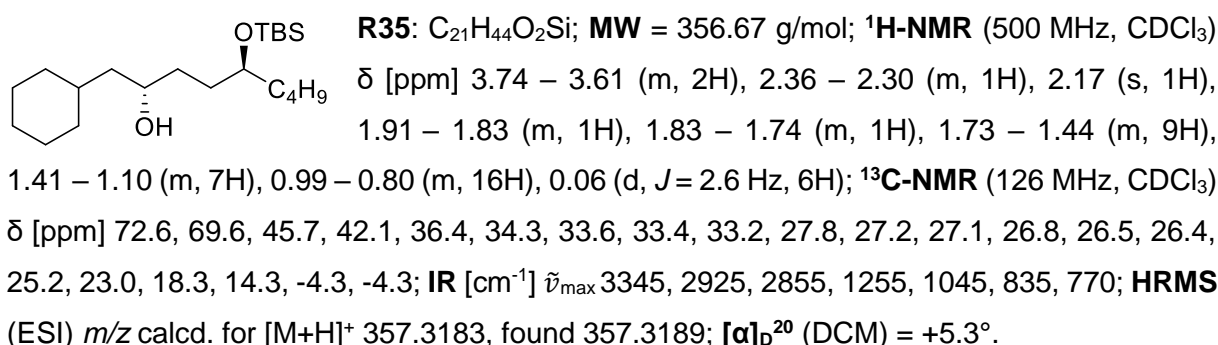


5.9.4 Opening of *tert*-butyl(((*S*)-1-((2*S*,3*R*)-3-(cyclohexylmethyl)oxiran-2-yl)hexan-2-yl)oxy)dimethylsilane

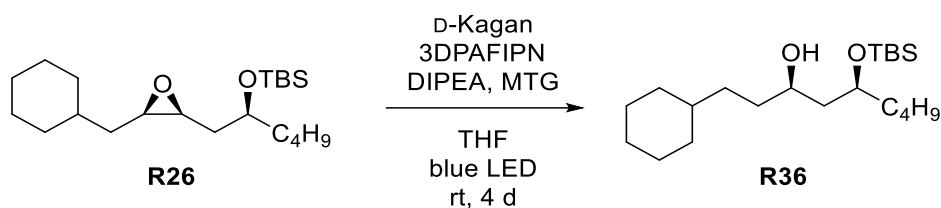
5.9.4.1



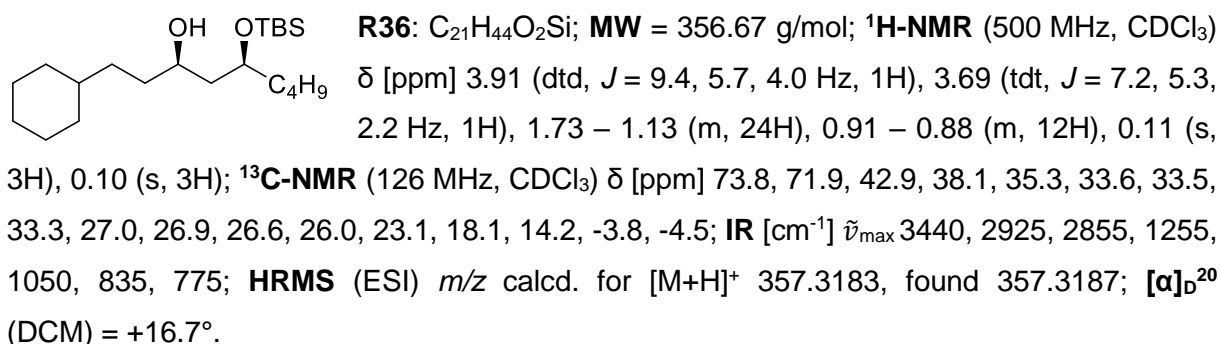
According to **GP11** L-Kagan (10 mol%, 0.05 mmol, 26.3 mg), **R26** (1.0 eq., 0.5 mmol, 177.3 mg), 3DPAFIPN (3 mol%, 0.015 μmol, 10.0 mg), DIPEA (3.0 eq., 1.5 mmol, 0.26 mL) and MTG (20 mol%, 0.1 mmol, 9 μL) are reacted in THF (0.1 M, 5 mL) under irradiation with blue light at room temperature for 4 days. After purification, **R35** (104.1 mg, 0.292 mmol, 59%, *d.r.* = 1:99) is obtained as a pale-yellow oil. *r.r.* (1,3:1,4) = 15:85.



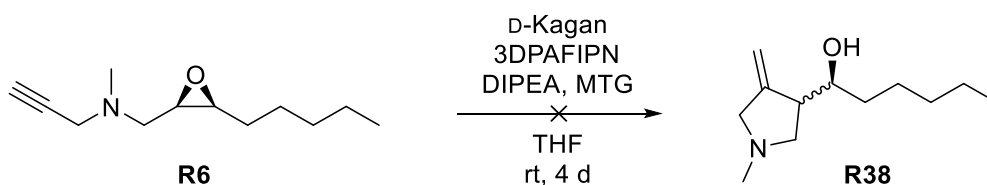
5.9.4.2



According to **GP11** D-Kagan (10 mol%, 0.05 mmol, 26.3 mg), **R26** (1.0 eq., 0.5 mmol, 177.3 mg), 3DPAFIPN (3 mol%, 0.015 μmol , 10.0 mg), DIPEA (3.0 eq., 1.5 mmol, 0.26 mL) and MTG (20 mol%, 0.1 mmol, 9 μL) are reacted in THF (0.1 M, 5 mL) under irradiation with blue light at room temperature for 4 days. After purification, **R36** (139.6 mg, 0.391 mmol, 78%, *d.r.* = 99:1) is obtained as a pale-yellow oil. *r.r.* (1,3:1,4) = 94:6.

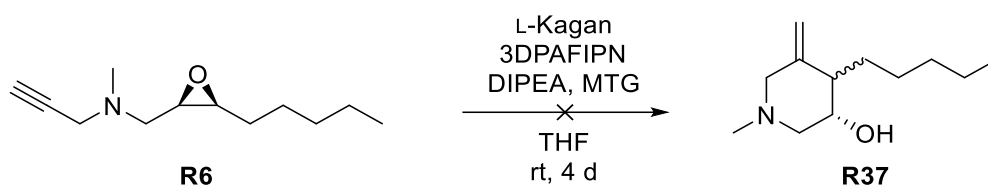
5.9.5 Opening of *N*-(((2*R*,3*S*)-3-hexyloxiran-2-yl)methyl)-*N*-methylprop-2-yn-1-amine

5.9.5.1



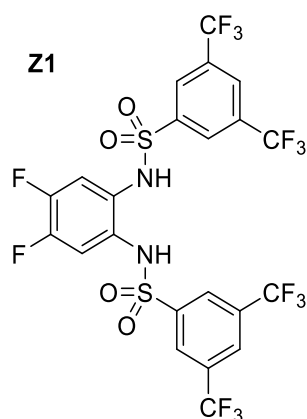
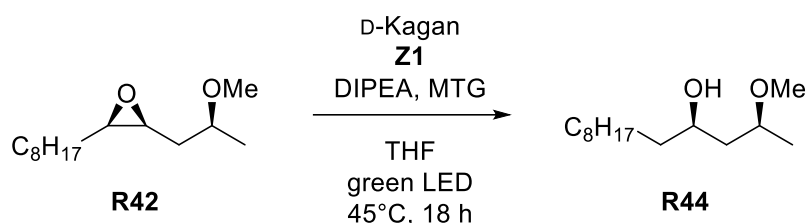
According to **GP11** D-Kagan (10 mol%, 0.05 mmol, 26.3 mg), **R6** (1.0 eq., 0.5 mmol, 97.7 mg), 3DPAFIPN (3 mol%, 0.015 μmol , 10.0 mg), DIPEA (3.0 eq., 1.5 mmol, 0.26 mL) and MTG (20 mol%, 0.1 mmol, 9 μL) are reacted in THF (0.1 M, 5 mL) under irradiation with blue light at room temperature for 4 days. According to TLC, no conversion is observed.

5.9.5.2



According to **GP11** L-Kagan (10 mol%, 0.05 mmol, 26.3 mg), **R6** (1.0 eq., 0.5 mmol, 97.7 mg), 3DPAFIPN (3 mol%, 0.015 μ mol, 10.0 mg), DIPEA (3.0 eq., 1.5 mmol, 0.26 mL) and MTG (20 mol%, 0.1 mmol, 9 μ L) are reacted in THF (0.1 M, 5 mL) under irradiation with blue light at room temperature for 4 days. According to TLC, no conversion is observed.

5.10 Regiodivergent Epoxide Openings with Sulfonamides

5.10.1 Opening of (2*S*,3*R*)-2-((*S*)-2-methoxypropyl)-3-octyloxirane

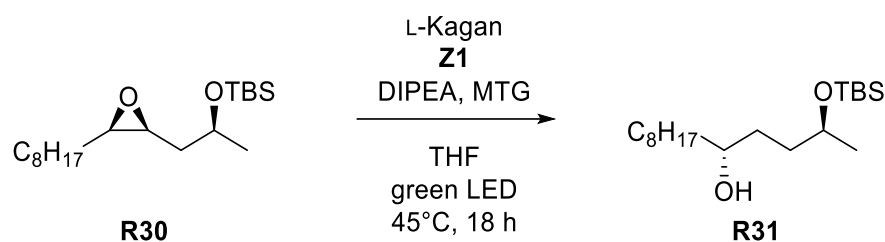
According to **GP12**, D-Kagan (15 mol%, 37.5 μmol , 19.7 mg), **R42** (1.0 eq., 0.25 mmol, 57.1 mg, *d.r.* = 93:7), **Z1** (15 mol%, 37.5 μmol , 26.1 mg), DIPEA (3.0 eq., 0.75 mmol, 0.13 mL) and MTG (20 mol%, 0.05 mmol, 4 μL) are reacted in THF (1.5 mL) under irradiation with green light at 45°C for 18 h. After purification, **R44** is obtained as a colorless oil (38.4 mg, 0.167 mmol, 66%, *d.r.* = 99:1). *r.r.* (1,3:1,4) = 90:10.

R44: $\text{C}_{14}\text{H}_{30}\text{O}_2$; **MW** = 230.39 g/mol; **$^1\text{H-NMR}$** (500 MHz, CDCl_3) δ [ppm] 3.80 – 3.73 (m, 1H), 3.62 – 3.52 (m, 1H), 3.40 (s, 1H), 3.34 (s, 3H), 1.59 – 1.19 (m, 18H), 1.16 (d, J = 6.1 Hz, 3H), 0.87 (t, J = 6.9 Hz, 3H); **$^{13}\text{C-NMR}$** (126 MHz, CDCl_3) δ [ppm] 78.6, 72.1, 55.9, 43.8, 37.8, 32.0, 29.9, 29.8, 29.7, 29.5, 25.6, 22.8, 19.3, 14.2; **IR** [cm^{-1}] $\tilde{\nu}_{\text{max}}$ 3435, 2825, 1465, 1375, 1125, 1080; **HRMS** (ESI) m/z calcd. for $[\text{M}+\text{H}]^+$ 231.2319, found 231.2318; **$[\alpha]_{\text{D}}^{20}$** (DCM) = +25.4°.

The analytical data is in agreement with the literature.^[136]

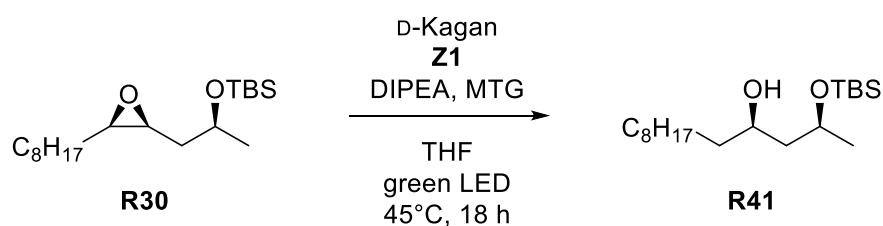
5.10.2 Opening of *tert*-butyldimethyl(((*S*)-1-((2*S*,3*R*)-3-octyloxiran-2-yl)propan-2-yl)oxy)silane

5.10.2.1



According to **GP12**, L-Kagan (15 mol%, 37.5 μ mol, 19.7 mg), **R30** (1.0 eq., 0.25 mmol, 82.2 mg, *d.r.* = 99:1), **Z1** (15 mol%, 37.5 μ mol, 26.1 mg), DIPEA (3.0 eq., 0.75 mmol, 0.13 mL) and MTG (20 mol%, 0.05 mmol, 4 μ L) are reacted in THF (1.5 mL) under irradiation with green light at 45°C for 18 h. After purification, **R31** is obtained as a colorless oil (57.4 mg, 0.174 mmol, 69%, *d.r.* = 1:99). *r.r.* (1,3:1,4) = 7:93.

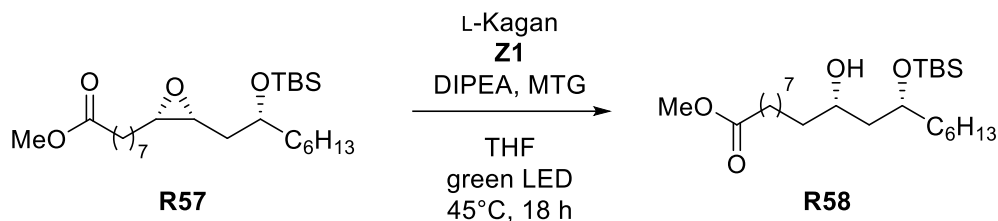
5.10.2.2



According to **GP12**, D-Kagan (15 mol%, 37.5 μ mol, 19.7 mg), **R30** (1.0 eq., 0.25 mmol, 82.2 mg, *d.r.* = 99:1), **Z1** (15 mol%, 37.5 μ mol, 26.1 mg), DIPEA (3.0 eq., 0.75 mmol, 0.13 mL) and MTG (20 mol%, 0.05 mmol, 4 μ L) are reacted in THF (1.5 mL) under irradiation with green light at 45°C for 18 h. After purification, **R41** is obtained as a colorless oil (59.7 mg, 0.181 mmol, 73%, *d.r.* = 99:1). *r.r.* (1,3:1,4) = 94:6.

5.10.3 Opening of methyl 8-((2*S*,3*R*)-3-((*R*)-2-((*tert*-butyldimethylsilyloxy)-octyl)oxiran-2-yl)octanoate

5.10.3.1

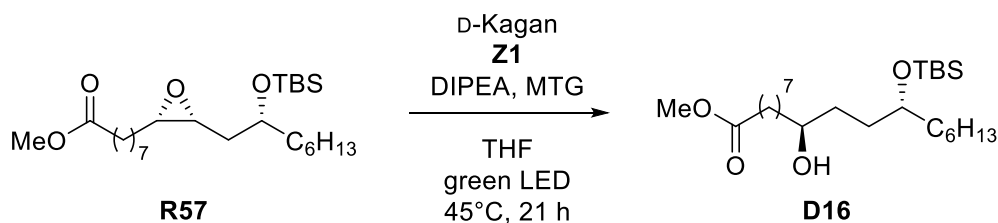


According to **GP12**, L-Kagan (15 mol%, 37.5 μ mol, 19.7 mg), **R57** (1.0 eq., 0.25 mmol, 110.7 mg, *d.r.* = 99:1), **Z1** (15 mol%, 37.5 μ mol, 26.1 mg), DIPEA (3.0 eq., 0.75 mmol, 0.13 mL) and MTG (20 mol%, 0.05 mmol, 4 μ L) are reacted in THF (1.5 mL) under irradiation with green light at 45°C for 18 h. After purification, **R58** is obtained as a colorless oil (82.4 mg, 0.186 mmol, 74%, *d.r.* = 99:1). *r.r.* (1,3:1,4) = 91:9.

R58: C₂₅H₅₂O₄Si; MW = 444.77 g/mol; ¹H-NMR (500 MHz, CDCl₃) δ [ppm] 3.90 (dtd, *J* = 9.5, 5.7, 4.1 Hz, 1H), 3.71 (ddd, *J* = 11.4, 5.6, 3.3 Hz, 1H), 3.65 (s, 3H), 2.28 (t, *J* = 7.5 Hz, 2H), 1.64 – 1.21 (m, 27H), 0.89 – 0.85 (m, 12H), 0.10 (s, 3H), 0.08 (s, 3H); ¹³C-NMR (126 MHz, CDCl₃) δ [ppm] 174.4, 73.8, 71.4, 51.5, 42.9, 38.3, 37.9, 34.2, 32.0, 29.8, 29.6, 29.5, 29.3, 29.3, 26.0, 25.5, 25.1, 24.7, 22.7, 18.1, 14.2, -3.8, -4.5; IR [cm⁻¹] $\tilde{\nu}_{\max}$ 3455, 2930, 2855, 1740, 1255, 1070, 835, 775; HRMS (ESI) *m/z* calcd. for [M+H]⁺ 445.3708, found 445.3705; [α]_D²⁰ (DCM) = -14.8°.

The analytical data is in agreement with the literature.^[136]

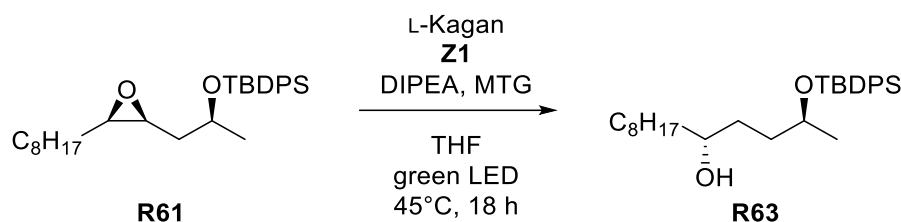
5.10.3.2



According to **GP12**, L-Kagan (15 mol%, 37.5 μ mol, 19.7 mg), **R57** (1.0 eq., 0.25 mmol, 110.7 mg, *d.r.* = 99:1), **Z1** (15 mol%, 37.5 μ mol, 26.1 mg), DIPEA (3.0 eq., 0.75 mmol, 0.13 mL) and MTG (20 mol%, 0.05 mmol, 4 μ L) are reacted in THF (1.5 mL) under irradiation with green light at 45°C for 18 h. After purification, **D16** is obtained as a colorless oil (75.1 mg, 0.169 mmol, 68%, *d.r.* = 1:99). *r.r.* (1,3:1,4) = 8:92.

5.10.4 Opening of *tert*-butyl(((*S*)-1-((2*S*,3*R*)-3-octyloxiran-2-yl)propan-2-yl)oxy)diphenylsilane

5.10.4.1

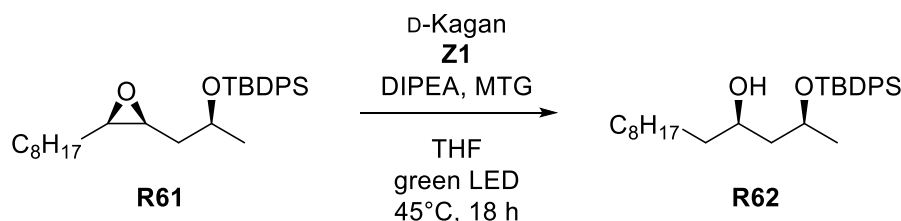


According to **GP12**, L-Kagan (15 mol%, 75 μ mol, 39.4 mg), **R61** (1.0 eq., 0.5 mmol, 226.4 mg, *d.r.* = 99:1), **Z1** (15 mol%, 75 μ mol, 52.2 mg), DIPEA (3.0 eq., 1.5 mmol, 0.26 mL) and MTG (20 mol%, 0.1 mmol, 9 μ L) are reacted in THF (3 mL) under irradiation with green light at 45°C for 18 h. After purification, **R63** is obtained as a colorless oil (163.7 mg, 0.360 mmol, 72%, *d.r.* = 1:99). *r.r.* (1,3:1,4) = 10:90.

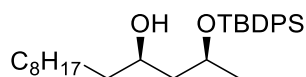
R63: C₂₉H₄₆O₂Si; MW = 454.77 g/mol; ¹H-NMR (500 MHz, CDCl₃) δ [ppm] 7.69 (ddd, *J* = 8.1, 6.6, 1.5 Hz, 4H), 7.45 – 7.40 (m, 2H), 7.40 – 7.35 (m, 4H), 3.89 (ddd, *J* = 5.9, 5.9, 5.9 Hz, 1H), 3.51 – 3.45 (m, 1H), 1.64 (s, 2H), 1.60 – 1.21 (m, 17H), 1.10 – 1.05 (m, 12H), 0.89 (t, *J* = 6.9 Hz, 3H); ¹³C-NMR (126 MHz, CDCl₃) δ [ppm] 136.0, 136.0, 134.8, 134.5, 129.7, 129.6, 127.7, 127.6, 72.2, 69.8, 37.6, 35.6, 33.1, 32.0, 29.9, 29.7, 29.4, 27.2, 25.8, 23.1, 22.8, 19.4, 14.3; IR [cm⁻¹] $\tilde{\nu}_{\max}$ 3345, 2925, 2855, 1105, 700, 610, 505, 485; HRMS (ESI) *m/z* calcd. for [M+H]⁺ 455.3340, found 455.3337; [α]_D²⁰ (CHCl₃) = -12.9°.

The analytical data is in agreement with the literature.^[136]

5.10.4.2



According to **GP12**, D-Kagan (15 mol%, 75 μ mol, 39.4 mg), **R61** (1.0 eq., 0.5 mmol, 226.4 mg, *d.r.* = 99:1), **Z1** (15 mol%, 75 μ mol, 52.2 mg), DIPEA (3.0 eq., 1.5 mmol, 0.26 mL) and MTG (20 mol%, 0.1 mmol, 9 μ L) are reacted in THF (3 mL) under irradiation with green light at 45°C for 18 h. After purification, **R62** is obtained as a colorless oil (168.5 mg, 0.371 mmol, 74%, *d.r.* = 99:1). *r.r.* (1,3:1,4) = 90:10.

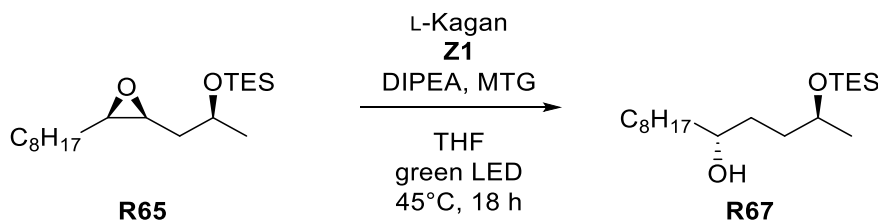


R62: C₂₉H₄₆O₂Si; **MW** = 454.77 g/mol; **¹H-NMR** (500 MHz, CDCl₃) δ [ppm] 7.77 – 7.71 (m, 4H), 7.47 – 7.36 (m, 6H), 4.13 (ddd, *J* = 8.2, 6.1, 4.7 Hz, 1H), 3.80 (tdt, *J* = 7.0, 5.1, 2.8 Hz, 1H), 2.84 (s, 1H), 1.67 (ddd, *J* = 14.3, 9.1, 8.2 Hz, 1H), 1.55 (ddd, *J* = 14.3, 4.7, 2.8 Hz, 1H), 1.46 – 1.35 (m, 3H), 1.28 (s, 13H), 1.06 (s, 9H), 1.01 (d, *J* = 6.1 Hz, 3H), 0.92 – 0.87 (m, 3H); **¹³C-NMR** (126 MHz, CDCl₃) δ [ppm] 136.0, 136.0, 134.6, 133.7, 129.9, 129.7, 127.8, 127.6, 71.0, 70.7, 46.5, 37.9, 32.1, 29.9, 29.8, 29.7, 29.5, 27.1, 25.6, 24.3, 22.8, 19.3, 14.3; **IR** [cm⁻¹] $\tilde{\nu}_{\max}$ 3450, 2925, 2855, 1110, 700, 505, 485; **HRMS** (ESI) *m/z* calcd. for [M+H]⁺ 455.3340, found 455.3350; **[α]_D²⁰** (CHCl₃) = +4.2°.

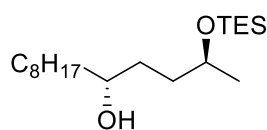
The analytical data is in agreement with the literature.^[136]

5.10.5 Opening of triethyl(((S)-1-((2S,3R)-3-octyloxiran-2-yl)propan-2-yl)oxy)silane

5.10.5.1



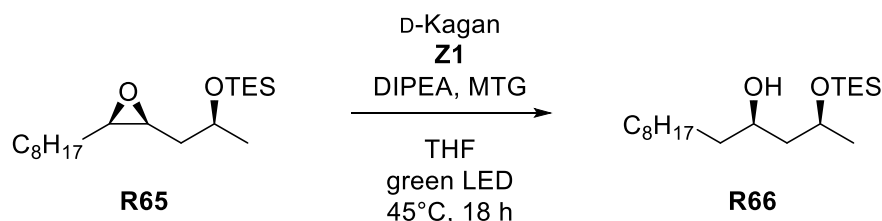
According to **GP12**, L-Kagan (15 mol%, 75 μmol, 39.4 mg), **R65** (1.0 eq., 0.5 mmol, 164.3 mg, *d.r.* = 99:1), **Z1** (15 mol%, 75 μmol, 52.2 mg), DIPEA (3.0 eq., 1.5 mmol, 0.26 mL) and MTG (20 mol%, 0.1 mmol, 9 μL) are reacted in THF (3 mL) under irradiation with green light at 45°C for 18 h. After purification, **R67** is obtained as a colorless oil (115.4 mg, 0.350 mmol, 70%, *d.r.* = 1:99). *r.r.* (1,3:1,4) = 7:93.



R67: C₁₉H₄₂O₂Si; **MW** = 330.63 g/mol; **¹H-NMR** (500 MHz, CD₂Cl₂) δ [ppm] 3.90 – 3.83 (m, 1H), 3.55 – 3.49 (m, 1H), 2.00 (s, 1H), 1.59 – 1.24 (m, 19H), 1.14 (d, *J* = 6.2 Hz, 3H), 0.96 (t, *J* = 7.9 Hz, 9H), 0.88 (ddd, *J* = 555.2, 13.9, 7.1 Hz, 3H), 0.60 (dt, *J* = 24.3, 7.7 Hz, 6H); **¹³C-NMR** (126 MHz, CD₂Cl₂) δ [ppm] 72.3, 69.0, 38.1, 36.3, 33.8, 32.3, 30.2, 30.0, 29.7, 26.1, 23.7, 23.1, 14.3, 7.0, 5.3; **IR** [cm⁻¹] $\tilde{\nu}_{\max}$ 3310, 3215, 2915, 1065, 1055, 1020, 720; **HRMS** (APCI) *m/z* calcd. for [M+H]⁺ 331.3027, found 331.3026; **[α]_D²⁰** (CHCl₃) = +4.7°.

The analytical data is in agreement with the literature.^[136]

5.10.5.2



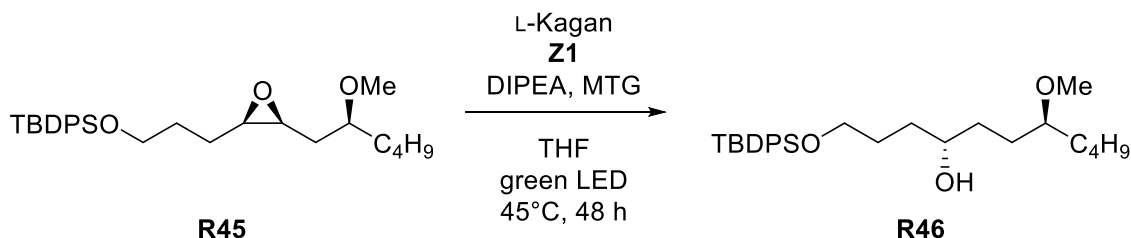
According to **GP12**, D-Kagan (15 mol%, 75 μ mol, 39.4 mg), **R65** (1.0 eq., 0.5 mmol, 164.3 mg, *d.r.* = 99:1), **Z1** (15 mol%, 75 μ mol, 52.2 mg), DIPEA (3.0 eq., 1.5 mmol, 0.26 mL) and MTG (20 mol%, 0.1 mmol, 9 μ L) are reacted in THF (3 mL) under irradiation with green light at 45°C for 18 h. After purification, **R66** is obtained as a colorless oil (124.4 mg, 0.376 mmol, 75%, *d.r.* = 98:2). *r.r.* (1,3:1,4) = 93:7.

R66: C₁₉H₄₂O₂Si; MW = 330.63 g/mol; ¹H-NMR (500 MHz, CDCl₃) δ [ppm] 4.13 – 4.04 (m, 1H), 3.75 (tt, *J* = 6.7, 4.2 Hz, 1H), 3.61 (s, 1H), 1.55 – 1.23 (m, 18H), 1.19 (d, *J* = 6.1 Hz, 3H), 0.97 (t, *J* = 7.9 Hz, 9H), 0.87 (t, *J* = 6.9 Hz, 3H), 0.64 (q, *J* = 7.9 Hz, 6H); ¹³C-NMR (126 MHz, CDCl₃) δ [ppm] 71.9, 70.4, 45.9, 37.9, 32.1, 29.9, 29.8, 29.7, 29.5, 25.6, 24.8, 22.8, 14.3, 6.9, 5.3; IR [cm⁻¹] $\tilde{\nu}_{\max}$ 3345, 2925, 2855, 1070, 1005, 730, 685; HRMS (APCI) *m/z* calcd. for [M+H]⁺ 331.3027, found 331.3027; [α]_D²⁰ (CHCl₃) = +3.3°.

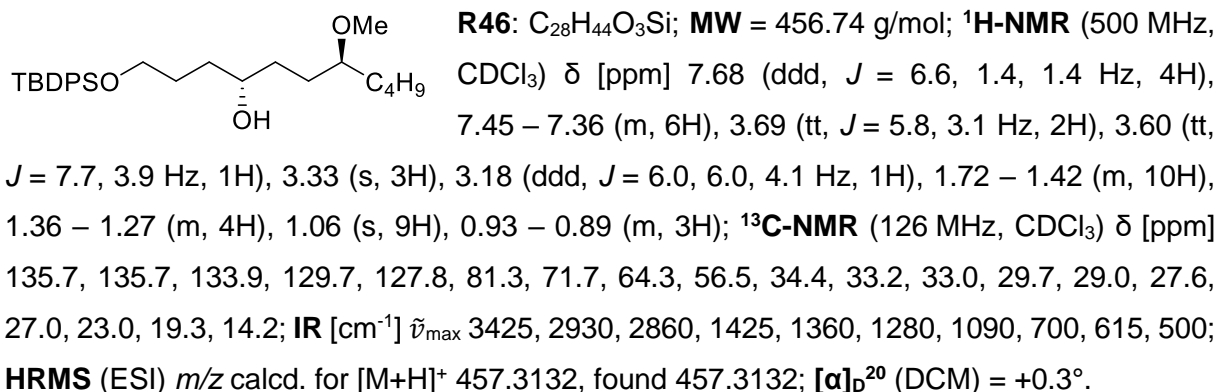
The analytical data is in agreement with the literature.^[136]

5.10.6 Opening of *tert*-butyl(3-((2*R*,3*S*)-3-((*S*)-2-methoxyhexyl)oxiran-2-yl)propoxy)diphenylsilane

5.10.6.1

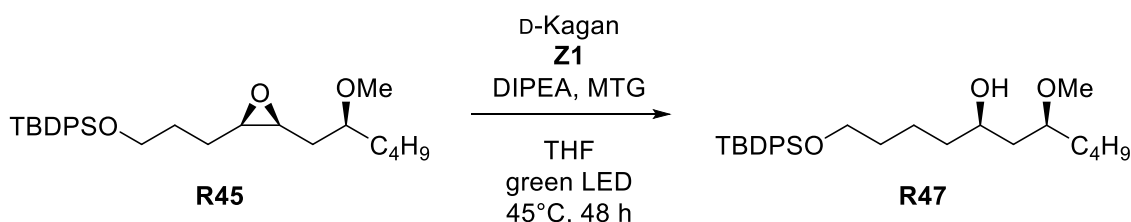


According to **GP12**, L-Kagan (15 mol%, 75 μ mol, 39.4 mg), **R45** (1.0 eq., 0.5 mmol, 227.4 mg, *d.r.* = 96:4), **Z1** (15 mol%, 75 μ mol, 52.2 mg), DIPEA (3.0 eq., 1.5 mmol, 0.26 mL) and MTG (20 mol%, 0.1 mmol, 9 μ L) are reacted in THF (3 mL) under irradiation with green light at 45°C for 48 h. After purification, **R46** is obtained as a colorless oil (177.3 mg, 0.388 mmol, 78%, *d.r.* = 1:99). *r.r.* (1,3:1,4) = 6:94.

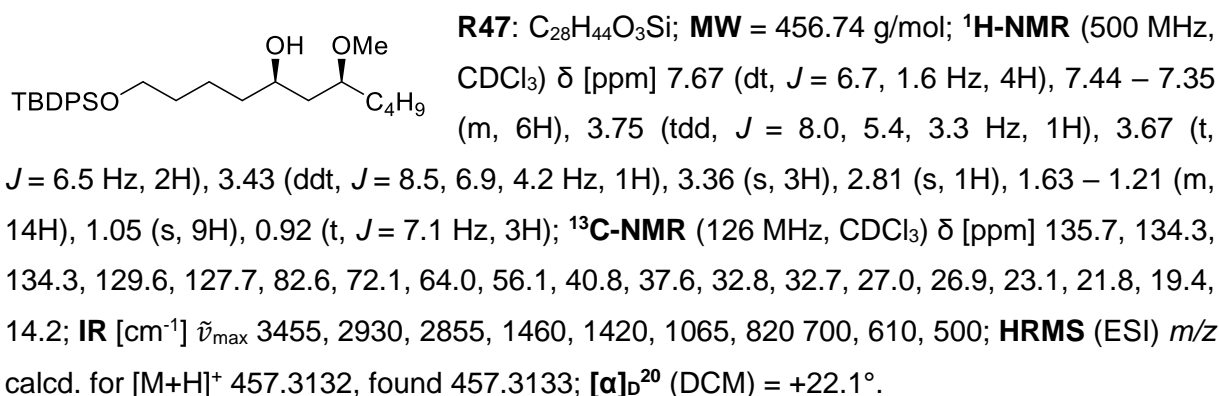


The analytical data is in agreement with the literature.^[136]

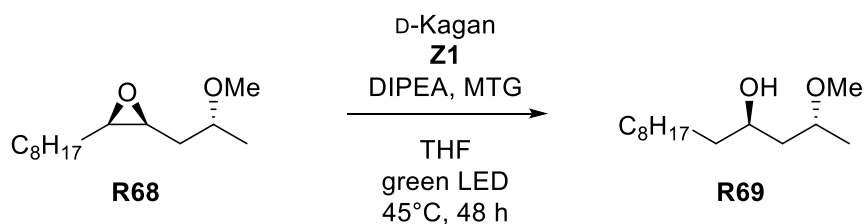
5.10.6.2



According to **GP12**, D-Kagan (15 mol%, 75 μ mol, 39.4 mg), **R45** (1.0 eq., 0.5 mmol, 227.4 mg, *d.r.* = 96:4), **Z1** (15 mol%, 75 μ mol, 52.2 mg), DIPEA (3.0 eq., 1.5 mmol, 0.26 mL) and MTG (20 mol%, 0.1 mmol, 9 μ L) are reacted in THF (3 mL) under irradiation with green light at 45°C for 48 h. After purification, **R47** is obtained as a colorless oil (159.4 mg, 0.349 mmol, 70%, *d.r.* = 99:1). *r.r.* (1,3:1,4) = 94:6.



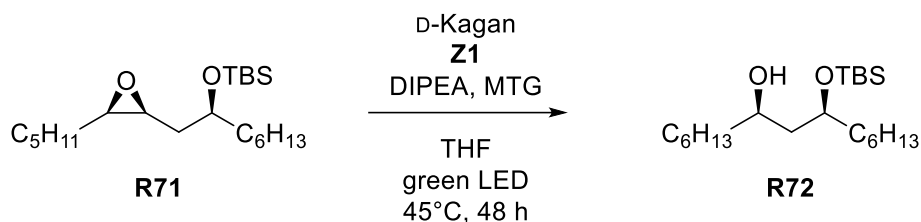
The analytical data is in agreement with the literature.^[136]

5.10.7 Opening of (2*S*,3*R*)-2-((*R*)-2-methoxypropyl)-3-octyloxirane

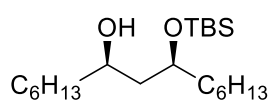
According to **GP12**, D-Kagan (15 mol%, 75 μ mol, 39.4 mg), **R68** (1.0 eq., 0.5 mmol, 114.2 mg, *d.r.* = 99:1), **Z1** (15 mol%, 75 μ mol, 52.2 mg), DIPEA (3.0 eq., 1.5 mmol, 0.26 mL) and MTG (20 mol%, 0.1 mmol, 9 μ L) are reacted in THF (3 mL) under irradiation with green light at 45°C for 48 h. After purification, **R69** is obtained as a colorless oil (82.7 mg, 0.359 mmol, 72%, *d.r.* = 1:99). *r.r.* (1,3:1,4) = 90:10.

R69: C₁₄H₃₀O₂; MW = 230.39 g/mol; ¹H-NMR (500 MHz, CDCl₃) δ [ppm] 3.86 (tdd, *J* = 7.5, 4.7, 2.9 Hz, 1H), 3.69 – 3.62 (m, 1H), 3.33 (s, 3H), 1.66 – 1.55 (m, 2H), 1.51 – 1.21 (m, 17H), 1.19 (d, *J* = 6.2 Hz, 3H), 0.87 (t, *J* = 6.9 Hz, 3H); ¹³C-NMR (126 MHz, CDCl₃) δ [ppm] 75.1, 68.8, 56.3, 42.5, 37.8, 32.0, 29.9, 29.8, 29.7, 29.5, 25.9, 22.8, 18.8, 14.3; IR [cm⁻¹] $\tilde{\nu}_{\max}$ 3425, 2925, 2855, 1465, 1375, 1150, 1125, 1085; HRMS (EI) *m/z* calcd. for [M-H₂O]⁺ 212.2135, found 212.2137; [α]_D²⁰ (DCM) = -18.7°.

The analytical data is in agreement with the literature.^[136]

5.10.8 Opening of *tert*-butyldimethyl(((*S*)-1-((2*S*,3*R*)-3-pentyloxiran-2-yl)octan-2-yl)oxy)silane

According to **GP12**, D-Kagan (15 mol%, 75 μ mol, 39.4 mg), **R71** (1.0 eq., 0.5 mmol, 178.3 mg, *d.r.* = 99:1), **Z1** (15 mol%, 75 μ mol, 52.2 mg), DIPEA (3.0 eq., 1.5 mmol, 0.26 mL) and MTG (20 mol%, 0.1 mmol, 9 μ L) are reacted in THF (3 mL) under irradiation with green light at 45°C for 48 h. After purification, **R72** is obtained as a colorless oil (138.5 mg, 0.386 mmol, 77%, *d.r.* = 99:1). *r.r.* (1,3:1,4) = 94:6.



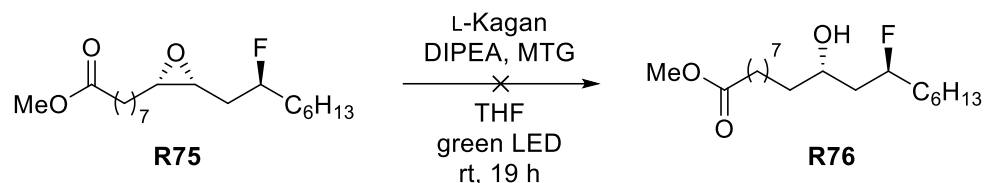
R72: C₂₁H₄₆O₂Si; **MW** = 358.68 g/mol; **¹H-NMR** (500 MHz, CDCl₃) δ [ppm] 3.91 (dtd, *J* = 9.4, 5.7, 4.0 Hz, 1H), 3.72 (dtd, *J* = 9.5, 4.6, 2.1 Hz, 1H), 3.20 (s, 1H), 1.60 (ddd, *J* = 14.3, 4.0, 2.3 Hz, 1H), 1.53 – 1.22 (m, 20H), 0.92 – 0.85 (m, 16H), 0.11 (s, 3H), 0.09 (s, 3H); **¹³C-NMR** (126 MHz, CDCl₃) δ [ppm] 73.8, 71.5, 43.0, 38.4, 38.0, 32.0, 32.0, 29.7, 29.6, 26.0, 25.5, 24.8, 22.8, 22.7, 18.1, 14.2, 14.2, -3.8, -4.5; **IR** [cm⁻¹] $\tilde{\nu}_{\max}$ 3440, 2955, 2930, 2855, 1255, 1070, 1005, 835, 810, 775; **HRMS** (ESI) *m/z* calcd. for [M+Na]⁺ 381.3159, found 381.3156; **[α]_D²⁰** (DCM) = +21.8°.

The analytical data is in agreement with the literature.^[136]

5.11 Regiodivergent Epoxide Openings under other Conditions

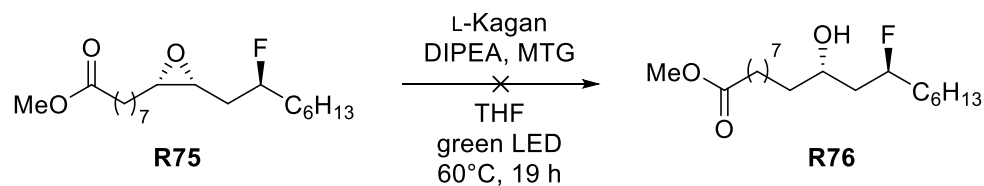
5.11.1 Opening of methyl 8-((2*S*,3*R*)-3-((*S*)-2-fluorooctyl)oxiran-2-yl)octanoate

5.11.1.1

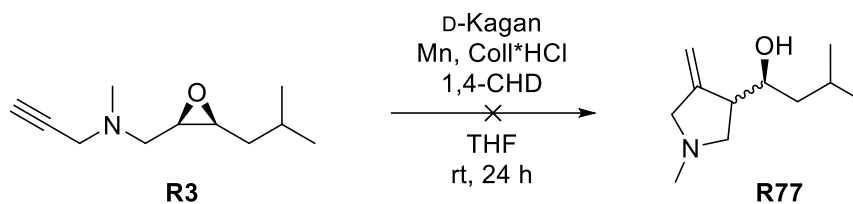


The reaction is performed in a heat-dried *Schlenk* tube under argon atmosphere. L-Kagan (10 mol%, 0.05 mmol, 26.3 mg) is placed in the tube and evacuated for 30 min. After flushing with argon, THF (0.17 M, 3 mL) and epoxide **R75** (1.0 eq., 0.5 mmol, 165.2 mg) are added, followed by DIPEA (3.0 eq., 1.5 mmol, 0.26 mL) and MTG (20 mol%, 0.1 mmol, 9 μ L). The reaction is stirred under irradiation with green light at room temperature for 19 h. After the reaction is finished, 5 mL of phosphate buffer solution and 5 mL of Et₂O are added. The reaction is stirred for 10 min. According to TLC, no conversion is observed.

5.11.1.2



The reaction is performed in a heat-dried *Schlenk* tube under argon atmosphere. L-Kagan (10 mol%, 0.05 mmol, 26.3 mg) is placed in the tube and evacuated for 30 min. After flushing with argon, THF (0.17 M, 3 mL) and epoxide **R75** (1.0 eq., 0.5 mmol, 165.2 mg) are added, followed by DIPEA (3.0 eq., 1.5 mmol, 0.26 mL) and MTG (20 mol%, 0.1 mmol, 9 μ L). The reaction is stirred under irradiation with green light at 60°C for 19 h. After the reaction is finished, 5 mL of phosphate buffer solution and 5 mL of Et₂O are added. The reaction is stirred for 10 min. According to TLC, no conversion is observed.

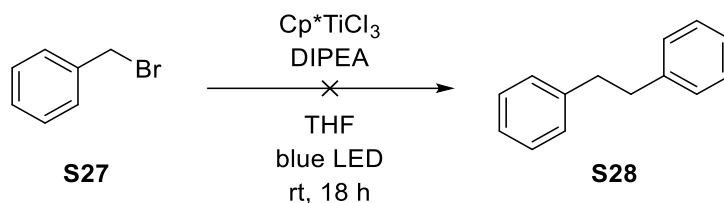
5.11.2 Opening of *N*-(((2*R*,3*S*)-3-isobutyloxiran-2-yl)methyl)-*N*-methylprop-2-yn-1-amine

The reaction is performed according to the literature.^[268] In a heat-dried *Schlenk* tube, Coll*HCl (1.5 eq., 0.9 mmol, 142 mg) is heated slightly under vacuum until sublimation. After cooling to room temperature and flushing with argon, D-Kagan (10 mol%, 0.06 mmol, 31.5 mg), Mn (2.0 eq., 1.2 mmol, 65.9 mg) and THF (0.3 M, 3 mL) are added and the mixture is stirred for 30 min until a color change from red to green occurs. **R3** (1.0 eq., 0.6 mmol, 110 mg) and 1,4-CHD (4.35 eq., 2.61 mmol, 0.25 mL) are added and the reaction is stirred at room temperature for 24 h. It is quenched by the addition of aqueous phosphate buffer (4 mL). According to TLC, no conversion is observed.

5.12 Other Syntheses

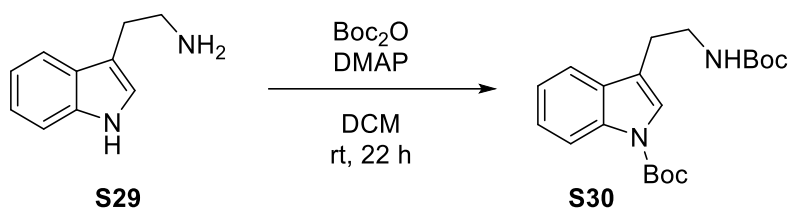
5.12.1 Dehalogenations

5.12.1.1 Debromination of (bromomethyl)benzene

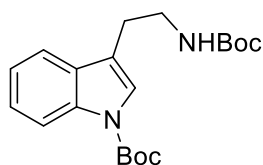


Cp^*TiCl_3 (10 mol%, 0.05 mmol, 14.5 mg) and DIPEA (3.0 eq., 1.50 mmol, 0.26 mL) are placed in a heat-dried *Schlenk* tube under argon and dry THF (5 mL) is added. **S27** (1.0 eq., 0.50 mmol, 0.06 mL) and THF (0.5 M, 5 mL) are added, and the reaction mixture is stirred at room temperature under irradiation with blue LEDs for 18 h. According to TLC, no conversion is observed.

5.12.1.2 Synthesis of tert-butyl 3-(2-((tert-butoxycarbonyl)amino)ethyl)-1H-indole-1-carboxylate



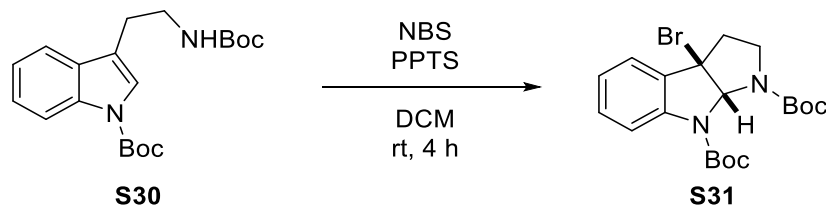
2-(1H-indol-3-yl)ethan-1-amine (**S29**, 1.0 eq., 62.4 mmol, 10.0 g) is placed in a heat-dried *Schlenk* flask under argon and dissolved in dry DCM (0.4 M, 150 mL). The solution is cooled to 0°C, Boc_2O (2.1 eq., 131.1 mmol, 30.1 mL) and DMAP (5 mol%, 3.12 mmol, 381 mg) are added and the reaction is stirred at room temperature for 22 h. After major conversion is observed by TLC, the solvent is removed under reduced pressure and the mixture is diluted with EA and washed with sat. aq. NaHCO_3 solution and brine. The layers are separated and the organic layer is dried over MgSO_4 , and the solvent is removed. The crude product (yellow viscous oil) is purified by flash column chromatography (SiO_2 , CH/EA 7:1). **S30** is obtained as a colorless solid (11.5 mmol, 4.15 g, 18%).



S30: $\text{C}_{20}\text{H}_{28}\text{N}_2\text{O}_4$; **MW** = 360.45 g/mol; **$^1\text{H-NMR}$** (400 MHz, CDCl_3) δ [ppm] 8.13 (s, 1H), 7.54 (dt, $J = 7.7, 1.0$ Hz, 1H), 7.41 (s, 1H), 7.32 (ddd, $J = 8.4, 7.2, 1.4$ Hz, 1H), 7.27 – 7.20 (m, 1H), 4.62 (s, 1H), 3.45 (d, $J = 7.3$ Hz, 2H), 2.93 – 2.83 (m, 2H), 1.67 (s, 9H), 1.44 (s, 9H).

The analytical data is in agreement with the literature.^[341]

5.12.1.3 Synthesis of di-tert-butyl (3aR,8aR)-3a-bromo-2,3,3a,8a-tetrahydropyrrolo[2,3-b]indole-1,8-dicarboxylate



S30 (1.0 eq., 11.5 mmol, 4.15 g) is dissolved in DCM (0.1 M, 120 mL). PPTS (1.0 eq., 11.5 mmol, 2.89 g) and NBS (2.0 eq., 23.0 mmol, 4.10 g) are added and the reaction mixture is stirred at room temperature for 4 h. It is diluted with DCM, washed with brine and H₂O and the layers are separated. The organic phase is dried over MgSO₄, and the solvent is removed under reduced pressure. The crude product is purified by flash column chromatography (SiO₂, CH/EA 20:1) and **S31** is obtained as a colorless solid (1.64 mmol, 811 mg, 14%).

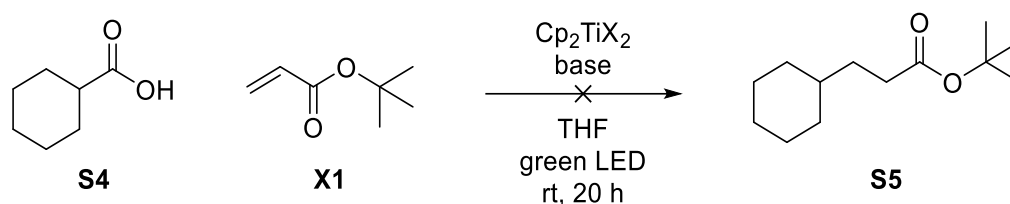


S31: C₂₀H₂₇BrN₂O₄; MW = 439.35 g/mol; ¹H-NMR (400 MHz, CDCl₃) δ [ppm] 7.58 (s, 1H), 7.38 – 7.33 (m, 1H), 7.31 – 7.25 (m, 1H), 7.09 (td, J = 7.5, 1.0 Hz, 1H), 6.44 (s, 1H), 3.78 – 3.66 (m, 1H), 2.85 – 2.68 (m, 3H), 1.58 (s, 9H), 1.49 (s, 9H).

The analytical data is in agreement with the literature.^[342]

5.12.2 Decarboxylations

5.12.2.1 Synthesis of tert-butyl 3-cyclohexylpropanoate

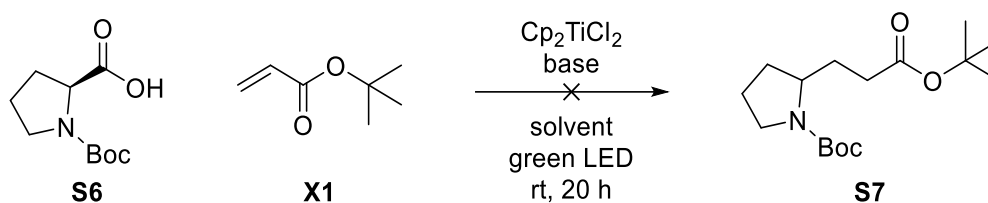


- I) According to **GP13**, Cp₂TiCl₂ (10 mol%, 0.05 mmol, 12.5 mg), cyclohexanecarboxylic acid (**S4**, 1.0 eq., 0.5 mmol, 64.1 mg), DABCO (10 mol%, 0.05 mmol, 5.6 mg) and **X1** (2.0 eq., 1.0 mmol, 0.15 mL) are reacted in dry THF (0.05 M, 10 mL) at room temperature under irradiation with green light for 20 h. The reaction mixture showed a colorless precipitate. According to TLC, no conversion is observed.

- II) According to **GP13**, Cp_2TiBr_2 (10 mol%, 0.05 mmol, 16.9 mg), cyclohexanecarboxylic acid (**S4**, 1.0 eq., 0.5 mmol, 64.1 mg), DABCO (10 mol%, 0.05 mmol, 5.6 mg) and **X1** (2.0 eq., 1.0 mmol, 0.15 mL) are reacted in dry THF (0.05 M, 10 mL) at room temperature under irradiation with green light for 20 h. The reaction mixture showed a colorless precipitate. According to TLC, no conversion is observed.
- III) According to **GP13**, $\text{Cp}_2\text{Ti}(\text{TFA})_2$ (10 mol%, 0.05 mmol, 20.2 mg), cyclohexanecarboxylic acid (**S4**, 1.0 eq., 0.5 mmol, 64.1 mg), DABCO (10 mol%, 0.05 mmol, 5.6 mg) and **X1** (2.0 eq., 1.0 mmol, 0.15 mL) are reacted in dry THF (0.05 M, 10 mL) at room temperature under irradiation with green light for 20 h. According to TLC, no conversion is observed.
- IV) According to **GP13**, $\text{Cp}_2\text{Ti}(\text{OMs})_2$ (10 mol%, 0.05 mmol, 18.4 mg), cyclohexanecarboxylic acid (**S4**, 1.0 eq., 0.5 mmol, 64.1 mg), DABCO (10 mol%, 0.05 mmol, 5.6 mg) and **X1** (2.0 eq., 1.0 mmol, 0.15 mL) are reacted in dry THF (0.05 M, 10 mL) at room temperature under irradiation with green light for 20 h. The reaction mixture showed a colorless precipitate. According to TLC, no conversion is observed.
- V) According to **GP13**, Cp_2TiCl_2 (10 mol%, 0.05 mmol, 12.5 mg), cyclohexanecarboxylic acid (**S4**, 1.0 eq., 0.5 mmol, 64.1 mg), DABCO (1.0 eq., 0.5 mmol, 56.1 mg) and **X1** (2.0 eq., 1.0 mmol, 0.15 mL) are reacted in dry THF (0.05 M, 10 mL) at room temperature under irradiation with green light for 20 h. The reaction mixture showed a colorless precipitate. According to TLC, no conversion is observed.
- VI) According to **GP13**, $\text{Cp}_2\text{Ti}(\text{TFA})_2$ (10 mol%, 0.05 mmol, 20.2 mg), cyclohexanecarboxylic acid (**S4**, 1.0 eq., 0.5 mmol, 64.1 mg), DABCO (1.0 eq., 0.5 mmol, 56.1 mg) and **X1** (2.0 eq., 1.0 mmol, 0.15 mL) are reacted in dry THF (0.05 M, 10 mL) at room temperature under irradiation with green light for 20 h. According to TLC, no conversion is observed.

- VII) According to **GP13**, Cp_2TiCl_2 (10 mol%, 0.05 mmol, 12.5 mg), cyclohexanecarboxylic acid (**S4**, 1.0 eq., 0.5 mmol, 64.1 mg), NEt_3 (0.5 eq., 0.25 mmol, 35 μL) and **X1** (2.0 eq., 1.0 mmol, 0.15 mL) are reacted in dry THF (0.05 M, 10 mL) at room temperature under irradiation with green light for 20 h. According to TLC, no conversion is observed.
- VIII) According to **GP13**, Cp_2TiCl_2 (10 mol%, 0.05 mmol, 12.5 mg), cyclohexanecarboxylic acid (**S4**, 1.0 eq., 0.5 mmol, 64.1 mg), collidine (0.5 eq., 0.25 mmol, 33 μL) and **X1** (2.0 eq., 1.0 mmol, 0.15 mL) are reacted in dry THF (0.05 M, 10 mL) at room temperature under irradiation with green light for 20 h. According to TLC, no conversion is observed.

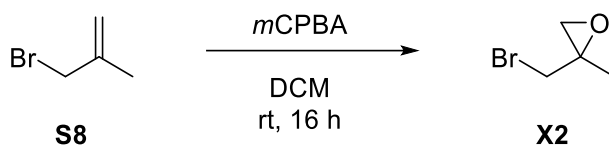
5.12.2.2 Synthesis of *tert*-butyl 2-(3-(*tert*-butoxy)-3-oxopropyl)pyrrolidine-1-carboxylate



- I) According to **GP13**, Cp_2TiCl_2 (10 mol%, 0.05 mmol, 12.5 mg), (*tert*-butoxycarbonyl)-L-proline (**S6**, 1.0 eq., 0.5 mmol, 107.6 mg), NEt_3 (0.5 eq., 0.25 mmol, 35 μL) and **X1** (2.0 eq., 1.0 mmol, 0.15 mL) are reacted in dry THF (0.05 M, 10 mL) at room temperature under irradiation with green light for 20 h. According to TLC, no conversion is observed.
- II) According to **GP13**, Cp_2TiCl_2 (10 mol%, 0.05 mmol, 12.5 mg), (*tert*-butoxycarbonyl)-L-proline (**S6**, 1.0 eq., 0.5 mmol, 107.6 mg), collidine (0.5 eq., 0.25 mmol, 33 μL) and **X1** (2.0 eq., 1.0 mmol, 0.15 mL) are reacted in dry THF (0.05 M, 10 mL) at room temperature under irradiation with green light for 20 h. According to TLC, no conversion is observed.
- III) According to **GP13**, Cp_2TiCl_2 (10 mol%, 0.05 mmol, 12.5 mg), (*tert*-butoxycarbonyl)-L-proline (**S6**, 1.0 eq., 0.5 mmol, 107.6 mg), NEt_3 (0.5 eq., 0.25 mmol, 35 μL) and **X1** (2.0 eq., 1.0 mmol, 0.15 mL) are reacted in dry DMF (0.05 M, 10 mL) at room temperature under irradiation with green light for 20 h. According to TLC, no conversion is observed.

- IV) According to **GP13**, Cp_2TiCl_2 (10 mol%, 0.05 mmol, 12.5 mg), (*tert*-butoxycarbonyl)-L-proline (**S6**, 1.0 eq., 0.5 mmol, 107.6 mg), NEt_3 (0.5 eq., 0.25 mmol, 35 μL) and **X1** (2.0 eq., 1.0 mmol, 0.15 mL) are reacted in dry DMPU (0.05 M, 10 mL) at room temperature under irradiation with green light for 20 h. According to TLC, no conversion is observed.
- V) According to **GP13**, Cp_2TiCl_2 (10 mol%, 0.05 mmol, 12.5 mg), (*tert*-butoxycarbonyl)-L-proline (**S6**, 1.0 eq., 0.5 mmol, 107.6 mg), NEt_3 (0.5 eq., 0.25 mmol, 35 μL) and **X1** (2.0 eq., 1.0 mmol, 0.15 mL) are reacted in dry MeCN (0.05 M, 10 mL) at room temperature under irradiation with green light for 20 h. According to TLC, no conversion is observed.
- VI) According to **GP13**, Cp_2TiCl_2 (10 mol%, 0.05 mmol, 12.5 mg), (*tert*-butoxycarbonyl)-L-proline (**S6**, 1.0 eq., 0.5 mmol, 107.6 mg), NEt_3 (0.5 eq., 0.25 mmol, 35 μL) and **X1** (2.0 eq., 1.0 mmol, 0.15 mL) are reacted in dry DME (0.05 M, 10 mL) at room temperature under irradiation with green light for 20 h. According to TLC, no conversion is observed.

5.12.3 Synthesis of 2-(bromomethyl)-2-methyloxirane

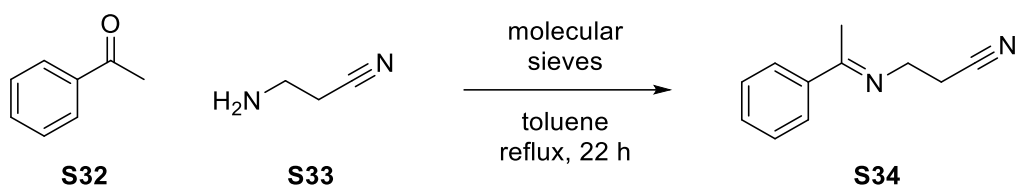


3-Bromo-2-methylprop-1-ene (**S8**, 1.0 eq., 14.8 mmol, 1.49 mL) is dissolved in DCM (0.5 M, 30 mL) and cooled to 0°C, *m*CPBA (77% in water, 1.6 eq., 23.3 mmol, 4.02 g) is slowly added and the reaction is stirred for 16 h at room temperature. The reaction mixture is washed with 10% aq. KOH solution, the phases are separated, and the organic phase is washed with water and 2x with sat. aq. NaHCO_3 solution. The organic layer is dried over MgSO_4 , and the solvent is removed under reduced pressure. **X2** is obtained as a colorless oil (13.6 mmol, 2.06 g, 92%) without further purification.

X2: $\text{C}_4\text{H}_7\text{BrO}$; **MW** = 151.00 g/mol; **$^1\text{H-NMR}$** (500 MHz, CDCl_3) δ [ppm] 3.40 (dd, J = 10.5, 0.8 Hz, 1H), 3.33 (d, J = 10.5 Hz, 1H), 2.83 – 2.79 (m, 2H), 1.50 (s, 3H).

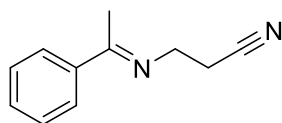
The analytical data is in agreement with the literature.^[343]

5.12.4 Synthesis of 3-((1-phenylethylidene)amino)propanenitrile



5.12.4.1

The synthesis is performed according to the literature.^[344] In a flame-dried *Schlenk* flask with a reflux condenser acetophenone (**S32**, 1.0 eq., 20.0 mmol, 2.33 mL) is dissolved in toluene (1.0 M, 20 mL) under argon atmosphere. 5 Å molecular sieves and **S33** (1.2 eq., 24.0 mmol, 1.75 mL) are added subsequently and the reaction mixture is heated to 110°C and stirred for 22 h. After cooling to room temperature, it is diluted with toluene, the molecular sieves are removed, and they are rinsed with DCM. The solvent is evaporated, and remaining **S33** is removed under reduced pressure (< 6 mbar) at 60°C. The crude product is obtained as a pale-yellow oil. As the product is hygroscopic, the reaction conversion is determined by ¹H-NMR analysis to be 60% (**S34**:**S32** = 3:2).

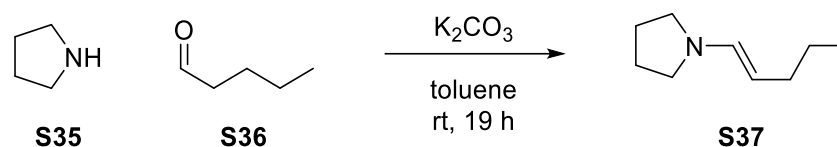


S34: C₁₁H₁₂N₂; MW = 172.23 g/mol; ¹H-NMR (400 MHz, CDCl₃) δ [ppm] 7.99 – 7.94 (m, 1H), 7.81 (dt, *J* = 6.0, 2.4 Hz, 2H), 7.60 – 7.54 (m, 1H), 7.50 – 7.44 (m, 1H), 3.71 (t, *J* = 6.9 Hz, 2H), 2.83 (t, *J* = 6.9 Hz, 2H), 2.32 – 2.26 (m, 3H).

The analytical data is in agreement with the literature.^[345]

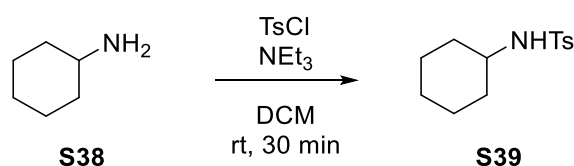
5.12.4.2

The synthesis is performed according to the literature.^[344] In a flame-dried *Schlenk* flask with a reflux condenser acetophenone (**S32**, 1.0 eq., 20.0 mmol, 2.33 mL) is dissolved in toluene (1.0 M, 20 mL) under argon atmosphere. 4 Å molecular sieves and **S33** (1.2 eq., 24.0 mmol, 1.75 mL) are added subsequently and the reaction mixture is heated to 110°C and stirred for 22 h. After cooling to room temperature, it is diluted with toluene, the molecular sieves are removed, and they are rinsed with DCM. The solvent is evaporated, and remaining **S33** is removed under reduced pressure (< 6 mbar) at 60°C. The crude product is obtained as a pale-yellow oil. As the product is hygroscopic, the reaction conversion is determined by ¹H-NMR analysis to be 60% (**S34**:**S32** = 3:2).

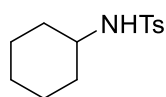
5.12.5 Synthesis of (*E*)-1-(pent-1-en-1-yl)pyrrolidine

The synthesis is performed according to the literature.^[346] In a heat-dried *Schlenk* flask potassium carbonate (2.05 eq., 28.7 mmol, 3.97 g) is suspended in dry toluene (0.7 M, 10 mL) under argon atmosphere. Pyrrolidine (**S35**, 1.0 eq., 14.0 mmol, 1.15 mL) is added and the solution is cooled to 0°C. Pentanal (**S36**, 2.0 eq., 28.0 mmol, 2.98 mL) is added and the reaction is stirred at room temperature for 19 h. The suspension is filtered and from the combined filtrate the remaining aldehyde as well as the solvent are removed under reduced pressure. The crude product is purified by distillation (1 mbar, 45°C). The product (*E*)-1-(pent-1-en-1-yl)pyrrolidine (**S37**, 7.47 mmol, 1.04 g, 53%) is obtained as hygroscopic colorless oil and stored under argon atmosphere at -18°C.

S37: C₉H₁₇N; MW = 139.24 g/mol; ¹H-NMR (500 MHz, C₆D₆) δ [ppm] 6.17 (dt, *J* = 13.6, 1.1 Hz, 1H), 4.25 (dt, *J* = 13.9, 7.1 Hz, 1H), 2.84 – 2.76 (m, 4H), 2.13 (qd, *J* = 7.1, 1.1 Hz, 2H), 1.53 – 1.46 (m, 6H), 1.00 (t, *J* = 7.4 Hz, 3H); ¹³C-NMR (126 MHz, C₆D₆) δ [ppm] 136.4, 98.4, 49.2, 33.5, 25.5, 25.1, 13.9; IR [cm⁻¹] $\tilde{\nu}_{\text{max}}$ 2955, 2925, 2870, 2830, 1655, 1360, 930; HRMS (ESI) *m/z* calcd. for [M+H]⁺ 140.1434, found 140.1436.

5.12.6 Synthesis of *N*-cyclohexyl-4-methylbenzenesulfonamide

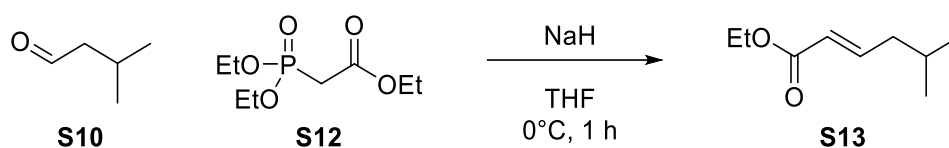
The synthesis is performed according to the literature.^[347] Cyclohexanamine (**S38**, 1.0 eq., 20.0 mmol, 2.29 mL) is dissolved in DCM (0.3 M, 65 mL) and TsCl (1.1 eq., 22.0 mmol, 4.19 g) and NEt₃ (2.5 eq., 50.0 mmol, 6.97 mL) are successively added. The reaction mixture is stirred at room temperature for 30 min. It is then diluted with aq. HCl (10 wt%, 10 mL) and the phases are separated. The aqueous layer is extracted with DCM (3x) and with EA. The combined organic layers are washed with brine, dried over MgSO₄ and the solvent is removed under reduced pressure. The crude product is purified by flash column chromatography (SiO₂, CH/EA 4:1). **S39** is obtained as a colorless solid (19.8 mmol, 5.02 g, 99%).



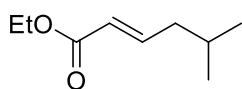
S39: C₁₃H₁₉NO₂S; **MW** = 253.36 g/mol; **¹H-NMR** (500 MHz, CDCl₃) δ [ppm] 7.76 (d, *J* = 8.2 Hz, 2H), 7.28 (dd, *J* = 8.1, 0.9 Hz, 2H), 4.72 (s, 1H), 3.11 (ddd, *J* = 10.7, 8.3, 5.3 Hz, 1H), 2.41 (s, 3H), 1.73 (dtd, *J* = 11.9, 4.5, 2.5 Hz, 2H), 1.61 (dt, *J* = 13.4, 3.9 Hz, 2H), 1.54 – 1.44 (m, 1H), 1.28 – 1.05 (m, 5H); **¹³C-NMR** (126 MHz, CDCl₃) δ [ppm] 143.2, 138.6, 129.7, 127.0, 52.7, 46.0, 34.0, 25.3, 24.8, 21.6, 8.8.

The analytical data is in agreement with the literature.^[348]

5.12.7 Synthesis of ethyl (*E*)-5-methylhex-2-enoate



In a heat-dried *Schlenk* flask, **S12** (1.15 eq., 115.0 mmol, 22.8 mL) is dissolved in dry THF (0.4 M, 250 mL) under argon atmosphere and the solution is cooled to 0°C. NaH (60% dispersion in mineral oil, 1.15 eq., 115.0 mmol, 4.60 g) is added portion wise, then the aldehyde **S10** (1.00 eq., 100.0 mmol, 10.8 mL) is added and the mixture is stirred at 0°C for 1 h. The reaction is quenched by the addition of sat. aq. NH₄Cl solution and the layers are separated. The aqueous layer is extracted with Et₂O (3x) and the combined organic phases are washed with water and brine. The solvent is removed under reduced pressure (>50 mbar) and the crude product is purified by flash column chromatography (SiO₂, CH/EA 5:1). **S13** (97.4 mmol, 15.22 g, 97%) is obtained as a colorless oil.



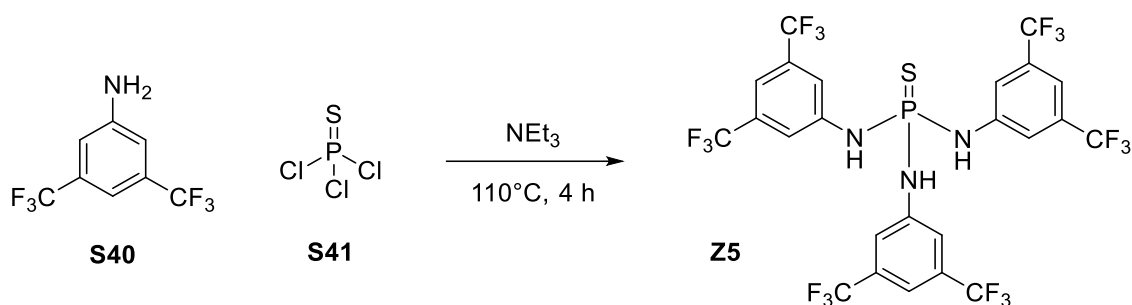
S13: C₉H₁₆O₂; **MW** = 156.23 g/mol; **¹H-NMR** (400 MHz, CDCl₃) δ [ppm] 6.94 (dt, *J* = 15.3, 7.5 Hz, 1H), 5.80 (dt, *J* = 15.7, 1.4 Hz, 1H), 4.18 (q, *J* = 7.2 Hz, 2H), 2.11 – 2.05 (m, 2H), 1.75 (dq, *J* = 13.4, 6.7 Hz, 1H), 1.28 (t, *J* = 7.1 Hz, 3H), 0.92 (d, *J* = 6.6 Hz, 6H).

The analytical data is in agreement with the literature.^[349]

S16: C₆H₁₂O; **MW** = 100.16 g/mol; **¹H-NMR** (400 MHz, CDCl₃) δ [ppm] 5.70 – 5.53 (m, 2H), 4.10 – 4.05 (m, 2H), 2.30 (pdd, *J* = 6.8, 5.9, 1.0 Hz, 1H), 2.03 (s, 1H), 0.99 (d, *J* = 6.8 Hz, 6H).

The analytical data is in agreement with the literature.^[102]

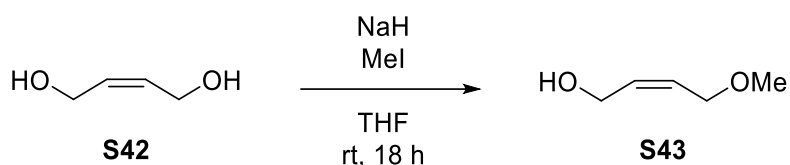
5.12.10 Synthesis of tris-*N,N',N''*-(3,5-di(trifluoromethyl)phenyl)thiophosphoric triamide



The reaction is performed in heat-dried glassware under argon atmosphere. The aniline **S40** (3.3 eq., 33.0 mmol, 5.11 mL) is dissolved in NEt₃ (30.0 eq., 300.0 mmol, 41.8 mL) and the solution is cooled to 0°C. SPCl₃ (1.0 eq., 10.0 mmol, 1.02 mL) is added dropwise and the reaction mixture is heated to 110°C and stirred for 4 h. It is cooled to room temperature and quenched by the addition of sat. aq. NH₄Cl solution. The layers are separated, and the aqueous layer is extracted with DCM (3x). The combined organic layers are washed with brine and dried over MgSO₄, the solvent is removed under reduced pressure. The crude product is purified by flash column chromatography (SiO₂, CH/EA 9:1) and subsequent recrystallization from heptane. **Z5** is obtained as a colorless solid (1.89 mmol, 1.41 g, 19%).

Z5: C₂₄H₁₂F₁₈N₃PS; **MW** = 747.39 g/mol; **¹H-NMR** (500 MHz, DMSO-*d*₆) δ [ppm] 9.46 (d, *J* = 8.9 Hz, 3H), 7.76 (d, *J* = 1.7 Hz, 6H), 7.58 (s, 3H); **¹³C-NMR** (176 MHz, DMSO-*d*₆) δ [ppm] 142.7, 130.9 (q, *J* = 32.7 Hz), 123.2 (q, *J* = 272.7 Hz), 118.5 (q, *J* = 7.7 Hz), 114.2; **¹⁹F-NMR** (470 MHz, DMSO-*d*₆) δ [ppm] -61.85; **³¹P-NMR** (202 MHz, DMSO-*d*₆) δ [ppm] 39.44.

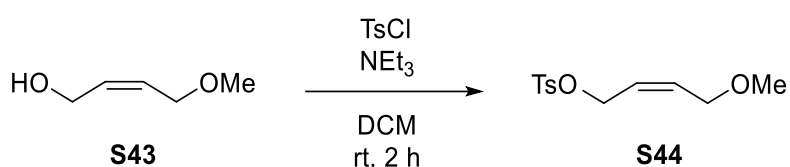
The analytical data is in agreement with the literature.^[350]

5.12.11 Synthesis of (*Z*)-4-methoxybut-2-en-1-ol

The reaction is performed in heat-dried glassware under argon atmosphere. The diol **S42** (1.0 eq., 100.0 mmol, 8.22 mL) is dissolved in THF (0.5 M, 200 mL) and the solution is cooled to 0°C. NaH (60% dispersion in mineral oil, 1.0 eq., 100.0 mmol, 4.00 g) is added and the mixture is warmed up to room temperature. MeI (1.0 eq., 100.0 mmol, 6.23 mL) is added and the reaction is stirred overnight at room temperature. It is quenched by the addition of sat. aq. Na₂S₂O₃ solution, the layers are separated, and the aqueous layer is extracted with Et₂O. The combined organic phases are dried over MgSO₄, and the solvent is evaporated. The crude product is purified by flash column chromatography (SiO₂, CH/EA 1:1). **S43** is obtained as a colorless oil (56.4 mmol, 5.76 g, 56%).

S43: C₅H₁₀O₂; **MW** = 102.13 g/mol; **¹H-NMR** (400 MHz, CDCl₃) δ [ppm] 5.85 – 5.77 (m, 1H), 5.68 (dtt, *J* = 11.3, 6.3, 1.3 Hz, 1H), 4.22 – 4.17 (m, 2H), 4.00 (ddd, *J* = 6.4, 1.5, 0.8 Hz, 2H), 3.34 (d, *J* = 0.9 Hz, 3H), 2.17 (s, 1H).

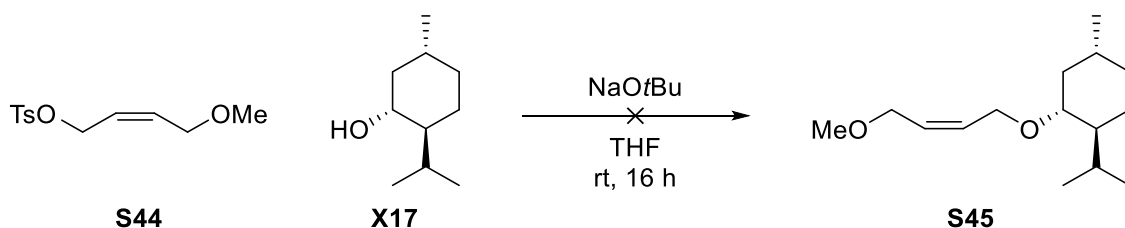
The analytical data is in agreement with the literature.^[351]

5.12.12 Synthesis of (*Z*)-4-methoxybut-2-en-1-yl 4-methylbenzenesulfonate

The alcohol **S43** (1.0 eq., 56.4 mmol, 5.76 g) is dissolved in DCM (0.3 M, 180 mL). NEt₃ (2.5 eq., 141.0 mmol, 19.6 mL) and TsCl (1.1 eq., 62.0 mmol, 11.83 g) are subsequently added and the reaction mixture is stirred for 2 h at room temperature. It is diluted with aq. HCl solution (10 wt%, 30 mL). The phases are separated, and the aqueous phase is extracted with DCM (3x). The combined organic layers are washed with brine and dried over MgSO₄. The solvent is evaporated, and the crude product is purified by flash column chromatography (SiO₂, CH/EA 1:1). **S44** is obtained as a colorless solid (18.08 mmol, 4.64 g, 32%).

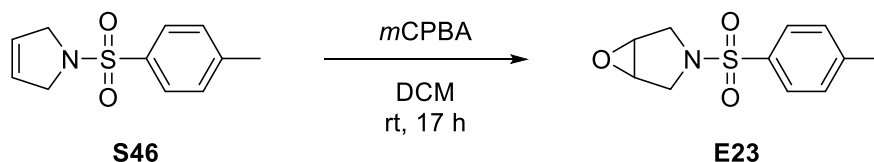

S44: C₁₂H₁₆O₄S; MW = 256.32 g/mol; ¹H-NMR (500 MHz, C₆D₆) δ [ppm] 7.96 – 7.88 (m, 2H), 7.45 – 7.38 (m, 2H), 5.86 – 5.69 (m, 2H), 4.15 – 4.09 (m, 2H), 4.08 – 4.00 (m, 2H), 3.35 (s, 3H), 2.49 (s, 3H); ¹³C-NMR (126 MHz, C₆D₆) δ [ppm] 146.9, 141.9, 130.9, 130.4, 128.5, 127.2, 67.8, 58.4, 39.3, 22.0; IR [cm⁻¹] $\tilde{\nu}_{\max}$ 1595, 1375, 1170, 1080, 810, 650, 565, 525; HRMS (ESI) *m/z* calcd. for [M+H]⁺ 257.0842, found 257.0840.

5.12.13 Synthesis of (1*S*,2*R*,4*R*)-1-isopropyl-2-(((*Z*)-4-methoxybut-2-en-1-yl)oxy)-4-methylcyclohexane

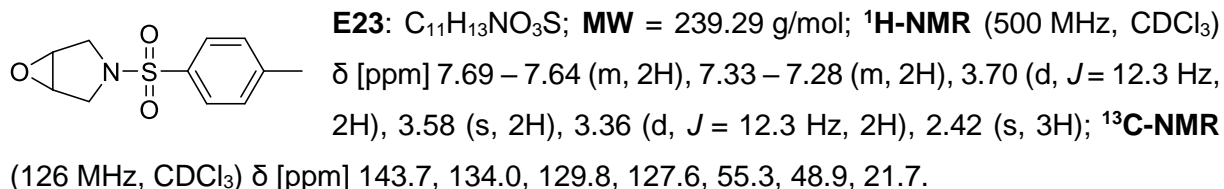


L-menthol (**X17**, 1.2 eq., 18.0 mmol, 2.81 g) is dissolved in THF (0.5 M, 30 mL). NaOtBu (1.2 eq., 18.0 mmol, 1.73 g) is added and the mixture is stirred for 30 min and cooled to 0°C. **S44** (1.0 eq., 15.0 mmol, 3.84 g) is slowly added (caution, heat evolution) and the reaction is stirred at room temperature for 16 h. It is quenched by the addition of sat. aq. NH₄Cl solution, the layers are separated, and the aqueous layer is extracted with EA. The combined organic phases are washed with brine, dried over MgSO₄, and the solvent is evaporated. According to the crude ¹H-NMR data, no desired **S45** is obtained.

5.12.14 Synthesis of 3-tosyl-6-oxa-3-azabicyclo[3.1.0]hexane

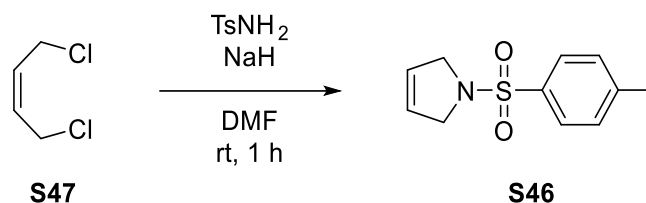


The reaction is performed under ambient conditions. To a solution of *m*CPBA (70% in water, 1.5 eq., 135.0 mmol, 33.3 g) in DCM (0.3 M, 250 mL) **S46** (1.0 eq., 90.0 mmol, 20.1 g) is added portionwise. The reaction is stirred at room temperature for 17 h. The majority of the solvent is evaporated and the precipitate is filtered off. The solution is washed with sat. aq. NaHCO₃ solution (3x) and the layers are separated. The organic layer is dried over MgSO₄ and the solvent is removed under reduced pressure. The crude product is recrystallized from EA. **E23** (40.7 mmol, 9.74 g, 45%) is obtained as a colorless solid.

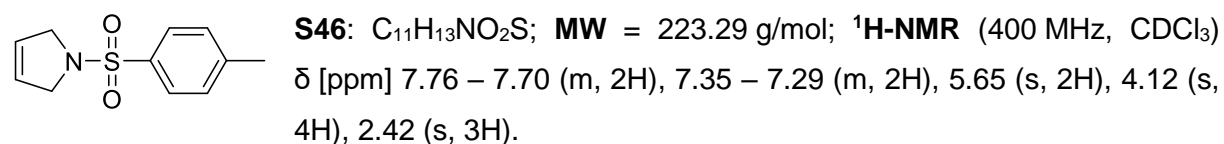


The analytical data is in agreement with the literature.^[352]

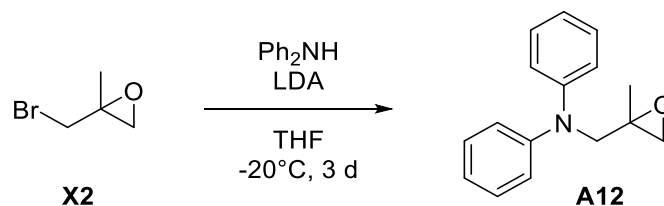
5.12.15 Synthesis of 1-tosyl-2,5-dihydro-1*H*-pyrrole



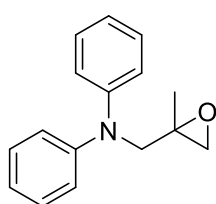
The reaction is performed in a heat-dried *Schlenk* flask under argon atmosphere. The alkene **S47** (1.1 eq., 101.2 mmol, 10.6 mL) and TsNH₂ (1.0 eq., 92.0 mmol, 15.75 g) are dissolved in DMF (0.5 M, 200 mL). At room temperature, NaH (60% dispersion in mineral oil, 2.0 eq., 184.0 mmol, 7.36 g) is added portionwise and the reaction mixture is stirred at room temperature for 1 h. It is poured into water (400 mL) and the mixture is stirred for 30 min. The precipitated solid is collected and washed with water and pentane and dried *in vacuo*. The product is obtained without further purification as light brown solid (90.4 mmol, 20.18 g, 98%).



The analytical data is in agreement with the literature.^[352,353]

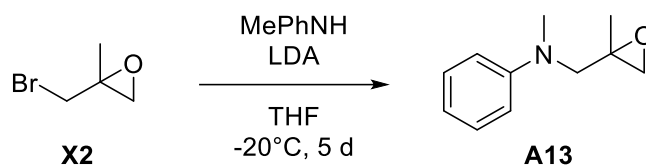
5.12.16 Synthesis of *N*-((2-methyloxiran-2-yl)methyl)-*N*-phenylaniline

The synthesis is performed according to the literature^[343] in heat-dried glassware under argon atmosphere. Diisopropyl amine (1.6 eq., 32.0 mmol, 4.52 mL) is dissolved in dry THF (0.4 M, 50 mL) and the solution is cooled to 0°C, then *n*BuLi (2.5 M solution in hexane, 1.6 eq., 32.0 mmol, 12.80 mL) is slowly added. The mixture is stirred for 1 h, cooled to -20°C and Ph₂NH (1.0 eq., 20.0 mmol, 3.38 g) is added. The mixture is stirred for 30 min, epoxide **X2** (1.2 eq., 24.0 mmol, 3.62 g) is added and the reaction is stirred for 3 d while warming to room temperature. It is quenched by the addition of sat. aq. NH₄Cl solution, the layers are separated, and the aqueous layer is extracted with EA (3x). The combined organic phases are washed with brine and dried over MgSO₄. The solvent is removed under reduced pressure. The crude product is purified by flash column chromatography (SiO₂, CH/EA 30:1). **A12** is obtained as a colorless solid (13.06 mmol, 3.13 g, 65%).

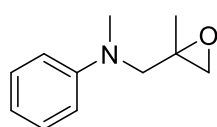


A12: C₁₆H₁₇NO; **MW** = 239.32 g/mol; **¹H-NMR** (500 MHz, CDCl₃) δ [ppm] 7.27 – 7.22 (m, 4H), 7.03 – 6.99 (m, 4H), 6.94 (tt, *J* = 7.4, 1.1 Hz, 2H), 3.90 (d, *J* = 1.2 Hz, 2H), 2.68 (dd, *J* = 4.7, 0.9 Hz, 1H), 2.56 (d, *J* = 4.8 Hz, 1H), 1.38 (d, *J* = 0.7 Hz, 3H); **¹³C-NMR** (126 MHz, CDCl₃) δ [ppm] 148.6, 129.4, 121.7, 121.1, 56.9, 56.7, 52.6, 19.9.

The analytical data is in agreement with the literature.^[139]

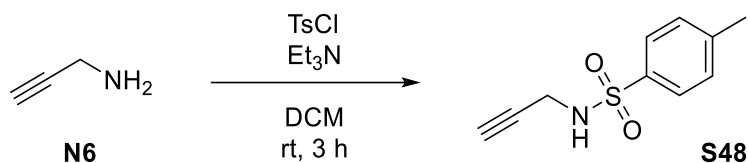
5.12.17 Synthesis of *N*-methyl-*N*-((2-methyloxiran-2-yl)methyl)aniline

The synthesis is performed according to the literature^[343] in heat-dried glassware under argon atmosphere. Diisopropyl amine (1.6 eq., 16.57 mmol, 2.34 mL) is dissolved in dry THF (0.4 M, 25 mL) and the solution is cooled to 0°C, then *n*BuLi (2.5 M solution in hexane, 1.6 eq., 16.57 mmol, 6.63 mL) is slowly added. The mixture is stirred for 1 h, cooled to -20°C and MePhNH (1.0 eq., 10.36 mmol, 1.12 mL) is added. The mixture is stirred for 30 min, epoxide **X2** (1.2 eq., 12.43 mmol, 1.88 g) is added and the reaction is stirred for 5 d while warming to room temperature. It is quenched by the addition of sat. aq. NH₄Cl solution, the layers are separated, and the aqueous layer is extracted with EA (3x). The combined organic phases are washed with brine and dried over MgSO₄, the solvent is removed under reduced pressure. The crude product is purified by flash column chromatography (SiO₂, CH/EA 30:1). **A13** is obtained as a pale-yellow oil (4.96 mmol, 878 mg, 48%).

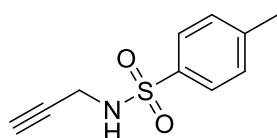


A13: C₁₁H₁₅NO; MW = 177.25 g/mol; ¹H-NMR (500 MHz, CDCl₃) δ [ppm] 7.28 – 7.22 (m, 2H), 6.75 – 6.71 (m, 3H), 3.55 (d, *J* = 15.7 Hz, 1H), 3.41 (d, *J* = 15.7 Hz, 1H), 2.98 (s, 3H), 2.67 (d, *J* = 4.9 Hz, 1H), 2.62 (d, *J* = 4.8 Hz, 1H), 1.37 (d, *J* = 0.7 Hz, 3H); ¹³C-NMR (126 MHz, CDCl₃) δ [ppm] 149.9, 129.3, 116.8, 112.3, 57.2, 56.8, 51.9, 39.2, 19.5.

The analytical data is in agreement with the literature.^[354]

5.12.18 Synthesis of 4-methyl-*N*-(prop-2-yn-1-yl)benzenesulfonamide

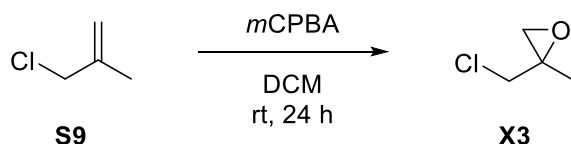
Prop-2-yn-1-amine (**N6**, 1.0 eq., 20.0 mmol, 1.30 mL) is dissolved in DCM (0.3 M, 60 mL) and TsCl (1.1 eq., 22.0 mmol, 4.19 g) and NEt₃ (1.5 eq., 30.0 mmol, 4.18 mL) are successively added. The reaction mixture is stirred at room temperature for 3 h. It is then diluted with water (60 mL) and the phases are separated. The aqueous layer is extracted with DCM (3x) and with EA. The combined organic layers are washed with brine, dried over MgSO₄ and the solvent is removed under reduced pressure. The crude product is purified by flash column chromatography (SiO₂, CH/Ea 3:1). **S48** is obtained as a colorless solid (19.9 mmol, 4.16 g, 99%).



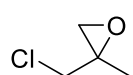
S48: C₁₀H₁₁NO₂S; MW = 209.26 g/mol; ¹H-NMR (400 MHz, CDCl₃) δ [ppm] 7.80 – 7.75 (m, 2H), 7.34 – 7.29 (m, 2H), 4.70 (s, 1H), 3.85 – 3.80 (m, 2H), 2.43 (s, 3H), 2.10 (t, *J* = 2.5 Hz, 1H).

The analytical data is in agreement with the literature.^[355]

5.12.19 Synthesis of 2-(chloromethyl)-2-methyloxirane



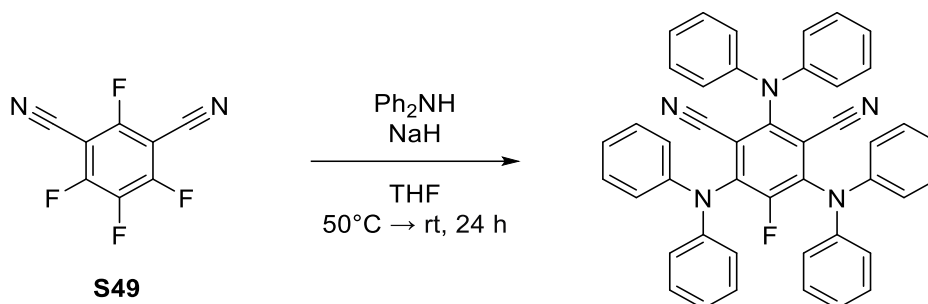
3-Chloro-2-methylprop-1-ene (**S9**, 1.0 eq., 20.0 mmol, 1.95 mL) is dissolved in DCM (0.5 M, 40 mL) and cooled to 0°C, *m*CPBA (70% in water, 1.1 eq., 22.0 mmol, 5.42 g) is slowly added and the reaction is stirred for 24 h at room temperature. The reaction mixture is washed with 10% aq. KOH solution, the phases are separated, and the organic phase is washed with water and 2x with sat. aq. NaHCO₃ solution. The organic layer is dried over MgSO₄ and the solvent is removed under reduced pressure. **X3** is obtained as a colorless oil (14.5 mmol, 2.39 g, 73%) without further purification.



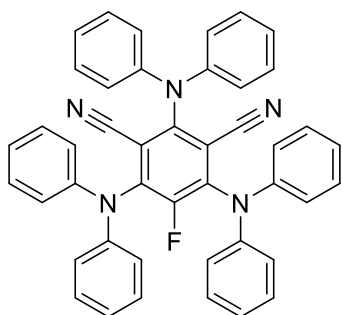
X3: C₄H₇ClO; MW = 106.55 g/mol; ¹H-NMR (400 MHz, CDCl₃) δ [ppm] 3.57 – 3.46 (m, 2H), 2.83 – 2.72 (m, 2H), 1.47 (s, 3H).

The analytical data is in agreement with the literature.^[356]

5.12.20 Synthesis of 2,4,6-tris(diphenylamino)-5-fluoroisophthalonitrile (3DPAFIPN)



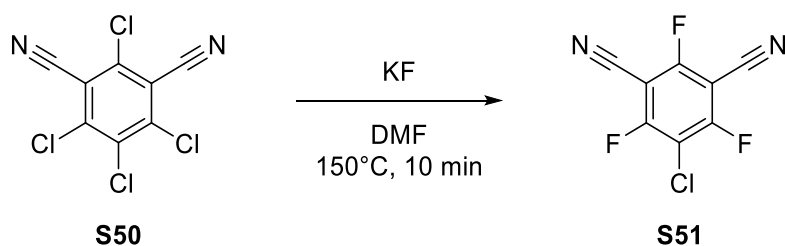
The synthesis is performed according to the literature.^[298] In a heat-dried *Schlenk* flask under argon atmosphere, Ph_2NH (5.0 eq., 10.0 mmol, 1.69 g) is dissolved in dry THF (0.1 M, 20 mL). NaH (60% dispersion in mineral oil, 7.5 eq., 15.0 mmol, 600 mg) is slowly added at room temperature, then the mixture is heated to 50°C (gas evolution). After stirring for 30 min, it is cooled to room temperature and **S49** (1.0 eq., 2.0 mmol, 400 mg) is added. The reaction is stirred at room temperature for 24 h. It is quenched by the addition of water, the yellow precipitate is filtered off and washed with water and EtOH. The crude product is dried *in vacuo*, then recrystallized from hexane/DCM. 3DPAFIPN is obtained as bright yellow solid (1.85 mmol, 1.20 g, 93%).



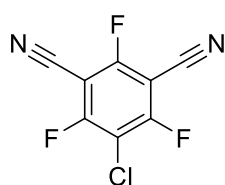
3DPAFIPN: $\text{C}_{44}\text{H}_{30}\text{FN}_5$; **MW** = 647.76 g/mol; **$^1\text{H-NMR}$** (400 MHz, CDCl_3) δ [ppm] 7.29 – 7.22 (m, 12H), 7.09 – 7.03 (m, 6H), 7.02 – 6.96 (m, 12H); **$^{13}\text{C-NMR}$** (101 MHz, CDCl_3) δ [ppm] 145.7, 145.4, 143.2 (d, $J = 11.1$ Hz), 129.6, 129.5, 124.7, 124.2, 122.9, 122.9, 112.8 (d, $J = 3.4$ Hz), 109.1 (d, $J = 3.3$ Hz).

The analytical data is in agreement with the literature.^[298,357]

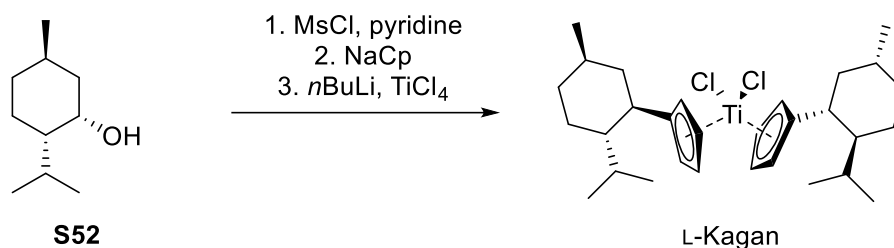
5.12.21 Synthesis of 5-chloro-2,4,6-trifluoroisophthalonitrile



The synthesis is performed according to the literature.^[358] In a heat-dried *Schlenk* flask under argon atmosphere, **S50** (1.0 eq., 25.0 mmol, 6.65 g) and KF (4.0 eq., 100.0 mmol, 5.81 g) are dissolved in dry DMF (0.3 M, 75 mL). The reaction mixture is heated to 150°C and stirred for 10 min. After cooling to room temperature, the reaction is quenched by the addition of water (300 mL). The grey precipitate is collected and washed with water (3x), then dried *in vacuo*. **S51** is obtained as a colorless crystalline solid (15.4 mmol, 3.33 g, 62%).



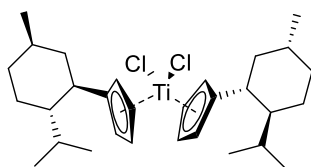
S51: C₈ClF₃N₂; **MW** = 216.55 g/mol; **¹⁹F-NMR** (470 MHz, CDCl₃) δ [ppm] -91.0 (d, *J* = 1.8 Hz), -95.8 (t, *J* = 1.8 Hz); **¹³C-NMR** (126 MHz, CDCl₃) δ [ppm] 162.5 (dt, *J* = 272.8, 6.2 Hz), 162.4 (dt, *J* = 274.8, 6.3 Hz), 110.2 (d, *J* = 5.3 Hz), 105.9 (d, *J* = 1.6 Hz), 92.5 – 92.2 (m); **HRMS** (EI) *m/z* calcd. for [M]⁺ 215.9697, found 215.9700.

5.12.22 Synthesis of the L-Kagan Complex (Bis(η^5 -L-menthyl-cyclopentadienyl)-titan(IV) dichloride)

The reaction is performed according to the literature.^[84,217] A solution of D-neomenthol (**S52**, 1.0 eq., 28.8 mmol, 5.0 mL) in dry pyridine (5 mL) is added to a solution of MsCl (1.4 eq., 40.3 mmol, 3.12 mL) in dry pyridine (22 mL) at -10°C under argon atmosphere. The reaction mixture is stirred at -10°C for 30 min and at 0°C for 5 h. The reaction is quenched by the addition of a mixture of aq. HCl (7 M, 12 mL) and ice (50 mL). The phases are separated, and the aqueous layer is extracted with Et₂O. The combined organic layers are dried over MgSO₄, and the solvent is removed under reduced pressure. The crude product is used without further purification.

NaH (60% dispersion in mineral oil, 2.3 eq., 66.2 mmol, 2.65 g) is dissolved in dry THF (45 mL) and freshly cracked cyclopentadiene (CpH, 1.8 eq., 51.8 mmol, 4.35 mL) is added dropwise to the solution at 0°C. The reaction mixture is stirred at 0°C for 1 h and then a solution of the mesylated neomenthol in dry THF (12 mL) is added at 0°C. The reaction is stirred at room temperature for 23 h and quenched by the addition of water. The phases are separated, and the aqueous layer is extracted with pentane. The combined organic layers are washed with brine, dried over MgSO₄ and the solvent is evaporated. The crude product is used without further purification.

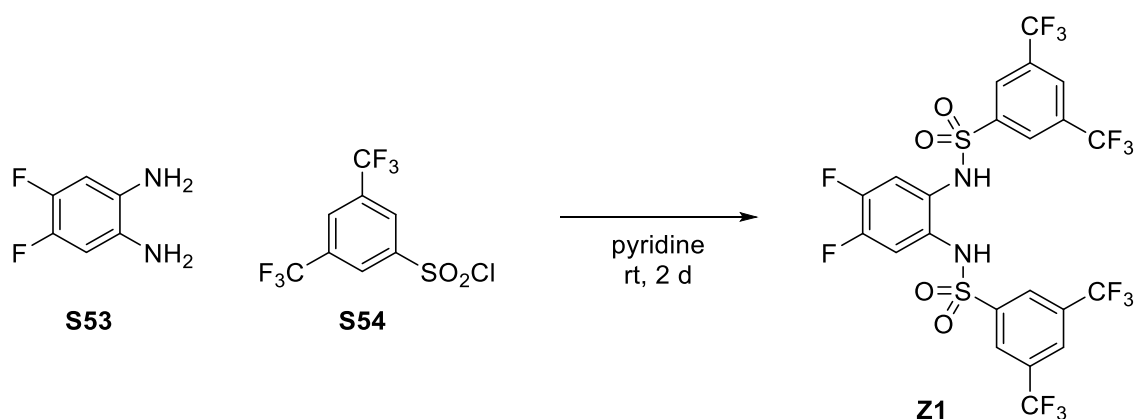
It is dissolved in dry THF (25 mL) and *n*BuLi (2.5 M solution in hexane, 1.05 eq., 30.2 mmol, 12.1 mL) is added dropwise at 0°C. This solution is added to a solution of TiCl₄ (0.5 eq., 14.4 mmol, 1.58 mL) in dry Et₂O (62 mL) at 0°C. The reaction mixture is stirred at room temperature for 20 h. The solvent is removed under reduced pressure and the residue is diluted with MTBE. After filtration over a plug of *Celite*[®], the residue is washed with MTBE until the filtrate becomes colorless. The residue is dissolved in DCM, the solvent is evaporated. The crude product is recrystallized from CHCl₃, dissolved in DCM, then washed with aq. HCl (1 M). After drying over MgSO₄, the L-Kagan complex is obtained as orange solid (6.01 mmol, 3.16 g, 42%).



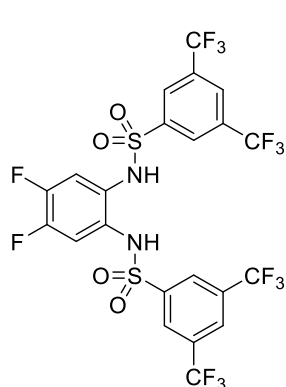
L-Kagan: C₃₀H₄₆Cl₂Ti; **MW** = 525.47 g/mol; **¹H-NMR** (500 MHz, CDCl₃) δ [ppm] 6.74 (td, *J* = 3.2, 2.0 Hz, 2H), 6.40 (q, *J* = 2.3 Hz, 2H), 6.28 (dt, *J* = 3.2, 2.2 Hz, 2H), 6.19 (q, *J* = 2.8 Hz, 2H), 2.74 (td, *J* = 11.3, 3.0 Hz, 2H), 1.77 (dq, *J* = 12.8, 3.2 Hz, 2H), 1.69 (dq, *J* = 13.0, 3.2 Hz, 2H), 1.60 (dq, *J* = 11.9, 2.9 Hz, 2H), 1.53 – 1.36 (m, 4H), 1.16 – 0.92 (m, 8H), 0.89 (d, *J* = 6.5 Hz, 6H), 0.85 (d, *J* = 6.8 Hz, 6H), 0.79 (d, *J* = 6.9 Hz, 6H); **¹³C-NMR** (126 MHz, CDCl₃) δ [ppm] 145.6, 126.9, 121.2, 115.1, 109.6, 51.0, 42.2, 40.9, 35.3, 32.5, 27.5, 24.8, 22.9, 21.8, 15.7.

The analytical data is in agreement with the literature.^[217,359]

5.12.23 Synthesis of *N*-(2-((3,5-bis(trifluoromethyl)phenyl)sulfonamido)-4,5-difluorophenyl)-3,5-bis(trifluoromethyl)benzenesulfonamide



The synthesis is performed according to the literature.^[151] 4,5-Difluorobenzene-1,2-diamine (**S53**, 1.0 eq., 6.76 mmol, 0.975 g) is refluxed with decolorizing charcoal in dry DCM under argon atmosphere prior to the reaction. It is then recrystallized from petrol ether/DCM (2:1). In heat-dried glassware, it is dissolved in dry pyridine (0.6 M, 12 mL) and cooled to 0°C. **S54** (2.0 eq., 13.53 mmol, 4.23 g) is added and after stirring for 30 min at 0°C, the mixture is warmed up to room temperature. It is stirred for 2 d. Water (200 mL) is added and the mixture is heated to 45°C for 1 h. The solvent is removed under reduced pressure and the crude product is recrystallized from EtOH/H₂O (4:1, 2x). **Z1** is dried *in vacuo* and obtained as a colorless solid (3.81 mmol, 2.65 g, 56%).

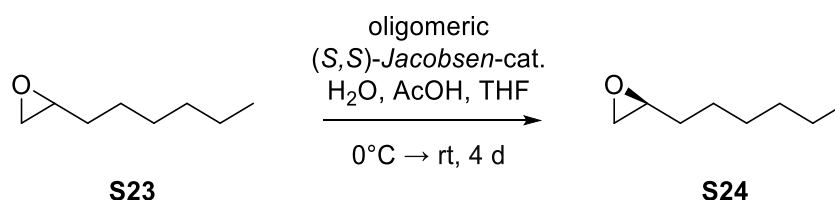


Z1: C₂₂H₁₀F₁₄N₂O₄S₂; **MW** = 696.43 g/mol; **¹H-NMR** (500 MHz, THF-d₈) δ [ppm] 9.13 (s, 2H), 8.36 (s, 2H), 8.24 (s, 4H), 7.01 (t, *J* = 9.5 Hz, 2H); **¹³C-NMR** (126 MHz, THF-d₈) δ [ppm] 149.0 (dd, *J* = 251.9, 15.3 Hz), 142.9, 133.3 (q, *J* = 34.3 Hz), 128.8 (dd, *J* = 5.7, 5.7 Hz), 128.6 (d, *J* = 4.0 Hz), 127.8 – 127.6 (m), 123.5 (q, *J* = 273.0 Hz), 115.4 (dd, *J* = 14.3, 7.6 Hz); **¹⁹F-NMR** (470 MHz, THF-d₈) δ [ppm] -63.8, -138.1; **IR** [cm⁻¹] $\tilde{\nu}_{\max}$ 3345, 3270, 3090, 1530, 1355, 1280, 1170, 1135, 1115, 930, 905, 700, 680, 580; **HRMS** (EI) *m/z*

calcd. for [M]⁺ 695.9853, found 695.9855; **mp**: 198-200°C (decomposition).

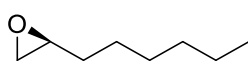
The analytical data is in agreement with the literature.^[136]

5.12.24 Synthesis of (S)-2-hexyloxirane



The reaction is performed under ambient conditions based on a literature known procedure.^[360]

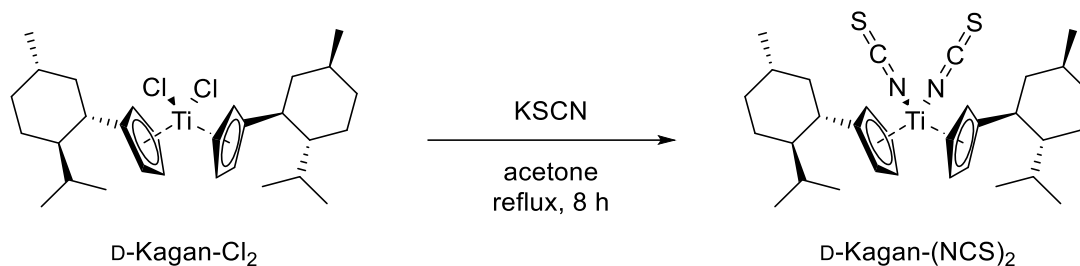
In a round bottom flask, oligomeric (*S,S*)-Jacobsen-catalyst (0.1 mg/mmol, 6.0 mg), AcOH (3 mol%, 1.77 mmol, 0.1 mL) and THF (0.2 eq., 11.8 mmol, 1.0 mL) are added to the racemic epoxide **S23** (1.0 eq., 58.9 mmol, 9.0 mL) and the mixture is cooled to 0°C. Water (0.55 eq., 32.4 mmol, 0.58 mL) is added and the reaction is stirred vigorously while warming to room temperature for 4 d. The crude product is purified by flash column chromatography (SiO₂, DCM). **S24** (25.1 mmol, 3.22 g, 43%) is obtained as a colorless oil.



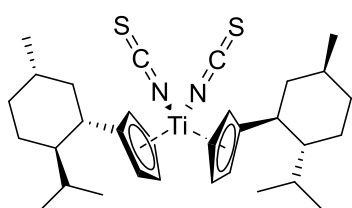
S24: C₈H₁₆O; **MW** = 128.22 g/mol.

e.r. = 99.9:0.1.

5.12.25 Synthesis of D-Kagan-(NCS)₂ (Bis(η^5 -D-menthyl-cyclopentadienyl)-titan(IV) diisothiocyanate)



The reaction is performed under ambient conditions based on a literature known procedure.^[361] D-Kagan-Cl₂ (1.0 eq., 5.0 mmol, 2.63 g) and KSCN (7.2 eq., 36.0 mmol, 3.50 g) are dissolved in acetone (0.2 M, 25 mL). The solution is heated to 60°C and stirred for 8 h. After cooling to room temperature, water (25 mL) is added and a dark-red precipitate is obtained. It is filtered off and washed with water. The product is obtained without further purification as dark-red crystalline solid (1.94 mmol, 1.11 g, 39%).



D-Kagan-(NCS)₂: C₃₂H₄₆N₂S₂Ti; **MW** = 570.72 g/mol; **¹H-NMR** (400 MHz, C₆D₆) δ [ppm] 6.00 (q, J = 2.3 Hz, 2H), 5.75 (td, J = 3.1, 2.0 Hz, 2H), 5.58 (dt, J = 3.0, 2.2 Hz, 2H), 5.28 (q, J = 2.8 Hz, 2H), 2.80 (td, J = 11.4, 3.0 Hz, 2H), 2.05 (dq, J = 12.4, 2.8 Hz, 2H), 1.76 (dddd, J = 14.8, 12.5, 5.9, 3.1 Hz, 4H), 1.63 – 1.55 (m, 2H), 1.30 (pd, J = 6.9, 2.6 Hz, 2H), 1.19 (q, J = 12.2 Hz, 2H), 1.13 (d, J = 6.4 Hz, 6H), 1.11 – 1.03 (m, 2H), 0.91 (ddt, J = 13.4, 9.0, 3.0 Hz, 4H), 0.78 (d, J = 6.8 Hz, 6H), 0.71 (d, J = 6.8 Hz, 6H); **¹³C-NMR** (101 MHz, C₆D₆) δ [ppm] 159.1, 145.1, 119.6, 118.7, 117.3, 108.9, 50.9, 41.9, 41.6, 35.4, 33.2, 27.9, 25.1, 23.1, 21.7, 15.8; **IR** [cm⁻¹] $\tilde{\nu}_{\text{max}}$ 2950, 2900, 2890, 2840, 2045, 2010, 1440, 1370, 900, 855, 845, 835, 670, 490, 425; **HRMS** (ESI) m/z calcd. for [M-NCS]⁺ 512.2828, found 512.2824; **mp**: 225°C; **[α]_D²⁰** (CH₂Cl₂) = -766.7°.

6 References

- [1] I. Dincer, *Renew. Sustain. Energy Rev.* **2000**, *4*, 157–175.
- [2] M. Tariq, S. Bhardwaj, M. Rashid, *EPES* **2013**, *2*, 41–43.
- [3] R. Baños, F. Manzano-Agugliaro, F. G. Montoya, C. Gil, A. Alcayde, J. Gómez, *Renew. Sustain. Energy Rev.* **2011**, *15*, 1753–1766.
- [4] R. K. Pachauri, L. Mayer *Climate change 2014. Synthesis report*, Intergovernmental Panel on Climate Change, Geneva, Switzerland, **2015**.
- [5] A. Qazi, F. Hussain, N. A. Rahim, G. Hardaker, D. Alghazzawi, K. Shaban, K. Haruna, *IEEE Access* **2019**, *7*, 63837–63851.
- [6] C. Bhowmik, S. Bhowmik, A. Ray, K. M. Pandey, *Renew. Sustain. Energy Rev.* **2017**, *71*, 796–813.
- [7] Statistisches Bundesamt, *Umweltökonomische Gesamtrechnungen - Energiegesamtrechnung, 2000-2019, Table 3.4*, Wiesbaden, **2021**.
- [8] J. H. Clark, *Green Chem.* **1999**, *1*, 1–8.
- [9] I. T. Horváth, P. T. Anastas, *Chem. Rev.* **2007**, *107*, 2169–2173.
- [10] P. T. Anastas, M. M. Kirchhoff, *Acc. Chem. Res.* **2002**, *35*, 686–694.
- [11] P. T. Anastas, J. C. Warner, *Green chemistry. Theory and practice*, 1. Ed., Oxford University Press, Oxford, **2000**.
- [12] J. B. Manley, P. T. Anastas, B. W. Cue, *J. Clean. Prod.* **2008**, *16*, 743–750.
- [13] B. M. Trost, A. B. Pinkerton, *J. Org. Chem.* **2001**, *66*, 7714–7722.
- [14] J. Habermann, S. V. Ley, J. S. Scott, *J. Chem. Soc. Perkin 1* **1999**, 1253–1256.
- [15] R. A. Sheldon, *Pure Appl. Chem.* **2000**, *72*, 1233–1246.
- [16] P. T. Anastas, E. S. Beach, *Green Chem. Lett. Rev.* **2007**, *1*, 9–24.
- [17] E. Taibi, D. Gielen, M. Bazilian, *Renew. Sustain. Energy Rev.* **2012**, *16*, 735–744.
- [18] K. H. Nealson, P. G. Conrad, *Philos. Trans. R. Soc. Lond. B Biol. Sci.* **1999**, 1923–1939.
- [19] A. Hermann, *Phys. J.* **1965**, *21*, 168–171.
- [20] O. Lapina, B. Bal'zhinimaev, S. Boghosian, K. Eriksen, R. Fehrmann, *Catal. Today* **1999**, *51*, 469–479.
- [21] X. Yin, L. Lin, H. T. Chung, S. Komini Babu, U. Martinez, G. M. Purdy, P. Zelenay, *ECS Trans.* **2017**, *11*, 1273–1281.
- [22] W. Ostwald, GB190200698A, **1902**.
- [23] W. S. Knowles, *J. Chem. Educ.* **1986**, *63*, 222.
- [24] T.-K. Yang, D.-S. Lee, J. Haas in *Encyclopedia of Reagents for Organic Synthesis*, John Wiley & Sons, Ltd, Chichester, UK, **2001**.
- [25] V. Alekseenko, A. Alekseenko, *J. Geochem. Explor.* **2014**, *147*, 245–249.
- [26] D. R. Lide *CRC handbook of chemistry and physics*, CRC Press, Boca Raton, **2004**.

- [27] Z. Xie, Z. Liu, Y. Wang, Z. Jin, *Natl. Sci. Rev.* **2015**, *2*, 167–182.
- [28] J. G. de Vries, S. D. Jackson, *Catal. Sci. Technol.* **2012**, *2*, 2009.
- [29] K. J. Laidler, *Pure Appl. Chem.* **1996**, *68*, 149–192.
- [30] B. Srinivasan, *FEBS J.* **2021**, DOI: 10.1111/febs.16124.
- [31] K. C. Nicolaou, P. G. Bulger, D. Sarlah, *Angew. Chem. Int. Ed.* **2005**, *44*, 4490–4527; *Angew. Chem.* **2005**, *117*, 4564–4601.
- [32] X. Chen, J. She, Z. Shang, J. Wu, H. Wu, P. Zhang, *Synthesis* **2008**, *2008*, 3478–3486.
- [33] H. E. Zimmerman, J. English Jr., *J. Am. Chem. Soc.* **1954**, *9*, 2285–2290.
- [34] R. A. Sheldon, I. Arends, U. Hanefeld, *Green chemistry and catalysis*, Wiley-VCH, Weinheim, **2007**.
- [35] A. S. Kashin, V. P. Ananikov, *J. Org. Chem.* **2013**, *78*, 11117–11125.
- [36] Nobel Prize Outreach, "The Nobel Prize in Chemistry 2001. William Knowles, Ryoji Noyori, Barry Sharpless", available at <https://www.nobelprize.org/prizes/chemistry/2001/summary/>, **2001**. 04.05.2022.
- [37] Nobel Prize Outreach, "The Nobel Prize in Chemistry 2005. Yves Chauvin, Robert H. Grubbs, Richard R. Schrock", available at <https://www.nobelprize.org/prizes/chemistry/2005/summary/>, **2005**. 04.05.2022.
- [38] Nobel Prize Outreach, "The Nobel Prize in Chemistry 2010. Richard F. Heck, Ei-ichi Negishi, Akira Suzuki", available at <https://www.nobelprize.org/prizes/chemistry/2010/summary/>, **2010**. 04.05.2022.
- [39] Nobel Prize Outreach, "The Nobel Prize in Chemistry 2021. Benjamin List, David W.C. MacMillan", available at <https://www.nobelprize.org/prizes/chemistry/2021/summary/>, **2021**. 04.05.2022.
- [40] M. Schidlowski, *Nature* **1988**, *333*, 313–318.
- [41] J. Gal, *Chirality* **2012**, *24*, 959–976.
- [42] U. Lepola, A. Wade, H. F. Andersen, *Int. Clin. Psychopharmacol.* **2004**, *19*, 149–155.
- [43] J. Hyttel, K. P. Bøgesø, J. Perregaard, C. Sánchez, *J. Neural Transm. Gen. Sect.* **1992**, *88*, 157–160.
- [44] J. M. Finfield, D. H. Sherman, M. Kreitman, R. M. Williams, *Angew. Chem. Int. Ed.* **2012**, *51*, 4802–4836; *Angew. Chem.* **2012**, *124*, 4886–4920.
- [45] G. P. Moss, *Pure Appl. Chem.* **1996**, *68*, 2193–2222.
- [46] K.-E. Jaeger, T. Eggert, *Curr. Opin. Biotechnol.* **2004**, *15*, 305–313.
- [47] E. Fischer, *Ber. Dtsch. Chem. Ges.* **1894**, *27*, 2985–2993.
- [48] K. J. Laidler, *Physical chemistry with biological applications*, Benjamin/Cummings, Menlo Park, California, **1978**.
- [49] R. Noyori, M. Yamakawa, S. Hashiguchi, *J. Org. Chem.* **2001**, *66*, 7931–7944.

- [50] H. C. Kolb, M. S. VanNieuwenhze, K. B. Sharpless, *Chem. Rev.* **1994**, *94*, 2483–2547.
- [51] R. Noyori, *Angew. Chem. Int. Ed.* **2002**, *41*, 2008–2022; *Angew. Chem.* **2002**, *114*, 2108–2032.
- [52] W. S. Knowles, *Angew. Chem. Int. Ed.* **2002**, *41*, 1998–2007; *Angew. Chem.* **2002**, *114*, 2096–2105.
- [53] B. D. Vineyard, W. S. Knowles, M. J. Sabacky, G. L. Bachman, D. J. Weinkauff, *J. Am. Chem. Soc.* **1977**, *99*, 5946–5952.
- [54] R. Noyori, S. Hashiguchi, *Acc. Chem. Res.* **1997**, *30*, 97–102.
- [55] E. N. Jacobsen, I. Marko, W. S. Mungall, G. Schroeder, K. B. Sharpless, *J. Am. Chem. Soc.* **1988**, *110*, 1968–1970.
- [56] W. S. Knowles, *Acc. Chem. Res.* **1983**, *16*, 106–112.
- [57] H.-J. Drexler, S. Zhang, A. Sun, A. Spannenberg, A. Arrieta, A. Preetz, D. Heller, *Tetrahedron Asymmetry* **2004**, *15*, 2139–2150.
- [58] E. Dolja, *Dissertation*, University of Bonn, Bonn, **2019**.
- [59] E. T. Kool, *Annu. Rev. Biochem.* **2002**, *71*, 191–219.
- [60] L. Pravda, K. Berka, R. Svobodová Vařeková, D. Sehnal, P. Banáš, R. A. Laskowski, J. Koča, M. Otyepka, *BMC Bioinformatics* **2014**, *15*, 379.
- [61] D. Ringe, G. A. Petsko, *Science* **2008**, *320*, 1428–1429.
- [62] K. Schmidt-Rohr, *Life* **2021**, *11*, 1191–1212.
- [63] O. Virtanen, E. Constantinidou, E. Tyystjärvi, *J. Biol. Educ.* **2020**, 1–8.
- [64] N. Cox, D. A. Pantazis, W. Lubitz, *Annu. Rev. Biochem.* **2020**, *89*, 795–820.
- [65] J. W. Verhoeven, *Pure Appl. Chem.* **1996**, *68*, 2223–2286.
- [66] D. A. Nicewicz, D. W. C. MacMillan, *Science* **2008**, *322*, 77–80.
- [67] M. A. Ischay, M. E. Anzovino, J. Du, T. P. Yoon, *J. Am. Chem. Soc.* **2008**, *130*, 12886–12887.
- [68] J. M. R. Narayanam, J. W. Tucker, C. R. J. Stephenson, *J. Am. Chem. Soc.* **2009**, *131*, 8756–8757.
- [69] N. Y. Shin, J. M. Ryss, X. Zhang, S. J. Miller, R. R. Knowles, *Science* **2019**, *366*, 364–369.
- [70] D. M. Niedzwiedzki, R. E. Blankenship, *Photosynth. Res.* **2010**, *106*, 227–238.
- [71] M. H. Shaw, J. Twilton, D. W. C. MacMillan, *J. Org. Chem.* **2016**, *81*, 6898–6926.
- [72] C. K. Prier, D. A. Rankic, D. W. C. MacMillan, *Chem. Rev.* **2013**, *113*, 5322–5363.
- [73] Z. Zhang, *Dissertation*, University of Bonn, Bonn, **2019**.
- [74] G. Zimmerman, L.-Y. Chow, U.-J. Paik, *J. Am. Chem. Soc.* **1958**, *80*, 3528–3531.
- [75] M. Latrache, N. Hoffmann, *Chem. Soc. Rev.* **2021**, *50*, 7418–7435.
- [76] T. D. Walsh, *J. Am. Chem. Soc.* **1969**, *91*, 515–516.

- [77] A. Windaus, O. Linsert, A. Lüttringhaus, G. Weidlich, *Eur. J. Org. Chem.* **1932**, 492, 226–241.
- [78] M. Wacker, M. F. Holick, *Dermatoendocrinol.* **2013**, 5, 51–108.
- [79] J. A. MacLaughlin, R. R. Anderson, M. F. Holick, *Science* **1982**, 216, 1001–1003.
- [80] L. Y. Matsuoka, J. Wortsman, J. G. Haddad, B. W. Hollis, *J. Lab. Clin. Med.* **1989**, 114, 301–305.
- [81] C. M. Manna, A. Kaur, L. M. Yablon, F. Haeffner, B. Li, J. A. Byers, *J. Am. Chem. Soc.* **2015**, 137, 14232–14235.
- [82] V. Bhat, E. R. Welin, X. Guo, B. M. Stoltz, *Chem. Rev.* **2017**, 117, 4528–4561.
- [83] H. Pellissier, *Tetrahedron* **2008**, 64, 1563–1601.
- [84] A. Gansäuer, S. Narayan, N. Schiffer-Ndene, H. Bluhm, J. E. Oltra, J. M. Cuerva, A. Rosales, M. Nieger, *J. Organomet. Chem.* **2006**, 691, 2327–2331.
- [85] E. Cesarotti, H. B. Kagan, R. Goddard, C. Krüger, *J. Organomet. Chem.* **1978**, 162, 297–309.
- [86] A. Gansäuer, M. Pierobon, H. Bluhm, *Angew. Chem. Int. Ed.* **1998**, 37, 101–103; *Angew. Chem.* **1998**, 110, 107–109.
- [87] R. W. Hoffmann, *Angew. Chem. Int. Ed.* **2003**, 42, 1096–1109; *Angew. Chem.* **2003**, 115, 1128–1142.
- [88] A. Gansäuer, H. Bluhm, T. Lauterbach, *Adv. Synth. Catal.* **2001**, 343, 785–787.
- [89] M. Hesse, H. Meier, B. Zeeh, S. Bienz, L. Bigler, T. Fox, *Spektroskopische Methoden in der organischen Chemie*, 8. Ed., Georg Thieme Verlag, Stuttgart, New York, **2012**.
- [90] H. B. Kagan, *Tetrahedron* **2001**, 57, 2449–2468.
- [91] E. Dolja, N. Funken, D. Slak, G. Schnakenburg, A. Gansäuer, *ChemCatChem* **2019**, 11, 5421–5424.
- [92] A. Gansäuer, *Synlett* **2020**, 32, 447–456.
- [93] N. Funken, Y.-Q. Zhang, A. Gansäuer, *Chem. Eur. J.* **2017**, 23, 19–32.
- [94] H. Weißbarth, F. Mühlhaus, A. Gansäuer, *Synthesis* **2020**, 52, 2940–2947.
- [95] A. Gansäuer, C.-A. Fan, F. Keller, J. Keil, *J. Am. Chem. Soc.* **2007**, 129, 3484–3485.
- [96] A. Gansäuer, C.-A. Fan, F. Keller, P. Karbaum, *Chem. Eur. J.* **2007**, 13, 8084–8090.
- [97] D. Slak, *Master Thesis*, University of Bonn, Bonn, **2019**.
- [98] A. Gansäuer, H. Bluhm, B. Rinker, S. Narayan, M. Schick, T. Lauterbach, M. Pierobon, *Chemistry* **2003**, 9, 531–542.
- [99] K. Daasbjerg, H. Svith, S. Grimme, M. Gerenkamp, C. Mück-Lichtenfeld, A. Gansäuer, A. Barchuk, F. Keller, *Angew. Chem. Int. Ed.* **2006**, 45, 2041–2044; *Angew. Chem.* **2006**, 118, 2095–2098.
- [100] A. Gansäuer, A. Barchuk, F. Keller, M. Schmitt, S. Grimme, M. Gerenkamp, C. Mück-Lichtenfeld, K. Daasbjerg, H. Svith, *J. Am. Chem. Soc.* **2007**, 129, 1359–1371.

- [101] A. Gansäuer, L. Shi, F. Keller, P. Karbaum, C.-A. Fan, *Tetrahedron: Asymmetry* **2010**, *21*, 1361–1369.
- [102] F. Mühlhaus, *Dissertation*, University of Bonn, Bonn, **2018**.
- [103] M. Adamietz, *Master Thesis*, University of Bonn, Bonn, **2019**.
- [104] A. Mullard, *Nat. Rev. Drug Discov.* **2019**, *18*, 85–89.
- [105] M. D. Burke, S. L. Schreiber, *Angew. Chem. Int. Ed.* **2004**, *43*, 46–58; *Angew. Chem.* **2004**, *116*, 48–60.
- [106] R. Breinbauer, I. R. Vetter, H. Waldmann, *Angew. Chem. Int. Ed.* **2002**, *41*, 2878–2890; *Angew. Chem.* **2002**, *114*, 3002–3014.
- [107] M. Feher, J. M. Schmidt, *J. Chem. Inf. Comput. Sci.* **2003**, *43*, 218–227.
- [108] S. L. Schreiber, *Science* **2000**, *287*, 1964–1969.
- [109] R. J. Spandl, A. Bender, D. R. Spring, *Org. Biomol. Chem.* **2008**, *6*, 1149–1158.
- [110] N. Funken, F. Mühlhaus, A. Gansäuer, *Angew. Chem. Int. Ed.* **2016**, *55*, 12030–12034; *Angew. Chem.* **2016**, *128*, 12209–12213.
- [111] M. Dieckmann, S. Rudolph, S. Dreisigacker, D. Menche, *J. Org. Chem.* **2012**, *77*, 10782–10788.
- [112] D. Menche, *ChemMedChem* **2021**, *16*, 2068–2074.
- [113] X. Just-Baringo, C. Morrill, D. J. Procter, *Tetrahedron* **2016**, *72*, 7691–7698.
- [114] T. Furumai, N. Nagahama, T. Okuda, *J. Antibiot.* **1968**, *21*, 85–90.
- [115] M. Tortosa, *Angew. Chem. Int. Ed.* **2011**, *50*, 3950–3953; *Angew. Chem.* **2011**, *123*, 4036–4039.
- [116] S. Peltier, J.-M. Oger, F. Lagarce, W. Couet, J.-P. Benoît, *Pharm. Res.* **2006**, *23*, 1243–1250.
- [117] H. Irschik, R. Jansen, K. Gerth, G. Höfle, H. Reichenbach, *J. Antibiot.* **1995**, *48*, 962–966.
- [118] S. W. M. Crossley, G. Tong, M. J. Lambrecht, H. E. Burdge, R. A. Shenvi, *J. Am. Chem. Soc.* **2020**, *142*, 11376–11381.
- [119] P. M. Blumberg, *Cancer Res.* **1988**, *48*, 1–8.
- [120] R. A. Hill, H. G. Cutler, S. R. Parker, US6060507A, **1997**.
- [121] W. M. Haynes *CRC handbook of chemistry and physics. A ready-reference book of chemical and physical data*, CRC Press, Boca Raton, Fla., **2015**.
- [122] M. Manßen, L. L. Schafer, *Chem. Soc. Rev.* **2020**, *49*, 6947–6994.
- [123] T. McCallum, X. Wu, S. Lin, *J. Org. Chem.* **2019**, *84*, 14369–14380.
- [124] S. P. Morcillo, D. Miguel, A. G. Campaña, L. Álvarez de Cienfuegos, J. Justicia, J. M. Cuerva, *Org. Chem. Front.* **2014**, *1*, 15–33.
- [125] A. Gansäuer, A. Fleckhaus, M. A. Lafont, A. Okkel, K. Kotsis, A. Anoop, F. Neese, *J. Am. Chem. Soc.* **2009**, *131*, 16989–16999.

- [126] W. A. Nugent, T. V. RajanBabu, *J. Am. Chem. Soc.* **1988**, *110*, 8561–8562.
- [127] T. V. RajanBabu, W. A. Nugent, *J. Am. Chem. Soc.* **1994**, *116*, 986–997.
- [128] A. K. Yudin *Aziridines and epoxides in organic synthesis*, Wiley-VCH, Weinheim, **2006**.
- [129] A. Gansäuer, *Chem. Commun.* **1997**, 457–458.
- [130] Z. Zhang, R. B. Richrath, A. Gansäuer, *ACS Catal.* **2019**, *9*, 3208–3212.
- [131] T. Liedtke, P. Spannring, L. Riccardi, A. Gansäuer, *Angew. Chem. Int. Ed.* **2018**, *57*, 5006–5010; *Angew. Chem.* **2018**, *130*, 5100–5104.
- [132] C. Yao, T. Dahmen, A. Gansäuer, J. Norton, *Science* **2019**, *364*, 764–767.
- [133] G. Shizgal, *Master Thesis*, University of Bonn, Bonn, **2018**.
- [134] A. Panfilova, *Dissertation*, University of Bonn, Bonn, **2019**.
- [135] Z. Zhang, T. Hilche, D. Slak, N. R. Rietdijk, U. N. Oloyede, R. A. Flowers, A. Gansäuer, *Angew. Chem. Int. Ed.* **2020**, *59*, 9355–9359; *Angew. Chem.* **2020**, *132*, 9441–9445.
- [136] Z. Zhang, D. Slak, T. Krebs, E. Kuchuk, M. Leuschner, U. N. Oloyede, J. B. Stückrath, J. Schmidt, P. Vöhringer, S. Grimme, R. A. Flowers, A. Gansäuer, *Manuscript in Preparation* **2022**.
- [137] A. Gansäuer, S. Narayan, *Adv. Synth. Catal.* **2002**, *344*, 465–475.
- [138] A. Gansäuer, C. Kube, K. Daasbjerg, R. Sure, S. Grimme, G. D. Fianu, D. V. Sadasivam, R. A. Flowers, *J. Am. Chem. Soc.* **2014**, *136*, 1663–1671.
- [139] A. Gansäuer, M. Behlendorf, D. von Laufenberg, A. Fleckhaus, C. Kube, D. V. Sadasivam, R. A. Flowers, *Angew. Chem. Int. Ed.* **2012**, *51*, 4739–4742; *Angew. Chem.* **2012**, *124*, 4819–4823.
- [140] T. Chivers, E. D. Ibrahim, *J. Organomet. Chem.* **1974**, *77*, 241–246.
- [141] A. Gansäuer, H. Bluhm, M. Pierobon, *J. Am. Chem. Soc.* **1998**, *120*, 12849–12859.
- [142] J. Meinwald, S. S. Labana, M. S. Chadha, *J. Am. Chem. Soc.* **1963**, *85*, 582–585.
- [143] H. O. House, *J. Am. Chem. Soc.* **1955**, *77*, 3070–3075.
- [144] R. B. Richrath, *Dissertation*, University of Bonn, Bonn, **2019**.
- [145] A. Gansäuer, B. Rinker, M. Pierobon, S. Grimme, M. Gerenkamp, C. Mück-Lichtenfeld, *Angew. Chem. Int. Ed.* **2003**, *42*, 3687–3690; *Angew. Chem.* **2003**, *115*, 3815–3818.
- [146] A. Macchioni, *Chem. Rev.* **2005**, *105*, 2039–2073.
- [147] K. Fagnou, M. Lautens, *Angew. Chem. Int. Ed.* **2002**, *41*, 26–47; *Angew. Chem.* **2002**, *114*, 26–49.
- [148] R. B. Richrath, T. Olyschläger, S. Hildebrandt, D. G. Enny, G. D. Fianu, R. A. Flowers, A. Gansäuer, *Chemistry* **2018**, *24*, 6371–6379.
- [149] F. Mühlhaus, H. Weißbarth, T. Dahmen, G. Schnakenburg, A. Gansäuer, *Angew. Chem. Int. Ed.* **2019**, *58*, 14208–14212; *Angew. Chem.* **2019**, *131*, 14346–14350.
- [150] T. Hilche, P. H. Reinsberg, S. Klare, T. Liedtke, L. Schäfer, A. Gansäuer, *Chem. Eur. J.* **2021**, *27*, 4903–4912.

- [151] L. Schäfer, *Master Thesis*, University of Bonn, Bonn, **2019**.
- [152] A. Gansäuer, D. von Laufenberg, C. Kube, T. Dahmen, A. Michelmann, M. Behlendorf, R. Sure, M. Seddiqzai, S. Grimme, D. V. Sadasivam, G. D. Fianu, R. A. Flowers, *Chem. Eur. J.* **2015**, *21*, 280–289.
- [153] R. J. Enemaerke, J. Larsen, G. H. Hjöllund, T. Skrydstrup, K. Daasbjerg, *Organometallics* **2005**, *24*, 1252–1262.
- [154] A. Gansäuer, M. Moschioni, D. Bauer, *Eur. J. Org. Chem.* **1998**, *9*, 1923–1927.
- [155] Y.-Q. Zhang, N. Funken, P. Winterscheid, A. Gansäuer, *Angew. Chem. Int. Ed.* **2015**, *54*, 6931–6934; *Angew. Chem.* **2015**, *127*, 7035–7038.
- [156] D. S. G. Henriques, K. Zimmer, S. Klare, A. Meyer, E. Rojo-Wiechel, M. Bauer, R. Sure, S. Grimme, O. Schiemann, R. A. Flowers, A. Gansäuer, *Angew. Chem. Int. Ed.* **2016**, *55*, 7671–7675; *Angew. Chem.* **2016**, *128*, 7801–7805.
- [157] Y.-Q. Zhang, F. Bohle, R. Bleith, G. Schnakenburg, S. Grimme, A. Gansäuer, *Angew. Chem. Int. Ed.* **2018**, *57*, 13528–13532; *Angew. Chem.* **2018**, *130*, 13716–13720.
- [158] D. S. G. Henriques, E. Rojo-Wiechel, S. Klare, R. Mika, S. Höthker, J. H. Schacht, N. Schmickler, A. Gansäuer, *Angew. Chem. Int. Ed.* **2022**, *61*, e202114198; *Angew. Chem.* **2022**, *134*.
- [159] P. Funk, R. B. Richrath, F. Bohle, S. Grimme, A. Gansäuer, *Angew. Chem. Int. Ed.* **2021**, *60*, 5482–5488; *Angew. Chem.* **2021**, *133*, 5542–5548.
- [160] M. Castro Rodríguez, I. Rodríguez García, R. N. Rodríguez Maecker, L. Pozo Morales, J. E. Oltra, A. Rosales Martínez, *Org. Process Res. Dev.* **2017**, *21*, 911–923.
- [161] P. R. D. Murray, J. H. Cox, N. D. Chiappini, C. B. Roos, E. A. McLoughlin, B. G. Hejna, S. T. Nguyen, H. H. Ripberger, J. M. Ganley, E. Tsui, N. Y. Shin, B. Koronkiewicz, G. Qiu, R. R. Knowles, *Chem. Rev.* **2022**, *122*, 2017–2291.
- [162] C. Starr, C. A. Evers, L. Starr, *Biology. Concepts and applications*, 6. Ed., Thomson, Brooks/Cole, Belmont, CA, **2006**.
- [163] N. A. Romero, D. A. Nicewicz, *Chem. Rev.* **2016**, *116*, 10075–10166.
- [164] E. Speckmeier, T. G. Fischer, K. Zeitler, *J. Am. Chem. Soc.* **2018**, *140*, 15353–15365.
- [165] H. Cano-Yelo, A. Deronzier, *J. Chem. Soc., Perkin Trans. 2* **1984**, 1093–1098.
- [166] K. Kalyanasundaram, *Coord. Chem. Rev.* **1982**, *46*, 159–244.
- [167] H. Kotani, K. Ohkubo, S. Fukuzumi, *J. Am. Chem. Soc.* **2004**, *126*, 15999–16006.
- [168] C. Wegeberg, O. S. Wenger, *J. Am. Chem. Soc.* **2021**, *1*, 1860–1876.
- [169] W.-J. Zhou, X.-D. Wu, M. Miao, Z.-H. Wang, L. Chen, S.-Y. Shan, G.-M. Cao, D.-G. Yu, *Chem. Eur. J.* **2020**, *26*, 15052–15064.
- [170] L. A. Büldt, O. S. Wenger, *Chem. Sci.* **2017**, *8*, 7359–7367.
- [171] C. Pac, M. Ihama, M. Yasuda, Y. Miyauchi, H. Sakurai, *J. Am. Chem. Soc.* **1981**, *103*, 6495–6497.

- [172] Y. Guindon, G. Jung, B. Guérin, W. W. Ogilvie, *Synlett* **1998**, 1998, 213–220.
- [173] H. Cano-Yelo, A. Deronzier, *Tetrahedron Lett.* **1984**, 25, 5517–5520.
- [174] A. G. Condie, J. C. González-Gómez, C. R. J. Stephenson, *J. Am. Chem. Soc.* **2010**, 132, 1464–1465.
- [175] S. Cai, X. Zhao, X. Wang, Q. Liu, Z. Li, D. Z. Wang, *Angew. Chem. Int. Ed.* **2012**, 51, 8050–8053; *Angew. Chem.* **2012**, 124, 8174–8177.
- [176] Y. Cheng, J. Yang, Y. Qu, P. Li, *Org. Lett.* **2012**, 14, 98–101.
- [177] S. Fukuzumi, S. Mochizuki, T. Tanaka, *J. Phys. Chem.* **1990**, 94, 722–726.
- [178] J. W. Tucker, J. M. R. Narayanam, S. W. Krabbe, C. R. J. Stephenson, *Org. Lett.* **2010**, 12, 368–371.
- [179] L. Furst, J. M. R. Narayanam, C. R. J. Stephenson, *Angew. Chem. Int. Ed.* **2011**, 50, 9655–9659; *Angew. Chem.* **2011**, 123, 9829–9833.
- [180] S. Lin, M. A. Ischay, C. G. Fry, T. P. Yoon, *J. Am. Chem. Soc.* **2011**, 133, 19350–19353.
- [181] J. Du, K. L. Skubi, D. M. Schultz, T. P. Yoon, *Science* **2014**, 344, 392–396.
- [182] E. L. Tyson, E. P. Farney, T. P. Yoon, *Org. Lett.* **2012**, 14, 1110–1113.
- [183] J. Du, T. P. Yoon, *J. Am. Chem. Soc.* **2009**, 131, 14604–14605.
- [184] M. Rueda-Becerril, O. Mahé, M. Drouin, M. B. Majewski, J. G. West, M. O. Wolf, G. M. Sammis, J.-F. Paquin, *J. Am. Chem. Soc.* **2014**, 136, 2637–2641.
- [185] A. Noble, D. W. C. MacMillan, *J. Am. Chem. Soc.* **2014**, 136, 11602–11605.
- [186] S. Ventre, F. R. Petronijevic, D. W. C. MacMillan, *J. Am. Chem. Soc.* **2015**, 137, 5654–5657.
- [187] M. J. Schnermann, L. E. Overman, *Angew. Chem. Int. Ed.* **2012**, 51, 9576–9580; *Angew. Chem.* **2012**, 124, 9714–9718.
- [188] Z. Zuo, D. W. C. MacMillan, *J. Am. Chem. Soc.* **2014**, 136, 5257–5260.
- [189] N. J. Turro, *Modern molecular photochemistry of organic molecules*, Univ. Science Books, Sausalito, Calif., **2007**.
- [190] T. Hofbeck, H. Yersin, *Inorg. Chem.* **2010**, 49, 9290–9299.
- [191] S. Z. Zard, *Radical reactions in organic synthesis*, 1. Ed., Oxford University Press, Oxford, **2003**.
- [192] P. Renaud, M. P. Sibi *Radicals in organic synthesis*, Wiley-VCH, Weinheim, **2001**.
- [193] A. J. McCarroll, J. C. Walton, *Angew. Chem. Int. Ed.* **2001**, 40, 2224–2248; *Angew. Chem.* **2001**, 113, 2282–2307.
- [194] H.-W. Shih, M. N. Vander Wal, R. L. Grange, D. W. C. MacMillan, *J. Am. Chem. Soc.* **2010**, 132, 13600–13603.
- [195] D. A. Nagib, M. E. Scott, D. W. C. MacMillan, *J. Am. Chem. Soc.* **2009**, 131, 10875–10877.

- [196] E. R. Welin, A. A. Warkentin, J. C. Conrad, D. W. C. MacMillan, *Angew. Chem. Int. Ed.* **2015**, *54*, 9668–9672; *Angew. Chem.* **2015**, *127*, 9804–9808.
- [197] S. H. Lau, M. A. Borden, T. J. Steiman, L. S. Wang, M. Parasram, A. G. Doyle, *J. Am. Chem. Soc.* **2021**, *143*, 15873–15881.
- [198] M. Silvi, P. Melchiorre, *Nature* **2018**, *554*, 41–49.
- [199] L. Zhang, E. Meggers, *Acc. Chem. Res.* **2017**, *50*, 320–330.
- [200] A. Inagaki, S. Edure, S. Yatsuda, M. Akita, *Chem. Commun.* **2005**, 5468–5470.
- [201] A. Inagaki, H. Nakagawa, M. Akita, K. Inoue, M. Sakai, M. Fujii, *Dalton Trans.* **2008**, 6709–6723.
- [202] A. Inagaki, S. Yatsuda, S. Edure, A. Suzuki, T. Takahashi, M. Akita, *Inorg. Chem.* **2007**, *46*, 2432–2445.
- [203] K. Murata, M. Ito, A. Inagaki, M. Akita, *Chem. Lett.* **2010**, *39*, 915–917.
- [204] H. Nitadori, T. Takahashi, A. Inagaki, M. Akita, *Inorg. Chem.* **2012**, *51*, 51–62.
- [205] T. Hamada, H. Ishida, S. Usui, Y. Watanabe, K. Tsumura, K. Ohkubo, *J. Chem. Soc. Chem. Commun.* **1993**, 909–911.
- [206] T. Hamada, H. Ishida, S. Usui, K. Tsumura, K. Ohkubo, *J. Mol. Catal.* **1994**, *88*, L1–L5.
- [207] J. Großkopf, T. Kratz, T. Rigotti, T. Bach, *Chem. Rev.* **2022**, *122*, 1626–1653.
- [208] F. Pecho, Y. Sempere, J. Gramüller, F. M. Hörmann, R. M. Gschwind, T. Bach, *J. Am. Chem. Soc.* **2021**, *143*, 9350–9354.
- [209] D. P. Schwinger, T. Bach, *Acc. Chem. Res.* **2020**, *53*, 1933–1943.
- [210] C. Müller, A. Bauer, T. Bach, *Angew. Chem. Int. Ed.* **2009**, *48*, 6640–6642; *Angew. Chem.* **2009**, *121*, 6767–6769.
- [211] R. Brimiouille, T. Bach, *Science* **2013**, *342*, 840–843.
- [212] Z.-T. Tsai, C. H. Brubaker, *J. Organomet. Chem.* **1979**, *166*, 199–210.
- [213] R. W. Harrigan, G. S. Hammond, H. B. Gray, *J. Organomet. Chem.* **1974**, *81*, 79–85.
- [214] J. W. Kenney, D. R. Boone, D. R. Striplin, Y. H. Chen, K. B. Hamar, *Organometallics* **1993**, *12*, 3671–3676.
- [215] G. V. Loukova, V. V. Strelets, *J. Organomet. Chem.* **2000**, *606*, 203–206.
- [216] G. V. Loukova, V. A. Smirnov, *Chem. Phys. Lett.* **2000**, *329*, 437–442.
- [217] M. Heinz, *Master Thesis*, University of Bonn, Bonn, **2020**.
- [218] W. C. Finch, E. V. Anslyn, R. H. Grubbs, *J. Am. Chem. Soc.* **1988**, *110*, 2406–2413.
- [219] K. Nakajima, Y. Miyake, Y. Nishibayashi, *Acc. Chem. Res.* **2016**, *49*, 1946–1956.
- [220] H. Weißbarth, *Dissertation*, University of Bonn, Bonn, **2021**.
- [221] A. Gansäuer, P. Karbaum, D. Schmauch, M. Einig, L. Shi, A. Anoop, F. Neese, *Chem. Asian J.* **2014**, *9*, 2289–2294.
- [222] B. D. Fairbanks, D. M. Love, C. N. Bowman, *Macromol. Chem. Phys.* **2017**, *218*, 1700073.

- [223] A. K. Sinha, D. Equbal, *Asian J. Org. Chem.* **2019**, *8*, 32–47.
- [224] A. B. Lowe, *Polym. Chem.* **2014**, *5*, 4820–4870.
- [225] F. Dénès, M. Pichowicz, G. Povie, P. Renaud, *Chem. Rev.* **2014**, *114*, 2587–2693.
- [226] K. Gilmore, I. V. Alabugin, *Chem. Rev.* **2011**, *111*, 6513–6556.
- [227] A. Gansäuer, M. Otte, L. Shi, *J. Am. Chem. Soc.* **2011**, *133*, 416–417.
- [228] M. Albert, L. Fensterbank, E. Lacôte, M. Malacria in *Top. Curr. Chem.*, Vol. 264, Springer, Berlin, **2006**.
- [229] M. Parasram, B. J. Shields, O. Ahmad, T. Knauber, A. G. Doyle, *ACS Catal.* **2020**, *10*, 5821–5827.
- [230] S. Lin, Y. Chen, F. Li, C. Shi, L. Shi, *Chem. Sci.* **2019**, *11*, 839–844.
- [231] S. Protti, T. Yoon, H. Han, *ACS Sustain. Chem. Eng.* **2021**, *9*, 13125–13127.
- [232] A. Gualandi, F. Calogero, M. Mazzarini, S. Guazzi, A. Fermi, G. Bergamini, P. G. Cozzi, *ACS Catal.* **2020**, *10*, 3857–3863.
- [233] A. Fermi, A. Gualandi, G. Bergamini, P. G. Cozzi, *Eur. J. Org. Chem.* **2020**, 6955–6965.
- [234] Z. Zhang, *Unpublished Results*.
- [235] K. Döppert, H.-P. Klein, U. Thewalt, *J. Organomet. Chem.* **1986**, *303*, 205–211.
- [236] G. Frey, J. N. Hausmann, J. Streuff, *Chem. Eur. J.* **2015**, *21*, 5693–5696.
- [237] A. Gansäuer, *Synlett* **1997**, 363–364.
- [238] A. Gansäuer, D. Bauer, *J. Org. Chem.* **1998**, *63*, 2070–2071.
- [239] T. Wirth, *Angew. Chem. Int. Ed.* **1996**, *35*, 61–63; *Angew. Chem.* **1996**, *108*, 65–67.
- [240] H.-P. Looock, B. Simard, S. Wallin, C. Linton, *J. Chem. Phys.* **1998**, *109*, 8980–8992.
- [241] Y.-R. Luo, *Comprehensive Handbook of Chemical Bond Energies*, CRC Press, Boca Raton, **2007**.
- [242] F. R. Wild, L. Zsolnai, G. Huttner, H. H. Brintzinger, *J. Organomet. Chem.* **1982**, *232*, 233–247.
- [243] K. P. Bryliakov, D. E. Babushkin, E. P. Talsi, A. Z. Voskoboynikov, H. Gritzko, L. Schröder, H.-R. H. Damrau, U. Wieser, F. Schaper, H. H. Brintzinger, *Organometallics* **2005**, *24*, 894–904.
- [244] S. M. Baldwin, J. E. Bercaw, H. H. Brintzinger, *J. Am. Chem. Soc.* **2010**, *132*, 13969–13971.
- [245] M. J. Schneider, J. Suhm, R. Mülhaupt, M.-H. Prosenc, H.-H. Brintzinger, *Macromolecules* **1997**, *30*, 3164–3168.
- [246] W. Kaminsky *Advances in Polymer Science*, Springer Berlin Heidelberg, Berlin, Heidelberg, **2013**.
- [247] T. Hilche, T. Krebs, H. Weißbarth, F. Lang, G. Schnakenburg, A. Gansäuer, *Manuscript in Preparation* **2022**.

- [248] T. Krebs, *Dissertation in Preparation*, University of Bonn, Bonn, **2022**.
- [249] L. Candish, M. Freitag, T. Gensch, F. Glorius, *Chem. Sci.* **2017**, *8*, 3618–3622.
- [250] J. W. Tucker, C. R. J. Stephenson, *J. Org. Chem.* **2012**, *77*, 1617–1622.
- [251] K. L. Skubi, T. R. Blum, T. P. Yoon, *Chem. Rev.* **2016**, *116*, 10035–10074.
- [252] L. Chu, C. Ohta, Z. Zuo, D. W. C. MacMillan, *J. Am. Chem. Soc.* **2014**, *136*, 10886–10889.
- [253] P. D. van Poelje, E. E. Snell, *Annu. Rev. Biochem.* **1990**, *59*, 29–59.
- [254] R. Brückner, *Reaktionsmechanismen. Organische Reaktionen, Stereochemie, moderne Synthesemethoden*, 3. Ed., Spektrum Akad. Verl., Berlin, Heidelberg, **2011**.
- [255] N. T. Anh, O. Eisenstein, *Tetrahedron Letters* **1976**, *17*, 155–158.
- [256] E. Osypchuk, *Bachelor Thesis*, University of Bonn, Bonn, **2021**.
- [257] M. Tokunaga, J. F. Larrow, F. Kakiuchi, E. N. Jacobsen, *Science* **1997**, *277*, 936–938.
- [258] S. E. Schaus, B. D. Brandes, J. F. Larrow, M. Tokunaga, K. B. Hansen, A. E. Gould, M. E. Furrow, E. N. Jacobsen, *J. Am. Chem. Soc.* **2002**, *124*, 1307–1315.
- [259] C. Meister, H.-D. Scharf, *Synthesis* **1981**, *1981*, 733–736.
- [260] D. X. Hu, G. M. Shibuya, N. Z. Burns, *J. Am. Chem. Soc.* **2013**, *135*, 12960–12963.
- [261] R. Hiatt, S. W. Benson, *Int. J. Chem. Kinet.* **1972**, *4*, 479–486.
- [262] A. L. Beckwith, C. H. Schiesser, *Tetrahedron* **1985**, *41*, 3925–3941.
- [263] A. Citterio, F. Minisci, O. Porta, G. Sesana, *J. Am. Chem. Soc.* **1977**, *99*, 7960–7968.
- [264] A. Citterio, A. Arnoldi, F. Minisci, *J. Org. Chem.* **1979**, *44*, 2674–2682.
- [265] A. Gansäuer, M. Seddiqzai, T. Dahmen, R. Sure, S. Grimme, *Beilstein J. Org. Chem.* **2013**, *9*, 1620–1629.
- [266] B. Cosimelli, D. Spinelli, F. Costanzo, D. Tonelli, L. Lamartina, M. C. Sarvà, R. Seeber, *Tetrahedron* **2001**, *57*, 1857–1860.
- [267] C. K. Mann, *Anal. Chem.* **1964**, *36*, 2424–2426.
- [268] A. Gansäuer, L. Shi, M. Otte, *J. Am. Chem. Soc.* **2010**, *132*, 11858–11859.
- [269] S. Huo, E. Negishi, *Org. Lett.* **2001**, *3*, 3253–3256.
- [270] D. D. Ford, L. P. C. Nielsen, S. J. Zuend, C. B. Musgrave, E. N. Jacobsen, *J. Am. Chem. Soc.* **2013**, *135*, 15595–15608.
- [271] L. P. C. Nielsen, C. P. Stevenson, D. G. Blackmond, E. N. Jacobsen, *J. Am. Chem. Soc.* **2004**, *126*, 1360–1362.
- [272] J. M. Ready, E. N. Jacobsen, *Angew. Chem. Int. Ed.* **2002**, *41*, 1374–1377; *Angew. Chem.* **2002**, *114*, 1432–1435.
- [273] C. A. Brown, H. C. Brown, *J. Am. Chem. Soc.* **1963**, *85*, 1003–1005.
- [274] C. A. Brown, V. K. Ahuja, *J. Chem. Soc. Chem. Commun.* **1973**, 553–554.
- [275] E. D. Mihelich, K. Daniels, D. J. Eickhoff, *J. Am. Chem. Soc.* **1981**, *103*, 7690–7692.
- [276] R. R. Rodríguez-Berríos, G. Torres, J. A. Prieto, *Tetrahedron* **2011**, *67*, 830–836.

- [277] K. B. Sharpless, R. C. Michaelson, *J. Am. Chem. Soc.* **1973**, *95*, 6136–6137.
- [278] J. E. Baldwin, *J. Chem. Soc. Chem. Commun.* **1976**, 734–736.
- [279] J. E. Baldwin, R. C. Thomas, L. I. Kruse, L. Silberman, *J. Org. Chem.* **1977**, *42*, 3846–3852.
- [280] M. B. Smith, J. March, *March's advanced organic chemistry. Reactions, mechanisms, and structure*, 6. Ed., Wiley, New York, Weinheim, **2007**.
- [281] K. Daasbjerg, J. D. Oslob, B. Åkermark, P.-O. Norrby, *Acta Chem. Scand.* **1995**, *49*, 878–887.
- [282] P. Crotti, V. Di Bussolo, L. Favero, F. Macchia, M. Pineschi, *Tetrahedron Lett.* **1994**, *35*, 6537–6540.
- [283] C. Galli, G. Illuminati, L. Mandolini, P. Tamborra, *J. Am. Chem. Soc.* **1977**, *99*, 2591–2597.
- [284] D. F. DeTar, N. P. Luthra, *J. Am. Chem. Soc.* **1980**, *102*, 4505–4512.
- [285] G. Illuminati, L. Mandolini, *Acc. Chem. Res.* **1981**, *14*, 95–102.
- [286] A. C. Knipe, *J. Chem. Soc., Perkin Trans. 2* **1973**, 589–595.
- [287] N. L. Allinger, E. L. Eliel *Topics in Stereochemistry*, John Wiley & Sons, Inc, Hoboken, USA, **1973**.
- [288] J. N. Brønsted, *Recl. Trav. Chim. Pays Bas* **1923**, *42*, 718–728.
- [289] J. Li, K. Subramaniam, D. Smith, J. X. Qiao, J. J. Li, J. Qian-Cutrone, J. F. Kadow, G. D. Vite, B.-C. Chen, *Org. Lett.* **2012**, *14*, 214–217.
- [290] S. W. Wright, E. P. Arnold, X. Yang, *Tetrahedron Lett.* **2018**, *59*, 402–405.
- [291] V. Ji Ram, A. Sethi, M. Nath, R. Pratap in *The Chemistry of Heterocycles*, Elsevier, **2019**, 149–478.
- [292] E. Díez-Barra, A. de La Hoz, A. Sánchez-Migallón, J. Tejada, *Synth. Commun.* **1990**, *20*, 2849–2853.
- [293] W. J. Middleton, *J. Org. Chem.* **1975**, *40*, 574–578.
- [294] D. E. Levy *The organic chemistry of sugars*, Taylor & Francis, Boca Raton, **2006**.
- [295] T. Hilche, S. L. Younas, A. Gansäuer, J. Streuff, *ChemCatChem* **2022**, e202200530.
- [296] M. Marchini, G. Bergamini, P. G. Cozzi, P. Ceroni, V. Balzani, *Angew. Chem. Int. Ed.* **2017**, *56*, 12820–12821; *Angew. Chem.* **2017**, *129*, 12996–12997.
- [297] M. Montalti, A. Credi, L. Prodi, M. T. Gandolfi, *Handbook of Photochemistry*, CRC Press, Boca Raton, **2006**.
- [298] J. Luo, J. Zhang, *ACS Catal.* **2016**, *6*, 873–877.
- [299] N. Funken, *Dissertation*, University of Bonn, Bonn, **2016**.
- [300] A. M. Harned, *Tetrahedron* **2018**, *74*, 3797–3841.
- [301] J. P. Vigneron, M. Dhaenens, A. Horeau, *Tetrahedron* **1973**, *29*, 1055–1059.
- [302] J. Xu, T. Wei, Q. Zhang, *J. Org. Chem.* **2003**, *68*, 10146–10151.

- [303] M. P. Sibi, T. R. Rheault, *J. Am. Chem. Soc.* **2000**, *122*, 8873–8879.
- [304] G. B. Stone, *Tetrahedron Asymmetry* **1994**, *5*, 465–472.
- [305] T. Sakai, *Tetrahedron Asymmetry* **2004**, *15*, 2749–2756.
- [306] P. G. M. Wuts, *Greene's protective groups in organic synthesis*, 4. Ed., Wiley-Interscience, Hoboken, N.J, **2007**.
- [307] J. Mulzer, B. Schöllhorn, *Angew. Chem. Int. Ed.* **1990**, *29*, 431–432; *Angew. Chem.* **1990**, *102*, 433–435.
- [308] T. Yamazaki, T. Ichige, T. Kitazume, *Org. Lett.* **2004**, *6*, 4073–4076.
- [309] IFA, "Tributylstannan", available at <https://gestis.dguv.de/data?name=490279>.
25.07.22.
- [310] T. Brodmann, D. Janssen, M. Kalesse, *J. Am. Chem. Soc.* **2010**, *132*, 13610–13611.
- [311] T. Brodmann, M. Lorenz, R. Schäckel, S. Simsek, M. Kalesse, *Synlett* **2009**, *2009*, 174–192.
- [312] S. Spindler, L. M. Wingen, M. Schönenbroicher, M. Seul, M. Adamek, S. Essig, M. Kurz, N. Ziemert, D. Menche, *Org. Lett.* **2021**, *23*, 1175–1180.
- [313] K. Narasaka, F.-C. Pai, *Tetrahedron* **1984**, *40*, 2233–2238.
- [314] K.-M. Chen, G. E. Hardtmann, K. Prasad, O. Repič, M. J. Shapiro, *Tetrahedron Letters* **1987**, *28*, 155–158.
- [315] M. Kretschmer, M. Dieckmann, P. Li, S. Rudolph, D. Herkommer, J. Troendlin, D. Menche, *Chemistry* **2013**, *19*, 15993–16018.
- [316] A. K. Saksena, P. Mangiaracina, *Tetrahedron Letters* **1983**, *24*, 273–276.
- [317] D. A. Evans, K. T. Chapman, E. M. Carreira, *J. Am. Chem. Soc.* **1988**, *110*, 3560–3578.
- [318] D. A. Evans, A. H. Hoveyda, *J. Am. Chem. Soc.* **1990**, *112*, 6447–6449.
- [319] P. M. Bodnar, J. T. Shaw, K. A. Woerpel, *J. Org. Chem.* **1997**, *62*, 5674–5675.
- [320] K. Ralston, A. Hulme, *Synthesis* **2012**, *44*, 2310–2324.
- [321] H. Lebel, E. N. Jacobsen, *J. Org. Chem.* **1998**, *63*, 9624–9625.
- [322] M. Miyashita, T. Suzuki, M. Hoshino, A. Yoshikoshi, *Tetrahedron* **1997**, *53*, 12469–12486.
- [323] K. Mikami, S. Matsumoto, A. Ishida, S. Takamuku, T. Suenobu, S. Fukuzumi, *J. Am. Chem. Soc.* **1995**, *117*, 11134–11141.
- [324] S. Kiyooka, Y. Kaneko, M. Komura, H. Matsuo, M. Nakano, *J. Org. Chem.* **1991**, *56*, 2276–2278.
- [325] Y. Gao, J. M. Klunder, R. M. Hanson, H. Masamune, S. Y. Ko, K. B. Sharpless, *J. Am. Chem. Soc.* **1987**, *109*, 5765–5780.
- [326] R. M. Hanson, K. B. Sharpless, *J. Org. Chem.* **1986**, *51*, 1922–1925.
- [327] T. Katsuki, K. B. Sharpless, *J. Am. Chem. Soc.* **1980**, *102*, 5974–5976.

- [328] Z. You, A. H. Hoveyda, M. L. Snapper, *Angew. Chem. Int. Ed.* **2009**, *48*, 547–550; *Angew. Chem.* **2009**, *121*, 555–558.
- [329] H. E. Gottlieb, V. Kotlyar, A. Nudelman, *J. Org. Chem.* **1997**, *62*, 7512–7515.
- [330] D. A. L. Otte, D. E. Borchmann, C. Lin, M. Weck, K. A. Woerpel, *Org. Lett.* **2014**, *16*, 1566–1569.
- [331] K. Miyamoto, N. Tada, M. Ochiai, *J. Am. Chem. Soc.* **2007**, *129*, 2772–2773.
- [332] S. Yamashita, D. Hayashi, A. Nakano, Y. Hayashi, M. Hirama, *J. Antibiot.* **2016**, *69*, 31–50.
- [333] X.-T. Zhou, R. G. Carter, *Chem. Commun.* **2004**, 2138–2140.
- [334] M. Kumar Muthyala, S. Choudhary, K. Pandey, G. M. Shelke, M. Jha, A. Kumar, *Eur. J. Org. Chem.* **2014**, *2014*, 2365–2370.
- [335] A. Gansäuer, S. Hildebrandt, A. Michelmann, T. Dahmen, D. von Laufenberg, C. Kube, G. D. Fianu, R. A. Flowers, *Angew. Chem. Int. Ed.* **2015**, *54*, 7003–7006; *Angew. Chem.* **2015**, *127*, 7109–7112.
- [336] T. Liedtke, T. Hilche, S. Klare, A. Gansäuer, *ChemSusChem* **2019**, *12*, 3166–3171.
- [337] D. Wang, Z. Zhang, *Org. Lett.* **2003**, *5*, 4645–4648.
- [338] K. Otaka, K. Mori, *Eur. J. Org. Chem.* **1999**, *8*, 1795–1802.
- [339] S. Chatterjee, P. Dey, S. V. Kanojia, S. Chattopadhyay, D. Goswami, *Synth. Commun.* **2021**, *51*, 765–775.
- [340] M. Morita, S. Saito, R. Shinohara, R. Aoyagi, M. Arita, Y. Kobayashi, *Synlett* **2020**, *31*, 718–722.
- [341] W. Xie, G. Jiang, H. Liu, J. Hu, X. Pan, H. Zhang, X. Wan, Y. Lai, D. Ma, *Angew. Chem. Int. Ed.* **2013**, *52*, 12924–12927; *Angew. Chem.* **2013**, *125*, 13162–13165.
- [342] V. R. Espejo, J. D. Rainier, *J. Am. Chem. Soc.* **2008**, *130*, 12894–12895.
- [343] D. Slak, *Bachelor Thesis*, University of Bonn, Bonn, **2017**.
- [344] G. Frey, H.-T. Luu, P. Bichovski, M. Feurer, J. Streuff, *Angew. Chem. Int. Ed.* **2013**, *52*, 7131–7134; *Angew. Chem.* **2013**, *125*, 7271–7274.
- [345] P. Beak, C. R. Payet, *J. Org. Chem.* **1970**, *35*, 3281–3286.
- [346] M. E. Kuehne, W. G. Bornmann, I. Markó, Y. Qin, K. L. LeBoulluec, D. A. Frasier, F. Xu, T. Mulamba, C. L. Ensinger, L. S. Borman, A. E. Huot, C. Exon, F. T. Bizzarro, J. B. Cheung, S. L. Bane, *Org. Biomol. Chem.* **2003**, *1*, 2120–2136.
- [347] L. Andna, L. Miesch, *Org. Biomol. Chem.* **2019**, *17*, 5688–5692.
- [348] G. Laudadio, E. Barmpoutsis, C. Schotten, L. Struik, S. Govaerts, D. L. Browne, T. Noël, *J. Am. Chem. Soc.* **2019**, *141*, 5664–5668.
- [349] F. Felluga, G. Pitacco, E. Valentin, C. D. Venneri, *Tetrahedron: Asymmetry* **2008**, *19*, 945–955.

- [350] A. A. Rodriguez, H. Yoo, J. W. Ziller, K. J. Shea, *Tetrahedron Lett.* **2009**, *50*, 6830–6833.
- [351] K. J. Emery, T. Tuttle, J. A. Murphy, *Org. Biomol. Chem.* **2017**, *15*, 8810–8819.
- [352] Grigoriy Shizgal, *Master Thesis*, University of Bonn, Bonn, **2018**.
- [353] J. A. Varela, C. González-Rodríguez, S. G. Rubín, L. Castedo, C. Saá, *J. Am. Chem. Soc.* **2006**, *128*, 9576–9577.
- [354] A. Fleckhaus, *Dissertation*, University of Bonn, Bonn, **2010**.
- [355] A. Cervantes-Reyes, F. Rominger, M. Rudolph, A. S. K. Hashmi, *Adv. Synth. Catal.* **2020**, *362*, 2523–2533.
- [356] M. J. Pugia, B. E. Knudsen, C. V. Carson, R. A. Bartsch, *J. Org. Chem.* **1987**, *52*, 541–547.
- [357] C. Zhou, T. Lei, X.-Z. Wei, C. Ye, Z. Liu, B. Chen, C.-H. Tung, L.-Z. Wu, *J. Am. Chem. Soc.* **2020**, *142*, 16805–16813.
- [358] H. Sun, S. G. DiMagno, *Chem. Commun.* **2007**, 528–529.
- [359] E. Rojo Wiechel, *Dissertation*, University of Bonn, Bonn, **2017**.
- [360] A. Habel, W. Boland, *Org. Biomol. Chem.* **2008**, *6*, 1601–1604.
- [361] S. A. Giddings, *Inorg. Chem.* **1967**, *6*, 849–850.

7 Abbreviations

1,4-CHD	1,4-cyclohexadiene
3DPAFIPN	2,4,6-tris(diphenylamino)-5-fluoroisophthalonitrile
4CzIPN	2,4,5,6-tetrakis(9 <i>H</i> -carbazol-9-yl)isophthalonitrile
7-DHC	7-dehydrocholesterol
Ac	acetyl
acac	acetylacetonate
$[\alpha]_D^{20}$	specific rotation at 20°C
<i>ansa</i>	Latin: handle
aq.	aqueous
BINOL	1,1'-bi-2-naphthol
Boc	<i>tert</i> -butyloxycarbonyl
bpm	2,2'-bipyrimidine
bpy	2,2'-bipyridine
Bu	butyl
<i>c/Cy</i>	<i>cyclo</i>
calcd.	calculated
cat.	catalyst
CH	cyclohexane
CHD	see 1,4-CHD
COD	1,5-cyclooctadiene
Coll	collidine; 2,4,6-trimethylpyridine
conv.	conversion
Cp	cyclopentadienyl
Cp*	pentamethylcyclopentadienyl
CSA	camphor sulfonic acid
Cy	cyclohexyl
d	doublet
DABCO	1,4-diazabicyclo[2.2.2]octane
DAST	diethylaminosulfur trifluoride
DCM	dichloromethane
DEO	diastereodivergent epoxide opening
DFT	density functional theory
DIBAL-H	diisobutyl aluminum hydride

DIPAMP	di(phenylanisylmethylphosphine)
DIPEA	<i>N,N</i> -diisopropylethylamine
DMAP	dimethylaminopyridine
DME	dimethoxyethane
DMF	<i>N,N</i> -dimethylformamide
DMPU	dimethylpropyleneurea
DMPS	dimethylphenylsilyl
DMT	dimethyl terephthalate
DOS	diversity-oriented synthesis
EA	ethyl acetate
ebthi	1,2-ethylene-1,1'-bis(tetrahydroindenyl)
EDA	ethylenediamine
<i>ent</i>	enantiomer
Et	ethyl
E _T	triplet state energy
<i>et al.</i>	and co-workers/and others
<i>fac</i>	facial isomer
HAD	hydrogen atom donor
HAT	hydrogen atom transfer
Hept	heptyl
Hex	hexyl
HOMO	highest occupied molecular orbital
HRMS	high resolution mass spectrometry
<i>i</i>	<i>iso</i>
IR	infrared spectroscopy
ISC	inter system crossing
<i>J</i>	coupling constant [Hz]
K	Kelvin
kW	kilowatt
LDA	lithium diisopropylamide
LUMO	lowest unoccupied molecular orbital
Lut	2,6-lutidine
<i>m</i>	<i>meta</i>
M	molar [mol/L]

<i>m</i> CPBA	<i>meta</i> -chloroperoxybenzoic acid
Me	methyl
menbpy	4,4'-dimenthoxycarbonyl-2,2'-bipyridine
MLCT	metal-to-ligand charge-transfer
mp	melting point
Ms	methanesulfonyl
MTG	methylthioglycolate
MW	molecular weight
<i>n</i>	<i>normal</i>
NBS	<i>N</i> -bromosuccinimide
NMR	nuclear magnetic resonance spectroscopy
No.	number
OSET	outer-sphere electron transfer
OTG	<i>n</i> -octyl thioglycolate
<i>p</i>	<i>para</i>
PCET	proton-coupled electron transfer
Piv	pivaloyl
Ph	phenyl
ppm	parts per million
PPTS	pyridinium- <i>para</i> -toluenesulfonate
ppy	2-phenylpyridine
Pr	propyl
PRC	photoredox catalysis
PRCat	photoredox catalyst
rac. or <i>rac</i>	racemic
REO	regiodivergent epoxide opening
rt	room temperature
s	singlet
SCE	saturated calomel electrode
S _n	singlet-state (S ₀ = ground state)
sat.	saturated
SET	single-electron transfer
t	triplet
<i>t</i>	<i>tert</i>

T _n	triplet-state
TBDPS	<i>tert</i> -butyldiphenylsilyl
TBHP	<i>tert</i> -butyl hydroperoxide
Temp.	reaction temperature
TES	triethylsilyl
Tf	trifluoromethanesulfonyl
TFA	trifluoroacetate
THF	tetrahydrofuran
THQ	tetrahydroquinoline
[Ti]	titanocene catalyst
TIPS	triisopropylsilyl
TMB	1,3,5-trimethoxybenzene
TMS	trimethylsilyl
TOS	target-oriented synthesis
Ts	<i>para</i> -toluenesulfonyl
TW	terawatt
UV	ultraviolet
Vis	visible
wt%	percentage by weight (mass fraction)

8 Appendix

8.1 List of Figures

Figure 1: Selection of principles of Green Chemistry by <i>Anastas</i> . ^[10,11]	2
Figure 2: Structures of the two enantiomers of asparagine.	7
Figure 3: Structures of the two enantiomers of <i>Citalopram</i>	7
Figure 4: Basic overview of isomerism.....	8
Figure 5: Structure of (<i>R,R</i>)-DIPAMP and the (<i>R,R</i>)-DIPAMP rhodium(I) COD complex. ^[57] ..	9
Figure 6: Structure of chlorophyll <i>a</i> . ^[70]	11
Figure 7: Ru(II) and Ir(III) photoredox catalysts. ^[66,69,73]	12
Figure 8: Structures of D- and L-Kagan complex. ^[84]	13
Figure 9: Interaction of reduced L-Kagan catalyst and substrate prior to the epoxide opening. ^[94]	15
Figure 10: Display of diastereoisomeric mixture of epoxides for DEO reactions.....	18
Figure 11: 1,3- and 1,4-diol-motif in natural products and pharmaceutical drugs. ^[112,113]	22
Figure 12: Prominent structures of halide-ion-acceptors. ^[131,136,150,151]	25
Figure 13: Simplified photochemical molecular orbital scheme of [Ir(ppy) ₃] under irradiation with 375 nm light. ^[71,189]	28
Figure 14: Structures of bimetallic Ru-Pd-complex and enantiomerically pure Ru-PRCat. ^[72]	31
Figure 15: Triplet-energy (E _T) transfer from excited I41 to bound substrate in the hydrogen bond adduct. ^[210]	33
Figure 16: UV-Vis spectrum of Cp ₂ TiCl ₂ in MeCN (c = 0.5 μmol/mL). Maxima at 392 nm and 525 nm.	35
Figure 17: IR spectra of E2 (blue, O–H stretching modes at 3330 cm ⁻¹) and crude reaction mixture (C21 , red).	37
Figure 18: UV-Vis investigated titanocene carboxylate complexes.	42
Figure 19: UV-Vis spectra (5 μM in THF) of Cp ₂ TiCl ₂ (red, 5 μM in MeCN), T1 (blue), T2 (green), T3 (violet), T4 (yellow).....	42
Figure 20: Basic structure of REO-Arylation substrates. ^[149]	51
Figure 21: General structure of REO substrates.	64
Figure 22: New REO substrates (top) and attempted structures (bottom). [a] Synthesized by <i>Heinz</i> . ^[217]	68
Figure 23: Proposed stabilization by supramolecular binding of Z1 to Cp ₂ Ti(III)Cl (left) based on DFT calculations for comparable [Cp ₂ TiCl : Z4] (right). ^[150]	90
Figure 24: Comparison of required REO reagents, catalytic (top) and stoichiometric (bottom). ^[110,136]	95

Figure 25: Structure of chivosazol A.^[117]95

Figure 26: Enantio- and diastereomerically pure *pseudo*-symmetrical secondary 1,3-diols
obtained by the photochemical REO.^[136]96

8.2 List of Tables

Table 1: Scope of the photoexcited titanocene catalyzed epoxide opening.	39
Table 2: Titanocene catalyzed radical 5-exo cyclizations under photoredox conditions.	40
Table 3: UV-Vis absorptions of selected titanocene dichlorides.	41
Table 4: Investigated reaction conditions for pinacol coupling of benzaldehyde (P1).	44
Table 5: Investigated reaction conditions for epoxide openings of E1	46
Table 6: Investigated reaction conditions for decarboxylations of S4	50
Table 7: Investigated reaction conditions for decarboxylations of S6	50
Table 8: Selected scope of indoline and THQ synthesis via REO-arylation.	53
Table 9: Investigated reaction conditions for REO-arylations of A1	56
Table 10: Investigated reaction conditions for REO-arylations of A6	60
Table 11: Investigated reaction conditions for photochemical arylations.	61
Table 12: Investigated reaction conditions for photochemical arylations.	63
Table 13: Synthesis of REO substrates via the direct double S _N 2 route.	70
Table 14: Synthetic approaches to X11	71
Table 15: Unsuccessful synthetic approaches to new REO substrates.	73
Table 16: Ground state and excited state redox potentials E _{1/2} of 3DPAFIPN.	78
Table 17: REO reactions using 3DPAFIPN as catalyst.	79
Table 18: DEO reactions using 3DPAFIPN as catalyst.	83
Table 19: Selected DEO reactions using Bu ₃ SnH as HAD by <i>Adamietz</i>	87
Table 20: Results for the performance of sulfonamides in REO of R42 to R43	89
Table 21: REO reactions with sulfonamide Z1 at 45°C.	92

8.3 List of Schemes

Scheme 1: Comparison of sustainability in different acylations for <i>Ibuprofen</i> precursor I2 . ^[8,10,15]	3
Scheme 2: Simplified depiction of the enantioselective hydrogenation in the synthesis of L-DOPA. ^[52,56,58]	9
Scheme 3: Catalytic cycle of the asymmetric enantioselective hydrogenation DIPAMP employed enantiomerically pure. ^[56]	10
Scheme 4: Net equation of the photosynthesis. ^[62]	11
Scheme 5: Synthesis of vitamin D ₃ . ^[78,79]	12
Scheme 6: Regioselective epoxide opening using titanocene dichloride as achiral catalyst. ^[86]	14
Scheme 7: Titanocene catalyzed enantioselective opening of <i>meso</i> -epoxides. Conditions: 10 mol% L-Kagan, 2.5 eq. Coll*HCl, 1.0 eq. epoxide, 1.0 eq. CHD, 2.0 eq. Zn, 0.1 M in THF, rt, 22 h. ^[88]	15
Scheme 8: Regiodivergent epoxide opening (REO) by application of different catalyst enantiomers.	16
Scheme 9: Regiodivergent epoxide opening of an enantiomerically enriched substrate. Conditions: 10 mol% D- or L-Kagan, 1.0 eq. epoxide, 1.5 eq. Coll*HCl, 1.5 eq. Mn, 4.4 eq. CHD, 0.3 M in THF, rt, 16 h. ^[95,96]	17
Scheme 10: Calculation of enantiomeric ratios in a REO with D-Kagan and a catalyst selectivity of 90% (red) and 95% (green) exclusively under catalyst-control.	17
Scheme 11: Calculation of diastereoisomeric ratios in a DEO with D-Kagan and a catalyst selectivity of 90% (red) and 95% (green) exclusively under catalyst-control.	19
Scheme 12: Overview of possible DEO reaction products. Main products encircled.	20
Scheme 13: General synthesis of REO and DEO substrates from simple common precursors. a) VO(acac) ₂ , TBHP; b) <i>m</i> CPBA. ^[103,110]	21
Scheme 14: Synthesis of (-)-massoialactone via REO. Conditions: a) 1.0 eq. epoxide I30 , 1.5 eq., Lut*HCl, 1.5 eq. Mn, 7 mol% D-Kagan, 2.2 eq. Bu ₃ SnH, 0.17 M in THF, rt, 72 h; b) 1.0 eq. 1,3-diol I31 , 0.5 eq. TsOH, 0.05 M in benzene, reflux, 7 h. ^[93,110]	23
Scheme 15: General catalytic cycle of the titanocene catalyzed epoxide opening with <i>in situ</i> catalyst activation by reduction with manganese powder. Depiction of the resting state C5 by complex formation with Coll*HCl. ^[92,137,138]	24
Scheme 16: General catalytic cycle of the titanocene catalyzed radical arylation. ^[139]	26
Scheme 17: Catalytic cycle of photoredox catalysis coupled with the titanocene catalyzed epoxide opening. ^[130]	29
Scheme 18: Dual-catalysis by <i>MacMillan</i> coupling photoredox catalyst with imidazolidinone-based organocatalyst in enantioselective α -benzylation of aldehydes. ^[194] ...	30

Scheme 19: First enantioselective triplet-sensitized [2+2]-photocycloaddition by <i>Bach</i> . ^[207,210]	32
Scheme 20: Catalytic cycle of the titanocene catalyzed epoxide opening under photoredox conditions with DIPEA as reductive quencher and MTG as HAT-catalyst. ^[135] ..	36
Scheme 21: Optimized reaction conditions for the photochemical titanocene catalyzed epoxide opening. ^[135]	38
Scheme 22: Titanocene catalyzed diastereoselective pinacol coupling of benzaldehyde. Conditions: 1.0 eq. Zn, 1.5 eq. TMSCl, 1.0 eq. MgBr ₂ , 90% yield, <i>d.r.</i> (<i>syn:anti</i>) = 95:5. ^[154] ..	43
Scheme 23: General reaction conditions for pinacol coupling screening reactions. Conditions: 10 mol% Cp ₂ TiCl ₂ , 3.0 eq. amine, 1.5 eq. TMSCl, 1.0 eq. ZnCl ₂ , 0.05 M in THF.	43
Scheme 24: General reaction conditions for photoexcited titanocene catalyzed epoxide opening reactions. Conditions: 10 mol% titanocene catalyst [Ti], 3.0 eq. DIPEA, 20 mol% MTG, 0.05 M in THF.	45
Scheme 25: Photoexcited <i>Brintzinger</i> -titanocene catalyzed epoxide opening. Conditions: 10 mol% <i>rac</i> -(<i>ebthi</i>)TiCl ₂ , 3.0 eq. DIPEA, 20 mol% MTG, 0.05 M in THF.	47
Scheme 26: Epoxide opening applying <i>cHex</i> -(+)-CSA titanocene catalyst. Conditions: 10 mol% (<i>cHexCp</i>) ₂ Ti(CSA) ₂ , 3 mol% 3DPAFIPN, 2.0 eq. H1 , 0.05 M in THF.	47
Scheme 27: Catalytic cycle of the photochemical decarboxylation with subsequent alkylation by <i>MacMillan</i> . ^[252]	48
Scheme 28: General reaction conditions for photoexcited titanocene catalyzed decarboxylation of S4 . Conditions: 10 mol% titanocene precatalyst Cp ₂ TiX ₂ , 2.0 eq. X1 , 10 mol% to 1.0 eq. base, 0.05 M in THF. Conversion monitored by TLC.	49
Scheme 29: General reaction conditions for photoexcited titanocene catalyzed decarboxylation of S6 . Conditions: 10 mol% Cp ₂ TiCl ₂ , 2.0 eq. X1 , 0.5 eq. base, 0.05 M in respective solvent. Conversion monitored by TLC.	50
Scheme 30: Concept of product scope for the REO-arylation of epoxide A1 . ^[149]	52
Scheme 31: Catalytic cycle for the formation of indolines in the REO-arylation. ^[149]	52
Scheme 32: Synthesis of arylation substrates. X2 employed in the S _N 2-reaction.	54
Scheme 33: Modular synthesis of enantiomerically pure REO-arylation substrates. ^[149] [a] Performed by <i>Heinz</i> . ^[217] [b] Performed by <i>Weißbarth</i> . ^[220]	55
Scheme 34: General THQ synthesis from A1 in the REO-arylation with indoline A2 as side-product. Conditions: 10 mol% cat., 0.1 to 1.0 eq. additive if used, 0.05 M in THF.	56
Scheme 35: Proposed catalytic cycle for the THQ formation via photocatalyzed REO-arylation.	57
Scheme 36: REO by <i>Heinz</i> . ^[217] Conditions: 10 mol% D-Kagan, 3 mol% 3DPAFIPN, 2.0 eq. H1 , 1.5 eq. DMPU, 0.1 M in THF. Isolated yield.	59

Scheme 37: General THQ synthesis from A6 in the REO-arylation. Conditions: 10 mol% cat., 1.0 eq. additive if used, 0.05 M in THF.	59
Scheme 38: General indoline synthesis in photochemical arylations. Conditions: 10 mol% D-Kagan, 0.05 M in THF.....	61
Scheme 39: Classic radical arylation of A12 . Conditions: 10 mol% D-Kagan, 10 mol% Zn, 0.05 M in THF.	62
Scheme 40: Photochemical radical arylations of A12 . Conditions: 10 mol% catalyst, 0.05 M in THF.	62
Scheme 41: Proposed catalytic cycle for the photocatalyzed radical arylation of A12	64
Scheme 42: Synthesis of first enantiomerically enriched REO substrates by <i>Gansäuer</i> . ^[95] ..	65
Scheme 43: Synthetic approach to enantiomerically and diastereomerically pure REO substrates. ^[110] [a] Yield over two steps.	66
Scheme 44: Strategies for the synthesis of new REO substrates and screened nucleophiles.	67
Scheme 45: Double S _N 2-mechanism in the synthesis of REO substrates from enantiomerically pure α-bromo epoxides.	69
Scheme 46: Two-step route for the synthesis of R7 and desired 5- <i>exo</i> -cyclization.	71
Scheme 47: Preparation of REO-cyclization substrate R4 . Conditions: 1.2 eq. X9 , 1.2 eq. NaH, 0.67 M in THF.	72
Scheme 48: Application of AlMe ₃ as <i>Lewis</i> acid and <i>Brønsted</i> base ^[289] for the conversion of propargyl amine with X6 . Conditions: 1.2 eq. X6 , 1.0 eq. AlMe ₃ , 0.2 M in DCM.	72
Scheme 49: Intramolecular epoxidation of X12 via S _N 2-reaction. Conditions: 2.0 eq. K ₂ CO ₃ , 0.5 M in MeOH.....	72
Scheme 50: Synthesis of REO substrate R6 via two-step approach with AlMe ₃ . Conditions: 1) 1.2 eq. X7 , 1.0 eq. AlMe ₃ , 0.2 M in DCM, rt, 20 h; 2) 2.0 eq. K ₂ CO ₃ , 0.5 M in MeOH, 40°C, 1 h.	73
Scheme 51: Observed ketone formation by addition of <i>Grignard</i> reagent N15 to X9	74
Scheme 52: Alkyne addition to enantiomerically pure S2 (<i>e.r.</i> = 98:2). Conditions: 1.0 eq. S3 , 1.1 eq. <i>n</i> BuLi, 1.0 eq. BF ₃ *THF, 0.63 M in THF.	74
Scheme 53: Alkyne reduction to (<i>Z</i>)-β-hydroxy alkene X14 . Conditions: 0.25 eq. Ni(OAc) ₂ , 0.25 eq. NaBH ₄ , 0.5 eq. EDA, 0.5 M in MeOH.	74
Scheme 54: Derivatization of <i>syn</i> -β-hydroxy alcohols to substrates for the photochemical REO. Conditions: (fluorination) 1.1 eq. DAST, 0.1 M in DCM; (methylation) 1.94 eq. MeI, 1.46 eq. NaH, 0.3 M in THF; (silylation) 1.2 eq. silyl chloride, 2.5 eq. imidazole, 1.0 M in DMF. [a] Synthesized by <i>Zhang</i> . ^[136] [b] Contained inseparable impurity.	75
Scheme 55: <i>Syn</i> -selective epoxidation to REO substrate precursor R19 . Conditions: 5 mol% VO(acac) ₂ , 1.5 eq. TBHP, 0.1 M in DCM.....	76

Scheme 56: Proposed catalytic cycle for the 3DPAFIPN and L-Kagan catalyzed REO reaction. ^[73]	77
Scheme 57: Attempted photochemical parallel resolution of R5 . Conditions: 10 mol% D-Kagan, 2.5 mol% 4CzIPN, 1.5 eq. DMPU, 2.0 eq. H1 , 0.1 M in THF.	83
Scheme 58: Best performance of L-Kagan as photoredox catalyst in a REO-arylation from Table 9. Conditions: 10 mol% L-Kagan, 1.0 eq. Ph ₃ N, 0.05 M in THF.	88
Scheme 59: Best performance of D-Kagan as photoredox catalyst in an arylation reaction from Table 11. Conditions: 10 mol% D-Kagan, 0.05 M in THF.....	88
Scheme 60: Screening reaction for the performance of sulfonamides as chloride-acceptors in photochemical REO reactions. Conditions: 15 mol% L-Kagan, 15 mol% sulfonamide, 2.0 eq. DIPEA, 20 mol% MTG, 0.17 M in THF. ^[136]	89
Scheme 61: Proposed catalytic cycle of the sulfonamide assisted photochemical REO. ^[136]	91
Scheme 62: Organoselenium-mediated regioselective epoxide opening. ^[315,322]	96
Scheme 63: Titanocene dichloride as photoredox catalyst in epoxide openings and 5- <i>exo</i> -cyclizations.....	97
Scheme 64: Highly sustainable, atom-economic radical arylation of epoxides with substituted titanocenes under photoredox conditions. R = H or (cyclo)alkyl, substituent sizes from R = H to (<i>t</i> Bu)CyHex.....	98
Scheme 65: General overview of photochemical REOs. R/R' = alkyl or alcohol/ester-substituted alkyl. X = F, OMe, OTBS or other silyl-protecting group.	99

8.4 List of Publications

- I. A DIVERGENT DUO: PALLADIUM CATALYZED CARBOAMINATION IN ENANTIOSELECTIVE DESYMMETRIZATION AND REGIODIVERGENT CATALYSIS
E. Dolja, N. Funken, **D. Slak**, G. Schnakenburg, A. Gansäuer, *ChemCatChem* **2019**, *11*, 5421–5424.
DOI: 10.1002/cctc.201901784

- II. TITANOCENES AS PHOTOREDOX CATALYSTS USING GREEN LIGHT IRRADIATION
Z. Zhang, T. Hilche, **D. Slak**, N. R. Rietdijk, U. N. Oloyede, R. A. Flowers II, A. Gansäuer, *Angew. Chem. Int. Ed.* **2020**, *59*, 9355–9359; *Angew. Chem.* **2020**, *132*, 9441–9445.
DOI: 10.1002/ange.202001508 and 10.1002/anie.202001508

9 Acknowledgement – Danksagung

Zunächst möchte ich mich bei *Prof. Andreas Gansäuer* für die Aufnahme in seinen Arbeitskreis und die Möglichkeit danken, diese Arbeit unter seiner Betreuung anzufertigen. Ebenso bedanke ich mich bei *Prof. Arne Lützen* für die Übernahme der Zweitkorrektur, sowie bei *Prof. Robert Glaum* und *Prof. Matthias Wüst* für ihren Beitrag als weitere Mitglieder meiner Promotionskommission.

Ganz besonders gilt mein Dank allen, die mich in dieser herausfordernden Zeit unterstützt und immer wieder aufgebaut haben und es mir ermöglicht haben, wieder im Alltag Fuß zu fassen und positiv in die Zukunft zu sehen. Insbesondere gilt auch dabei mein Dank *Prof. Gansäuer*, der mir mit Rat und Verständnis immer zur Seite stand und mich stets unterstützt hat. Vielen Dank für Ihr Vertrauen, die Flexibilität im Arbeitsalltag und die Zeit, die ich mir nehmen durfte, um wieder völlig gesund zu werden. Danke auch hier besonders an *Grigoriy*, *Tim* und *Michael*, ihr wart mir immer eine große Hilfe, Stütze und Motivation und tragt einen großen Teil dazu bei, dass ich mich im Arbeitskreis so wohl gefühlt habe.

Bedanken möchte ich mich außerdem bei *Michael* und *Sebastian* für das Korrekturlesen dieser Arbeit, sowie bei *Tim*, *Hua*, *Marcel*, *Tobias* und *Nancy* für die erfolgreiche Zusammenarbeit in den Projekten für unsere Publikationen.

Zudem Danke an *Lydia* und *Regine*, für die schöne Zeit im Studium und in der Freizeit, sowie die Hilfe bei allen Fragen und Problemen.

Außerdem danke an *Hendrik* für die gute Zeit beim Bouldern und die Jahre im Arbeitskreis. Auch allen anderen aktuellen und ehemaligen Mitgliedern des Arbeitskreises möchte ich danken, für die schöne Zeit, die lustigen Kaffeepausen, die Grillabende und die allzeit gute Atmosphäre. Ich werde es sehr vermissen.

Auch bedanke ich mich bei meinem Freundeskreis aus dem Norden, hierbei insbesondere bei *Henrik*, der trotz der großen Entfernung immer ein offenes Ohr und einen guten Rat für mich hatte.

Herzlichsten Dank besonders an meine Familie, meine Eltern und meine Schwester *Anna* und an *Francesca*. Ohne Euch wäre ich heute nicht, wo ich jetzt bin, und da bin ich verdammt gerne.

Tausend Dank.

10 Zusammenfassung

DIE ENTWICKLUNG CHIRALER TITANOCENE ALS PHOTOREDOXKATALYSATOREN

Schlagworte: Titanocene, Katalyse, Photochemie, Stereoselektivität, Nachhaltigkeit

Die vorliegende Dissertation beschreibt die aktuellen Fortschritte in der Entwicklung von photochemisch aktivierten (chiralen) Titanocenen sowohl als Elektronen-Transfer-Katalysator als auch als Photoredoxkatalysator in Epoxidöffnungsreaktionen. Basierend auf der Entdeckung der photoredox-aktiven Eigenschaften von Titanocendichlorid und den daraus resultierenden erfolgreichen Anwendungen als Photoredoxkatalysator, sollte die Einsetzbarkeit als solcher in weiteren bekannten titanocenkatalysierten Reaktionen getestet werden. Zudem wurde die Nutzung anderer Titanocene mit verschiedenen photochemischen und elektronischen Eigenschaften untersucht. Durch die Entwicklung neuer Reaktionsbedingungen konnte außerdem der Verzicht auf vorher notwendige, nicht nachhaltige und giftige Reagenzien realisiert werden, indem diese durch Alternativen in katalytischen Mengen ersetzt werden konnten.

Radikalische Arylierungen sowie regio- und diastereodivergente Epoxidöffnungsreaktionen wurden durch Einsatz des als *Kagan* Komplexes bekannten chiralen und enantiomerenreinen Titanocens erfolgreich unter Herstellung verschiedener neuer Moleküle durchgeführt, einerseits in Kombination mit einem externen, organischen Photoredoxkatalysator, andererseits indem das Titanocen selbst diese Funktion übernimmt.

Erfreulicherweise werden bisher störende aber in der Synthese beliebte Silylschutzgruppen unter den neuen Reaktionsbedingungen toleriert, was die Darstellung selektiv einfach geschützter, enantio- und diastereomerenreiner 1,3- und 1,4-Diole ermöglicht. Hierbei werden außerdem die erzielten Ausbeuten der ursprünglichen Reaktionsbedingungen für bereits etablierte REO-Reaktionsprodukte erreicht.

Durch Anwendung der photochemischen Methode kann nicht nur eine wesentliche Verbesserung im Hinblick auf die Nachhaltigkeit erreicht werden, sondern auch eine Erweiterung der umsetzbaren Substratpalette, wodurch diese neuen Bedingungen auch für die Synthese von natürlich vorkommenden und oft biologisch aktiven Diolstrukturen in der Naturstoffsynthese oder der Herstellung von Pharmazeutika genutzt werden können.

11 Abstract

THE DEVELOPMENT OF CHIRAL TITANOCENES AS PHOTOREDOX CATALYSTS

Keywords: Titanocenes, Catalysis, Photochemistry, Stereoselectivity, Sustainability

This dissertation describes the advances in photochemically activated (chiral) titanocenes as both electron transfer and photoredox catalysts in epoxide opening reactions. Based on the discovery of the photoredox-active properties of titanocene dichloride and the resulting successful employment as photoredox catalyst, the applicability of these properties in other types of titanocene catalyzed reactions was investigated. The performance of various other titanocenes with different photochemical and electronic properties was also examined. Moreover, newly developed reaction conditions enabled the renunciation of previously required unsustainable and toxic reagents by replacing them with catalytic alternatives.

For radical arylations, as well as regio- and diastereodivergent epoxide openings, the chiral and enantiomerically pure titanocene known as *Kagan's* complex has been successfully used either in combination with an external, organic photoredox catalyst or as photoredox catalyst itself in the synthesis of various new compounds.

Gratifyingly, novel reaction conditions tolerating the presence of commonly used and previously obstructive silyl-protecting groups have been found, giving access to selectively monoprotected, enantio- and diastereomerically pure 1,3- and 1,4-diol-structures. Moreover, the yields of the originally used conditions for already established REO reaction products could be matched.

By this photochemical approach, not only an improvement regarding sustainability has been achieved, but also the substrate scope has been extended. This renders the method a potentially useful and reliable tool for the synthesis of naturally occurring and often biologically active diol-moieties in natural product or pharmaceutical drug synthesis.